UNIVERSIDADE DE LISBOA

FACULDADE DE FARMÁCIA

ROLE OF GLIAL CELLS AS CONTRIBUTORS TO THE ONSET AND PROPAGATION OF ALS DISEASE

Joana Carolina Marinho Cunha

Orientador(es): Prof. Doutora Dora Maria Tuna de Oliveira Brites
Doutora Ana Rita Mendonça Vaz Botelho

Tese especialmente elaborada para obtenção do grau de **Doutor em Farmácia**, especialidade de **Biologia Celular e Molecular**

2017

UNIVERSIDADE DE LISBOA

FACULDADE DE FARMÁCIA

ROLE OF GLIAL CELLS AS CONTRIBUTORS TO THE ONSET AND PROPAGATION OF ALS DISEASE

Joana Carolina Marinho Cunha

Orientador(es): Prof. Doutora Dora Maria Tuna de Oliveira Brites
Doutora Ana Rita Mendonça Vaz Botelho

Tese especialmente elaborada para obtenção do grau de **Doutor em Farmácia**, especialidade de **Biologia Celular e Molecular**

Júri

Presidente: Doutora Matilde da Luz dos Santos Duque da Fonseca e Castro, Professora Catedrática e Diretora da Faculdade de Farmácia da Universidade de Lisboa
Vogais:

- Doutora Ana Luísa Colaço Cardoso, Investigadora
  Centro de Neurociências e Biologia Celular da Universidade de Coimbra;
- Doutor Nuno Jorge Ramos Abreu da Silva Lamas, Professor Auxiliar Convidado
  Escola de Medicina da Universidade do Minho;
- Doutora Liliana Inácio Bernardino, Professora Auxiliar
  Faculdade de Ciências da Saúde da Universidade da Beira Interior;
- Doutor Mamede Alves de Carvalho, Professor Catedrático
  Faculdade de Medicina da Universidade de Lisboa;
- Doutora Dora Maria Tuna de Oliveira Brites, Investigadora Coordenadora
  Faculdade de Farmácia da Universidade de Lisboa, Orientadora.

2017

This thesis was supervised by:

Professor Dora Brites, PhD (supervisor)
Research Coordinator
Head of Neuron Glia Biology in Health and Disease
Research Institute for Medicines (iMed.ULisboa)
Faculty of Pharmacy, Universidade de Lisboa

Ana Rita Vaz, PhD (co-supervisor)
Post-doctoral fellow (Fundação para a Ciência e a Tecnologia)
Invited Assistant Professor
Research Institute for Medicines (iMed.ULisboa)
Faculty of Pharmacy, Universidade de Lisboa.

Experimental work was conducted at:

Neuron Glia Biology in Health and Disease Group, Research Institute for Medicines (iMed.ULisboa), Faculty of Pharmacy, Universidade de Lisboa.

Financial Support:

Joana Carolina Marinho Cunha was a PhD student in Pharmacy (Cellular and Molecular Biology) and a recipient of the fellowship SFRH/BD/91316/2012 from the Portuguese Fundação para a Ciência e a Tecnologia (FCT). The execution of this work was supported by FCT (project PTDC/SAU-FAR/118787/2010 to Professor Dora Brites, and in part by Project UID/DTP/04138/2013 to iMed.ULisboa), FEDER/COMPETE, Santa Casa da Misericórdia de Lisboa - Programa de Investigação Científica em Esclerose Lateral Amiotrófica (Project ELA-2015-002 to Professor Dora Brites), and to some extent benefited from the EU Joint Programme-Neurodegenerative Disease Research (JPND) project (JPCOFUND/003/2015 to Professor Dora Brites).

To my parents

Para os meus pais

Acknowledgements/Agradecimentos

E com o fim desta jornada, chega o momento de agradecer a todas as pessoas que de alguma maneira contribuíram para o meu percurso ao longo destes últimos anos.

O meu primeiro agradecimento é naturalmente dirigido à Professora Doutora Dora Brites, orientadora deste trabalho, a quem muito tenho que agradecer. Obrigada por me ter acolhido no seu grupo onde dei os primeiros passos na investigação como aluna de mestrado. Obrigada pela oportunidade que me deu e confiança que depositou em mim para desenvolver um projeto de doutoramento sob a sua orientação. Obrigada pela presença e apoio constante ao longo de todo o meu percurso. A dedicação, o gosto pela Ciência, o rigor e a exigência que a caracterizam ensinaram-me a querer ser sempre melhor pois só assim se atinge a excelência que deseja para todos os seus alunos. Muito obrigada por todos os ensinamentos e conselhos e por exigir nunca menos do que o melhor de mim. Tenho a certeza que tudo o que aprendi nestes últimos anos me vai ser útil para toda a minha vida. Muito obrigada.

Em segundo lugar, gostaria de agradecer-te Rita, não só pela tua coorientação mas por toda a amizade, apoio, companheirismo e confiança. Foi contigo que dei os primeiros passos no laboratório e, mais importante, que cresci como profissional. Acompanhaste de perto todos os meus dilemas, os dias sem fim, as frustrações, mas também todas as conquistas e a satisfação de tarefa cumprida. Partilhámos muitas conversas, desabafos, horas de fluxo, rataria, culturas, descoberta de técnicas novas e excursões pelos nossos adorados exossomas!!! Muito obrigada por acreditares em mim, por me dares sempre força e por estares sempre disponível para me ajudar, por mais árdua que seja a tarefa! Muito obrigada.

Gostaria também de dar uma palavra de agradecimento à Professora Doutora Alexandra Brito e ao Professor Doutor Rui Silva pela disponibilidade em me ajudar sempre que precisei e pelos conhecimentos que me foram transmitindo ao longo destes anos. Gostaria também de agradecer à Sofia e à Adelaide pela simpatia, boa disposição, disponibilidade e pelos almocinhos descontraídos. Em particular, obrigada Adelaide por todas as palavras de conforto. Obrigada pela tranquilidade que transmites capaz de amenizar qualquer situação. Obrigada ainda por todo o conhecimento, e tanto que é! Tem sido um prazer trabalhar mais de perto contigo nestes últimos meses. Admiro-te muito.

Gostaria de expressar os meus agradecimentos à Professora Doutora Ana Sebastião e ao Professor Doutor Alexandre Ribeiro da Faculdade de Medicina pela preciosa colaboração com o modelo animal transgénico da SOD1.

Gostaria ainda de agradecer a disponibilidade e importante ajuda da Professora Doutora Manuela Carvalheira relativa à utilização do equipamento ZetaSizer Nano S e Z no Instituto Nacional de Engenharia, Tecnologia e Inovação (INETI), bem como ao Professor Doutor José Paulo Farinha e à Doutora Tânia Ribeiro do Instituto Superior Técnico, relativamente ao equipamento NanoSight.

Por todos os ensinamentos de expressão génica e de todas as etapas adjacentes à transfeção de células, gostaria de agradecer à Professora Doutora Elsa Rodrigues, à Maria e ao Miguel. Obrigada por toda a ajuda e pela paciência e simpatia com que me auxiliaram com as minhas dúvidas infinitas. Diane, muito obrigado também por toda a ajuda com a produção dos vírus e as transduções.

Gostaria ainda de agradecer à Professora Doutora Maria da Conceição Lima por me ter recebido no seu grupo de investigação em Coimbra e à Doutora Ana Luísa Cardoso pela simpatia e por me ter ensinado as técnicas necessárias à avaliação da expressão dos microRNAs que constituiu uma parte tão significativa do meu trabalho.

I would like to thank Professor Jari Koistinaho and the people from his lab for welcoming me in Kuopio during my training period and for providing me all the valuable knowledge on iPS cells maintenance and differentiation protocols. In particular, to Eila, Minna and Henna, who taught to me so much and were so gentle to me! I am also particularly grateful to Professor Tarja Malm, Professor Katja Kanninen, Sara Wojciechowski and to the girls of the Neuroinflammation Research Lab for all the sympathy and kindness. I really felt at home.

Gostaria também de agradecer às minhas companheiras de “cave” ao longo destes anos e todos os alunos de mestrado que foram passando pelo grupo que sempre contribuíram para um bom ambiente de trabalho!

Filipa, Marta e Gisela, obrigada por toda simpatia e boa disposição. É muito reconfortante poder trabalhar num ambiente assim, onde partilhamos ideias e “mãos” e nos ajudamos mutuamente com um sorriso nos lábios.

Cláudia, obrigada pela tua simplicidade e amizade. Entrámos juntas neste mundo encantado da microglia e foi tão bom poder partilhá-lo contigo. És uma pessoa fantástica, com uma atitude sempre positiva por mais adversidades que apareçam e, por isso mesmo, és um exemplo. E parabéns também pela etapa recentemente conquistada! Tu mereces…

Inês, apesar de mais distantes nestes últimos tempos, queria também agradecer-te toda a amizade dentro e fora do CPM e o exemplo de organização e trabalho eficaz que me transmitiste desde o primeiro momento que te vi trabalhar.

Um agradecimento muito especial para ti, Andreia. A nossa amizade foi crescendo nos últimos anos e hoje és sem dúvida uma pessoa muito importante para mim. Obrigada por todas as palavras de incentivo, todas as brincadeiras, todas as conversas e todos os

momentos com esse pequeno que levantam o ânimo a qualquer um. A mim então… Muito obrigada ainda pela “mãozinha” nesta fase final! Sei que posso contar sempre contigo e portanto, vou abusar!

Sem dúvida uma das pessoas mais importantes neste meu percurso, tenho que agradecer muito à minha companheira de todas as horas, minha amiga, minha irmã… Cátia. Devo-te tanto! Não tenho palavras para agradecer tudo aquilo que fizeste e que és para mim… Para além da tua amizade e de todos os bons momentos que passamos fora dos deveres laborais, foi e é um prazer trabalhar contigo. Tens uma capacidade de trabalho, organização e responsabilidade incríveis e é excecional poder trabalhar com uma pessoa assim. Funcionamos tão bem como equipa que quase parece que estamos na cabeça uma da outra. Foi difícil não te ter cá nestes últimos tempos… Fizeste-me tanta falta! Muito obrigada pelo teu apoio, pelas tuas palavras de conforto, pelas tuas gargalhadas, pelas tentativas de sussurro que acabavam sempre em conversas de gmail, pelas horas de fluxo e por tantas outras coisas! Obrigada por tudo!

Gostava ainda de expressar o meu agradecimento às meninas de mestrado que tive oportunidade de acompanhar no laboratório, Maria Inês, Sara e Catarina. Obrigada pela confiança e por me mostrarem que fui importante para vocês e que contribui para o vosso trabalho. Sara, obrigada por todo o companheirismo e esforço nestes últimos meses, foi um prazer trabalhar contigo lado a lado. Catarina, as tuas palavras meigas e de admiração neste último ano encheram-me o coração. Obrigada!

Obrigada a todos os companheiros do CPM, pela simpatia e entreajuda e por criarem um ambiente tão alegre e agradável para trabalhar. Os corredores são testemunhas das gargalhadas e da boa disposição que se faz sentir.

Quero também agradecer aos meus amigos de sempre. Nada como chegar a casa cansada de um dia longo de trabalho e receber aquela mensagem da Rapaziada que me põe logo bem-disposta. É tão bom saber que estarão sempre lá. Um obrigado especial às minhas meninas, pela vossa amizade incondicional. Não há nada que eu possa dizer que vocês não tenham uma solução para mim. Sou uma pessoa mais feliz por vos ter por perto.

Embora não de sempre, mas que serão com certeza para sempre, não posso deixar de agradecer aos Vizinhos! Miguel e André (voltamos à dupla “pimba”) obrigada por me terem acolhido tão bem quando cheguei ao CPM. Passámos bons momentos enquanto “colegas do lado” mas tornámo-nos grandes amigos que agora partilham muito mais que o local de trabalho. Obrigada pelas jantaradas, pelos cafezinhos, pelo Padel e por ouvirem todas as minhas lamúrias. Obrigada por tudo meus amigos!

Não posso também deixar de agradecer a toda minha família por me fazerem sentir sempre protegida e amada.

Titi, madrinha e padrinho, obrigada pela vossa preocupação e por me fazerem sentir especial. Tio Tujó, Tia Sónia, Gui e Tita, obrigada por todo o carinho e por me receberem sempre de braços abertos. É tão bom sentir que vos tenho aqui ao meu lado para qualquer ocasião.

Filipe, um obrigado especial para ti que também já és um bocadinho meu. É difícil expressar em palavras o que tenho para te agradecer já que “viveste” estes meus últimos anos bem de perto. Obrigada pelo apoio e por nunca me deixares desanimar. Obrigada pela paciência e por me fazeres esquecer do mundo lá fora, ainda que por breves momentos. Obrigada pelas palavras duras que precisava de ouvir. Obrigada por todos os momentos que temos vivido. Obrigada por todo o amor. Obrigada por tudo.

Resta-me agradecer às pessoas mais importantes da minha vida, os meus pais e o meu irmão. Mãe e Pai, muito obrigada pelo vosso amor incondicional. Obrigada pela compreensão, pelo apoio, pela dedicação, pelo sacrifício e por fazerem tudo ao vosso alcance para me fazerem a pessoa mais feliz do mundo. E sou porque vos tenho! Tudo o que sou e tudo o que alcancei devo a vocês… Obrigada por me encherem o coração! Muito obrigada por tudo! Maninho, não é fácil que estejas tão longe de nós mas sinto-me muito feliz por ver tudo o que conseguiste alcançar e como te sentes tão realizado e feliz! Obrigada por teres tomado tão bem conta de mim e acredita que seguir o teu exemplo fez de mim uma pessoa melhor. Tenho muito orgulho em ti.

Index

Figure Index

Table Index

Publications

Papers directly related with the present thesis

1. Cunha C, Gomes C, Vaz AR, Brites D. Exploring new inflammatory pathways and biomarkers during LPS-induced M1 polarization. Mediators Inflamm. 2016; 2016:6986175.

2. Pinto S[§], **Cunha C**[§], Barbosa M, Vaz AR, Brites D. Exosomes from NSC-34 cells transfected with hSOD1-G93A are enriched in miR-124 and promote a specific microglia phenotype signature. Front Neurosci. 2017; 11:273. [§]equal contribution

3. Cunha C, Santos C, Gomes C, Fernandes A, Correia AM, Sebastião AM, Vaz AR, Brites D. Downregulated glia interplay and increased miRNA-155 as promising markers to track ALS at an early stage. Mol Neurobiol. 2017; doi: 10.1007/s12035-017-0631-2.

4. Cunha C, Gomes C, Vaz AR, Brites D. *SOD1*^{G93A} spinal microglia switch from pro-inflammatory to heterogeneous phenotypes with *in vitro* aging and cross-talk with paired reactive astrocytes (to be submitted).

Papers not directly related with the present thesis

5. Caldeira C, **Cunha C**, Vaz AR, Falcão AS, Barateiro A, Seixas E, Fernandes A, Brites D. Key aging-associated alterations in primary microglia response to beta-amyloid stimulation. Front Aging Neurosci. 2017; 9:277.

6. Vaz AR, **Cunha C**, Gomes C, Schmucki N, Barbosa M, Brites D. Glycoursodeoxycholic acid reduces matrix metalloproteinase-9 and caspase-9 activation in a cellular model of superoxide dismutase-1 neurodegeneration. Mol Neurobiol. 2015; 51(3):864-77.

7. Caldeira C, Oliveira AF, **Cunha C**, Vaz AR, Falcão AS, Fernandes A, Brites D. Microglia change from a reactive to an age-like phenotype with the time in culture. Front Cell Neurosci. 2014; 8:152.

Book Chapters

Vaz AR, Gomes C, **Cunha C**, Brites D. Astrocytes in Amyotrophic Lateral Sclerosis: Harmful effects and strategies to afford neuroprotection. in: New Developments in Astrocytes Research. Nova Science Publishers, Inc., New York, USA. 2016, 75-116. ISBN: 978-1-63485-584-6 (e-book).

Peer-reviewed abstracts published in international journals

1. Vaz AR, **Cunha C**, Gomes C, Brites D. Reactive astrocytes from the spinal cord of mSOD1 mice pups trigger microglia M1 polarization, while switch mSOD1 microglia into M1/M2 phenotypes that lately become irresponsive. 2017. GLIA 65:E153.

2. Brites D, Monteiro M, Ribeiro AR, **Cunha C**, Vaz AR, Fernandes A. Role of neuron-microglia secretome and stress-related microRNAS in Alzheimer's disease. 2017. GLIA 65:E301.

3. Fernandes A, Caldeira C, Falcão AS, **Cunha C**, Vaz AR, Brites D. Temporal gene expression profile related to microglia reactivity in 3xTgAD mice. 2015. GLIA 63:E367.

4. Cunha C, Vaz AR, Brites D. Exploring motor neuron signaling dynamics to microglia in ALS. 2013. GLIA 61:S106.

Abbreviations

7-AAD	7-amino-actinomycin-D
AAV9	Adeno-associated virus serotype 9
AD	Alzheimer's disease
ALDH1L1	Aldehyde dehydrogenase family 1
ALS	Amyotrophic lateral sclerosis
AMPA	Alpha-amino-3-hydroxy-5-methyl-4-isoxazole propionic acid
Ang	Angiogenin
APOE	Alipoprotein E
Arg1	Arginase 1
ASC	Adaptor apoptosis-associated speck-like protein containing a CARD
ATF-1	Activating transcription factor 1
Atgs	Autophagy-related proteins
ATP	Adenosine tri-phosphate
ATX	Autotaxin
Aβ	Amyloid-β
BBB	Blood-brain barrier
BCL-2	B-cell lymphoma 2
BDNF	Brain-derived neurotrophic factor
BSA	Bovine serum albumin
BSCB	Blood-spinal cord barrier
C/EBP	CCAAT/enhancer-binding protein
C9ORF72	Chromosome 9 open reading frame 72
CCL	C-C motif chemokine ligand
CCR	C-C motif chemokine receptor
CD	Cluster of differentiation 11b
cDNA	Complementary DNA
CNS	Central nervous system
COX2	Cyclo-oxigenase-2
CR1	Complement receptor type-1
CR3	Complement receptor type-3
CSF	Cerebrospinal fluid
CSF-1R	Colony stimulating factor-1 receptor

CX3CL1	C-X3-C motif chemokine ligand 1
CX3CR1	C-X3-C motif chemokine receptor 1
Cx43	Connexin-43
CXCL	C-X-C motif chemokine ligand
CXCR	C-X-C motif chemokine receptor
DAMPs	Danger-associated molecular patterns
DGCR8	DiGeorge syndrome critical region gene 8
DLS	Dynamic Light-Scattering
DMEM	Dulbecco's Modified Eagle's Medium
DMEM-F12	Dulbecco's Modified Eagle's Medium - Ham’s F12 Medium
DNA	Deoxyribonucleic acid
DPR	Dipeptide repeats
EAAT2	Excitatory amino acid transporter 2
EAE	Experimental autoimmune encephalomyelitis
EGA	Estimated gestational age
EGF	Endothelial growth factor
EMA	European medical agency
EPSCs	Excitatory postsynaptic currents
ER	Endoplasmic reticulum
ERK	Extracellular signal-regulated kinase
ESCRT	Endosomal sorting complexes required for transport
EVs	Extracellular vesicles
FACS	Fluorescent-activated cell sorting
fALS	Familial ALS
FasL	Fas ligand
FBS	Fetal bovine serum
FDA	Food and Drug Administration
FIZZ1	Found in inflammatory zone 1
FTD	Frontotemporal dementia
FUS	Fused in sarcoma
G93A	Glycine to alanine point mutation at residue 93
GABA	Gamma amino butyric acid
Gas6	Growth-arrest specific factor-6
GDNF	Glial-cell derived neurotrophic factor
GFAP	Glial fibrillary acidic protein

GLT-1	Glutamate transporter 1
GluR2	Glutamate receptor 2
GM-CSF	Granulocyte macrophage colony-stimulating factor
H&E	Hematoxylin–eosin
HIV	Human immunodeficiency virus
HMGB1	High mobility group box 1
hnRNPA2B1	Heterogeneous nuclear ribonucleoprotein A2B1
Hsp	Heat-shock proteins
Iba1	Ionized calcium-binding adaptor molecule 1
IFN	Interferon
IFNRs	IFN receptors
IGF-1	Insulin growth factor 1
IL	Interleukin
IL1R	IL-1 receptor
ILVs	Intraluminal vesicles
iNOS	Inducible nitric oxide synthase
IP_3	Inositol triphosphate
iPSCs	Induced pluripotent stem cells
IRAK	Interleukin-1 receptor associated kinase
IRF8	Interferon regulatory factor 8
JAK	Cytokine-activated Janus kinase
LC3	Light chain 3
LMN	Lower motor neurons
LPS	Lipopolysaccharide
LTP	Long-term potentiation
MBP	Myelin basic protein
MCP-1	Monocyte chemoattractant protein 1
MEK	Mitogen-activated protein kinase
MERTK	MER receptor tyrosine kinase
MFG-E8	Milk fat globule-EGF 8
MHC-II	Major histocompatibility complex class II
miRNAs	MicroRNAs
MLKL	Mixed lineage kinase domain-like protein
MMP	Matrix metalloproteinase
MN	Motor neuron

MND	Motor neuron disease
MRI	Magnetic resonance imaging
mRNAs	Messenger RNAs
MS	Multiple sclerosis
MSC	Mesenchymal stem cells
mSOD1	Mutant SOD1
MVBs	Multivesicular bodies
NADPH	Nicotinamide adenine dinucleotide phosphate hydrogen
NF	Neurofilament
NFL	Neurofilament light chain
NF-κB	Nuclear factor-kappa B
NGS	RNA NextGen sequencing
NLRP3	NLR pyrin domain containing 3
NLRs	NOD-like receptors
NMDA	N-methyl-D-aspartate
NO	Nitric oxide
NO_2	Nitrites
NOD	Nucleotide binding and oligomerization domain
NOX2	NADPH oxidase 2
NSC	Neural stem cells
OPC	Oligodendrocyte progenitor cells
Optn	Optineurin
OSC	Organotypic slice cultures
PAMPs	Pathogen- associated molecular patterns
Panx1	Pannexin-1
PBS	Phosphate buffered saline
PD	Parkinson’s disease
PDCD4	Programmed cell death 4
PET	Positron emission tomography
PGE_2	Prostaglandin E2
PI3K	Phosphoinositide 3-kinase
PMSF	Phenylmethylsulfonyl fluoride
pNFH	Phosphorylated neurofilament heavy chain
PNI	Peripheral nerve injury
PPARγ	Peroxisome proliferator activated receptor γ

PPRs	Pattern-recognition receptors
PS	Phosphatidylserine
PTEN	Phosphatase and tensin homolog
qRT-PCR	Quantitative reverse transcriptase polymerase chain reaction
RAGE	Receptor for advanced glycation end products
RAN	Repeat-associated non-ATG
RIP1	Receptor-interacting serine/threonine-protein kinase 1
RISC	RNA-induced silencing complex
RNA	Ribonucleic Acid
ROS	Reactive oxygen species
RPMI	Roswell Park Memorial Institute
RT	Room temperature
sALS	Sporadic ALS
SC	Spinal cord
SDS-PAGE	Sodium dodecyl sulfate-polyacrylamide gel electrophoresis
SIGLEC	Sialic acid-binding immunoglobulin-like lectin
SIRPα	Signal regulatory protein alpha
SMA	Spinal muscular atrophy
SOCS1	Suppressor of cytokine signaling 1
SOD1	Copper-zinc superoxide dismutase 1
STAT	Signal transducer and activator of transcription
SVZ	Subventricular zone
TDP-43	TAR-DNA binding protein 43
TGF-β	Transforming growth factor-beta
TIM4	T-cell immunoglobulin mucin 4
TLR	Toll-like receptor
TNFR	TNF receptor
TNF-α	Tumor necrosis factor-alpha
TRAF6	TNF receptor associated factor 6
TREM2	Triggering receptor expressed on myeloid cells 2
UDP	Uridine 5'-diphosphate
UMN	Upper motor neurons
UTR	Untranslated region
VEGF	Vascular endothelial growth factor
VNR	Vitronectin receptors

V-PE	Phycoerythrin-conjugated annexin V
WB	Western blot
WT	Wild type

Abstract

Amyotrophic lateral sclerosis (ALS) is a motor neuron (MN) disease comprehending critical neuroinflammatory pathways, where microglia and astrocytes play a crucial role. ALS onset events are largely unknown and identification of disease steps during progression and dissemination, including the possible role of exosomes, are not clarified.

Several models were used to improve data validity and deepen knowledge in ALS. We identified innovative targets to regulate microglia M1 polarization, including NLRP3-inflammasome, HMGB1 alarmin and MFG-E8/lactadherin, and demonstrated the sorting of microglial microRNA(miR)-155/miR-146a into exosomes. We showed that ALS NSC-34 MNs and their exosomes are enriched in miR-124, which are captured and drive early N9-microglia M1 polarization, with later development of M1/M2 subpopulations containing increased miR-124/miR-146a/miR-155. Moving from *in vitro* models to the spinal cord of the *SOD1*^{G93A} ALS mouse model, we observed that depressed intercellular communication and increased miR-155 were early disease events preceding the inflammatory status of the symptomatic stage. Upregulated CX3CL1-CX3CR1, connexin-43/pannexin-1 and miR-124/miR-125b/miR-146a/miR-21 emerged as candidate targets for pathological neuroinflammation. Reduced MN number, together with aberrant/reactive astrocytes showing deficient glutamate transporters and GFAP, additionally characterized such state. Differently deregulated profiles of microglia isolated from the spinal cord of 7-day old *SOD1*^{G93A} mice, after short- and long-term cultures, highlighted that cells present transient phenotypes accordingly to ALS environmental progression-stimuli and ultimately acquire a less responsive phenotype to stimulation. Astrocytes isolated from these mice promoted diverse inflammatory polarized subtypes in wild-type and ALS microglia, thus accounting to microglia heterogeneous populations, while strengthened deregulated microglia-astrocyte cross-talk as part of ALS neurodegenerative mechanisms.

Our studies in ALS models reveal early promising biomarkers and novel targets to control excessive neuroinflammation and spread, including exosomal microRNAs. Due to multiple microglia phenotypes induced by MNs and their exosomes, and by reactive astrocytes, in the ALS disease, differentiated and combined therapeutic approaches may be recommended.

Keywords: Microglia subpopulations; Inflamma-miRs; Neuron-Glia interplay & Exosome trafficking; ALS biomarkers; SOD1G93A-experimental models

Resumo

A Esclerose Lateral Amiotrófica (ELA) é a terceira doença neurodegenerativa mais comum, caracterizada pela disfunção e morte dos neurónios motores superiores e inferiores do córtex motor, do tronco cerebral e da medula espinhal, com uma forte componente neuro-inflamatória. Os doentes com ELA sofrem de fraqueza e atrofia muscular progressiva e acabam por falecer por falência respiratória cerca de 3-5 anos após o aparecimento dos primeiros sintomas. Embora a maioria dos casos de ELA seja de etiologia desconhecida (esporádicos) diferentes mutações ocorrem em cerca de 10% dos doentes com a ELA familiar. Mutações na proteína superóxido dismutase 1 (SOD1) representam 20% dos casos familiares e 2% dos esporádicos, constituindo a base dos modelos de estudo da ELA. A doença é ainda incurável. De facto, o riluzole (que previne a excitotoxicidade do glutamato), aprovado pela *Food and Drug Administration* (FDA), apenas prolonga a vida dos doentes em alguns meses. Daí a procura de novas soluções terapêuticas, tanto mais que o edaravone (com ação anti-oxidante), recentemente aprovado pela FDA, para além de efeitos secundários marcados, é de eficácia discutível. Para além de não haver medicamentos que melhorem os sintomas ou atrasem a progressão da doença, o diagnóstico definitivo da ELA pode ser demorado (cerca de 11 meses), em grande parte por não haver biomarcadores precoces. A principal causa destas problemáticas reside no desconhecimento das causas subjacentes à doença.

Tal como noutras doenças neurodegenerativas, os agregados e inclusões de proteínas com enrolamento incorreto constituem características neuropatológicas da ELA. Apesar da toxicidade direta destes agregados não estar esclarecida, associa-se à doença muitos outros fatores, como: disfunção da mitocôndria, stresse oxidativo, excitotoxicidade mediada pelo glutamato e alterações no metabolismo do ácido ribonucleico (RNA). A neuroinflamação e a gliose assumem também grande relevância na patologia da ELA e amostras de autópsias de doentes com ELA evidenciam ativação da microglia, as células imunes do sistema nervoso central. Modelos animais demonstraram que estas células, juntamente com os astrócitos, possuem um fenótipo reativo e pro-inflamatório e contribuem para a morte dos neurónios motores. No entanto, os mecanismos de sinalização que despoletam a ativação das células gliais e a libertação de fatores neurotóxicos não são totalmente conhecidos. Mais ainda, sendo que a maior parte dos estudos são focados na fase sintomática da doença, muito pouco se sabe sobre os mecanismos patofisiológicos que precedem o aparecimento dos sintomas. Recentemente, tem-se explorado o papel dos exossomas na transmissão de proteínas/RNAs célula-a-célula. Apesar de se saber que os exossomas neuronais transportam proteínas com enrolamento incorreto para outras células,

incluindo a própria SOD1, disseminando a doença, muito pouco se sabe sobre o seu envolvimento na propagação da resposta inflamatória, e quase nada na patologia da ELA.

O trabalho experimental desenvolvido nesta tese focou-se, entre outros, no papel dos exossomas e dos microRNAs (miRNAs) associados à inflamação em modelos diversos de ELA, com o objetivo de:

(i) Caracterizar as vias de sinalização envolvidas na polarização da microglia de um estado vigilante para um fenótipo pro-inflamatório M1, usando a linha celular microglial N9 e estimulação com lipopolissacarídeo (LPS) (Capítulo II), para esclarecer, mais tarde, os mecanismos de ativação destas células transfetadas com a proteína SOD1 com a mutação G93A (*SOD1^{G93A}*), (tal como proposto no Capítulo VII);

(ii) Identificar os processos de ativação/desativação da microglia N9 na presença de exossomas libertados por neurónios motores, usando a linha celular NSC-34 transfetada para expressar *SOD1^{G93A}* (NSC-34/*SOD1^{G93A}*) (Capítulo III);

(iii) Analisar os fatores inflamatórios envolvidos na reatividade dos astrócitos/microglia, bem como e na desregulação da comunicação intercelular, usando a medula espinhal de murganhos *SOD1^{G93A},* quer na fase pré-sintomática, quer na sintomática, para identificar alvos terapêuticos específicos e biomarcadores de cada fase (Capítulo IV);

(iv) Contribuir para o esclarecimento dos processos de ativação/desativação microglial na medula espinhal de murganhos *SOD1^{G93A},* com sete dias de vida, considerando o tempo em cultura (curto ou prolongado) e a ação de astrócitos *SOD1^{G93A}* reativos obtidos do mesmo modelo (Capítulo V).

Os resultados obtidos no **Capítulo II** respeitam à polarização da microglia N9 para o fenótipo M1, identificado em doenças neurodegenerativas como a ELA, por estimulação com LPS. Nesta condição a microglia sobre-expressa marcadores característicos do fenótipo M1, adquire uma morfologia amebóide, prolifera e perde a capacidade de migrar para o quimioatrator ATP. Encontram-se ativadas as vias de sinalização dependentes do recetor tipo *toll 4* (TLR4), do fator nuclear-kappa B (NF-κB) e ainda do inflamassoma *NOD-like receptor pyrin domain containing 3* (NLRP3), havendo libertação da metaloproteinase 9 (MMP-9) e da alarmina *high mobility group box 1* (HMGB1). A microglia polarizada em M1 revelou maior capacidade fagocítica e aumento da produção e libertação do fator *milk fat globule-EGF factor 8* (MFG-E8). De assinalar, os resultados pioneiros demonstrando que a microglia N9 tratada com LPS tem expressão elevada de miRNA (miR)-155/miR-146a e diminuída de miR-124, perfil esse que mostrou ser reproduzido nos exossomas por ela libertados.

No **Capítulo III**, demonstrámos que os exossomas provenientes dos neurónios motores NSC-34/*SOD1*^{G93A} recapitulavam a sobre-expressão do miR-124 igualmente observado nas células e que eram preferencialmente captados pelas células da microglia N9, induzindo diversos fenótipos microgliais. O primeiro contacto da microglia com os exossomas manifesta-se na indução de um fenótipo M1 que progride para a existência de várias subclasses de microglia às 24 h, como sejam os subtipos M1, M2 e uma população com características de células senescentes. Esta heterogeneidade de fenótipos é também suportada pelo aumento simultâneo de miR-155, miR-146a e miR-124, este último bastante elevado sugerindo que possa ter sido transportado dos neurónios motores para a microglia pelos exossomas. A ativação do NF-κB e a diminuição da capacidade fagocítica da microglia foram observados em todas as condições experimentais, demonstrando serem mecanismos importantes na resposta da microglia N9 aos exossomas das células NSC-34/*SOD1*^{G93A}. Deste modo, este estudo indica que a transferência de exossomas entre os neurónios motores e a microglia pode constituir uma forma de propagação da doença e de sinalização da disfunção neuronal para células recetoras dos exossomas, ao mesmo tempo que destaca o miR-124 como um alvo a ser modulado.

No **Capítulo IV**, determinámos marcadores inflamatórios na medula espinhal do murganho transgénico *SOD1*^{G93A}, tanto na fase pré-sintomática (4-6 semanas de vida), como sintomática (12-14 semanas de vida) da doença. Observámos que na fase pré-sintomática, havia sub-expressão de proteína glial fibrilar ácida (GFAP), de S100B, de citocinas inflamatórias e de marcadores do fenótipo M2 microglial, a qual foi já considerada noutras situações como uma tentativa de travar o dano na fase precoce da doença neurodegenerativa. Na fase sintomática, pelo contrário, verificou-se existir uma elevação de um grande grupo de marcadores de inflamação, incluindo os inflama-miRNAs. Diferentes fenótipos da microglia coexistiam nesta fase, embora o M1 fosse prevalente. A elevação de S100B e de conexina-43, juntamente com diminuição dos transportadores de glutamato, foram consideradas como devidas ao fenótipo reativo dos astrócitos. Dada a consistência do aumento de miR-155 e diminuição de MFG-E8 em ambas as fases estudadas, estas moléculas surgem como biomarcadores da ELA, para além de potenciais alvos terapêuticos. Nestes incluímos também o inflamassoma NLRP3, o HMGB1, o miR-125b, o eixo recetor/quimiocina motivo C-X3-C (CX3CR1/CX3CL1), a conexina-43 e a panexina-1.

Por fim, no **Capítulo V**, demonstrámos que as células da microglia, obtidas da medula espinhal de murganhos *SOD1*^{G93A} com 7 dias, apresentam diferentes estadios de ativação, consoante o tempo em cultura. Se mantidas por um período curto, apresentam um fenótipo M1, semelhante ao encontrado na fase sintomática do ratinho *SOD1*^{G93A}. Contudo, transitam para uma mistura de fenótipos e adquirem características disfuncionais quando mantidas mais tempo em cultura, à imagem do indicado para as fases finais da doença, com perca da

capacidade de resposta a estímulos e com fenótipos que não são nem M1, nem M2. Os astrócitos dos mesmos animais confirmaram o seu fenótipo reativo e aberrante ao manifestarem aumento de S100B, bem como diminuição de GFAP e do transportador do glutamato 1 (GLT-1). Quando em co-cultura com a microglia induzem um fenótipo pro-inflamatório na microglia WT e levam a fenótipos heterogéneos na microglia *SOD1*^{G93A}, onde se incluem as polarizações M1 e M2. Curiosamente, a comunicação entre astrócitos e microglia *SOD1*^{G93A} mostrou ser essencial para haver sobre-expressão do inflamassoma NLRP3 e libertação do HMGB1.

Em suma, os resultados alcançados nesta tese esclarecem as alterações da homeostasia antes do aparecimento dos sintomas associados à ELA e os componentes inflamatórios da fase sintomática. A microglia mostrou transitar de um estadio inicial "imuno-suprimido", para uma polarização M1 e depois para fenótipos heterogéneos e até disfuncionais. Os astrócitos com um fenótipo reativo e aberrante mostraram causar alterações do fenótipo e das vias inflamatórias na microglia, como também aconteceu através dos exossomas libertados de neurónios motores. O trabalho realizado selecionou novos alvos terapêuticos para a descoberta de fármacos para a ELA e identificou o miR-155 e o MFG-E8 como biomarcadores precoces da doença. Tendo em conta os diversos mecanismos observados e a heterogeneidade fenotípica da microglia no decurso da doença, acreditamos que a estratégia terapêutica deve considerar o uso combinado de medicamentos dirigidos a vários alvos e ter em conta características específicas de cada estadio da doença.

Palavras-chave: Subpopulações microgliais; MicroRNAs inflamatórios; Comunicação Neuro-Glial & Tráfego mediado por exossomas; Biomarcadores da ELA; Modelos experimentais com mutação SOD1G93A

Chapter I

GENERAL INTRODUCTION

1. Microglial physiology in the CNS: phenotypes, drivers, and activation

Microglia are the typical immune cells within the central nervous system (CNS) and were first described by Pio del Rio Hortega in 1932. These non-neuronal cells exhibit a small cell soma with highly branched processes (Kettenmann et al. 2011), accounting for 5-20% of total glial cells (Arcuri et al. 2017; Vilhardt 2005). They populate CNS parenchyma throughout both white and gray matter (Kabba et al. 2017), although environment specificities underlie microglia region heterogeneity. As a unique non neuronal population, microglia belong to the mesodermal lineage that enter the brain during embryonic development (Ginhoux and Prinz 2015).

The way we envision microglia functionality nowadays overlap with the first observations of del Rio Hortega. Microglia are constantly monitoring their microenvironment and each specific cell only screens its confined space (Kettenmann et al. 2011). Through the ability to recognize a wide variety of signals, microglia are extremely sensitive to tissue disturbances and can change their morphology, as well as the expression profile and functional behavior upon stimulation, acquiring an activated phenotype (Colton 2009; Obst et al. 2017). Once activated, microglia initiate an inflammatory reaction in order to eliminate and contain the damage restoring tissue homeostasis. However, when facing an intense or chronic stimulus, microglia continuous production of inflammatory mediators can cause neuronal damage, leading to a neuroinflammatory environment with a feed-forward loop progression. Indeed, microglia-mediated neuroinflammation has been associated with different neurodegenerative conditions including Alzheimer's disease (AD), Parkinson's' disease (PD) and amyotrophic lateral sclerosis (ALS).

Despite being the first line of defense against pathogenic organisms, and the sensors of CNS homeostasis (Nimmerjahn et al. 2005), accumulating evidence indicate their crucial role for CNS physiology and development, as well as for neuronal circuitry formation and maintenance.

1.1. Microglia origin and CNS distribution

In his first publications, del Rio Hortega already suggested that microglial cells would be originated from the mesoderm and that they enter the developing brain with an amoeboid morphology. At that time, other authors also believed that microglia developed from the neuroepithelium like the other CNS cells. However, due to morphological and biochemical similarities between microglia, monocytes and macrophage populations, soon the scientific community accepted their myeloid origin (Arcuri et al. 2017; Ginhoux and Prinz 2015).

While in the following years it was believed that circulating monocytes entered the brain and differentiated into microglial cells whenever needed, increasing evidence showed that, in fact, microglia was originated from myeloid progenitors localized in the embryonic yolk sac, which is now established. These cells migrate to the brain rudiment around embryonic day 8.5-9 (E8.5-9), initially by interstitial migration and later via the circulatory system (Nayak et al. 2014), and the adult microglia population proliferates and differentiates from the initial embryonic progenitors (Alliot et al. 1999; Ginhoux et al. 2010) through the ability to self-renew (Perdiguero et al. 2015). Globally, three developmental stages that occur in synchrony with brain development under distinct regulatory circuits were recently indicated (Matcovitch-Natan et al. 2016): an early stage (E10.5 to E14), pre-microglia (E14 to postnatal day 9) and adult microglia (4 weeks and onwards). In the spinal cord, the microglial complex morphology characterized by several extensions and ramifications was indicated to take place at E15.5 (Rigato et al. 2011). Importantly, the expression of colony stimulating factor-1 receptor (CSF-1R) is essential to determine the embryonic fate of microglia (Ginhoux et al. 2010) and microglia development is also dependent on the transcription factors PU.1 and interferon regulatory factor 8 (IRF8) (Kierdorf et al. 2013).

In humans, embryonic hematopoiesis starts around day 19 of estimated gestational age (EGA) in the yolk sac, where cells are committed to the erythro-myeloid lineage (Brites et al. 2015). Then, this process moves to the liver at 4-5 weeks of EGA, and finally to the bone-marrow (10.5 weeks), where it remains until adulthood. The fact that microglial-like cells are observed in the fetuses' brain at 3 weeks of EGA underlines their yolk-sac derivation (Hutchins et al. 1990). In the spinal cord, microglia first appear at 9 weeks of EGA. Microglia distribution and differentiation continue until they became well-differentiated ramified cells around 35 weeks (Ginhoux et al. 2013).

In the first two postnatal weeks, mouse microglia proliferate at higher rates and distributes across the entire CNS regions, where they acquire their typical ramified shape. The specific CNS region determines imbalance in microglial numbers and morphology (Tambuyzer et al. 2009). Higher microglia density was found in grey *vs.* white matter, namely in hippocampus, olfactory telencephalon, basal ganglia and substancia nigra. Whereas ramified microglia are mostly located at the neuropil, longitudinal branched cells are aligned with axons of nerve fibers tracts (Lawson et al. 1990). More recently, it was reported that microglia density did not change between mouse cortex and spinal cord (Zhang et al. 2008); however, independent studies showed that microglia are less numerous in the spinal cord (Li et al. 2016b; Nikodemova et al. 2014). Data are missing regarding the distribution of microglia in the normal human adult CNS, as the majority of studies have been performed in pathological conditions. Immunostaining of brain samples from non-neurological associated damage showed that microglia numbers vary across brain regions in a 10-fold variation

(Mittelbronn et al. 2001; Olah et al. 2011) but, contrary to rodents, white matter is more populated than the grey matter. Interestingly, even within a specific region, microglial cells can have different phenotypes (Olah et al. 2011).

1.2. Microglial markers: classical and new perspectives

As descendents of myeloid precursor, microglia express specific macrophage markers that have been recognized for years (Kettenmann et al. 2011). These markers include F4/80, cluster of differentiation 11b (CD11b), ionized calcium-binding adaptor molecule 1 (Iba1) and C-X3-C chemokine receptor 1 (CX3CR1). CD39 and CD163 have also emerged as novel microglial markers (Butovsky et al. 2015; David and Kroner 2011). Within the brain, however, the discrimination between microglia and perivascular macrophages has been difficult, creating some uncertainty in microglial functions *in vivo*. Until recently, the low expression of CD45 in microglia was the segregation point as macrophages expressed high levels of this marker (Ginhoux and Prinz 2015). Nonetheless, novel transcriptome-based studies, reviewed in Sousa et al. (2017), have uncovered new specific transcripts that allow to distinguish microglia from other myeloid cells as well as other CNS cells, both in mice (Butovsky et al. 2014; Hickman et al. 2013; Zhang et al. 2014) and humans (Butovsky et al. 2014; Galatro et al. 2017). These markers are summarized in Table I.1.

Table I.1 - Microglia unique or enriched markers compared to other macrophages or CNS cells

Classical microglial markers		**Novel transcriptome signatures**		
Rodents	**Humans**	**Rodents**		**Humans**
CD11b	CD14	*Camp*	*S100a9*	*Aif1 (Iba1)*
CD39	CD16	*Ccr5*	*Sall1*	*Axl*
CD163	CD32	*Cd53*	*Selplg*	*Csfr1*
CX3CR1	CD40	*Crybb1*	*Siglech*	*Cx3cr1*
Iba1	CD68	*Csf1r*	*Smad7*	*C1qa*
F4/80	CD163	*Cx3cr1*	*Socs3*	*Itgam (Cd11b)*
$CD45^{low}$	CD45	*Fcrls*	*Rnase4*	*Gas6*
	ITGAM (CD11b)	*Gpr34*	*Tgfb1*	*Gpr34*
	HLA-DR	*Gpr84*	*Trfbr1*	*Mertk*
		Xexb	*Tmem119*	*P2ry12*
		Itgb5	*Trem2*	*Pros1*
		Ly86	*Tyrobp*	*Spi1 (PU.1)*
		Olfml3	miR-342-3p	*Tmem119*
		P2ry12	miR-99a	*Trem2*
		P2ry13	miR-125b-5p	*Tyrobp*
		PU.1		
		S100a8		

CD, cluster of differentiation; **HLA-DR**, human leucocyte antigen-D; **ITGAM**, integrin subunit alpha M.

Importantly, although rodent and human microglia functionality differs in certain aspects (Wolf et al. 2017), there are evidences of close gene signatures between them. Interestingly,

a data base was recently created where transcriptomes of glial cells, including microglia can be found (Holtman et al. 2015). As it will be addressed later, microglia transcriptome also changes throughout brain regions.

1.3. Microglial function in CNS homeostasis

During development, primitive macrophage amoeboid morphology underlies one of the most important microglial specialized functions: phagocytosis. Indeed, accumulating evidences indicate that microglia actively contribute to normal neuronal maturation and CNS development [for review see Mosser et al. (2017)]. Actually, microglia are responsible for the elimination of neuronal and glial cells, as almost 50% of these newly formed cells are eliminated in the developing CNS (Wolf et al. 2017), as well as by synaptic pruning during postnatal development (Paolicelli et al. 2011). Among other functions, microglia are also able to exert trophic actions in developing postnatal neurons (Ueno et al. 2013) and to promote neurogenesis in neural stem cells (NSC) from the subventricular zone (SVZ) (Walton et al. 2006). Interestingly, microglia was shown to equally exert a compensatory self-repairing mechanism associated with their pro-neurogenic role in chronic neurodegeneration (De Lucia et al. 2016). In humans, the regional distribution of microglia in the embryonic and fetal period strongly correlates to their role in synaptic pruning and clearance of neuronal debris (Monier et al. 2007). Human microglia is also able to promote NSC proliferation and survival *in vitro* (Liu et al. 2013a).

In 2005, two important reports changed the view of microglia latency under physiological conditions, the so called “resting” or “quiescent” phenotype. Microglia is in fact constantly moving their highly branched cellular ramifications making contact with all the surfaces that lie within their environment. These studies used *in vivo* two-photon microscopy in transgenic mice expressing enhanced green fluorescent protein (GFP) in *Cx3cr1* locus and showed that microglia processes were remarkably motile, continuously undergoing extension, withdrawal and cycles of *de novo* formation (Davalos et al. 2005; Nimmerjahn et al. 2005). Moreover, Nimmerjahn and colleagues (2005) also demonstrated that the brain parenchyma is completely screened by microglia once every few hours. Besides this highly dynamic surveillance, microglia also biochemically sense and interpret their environment. Through a variety of surface receptors, such as receptors for cytokines or chemokines, receptors for complement fragments, immunoglobulins, adhesion molecules and inflammatory stimuli, microglia can sense subtle changes (Nimmerjahn et al. 2005), being able to quickly respond to any insult to CNS homeostasis.

Several lines of evidence have indicated that microglia play a role in synaptic plasticity in the adult CNS, which give rise to the concept of “quad-partite” synapse (Schafer et al. 2013).

During parenchyma monitoring, microglia establish direct contact with neuronal synapses, with both axon terminals and dendritic spines (Wu et al. 2015b). These interactions usually occur for 5 min, once per hour, but variations in neuronal activity positively correlate with microglia synapse scavenging (Tremblay et al. 2010; Wake et al. 2009). Additionally, small dendritic spines can be eliminated by microglia, highlighting their function in synaptic shaping (Tremblay et al. 2010). *In vitro*, microglia conditioned media is able to induce long N-methyl-D-aspartate (NMDA) receptor mediated excitatory postsynaptic currents (EPSCs) in cortical slice cultures and long-term potentiation (LTP) in hippocampal neurons (Schafer et al. 2013), further indicating microglia active contribution to neuronal activity and synaptic transmission.

Finally, microglia can also exert trophic effects in neurons promoting growth, differentiation and circuitry formation by releasing a set of neurotrophic factors including neurothrophins, brain-derived neurotrophic factor (BDNF), glial-cell derived neurotrophic factor (GDNF), and insulin growth factor 1 (IGF-1), among others (Kettenmann et al. 2011; Kim and de Vellis 2005).

Importantly, the surveying state of microglia is maintained through intimate interactions with their CNS neighbors, especially neurons. The factors involved in microglia-neuron cross-talk will be addressed later in this Chapter.

1.4. Defining microglia activation: from neuroprotection to neurodegeneration

Any disturbance on CNS physiology, either by the sudden presence or abnormal concentration of a given factor, or even any disruption in environment inhibitory signals, can activate microglia. Of notice, the term “activation” does not mean that they were latent or resting (discussed above), but rather indicate a shift between states, as previously suggested (Hanisch and Kettenmann 2007). Microglia activation is an adaptive process specific for each stimulus and CNS region, and can lead to neuroprotective or neurotoxic outcomes. As it will be detailed in the following sections, microglia activation includes change of morphology and functional behavior, as well as alteration of the transcriptional program and production of inflammatory mediators (Kettenmann et al. 2011).

1.4.1. Morphology

Transformation of microglia morphology, from the surveillant ramified shape to an amoeboid morphology, has been used for long as the first indicator of microglia activation (Kreutzberg 1996; Tambuyzer et al. 2009). The overall shape transition includes retraction of processes and reduced morphological complexity (Kettenmann et al. 2011). Different morphologies and denominations have been proposed, including bipolar or rod-shape, bushy, primed, hypertrophic, amoeboid and dystrophic (Au and Ma 2017; Streit et al. 2004;

Torres-Platas et al. 2014; Zhang et al. 2008). While these shapes where recently observed in normal mouse and adult human brains (Torres-Platas et al. 2014), the loss of ramified morphology has been mostly associated with pathological conditions. The specific role of each morphology is, however, largely unknown. Some studies indicate that amoeboid microglia is acquired upon lipopolysaccharide (LPS) challenge (Papageorgiou et al. 2016), an endotoxin present in Gram-negative bacteria's membranes. Such morphology was found in AD and PD human samples (Doorn et al. 2013), as well as in mouse models of traumatic brain injury (TBI) (Loane and Kumar 2016) and ischemic stroke (Morrison and Filosa 2013). As recently reviewed, bipolar/rod-shape microglia seems to be associated with early neurodegenerative processes encompassing neuroprotective functions (Au and Ma 2017). Dystrophic morphology is characterized by disintegration of the cytoplasm, a process called cytorrhexis, accompanied by fragmentation of processes and loss of fine branches. Such degeneration was observed in human aged microglia (Streit et al. 2004), and described to be important in age-related disorders, such as AD (Brites 2015; Mosher and Wyss-Coray 2014).

1.4.2. Migration, phagocytosis and autophagy

Under physiological conditions, microglia is constantly screening their microenvironment, a process designated as motility (Davalos et al. 2005; Nimmerjahn et al. 2005). Upon injury, microglia rapidly extend their multiple processes towards the affected area without translocation of cell body. Microglia in surrounding areas can also be recruited and migrate towards the lesion site (chemotaxis). Both motility and chemotaxis are orchestrated by multiple chemotatic compounds, as indicated in Figure I.1. These include chemokines, such as C-C motif chemokine ligand 2 (CCL2) [also known as monocyte chemoattractant protein 1 (MCP-1)] and fractalkine [or C-X3-C chemokine ligand 1 (CX3CL1)], and ATP, among others (Calvo and Bennett 2011; Davalos et al. 2005; Madry and Attwell 2015), that can be released by neuronal and non-neuronal cells. Several studies have tried to discover the pathways underlying microglia migration ability that culminate with actin reorganization and polymerization (Fan et al. 2017). ATP-mediated microglial chemotaxis requires activation of $P2Y_{12}$ (Haynes et al. 2006) and $P2X_4$, with downstream activation of phosphoinositide 3-kinase (PI3K) pathway (Ohsawa et al. 2007; Ohsawa et al. 2010), and involves Ca^{2+} signaling (Lim et al. 2017). Interestingly, in acute spinal cord injury (SCI), nitric oxide (NO) mediates microglia migration to the lesion site, a process also mediated by ATP *in vivo* (Dibaj et al. 2010). It was recently showed that CCL2 induces migration of BV2 microglial cells through activation of *c*-jun and activating transcription factor 1 (ATF-1), probably following mitogen-activated protein kinase/extracellular signal-regulated kinase (MEK/ERK) and PI3K signaling pathways (Bose et al. 2016). Moreover, novel players are being discovered, such

as triggering receptor expressed on myeloid cells 2 (TREM2), as indicated by reduced chemotaxis of *Trem2*$^{-/-}$ microglia (Mazaheri et al. 2017). Importantly, once in the damaged area, microglia become activated, acquire an amoeboid effector shape and lose their chemotactic ability (Orr et al. 2009).

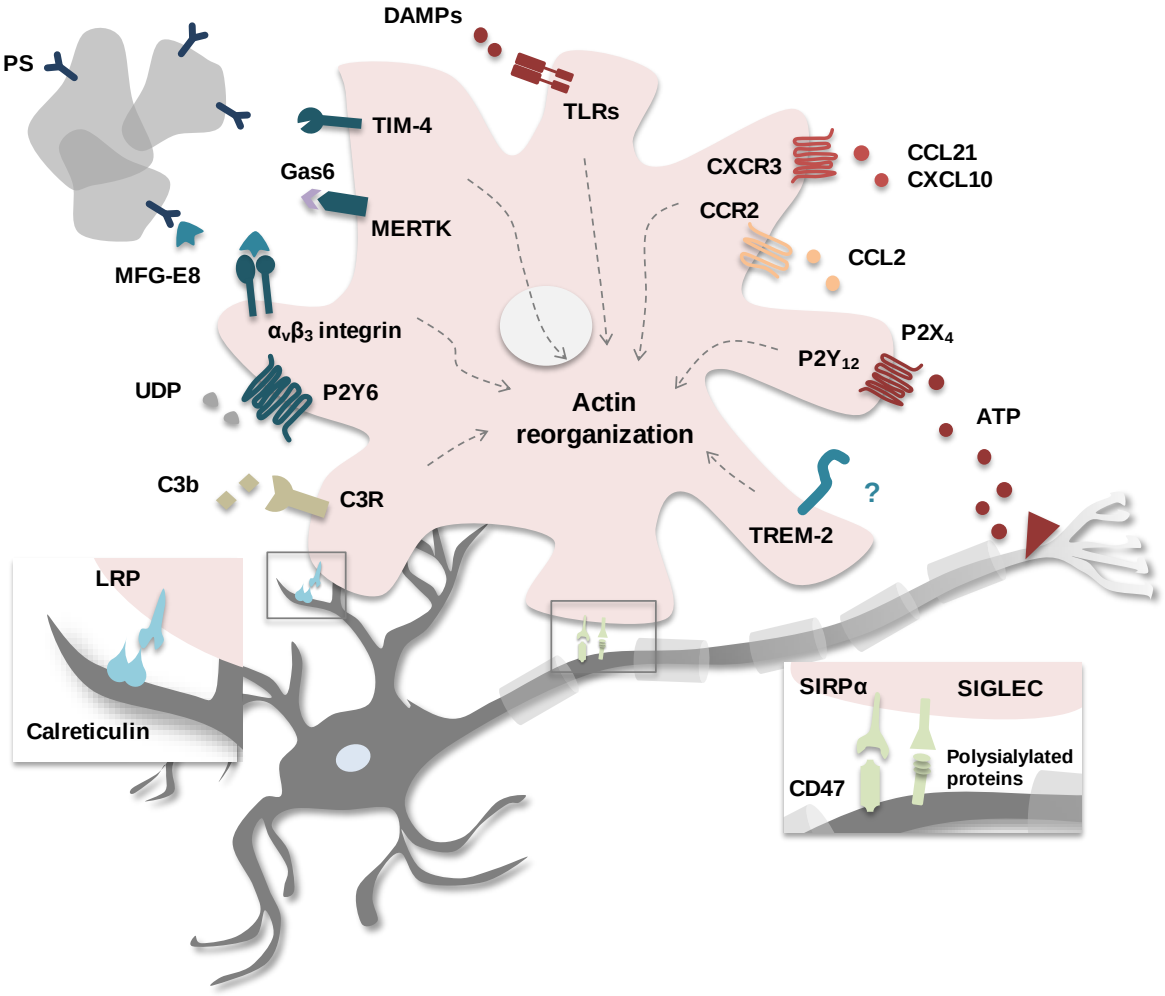

Figure I.1 - Microglial phagocytosis and migration are regulated by a number of specific ligand-receptor interactions. PS exposed at the surface of damaged neurons or neuronal debris can be recognized by several microglial receptors as an "eat-me" signal inducing microglia phagocytosis. These receptors include TIM4, MERTK/Gas6 complex and the adaptor molecule MFG-E8, which can be released and establish a bridge between PS and $\alpha_v\beta_3$ integrin. Calreticulin is another "eat-me" signal that is recognized by LRP. Other ligand-receptor pairs involved in phagocytosis include UDP leaking from injured and C3b that opsonizes neurons by binding de-sialylated glicoproteins, which can be recognized by $P2Y_6$ receptors and C3R, respectively. Whereas these interactions induce phagocytosis without pro-inflammatory responses, recognition of DAMPs by TLRs promotes the engulfment of extracellular material. Interestingly, although the TREM2 has been linked to distinct neuropathological conditions, its specific ligands remain unknown. In order to maintain the microglial steady/surveillance state, neurons also express "do not eat-me" signals, such as CD47 and polysialylated proteins recognized by microglial SIRPα and SIGLECs, respectively. Microglia recruitment to the sites of injury is mediated by different receptors as well. Stressed neurons release ATP, a well-known chemotactic agent that stimulates microglia migration through purinergic $P2Y_{12}$ and $P2X_4$ receptors. Finally, a number of chemokines also mediate microglia chemotaxis. For example, CCL2 binds specifically to CCR2 while CXCR3 recognizes different chemokines such as CCL21 and CXCL10.

PS, Phosphatidylserine; TIM4, T-cell immunoglobulin mucin 4; MERTK, MER receptor tyrosine kinase; Gas6, growth-arrest specific factor-6; MFG-E8, milk-fat globule endothelial growth factor E8; LRP, low-density lipoprotein receptor-related protein; C3R, C3 receptor; DAMPs, danger-associated molecular patterns; TLRs, Toll-like receptors; TREM2, triggering receptor expressed on myeloid cells 2; CD47, cluster of differentiation 47; SIRPα, signal regulatory protein alpha; SIGLECs, sialic acid-binding immunoglobulin-like lectins.

Phagocytosis is an endocytic mechanism involving vesicular internalization of solid particles, including pathogens and cellular debris, and is one of the most vital microglial functions. Microglia can phagocytose neural precursor cells during development (Cunningham et al. 2013), as well as synapses in neuronal circuitry formation (Paolicelli et al. 2011) and in physiological conditions (Tremblay et al. 2010), together with entire neurons and cellular debris upon injury, preventing inflammatory reactions and damage spread (Brown and Neher 2014; Neher et al. 2012). Importantly, microglia can also engulf live, possible healthy neurons, a process called phagoptosis (Neher et al. 2012). Phosphatidylserine (PS), which is confined to the inner leaflet of the neuronal plasma membrane, can be exposed at the surface of stressed or injured neurons in reversible or irreversible ways (Arcuri et al. 2017). As it constitutes an “eat-me” signal, PS can be recognized by different microglial receptors including T-cell immunoglobulin mucin 4 (TIM4) (Miyanishi et al. 2007), MER receptor tyrosine kinase (MERTK)/ growth-arrest specific factor-6 (Gas6) complex (Wu et al. 2005) and the adaptor molecule milk-fat globule endothelial growth factor E8 (MFG-E8) (Figure I.1). MFG-E8 can be released by microglia and establish a bridge between PS at the surface of neurons and microglial vitronectin receptors (VNRs), mainly $\alpha_v\beta_3$ integrin (Hanayama et al. 2002). To note, however, that at high concentrations, the MFG-E8 molecules can bind to PS and to integrins, thus inhibiting the bridge of both cell types (Kruse et al. 2010). Upregulation of MERKT or MFG-E8 occurs during brain ischemia and inflammation being involved in delayed neuronal death (Neher et al. 2013), highlighting the protective role of these receptors. As detailed in Figure I.1., microglia phagocytosis may involve other receptor-ligand pairs, as well (Arcuri et al. 2017; Napoli and Neumann 2009).

TREM2 belongs to the immunoglobulin family and induces phagocytosis of cellular debris. Nevertheless, the exact signal that TREM2 recognizes remains to be clarified (Brown and Neher 2014; Takahashi et al. 2005), though it was recently showed that it can sense a number of lipids, including PS (Wang et al. 2015b), as well as nucleic acids (Kawabori et al. 2015). While these receptors mediate a “silent” phagocytosis that occurs concomitantly with the secretion of anti-inflammatory factors (Neumann et al. 2009), activation of Toll-like receptors (TLRs) also stimulate microglia phagocytic ability. TLRs are crucial to recognize pathogens, as well as protein aggregates, such as amyloid-β (Aβ) fibrils (a pathological hallmark of AD), thus stimulating their elimination (Fu et al. 2014; Xiang et al. 2015). Although microglia phagocytosis is primarily protective, because TLR-mediated phagocytosis courses with the release of pro-inflammatory mediators, this mechanism may contribute to the pathogenesis of neurodegenerative diseases. In fact, LPS-stimulated microglia is able to phagocytose live neurons, both *in vitro* and *in vivo*, which was prevented by *Mfge8* knock-out (Fricker et al. 2012), and Aβ was similarly shown to induce microglia engulfment of viable neurons in culture (Tahara et al. 2006). On the other hand, loss of phagocytic ability can

cause accumulation of apoptotic/necrotic material and spread of inflammation (Arcuri et al. 2017; Neher et al. 2012). It has been shown that inefficient clearance of myelin debris after focal demyelinating insult impairs remyelination. Recently, Kawabe and coworkers (2017) showed that MFG-E8 can bind Aβ promoting its endocytosis. However, MFG-E8 levels are reduced in the brain of AD patients and mouse models, suggesting a role for decreased phagocytic ability and Aβ accumulation. Importantly, the expression of "don't eat-me signals" in neurons also contribute to regulate microglia phagocytosis, as reviewed in Arcuri et al. (2017). Furthermore, several phagocytosis-associated gene variants are being considered as risk factors to develop AD, including CD33, alipoprotein E (APOE) and complement receptor type-1 (CR1). Additionally, *TREM2* variants were associated with the risk to develop both AD and ALS (Cady et al. 2014; Neumann and Daly 2013).

Although the role of autophagy in microglia behavior is largely unknown, recent studies have established some connections between autophagy and microglia inflammatory response (Su et al. 2016). In brief, autophagy (that comprises three types: macroautophagy, microautophagy and chaperone-mediated autophagy) is a process where cytoplasmic material is captured in a membrane vesicular structure, the autophagosome, and delivered for degradation upon fusion of the autophagosome with lysosomes (Menzies et al. 2017; Plaza-Zabala et al. 2017). After digestion, the breakdown products are reintegrated in the cell metabolism. The autophagic machinery encompasses more than 35 proteins, commonly designated as autophagy-related proteins (Atgs), such as beclin-1 (Atg6) and light chain 3 (LC3, Atg8) (Budini et al. 2017; Plaza-Zabala et al. 2017). Whereas essential for cell homeostasis, autophagy can be induced under stress conditions, including nutrient starvation, endoplasmic reticulum (ER) stress or mitochondrial damage, among other, in order to restore normal cell functions. As post-mitotic cells, neuronal survival is critically influenced by the ability to eliminate intracellular toxic material, and defects in autophagy have been reported in many neurodegenerative pathologies (Menzies et al. 2017). Several lines of evidence indicate that autophagy can regulate microglia activation (Su et al. 2016). Inhibition of autophagy *in vitro* promoted activation of nuclear factor-kappa B (NF-κB) and release of pro-inflammatory cytokines in BV2 and primary mouse microglia, while LPS-induced microglia response was suppressed by an autophagic inducer (Ye et al. 2017). Additionally, autophagy rescued neuronal cell death caused by α-synuclein-mediated microglia activation (Bussi et al. 2017). Jin and colleagues (2017) recently showed that LC3 and beclin-1 were increased in activated microglia after TBI, but when autophagy was inhibited, microglia activation and neuronal death were more pronounced. Together, these findings suggest that autophagy can be beneficial to restrain microglia overactivation and neurotoxicity.

Autophagy and phagocytosis share similarities in the process of vesicular formation and material digestion. However, despite recent evidences showing that LC3 can be allocated to the formation of the phagosome upon phagocytosis in macrophages, this interaction was never studied in microglia (Plaza-Zabala et al. 2017).

1.4.3. Microglial receptors

As extensively reviewed by Kettenmann and his colleagues (2011), microglia express a wide variety of receptors and channels that underline their extraordinary sensitivity. Despite the well-known chemokines [C-C motif (CC) and C-X-C motif (CXC)] and cytokines [interleukin (IL), tumor necrosis factor-alpha (TNF-α) and interferon (IFN)] receptors, involved in microglia chemotaxis to lesion sites and regulation of the inflammatory response, the expression of neurotransmitter receptors, including adenosine receptors, glutamate receptors, cholinergic receptors, P2X and P2Y receptor, Alpha-Amino-3-Hydroxy-5-Methyl-4-Isoxazole Propionic Acid (AMPA) and Gamma Amino Butyric Acid (GABA) receptors (Guruswamy and ElAli 2017; Kettenmann et al. 2011), highlight microglia as modulators of neuronal synaptic transmission. Microglia can also recognize both pathogen- and danger-associated molecular patterns (PAMPs and DAMPs, respectively) through pattern-recognition receptors (PPRs). Lectin and mannose receptors, nucleotide binding and oligomerization domain (NOD)-like receptors (NLRs) and TLRs constitute this group (Banjara and Ghosh 2017; Kettenmann et al. 2011). Because DAMPs, also called alarmins, comprise host intracellular molecules and represent injury once in the extracellular space, activation of TLRs signaling pathways has been observed in different CNS pathologies, including ALS, PD and stroke (Paschon et al. 2015). Moreover, as it will be further addressed, microglia express unique receptors that enable specialized cross-talk with neurons.

1.4.3.1. The cytosolic NLRP3-inflammasome

Inflammasomes consist in intracellular multimolecular complexes involved in inflammation and have been described in neurons, astrocytes and microglia (Walsh et al. 2014). Inflammasome mediators include the adaptor apoptosis-associated speck-like protein containing a CARD (ASC), Caspase-1, responsible for cleavage of pro-IL-18 and pro-IL-1β into their active forms, and the NLRs (Walsh et al. 2014). Among the different NLRs described, NLR pyrin domain containing 3 (NLRP3) is the best characterized and it is specialized in the recognition of DAMPs (He et al. 2016b), such as ATP (Mariathasan et al. 2006), uric acid crystals (Martinon et al. 2006) and Aβ fibrils (Halle et al. 2008). NLPR3-inflammasome assembly occurs in a two-step signal process (He et al. 2016b; Walsh et al. 2014), as evidenced in Figure I.2. Activation of TLRs induces translocation of NF-κB into the

nucleus, with the subsequent transcription of NLRP3 and pro-IL-1β genes. A second signal, comprising ATP or mitochondrial reactive oxygen species (ROS), stimulates the formation of the complex where NLRP3 recruits ASC, which in turn recruits and activates caspase-1. The mechanisms underlying complex assembly are still not completely clarified but it was recently demonstrated that phosphorylation of the NLRP3 pyrin domain is required for NLRP3-ASC interaction (Stutz et al. 2017). AD, multiple sclerosis (MS) and ALS pathogenesis have been linked to higher expression of NLRP3-inflammasome components (Barateiro et al. 2015; Song et al. 2017). Interestingly, Bezbradica and colleagues (2017) recently showed that sterile stimulation (two DAMP signals) induces weaker and delayed NLRP3-inflammasome activation than bacterial-associated signals revealing a specific inflammasome response under neurodegenerative conditions.

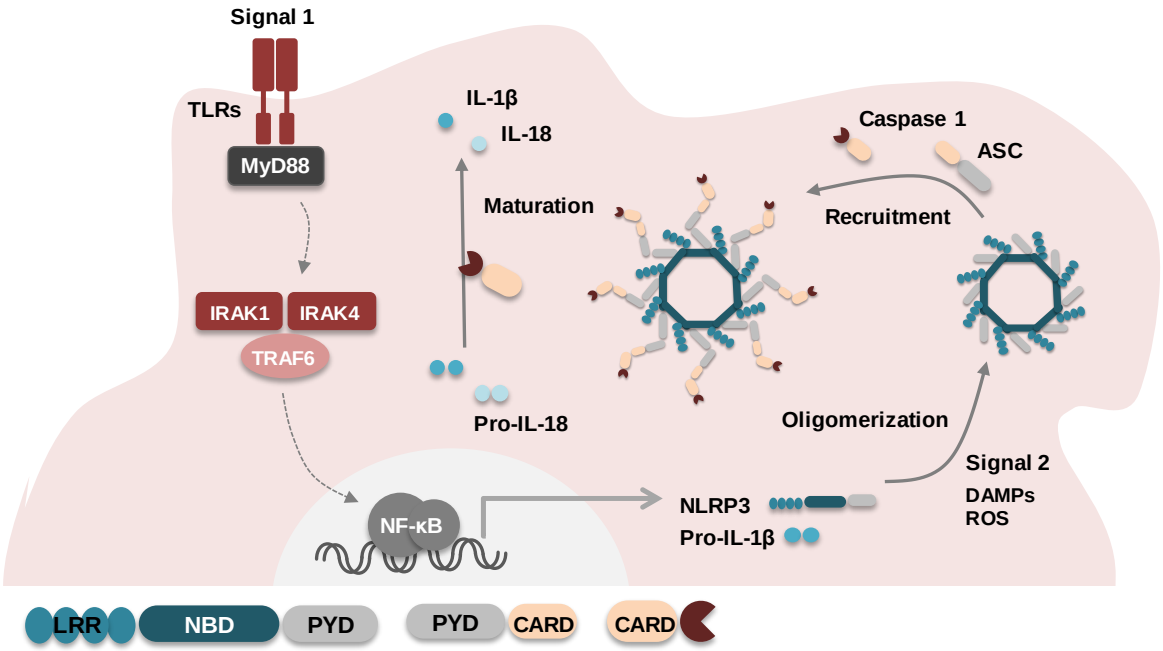

Figure I.2 - NLRP3-inflammasome activation mechanism. Activation of TLRs induces transactivation of NF-κB and the transcription of several pro-inflammatory genes. Among them are NLRP3 and IL-1β in its inactive pro-form (pro-IL-1β). Then, a second signal that includes DAMPs and mitochondrial ROS, for example, triggers the oligomerization of NLRP3 that is mediated by the NBD. The PYD of NLRP3 mediates protein-protein interactions between the LRR and the ASC (also contains a PYD) and, in turn ASC recruits caspase-1 by protein-protein interactions between CARD domains. After cleavage, active caspase-1 induces the maturation of pro-IL-18 and pro-IL-1β into their mature forms.
TLRs, toll-like receptors; NF-κB, nuclear factor-kappa B; NLRP3, NOD-like receptor pyrin domain containing 3; IL, interleukin; DAMPs, danger-associated molecular patterns; ROS, reactive oxygen species; NBD, nucleotide-binding domain; PYD, pyrin domain; LRR, carboxy-terminal leucine-rich repeat; ASC, adaptor apoptosis-associated speck-like protein containing a CARD.

1.4.4. Production of inflammatory mediators

As the resident immune cells within the CNS, microglia responses encompass the release of inflammatory mediators that either stimulate (pro-inflammatory), or inhibit (anti-inflammatory) inflammation, including cytokines, chemokines, ROS, DAMPs or alarmins and matrix metalloproteinases (MMPs) (Könnecke and Bechmann 2013; Lan et al. 2017;

Ransohoff and Perry 2009; Tambuyzer et al. 2009). Stimulation of TLR2 and TLR4 induces a pro-inflammatory response through activation of NF-κB, activator protein 1 (AP1) and interferon regulatory factor 3 (IRF3) (He et al. 2014; Lehnardt 2010). These transcription factors induce IL-1, IL-1β, TNF-α, IL-6 and IFN-γ gene expression and further production of ROS and NO (Kraft and Harry 2011). Once in the extracellular space, these cytokines will potentiate the inflammatory response by binding to their specific receptors. At the same time, MMP-2 and -9, as well as the chemokines CCL2 and CXCL10, to mention some, are additionally released contributing to extracellular matrix degradation and recruitment of microglia from the neighboring areas, respectively (Könnecke and Bechmann 2013; Tambuyzer et al. 2009; Zhao et al. 2017). It has also been shown that high mobility group box 1 (HMGB1) can be actively released by activated immune cells (Eun et al. 2013; Wu et al. 2012b). HMGB1 is mainly located at the nucleus, but shuttles between the nucleus and cytoplasm, exerting important biological activities that include nucleosome stability, gene transcription or autophagy stimulation, as extensively reviewed in Kang et al. (2014). Once released to the extracellular space, usually upon cell death (Magna and Pisetsky 2014), HMGB1 acts as an alarmin activating pro-inflammatory actions in microglia by binding to TLR2/4 or receptor for advanced glycation end products (RAGE), among others. Interestingly, HMGB1 release from immune cells occurs through a variety of pathways, including a NLRP3-inflammasome-dependent via (Lamkanfi et al. 2010). In opposite, microglia also release anti-inflammatory and neuroprotective agents, such as IL-4, IL-10, IL-13 and transforming growth factor-β (TGF-β). Such release requires the activation of signal transducer and activator of transcription (STAT) 3 and 6, and/or peroxisome proliferator activated receptor (PPARγ) pathway (Zhao et al. 2017). The release of such molecules is essential to reengage microglia into surveillant functions and to restore homeostasis after a toxic insult.

1.5. Microglia phenotypic plasticity

Until few years ago, microglial activation was defined as a switch-on/off process, but nowadays it is clear that microglia show incredible functional plasticity encompassing diverse phenotypes (Brites and Vaz 2014; Kettenmann et al. 2011). The different states of microglia polarization have started to be defined according to the activation of macrophage upon recognition of specific stimulus that induced the extremes of pro- vs. anti-inflammatory properties. As indicated in Table I.2, at least 7 phenotypes are currently categorized: surveillant (M0), classical activation or pro-inflammatory (M1) and alternative activation or anti-inflammatory (M2) [divided in wound-healing/anti-inflammatory (M2a), immunoregulatory (M2b) and acquired deactivation (M2c)], primed and dystrophic. As above mentioned the

surveillant phenotype, also known as M0 or steady state, is used to an alert, but not activated, microglia that controls CNS homeostasis (Nimmerjahn et al. 2005). The M1 phenotype is induced by LPS, or other TLRs agonists, as well as by IFN through TLR4/NF-κB and IFN receptors (IFNRs)/cytokine-activated Janus kinase (JAK)/STAT signaling, respectively (Chhor et al. 2013; Subramaniam and Federoff 2017). Hence, it is characterized by an increased production of pro-inflammatory cytokines, chemokines, proteases and redox species, like NO (Colton 2009; Kraft and Harry 2011). This phenotype is associated with neurotoxicity in cases of prolonged inflammatory environment and has been linked with neurodegeneration in PD and ALS, thus constituting a target for modulation (Song and Suk 2017; Subramaniam and Federoff 2017). The M2a phenotype is engaged in anti-inflammatory actions and is associated with repair after brain damage (Cherry et al. 2014). M2b is a regulator of the immune response that shares M1 and M2 properties and is induced by TLR agonists and immune complexes (Bell-Temin et al. 2015; Chhor et al. 2013). Finally, the M2c phenotype is required to restore CNS homeostasis, being promoted by TGF-β, IL-10 or even by phagocytosis of cell debris (Brites and Vaz 2014; Colton 2009; Wilcock 2012). The currently used microglial phenotypic markers are detailed in Table I.2.

Interestingly, whereas peripheral immune cells die after an M1-polarization, microglia have the ability to switch from the M1 to the M2 phenotype, and vice-versa. Concomitant high levels of inducible nitric oxide synthase (iNOS or NOS2) and arginase 1 (Arg1) in microglia were recently discovered after TBI and described as a transitional phenotype that the authors denominated as Mtran (Kumar et al. 2016). Therefore, the discrimination between distinct phenotypes is complex not only because they share markers and functions, but also due to the existence of transitional states. Recently, the M1/M2 polarization dichotomy started to be questioned since it cannot explain all the features of microglia reactivity under pathological circumstances (Ransohoff 2016). In fact, *in vivo* microglia face a multitude of signals, rather than a controlled *in vitro* polarization. Therefore, mounting evidence suggest that microglia acquire either a disease-specific or a mixture of phenotypes *in vivo* (Chiu et al. 2013; Peferoen et al. 2014b; Vincenti et al. 2016; Weekman et al. 2014). Although these limitations have to be taken into account, studying microglial phenotypes have evidenced important links between microglia activation and neurodegeneration, and microglia activation and disease progression stage (Subramaniam and Federoff 2017; Tang and Le 2016; Walker and Lue 2015). Most of the knowledge came from rodent microglia behavior, but the few reports that study human microglia indicate similar polarization features, as summarized in Table I.2.

Finally, primed and dystrophic/senescent microglia have been characterized as age-related phenotypes [reviewed in Deleidi et al. (2015), Koellhoffer et al. (2017) and Niraula et al. (2016)]. Primed microglia is described as having exacerbated pro-inflammatory responses

upon LPS challenge (Godbout et al. 2005), which is associated with the low-grade chronic inflammation in the aged CNS, designated as inflammaging (Deleidi et al. 2015). Throughout lifespan microglia are challenged by different situations that determine their primed state. This can be demonstrated by repetitive LPS injections where the first injection produces low levels of IL-1β and IL-12, whereas the second produces a much higher amount (Püntener et al. 2012). Markers of this phenotype include major histocompatibility complex class II (MHC-II), CD68 and TLRs together with downregulation of IL-10 and CD200 (Frank et al. 2006; Godbout et al. 2005; Letiembre et al. 2007). It has also been proposed that the chronic inflammation may also trigger the loss of microglia function (Koellhoffer et al. 2017) and lesions over the lifespan accelerate brain aging and bit-by-bit determines a dysfunctional microglia that lose their homeostatic and/or repairing capacity (Lourbopoulos et al. 2015). Thus, together with inflammaging, immunosenescence is also an aged-related feature. The major hallmarks of dystrophic microglia in the aged human brain are process shortening and enlargement, deramification of fine branches and cytorrhexis (Streit et al. 2004). Additionally, it was shown that microglia in the aged brain have lower ability to scavenge the brain, as well as to phagocytose (Rawji et al. 2016). While associated with normal aging mechanisms, these alterations in microglia underline microglia-mediated neurotoxicity in a variety of neurodegenerative and neuropsychiatric disorders (Deleidi et al. 2015). Overall, coexistence of heterogeneous microglia phenotypes have been found in several neurodegenerative diseases associated with chronic neuroinflammation and aging, and their effect in exacerbating neurodegeneration or inability to maintain homeostasis need to be further addressed in future studies.

1.5.1. Inflamma-miRNAs involved in regulation of microglia phenotype

MicroRNAs (miRNAs) are small, single stranded non-coding RNAs involved in regulation of gene expression at a post-transcriptional level. They directly bind to the 3’ untranslated region (UTRs) of a specific mRNA leading to repression of protein expression or induction of mRNA degradation (approximately 80% of miRNAs). MiRNA biogenesis occurs as canonical or non-canonical pathways, as detailed in Figure I.3. In the first case, miRNAs are transcribed from introns of protein-coding genes by RNA polymerase II into primary transcripts (pri-miRNAs) that fold as a hairpin loop structure. Then, pri-miRNA is converted to a shorter pre-miRNA by the enzymes Drosha and DiGeorge syndrome critical region gene 8 (DGCR8). In the second one, miRNAs transcripts, called mirtrons, are directly converted to pre-miRNAs by splicing. Pre-miRNAs are transported to the cytoplasm by exportin 5 and the formation of miRNA/miRNA* duplexes are catalyzed by Dicer. Whereas the complementary miRNA* strain is released and degraded, the mature miRNA (~22 nucleotides) binds to

Argonaute proteins and is incorporated in the RNA-induced silencing complex (RISC). This miRNA-RISC complex is finally transported by importin 8 to the specific target mRNA (Krol et al. 2010; O'Connell et al. 2010; Ponomarev et al. 2013; Tomankova et al. 2011).

MiRNAs play a central role in various biological processes including cellular differentiation, proliferation and survival (Ponomarev et al. 2013; Tomankova et al. 2011). Recently, the role of miRNAs in inflammation has been growing in interest. As reviewed in Tomankova et al. (2011), deregulation of miRNAs in the immune system may lead to sustained inflammation and, consequently, to chronic inflammatory diseases. Indeed, microglia phenotypes have been associated to variable expression of miRNAs, called inflammation-related miRNAs or inflamma-miRNAs, including miR-155, miR-125b, miR-101, miR-689, miR-21, miR-124, miR-145 and miR-146a, among others (Cardoso et al. 2012; Freilich et al. 2013; Ponomarev et al. 2011; Saba et al. 2012). Activation of pro-inflammatory pathways mediated by TLRs is associated with an increased expression of miR-155, miR-146a and miR-21 though their functions have different outcomes (He et al. 2014). Although in some situations it can inhibit MyD88 or NF-κB, exerting anti-inflammatory effects, miR-155 is a typical inducer of pro-inflammatory responses (Wu et al. 2016b). MiR-155 was shown to target multiple genes associated with the anti-inflammatory function of microglia. To name just a few, the suppressor of cytokine signaling 1 (SOCS1) involved in negative regulation of TLR/NF-κB transduction pathway, the SMAD2 that is a regulator of TGF-β signaling, and the transcription factor CCAAT/enhancer-binding protein beta (C/EBPβ) associated to the expression of Arg1, IL-10 and CD206 (Cardoso et al. 2012; Obora et al. 2017; Ponomarev et al. 2013). In opposite, miR-146a and miR-21 are involved in restoration of normal environment after damage. By targeting interleukin-1 receptor associated kinase 1 (IRAK1) and TNF receptor associated factor 6 (TRAF6), miR-146a negatively regulates the TLR2 transduction pathway in microglia (Saba et al. 2012). Relatively to miR-21, it is indicated to stimulate IL-10 production through repression of programmed cell death 4 (PDCD4) expression in macrophages (Sheedy et al. 2010). Importantly, miR-21 also regulates the pro-apoptotic proteins Fas ligand (FasL), as well as phosphatase and tensin homolog (PTEN), thus promoting cell survival (Wu et al. 2016b). Moreover, miR-125b and miR-101 were recently associated with microglia pro-inflammatory properties (Guedes et al. 2013). In particular, SMAD3, IRF4 and A20 are part of miR-125b regulation network. While the inhibition of the first two promote the expression of TNF-α, MHC-II, CD80 and CD86, that of A20 suppress NF-κB activation (Guedes et al. 2013; Parisi et al. 2013; Parisi et al. 2016). As one of the highest expressed miRNAs in the brain, mainly in neurons, miR-124 is required to maintain microglia in the surveillant state (Ponomarev et al. 2011). This effect is, in part, due to its capacity to keep low the levels of C/EBPα, as well as of CD45, MHC-II and iNOS. Additionally, miR-124 is able to downregulate M1-associated markers and to promote the M2

microglia phenotype (Ponomarev et al. 2011; Veremeyko et al. 2013), while suppressing microglia innate immunity by targeting TRAF6 (Qiu et al. 2015).

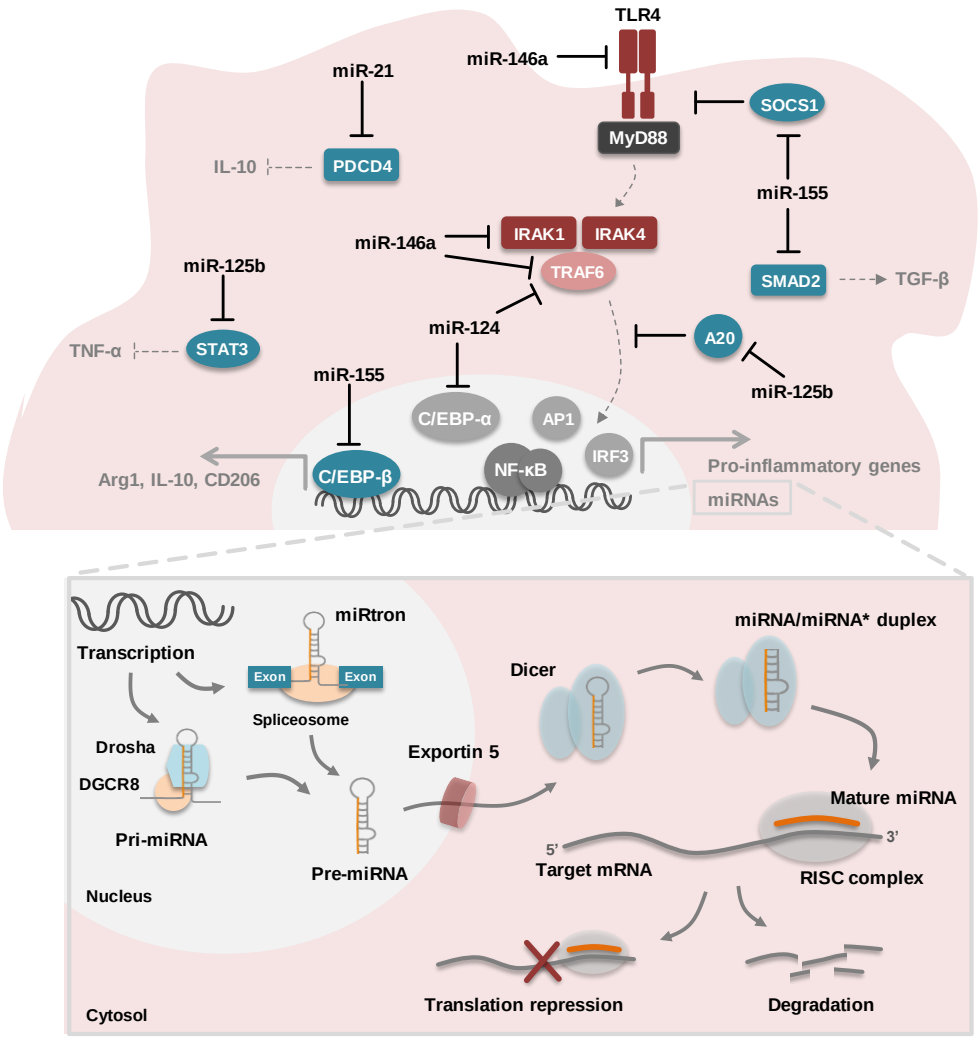

Figure I.3 - Inflamma-miRNAs production and gene regulation networks. Translocation of NF-κB, AP1 and IRF3 occur downstream of the activation of the TLR4 signaling pathway and induces the transcription of pro-inflammatory genes, including the inflammatory-related microRNAs (inflamma-miRNAs) miR-155, miR-146a and miR-21. MiR-155 potentiates the inflammatory environment by targeting the SOCS1 that inhibits TLR/NF-κB signaling pathway, the SMAD2 that is an inducer of TGF-β pathway and the transcription factor C/EBP-β, which induces the expression of anti-inflammatory genes. In opposite, TLR4, IRAK1 and TRAF6 are part of the gene regulation network of miR-146a highlighting its role in restraining microglia inflammatory responses. Likewise, decreased expression of PDCD4, upon miR-21 recognition, potentiates the production of IL-10. Whereas miR-124 targets C/EBP-α (transcription factor inducer of pro-inflammatory genes) and TRAF6, promoting anti-inflammatory actions, miR-125b acts together with miR-155 enhancing inflammation. Among the targets of miR-125b, A20 represses TLR/NF-κB signaling pathway and SMAD3 is involved in TNF-α expression. Biogenesis of miRNAs includes multiple and highly regulated mechanisms that start with the transcription of protein-coding regions by RNA polymerase II. In the canonical pathway, primary miRNA transcripts (pri-miRNA) are processed into a shorter pre-miRNA by the enzymes Drosha and DGCR8. In the non-canonical pathway, miRNAs are encoded in short introns (miRtrons) that are directly converted to pre-miRNAs by splicing. Pre-miRNAs are then transported to the cytosol by exportin 5 and converted to miRNA/miRNA* duplexes by DICER. The guided strand is then incorporated into RISC complex (miRNA* follows degradation) and binds to the UTR of target mRNAs inducing translation repression (partial complementarity) or mRNA degradation (near-perfect pairing).

NF-κB, nuclear factor-kappa B; AP1, activator protein 1; IRF3, interferon regulatory factor 3; TLR4, toll-like receptor 4; SOCS1, suppressor of cytokine signaling 1; TGF-β, transforming growth factor-beta; C/EBP, CCAAT/enhancer-binding protein; IRAK1, interleukin-1 receptor associated kinase 1; TRAF6, tumor necrosis factor receptor associated factor 6; PDCD4, programmed cell death 4; DGCR8, DiGeorge syndrome critical region gene 83'; UTR, untranslated region; mRNA, messenger RNAs.

Table I.2 - Rodent and human microglia phenotypic markers

Rodent microglia				**Human microglia**			
Inducers	**Effectors**		**Refs**	**Inducers**	**Effectors**		**Refs**
			M1 pro-inflammatory				
LPS IFN-γ	**Markers** CD80,CD86 MHC II C/EBPα iNOS **Inflammation** IL-6, IL-1β, IL-12 TNF-α, NO CCL2, CXCL10	**miRNAs** miR-155 miR-101 miR-125b low miR-124	(Chhor et al. 2013);(Wilcock 2012); (Freilich et al. 2013); (Guedes et al. 2013)	LPS + IFN-γ TNF-α + IFN-γ G-CSF followed by LPS + IFN-γ	**Markers** CD80 CCR7 CD14 MHC II **Inflammation** IL-6,IL-12 IL-1β TNF-α	**miRNAs** miR-155 miR-146a?	(Durafourt et al. 2012); (Walker and Lue 2015); (Moore et al. 2013);(Cardoso et al. 2016)
			M2a wound-healing/anti-inflammatory				
IL-4 IL-13	**Markers** Arg1,FIZZ Ym1 CD206, CD209 IL-1Ra, DAB2 **Inflammation** IL-4, IL-10 TGF-β	**miRNAs** miR-145 miR-124	(Chhor et al. 2013); (Bell-Temin et al. 2015); (Cherry et al. 2014); (Wilcock 2012); (Freilich et al. 2013)	IL-4 + IL-13 M-CSF followed by IL-4 + IL-13	**Markers** CD206 CD209 CD33 TREM2 **Inflammation** TGF-β		(Durafourt et al. 2012); (Walker and Lue 2015); (Cherry et al. 2014)
			M2b immunoregulatory				
TLR agonists Immune complexes	**Markers** SOCS3 MHC II CD86 **Inflammation** IL-10, IL-6 IL-1β, TNF-α	**miRNAs** miR-155 miR-146a	(Cherry et al. 2014); (Wilcock 2012)	IC + LPS or IL-1β	**Markers** CD16, CD32 CD33 TREM2 **Inflammation** TGF-β IL-10		(Walker and Lue 2015)
			M2c acquired deactivation				
IL-10 TGF-β Cell debris Glucocorticoids	**Markers** SOCS3 SPHK1 Arg1 **Inflammation** IL-10, TGF- β Reduced pro-inflammatory mediators	**miRNAs** miR-146a miR-21 miR-124	(Cherry et al. 2014); (Wilcock 2012); (David and Kroner 2011; Ponomarev et al. 2013)	IL-10	**Markers** CD163 **Inflammation** IL-10	**miRNAs** miR-146a?	(Walker and Lue 2015); (Cherry et al. 2014); (Cardoso et al. 2016)
			Primed				
Repetitive stimulation Aging	**Markers** TLRs MHC II CD68 **Inflammation** Exacerbated response upon activation	**miRNAs** miR-155 miR-146a miR-21	(Godbout et al. 2005); (Letiembre et al. 2007); (VanGuilder et al. 2011) (Olivieri et al. 2015)	Aging	**Inflammation** TLR NFKB1 TRAF6 TSPO		(Primiani et al. 2014)
			Dystrophic/senescent				
In vitro aging	**Markers** Loss of function	**miRNAs** miR-146a	(Caldeira et al. 2014)	Aging	**Markers** Cytorrehis Deramification Branches shortening		(Streit et al. 2004)

Among the inflamma-aging miRNAs, recent data indicate that miR-155, miR-146a and miR-21 are associated with DNA damage response-induced senescence that is observed under neurodegenerative conditions (Olivieri et al. 2015). Whereas miR-155 may inhibit or promote senescence depending on the specific gene expression program (Olivieri et al. 2015), miR-146a is upregulated in aged mice promoting macrophage dysfunction (Jiang et al. 2012), as well as in *in vitro* aged-microglia (Caldeira et al. 2014), being considered a marker of cell senescence.

1.6. *In vitro* models to study microglia activation

Microglia activation has been studied *in vivo*, *in vitro* and *ex vivo*. While *in vivo* microglia responses are constantly influenced by the surrounding environment, *in vitro* studies allow a more focused understanding of specific features of microglia biology, such as the release of inflammatory mediators, polarization specificities or chemotactic movement (Sousa et al. 2017; Stansley et al. 2012). Both primary microglia cultures, obtained from the cortex of newborn mice or rats, and more recently form adult rodents, and microglia secondary cell lines, developed by genetic immortalization of primary cells, are commonly used to explore microglia functioning in normal or pathological circumstances (Sousa et al. 2017). Primary microglia are able to produce pro- and anti-inflammatory responses depending on the stimulus, to phagocytose and migrate towards chemoattractants and, so, to induce neuroprotective or neurotoxic mechanisms (Caldeira et al. 2014; Neniskyte et al. 2011; Nikodemova and Watters 2011). However, despite the efforts, primary cultures still produce low number of cells and they are time-consuming. In this context, mouse BV2 cells (immortalized via *v-raf*/*v-myc* carrying retrovirus) (Blasi et al. 1990) and N9 cells (*v-myc* or *v-mil* of the avian retrovirus MH2) (Righi et al. 1989a) have been the most used lines. These cells are also able to perform typical microglial functions (Bussi et al. 2017; Cardoso et al. 2012; Mazaheri et al. 2017) and, although with some differences mainly in the length of responses, their behavior is similar to primary microglia (Nikodemova and Watters 2011; Stansley et al. 2012). The disadvantages in the use of cell lines rely on their increased proliferation and adhesion as well as on their homogeneous responses, which limit the representation of microglia diversity *in vivo*. Reported differences in microglia behavior *in vivo* or *in vitro* conditions may be caused by the fact that microglia are always activated to same extend when in culture and may lose their specific homeostatic gene signature (Bohlen et al. 2017; Butovsky et al. 2014). In fact, the interaction with neighboring cells, crucial for the modulation of microglial reactivity (Hanisch and Kettenmann 2007), is absent. Altogether, these particularities should be taking into account when manipulating microglia in culture, in order to correctly evaluate their behavior.

Other useful models to study microglia reactivity include mixed and cocultures with neurons or other glial cells, and the usage of *ex vivo* organotypic slice cultures (OSCs). Cocultures allow the study of interaction among two cell types by soluble factors, whereas mixed cultures have the increased advantage of also allowing the assessment of ligand-receptor interactions. The OSCs are the closest model to explore microglia function in their biological environment, both in physiology (Vinet et al. 2012) or pathology, such as in MS (Barateiro et al. 2015), as the three dimensional architecture of the brain is maintained.

Contemporary studies have started to explore microglia activation after acute isolation followed by transcriptomic analysis (Hirbec et al. 2017). The most common isolation procedures are fluorescent-activated cell sorting (FACS), usually based on CD11b positive and CD45 low expression, laser capture microdissection (LCM), and CD11b positive magnetic beads separation (few studies). After isolation, transcriptome analysis can be done by microarrays or RNA NextGen sequencing (NGS) (Hirbec et al. 2017). These techniques had a huge impact on the knowledge of microglia biology enabling the identification of novel microglial markers, as well as disease-specific and stage-specific behaviors (Butovsky et al. 2014; Chiu et al. 2013; Hickman et al. 2013), as already mentioned. Interestingly, the novel single-cell RNA sequencing approach is contributing to the idea that distinct microglial populations coexist in a variety of situations (Matcovitch-Natan et al. 2016).

Primary microglial cultures form human embryos and post-mortem individuals, as well as production of human cell lines (such as HMO6 or CHME3), have been additionally accomplished. Importantly, the development of new isolation techniques is continuous and very recently, Mizzee and colleagues (2017) have published a fast method to isolate and study the phenotype of post-mortem human microglia. Finally, the generation of human induced pluripotent stem cells (iPSCs) from skin fibroblasts (Takahashi et al. 2007) has opened new avenues in the neuroscience field and personalized medicine. Together with neuron and astrocytes differentiation, protocols for iPSCs-derivation into microglia-like cells are now being developed (Abud et al. 2017; Pandya et al. 2017).

2. Interactive networks between microglia and other CNS cells: homeostasis and injury

In normal CNS, microglia physiology is intimately regulated by the environment they encounter. Therefore, interaction with neurons as well as with astrocytes, oligodendrocytes, pericytes and endothelial cells are able to modulate microglia behavior. Since they are the vigilant cells of CNS homeostasis, any alteration in a specific cell type can activate microglia. In this section, the cross-talk between microglia and their CNS neighbors and how it may influence microglia phenotype will be described.

2.1. The fundamental cross-talk with neurons

Intercellular communication between neurons and microglia is mediated either by soluble or membrane-anchored factors that are recognized by specific receptors and are essential for maintaining the surveillance phenotype of microglia. The inhibitory or calming signals produced by neurons, namely CD200 and CX3CL1, can shape microglia responses and restrain their activation through binding to their specific receptors CD200R and CX3CR1, respectively, which have immunoreceptor tyrosine-based inhibition motifs (ITIMs) (Kabba et al. 2017; Ransohoff and Perry 2009; Zhao et al. 2017). Hoek and colleagues (2000) have shown that microglia in CD200-deficient mice exhibit a constitutively active phenotype with an increased subset of amoeboid phagocytic morphology and elevated levels of CD45 and complement receptor type-3 (CR3). More recently, it was additionally showed that *Cd200*$^{-/-}$ microglia polarize towards the M1-phenotype with increased levels of TLR4 and NF-κB (Denieffe et al. 2013). CX3CL1-CX3CR1 signaling has been the focus of several studies since the outcome of such interaction strongly depends on the physiological/pathological context (Cardona et al. 2006b; Limatola and Ransohoff 2014; Paolicelli et al. 2014). Mainly associated with neuroprotection, this axis is involved in numerous mechanisms, including synaptic pruning, neurogenesis and migration. *Cx3cr1*$^{-/-}$ mice were shown to exhibit high number of immature dendritic spines and inactive synapses during development, as well as reduced neuronal progenitors in neurogenic niches (Paolicelli et al. 2011). Disrupted CX3CL1 signaling also results in about 30% reduction in the process speed, as evidenced by observation of microglia dynamics in *ex vivo* time lapse imaging of mouse retina explants (Liang et al. 2009). This cross-talk axis is also important to maintain microglia viability, as showed in an *in vitro* study where CX3CL1 prevented microglia apoptosis (Boehme et al. 2000). Importantly, CX3CR1 knock-out was shown to aggravate neuronal loss in mouse models of PD and ALS, highlighting the role of CX3CR1 in reducing microglia pro-inflammatory responses (Cardona et al. 2006b). Moreover, CX3CL1 can exist as a soluble (cleaved by ADAM 10, 17 and occasionally by MMP-9), or membrane-bound factor, which is proposed to stimulate different microglial responses (Wolf et al. 2013), although further investigation is needed to clarify this issue. Reports indicate that this axis may participate in neurotoxic mechanisms as well. In mouse models of brain ischemia, CX3CL1-deficiency conferred neuroprotection by reducing infarction volume and mice mortality rate (Soriano et al. 2002), while CX3CR1 reduced expression was shown to decrease microglia activation and related production of IL-6, IL-1β and TNF-α (Liu et al. 2015b). Injection of $A\beta_{1-40}$ fibrils in the hippocampus revealed to upregulate CX3CR1, together with microglia activation and IL-1β production, which was reverted by CX3CR1 suppression, restoring synaptic plasticity and mice cognitive capacity (Wu et al. 2013).

Other cross-talk interactions between neurons and microglia include signal regulatory protein alpha (SIRPα) and its ligand CD47, as well as sialic acid-binding immunoglobulin-like lectins (SIGLEC) that recognize polysialylated proteins. Now concerning the SIRPα-CD47 axis, it has been referred to regulate migration, phagocytosis and immune homeostasis, while SIGLEC signaling attenuates microglia neurotoxicity (Kettenmann et al. 2011; Zhao et al. 2017). Both ligands also constitute “don’t-eat-me” signals that inhibit microglia phagocytosis (Arcuri et al. 2017; Brown and Neher 2014). Recently, it was showed that the neuronal soluble factors CSF-1 and IL-34, recognized by CSF-1R are critically important for microglia survival and maintenance of surveillance function (Wohleb 2016).

Upon injury, neurons often release increased amounts of ATP and UDP, which can be sensed by microglia leading to their activation (Davalos et al. 2005; Koizumi et al. 2007). As previously mentioned, ATP is recognized by $P2Y_{12}$ receptor (Haynes et al. 2006). It induces microglia chemotaxis that by facing an increased gradient of ATP become neurotoxic (Inoue 2002). Release of UDP, instead, induces phagocytic ability through $P2Y_6$ receptor (Lim et al. 2017). In addition, CX3CL1 cleavage (Chapman et al. 2000) and exposure of PS (Neniskyte et al. 2011) in injured neurons are leading events inducing microglial migration to damaged areas and clearance of neurons, respectively. Finally, neurons also upregulate a number of chemokines, including CCL21 and MCP1 that are recognized by CCR7/CXCR3 and CCR2, in order to recruit microglia to lesion sites (Kettenmann et al. 2011; Zhang et al. 2017). Under more severe situations, microglia are stimulated by DAMPs that are released upon neuronal death, mainly by necrosis since apoptosis usually occurs in an immunological silent manner (Pisetsky 2013). These factors include ATP and HMGB1, among others (Banjara and Ghosh 2017), which activate microglia through TLRs, RAGE and the NLRP3-inflammasome initiating an inflammatory response that although firstly neuroprotective, may trigger neurotoxicity in chronic situations. Interestingly, several of these neurodegenerative conditions are caused by accumulation of misfolded and aggregated proteins, such as Aβ and phosphorylated Tau in the case of AD, α-synuclein in PD, and copper-zinc superoxide dismutase 1 (SOD1) and TAR-DNA binding protein 43 (TDP-43) in ALS, that can also be recognized by microglia as danger signals (Block et al. 2007). Given the bi-directional signaling of neuron-microglia interaction, the activated microglia may release molecules that, in turn, will harm neurons. IL-1β and TNF-α are among the cytokines able to bind to neuronal IL-1R and TNFRs inducing changes in neuronal activity, as well as inducing neurodegeneration. In addition, release of ROS is a well-known neurotoxic mechanism mediated by activated microglia (Block et al. 2007). Therefore, neuron-microglia communication can induce a deleterious vicious circle that will perpetuate the neurotoxic injury, a crucial mechanism for the genesis of neurodegeneration.

2.2. A triad of glial cells in an immune privileged environment

Besides neurons, microglia share the CNS environment with the other glial cells (astrocytes and oligodendrocytes), as well as with endothelial cells, which are the main component of BBB and blood-spinal cord barrier (BSCB). Since microglia surveillance function is collectively maintained by a multitude of soluble and membrane-bound factors, all these cell types influence microglia phenotype in physiological conditions. In case of injury, the interplay between them likely contributes to microglia activation and vice-versa.

Astrocytes are the most frequent glial cell, accounting for 30% of the total CNS cells and have a star-shaped morphology (Sofroniew and Vinters 2010). They perform a number of vital functions for neuronal support that include release of neurotrophic factors and energy substrates, including the clearance of neurotransmitters (mainly glutamate) from the synaptic cleft. Together with microglia, they participate in the neuroimmune response and synapse modulation. Astrocyte end-feet are also structural elements of the BBB. Amongst the factors produced by astrocytes, TGF-β is a contributing element for microglia surveillance. It was shown that it reduces microglia production of pro-inflammatory cytokines and ROS. Together with CSF-1, IL-34 and cholesterol TGF-β was shown to promote microglia viability and their ramified morphology (Bohlen et al. 2017; Liu et al. 2011). Astrocytes have the ability to communicate through Ca^{2+} waves by transporting inositol triphosphate (IP_3) and ATP through gap-junctions (formed by docking of two hemichannels in the membranes of adjacent cells) (Montero and Orellana 2015). This mechanism can spread to microglia (Schipke et al. 2002; Verderio and Matteoli 2001). Connexin-43 (Cx43) is a major element of astrocytic gap-junctions, although also existing in microglia together with other hemichannels, enabling the release of a set of small molecules and its uptake by neighboring cells, such as glutamate or prostaglandin E2 (PGE_2), [reviewed in Gajardo-Gomez et al. (2016) and Montero et al. (2015)].

Being the sensor of the CNS, several lines of evidence indicate that microglia activation precedes astrocyte reactivity in a number of neuropathological circumstances that include experimental autoimmune encephalomyelitis (EAE), AD, ALS and neuropathic pain (Liu et al. 2011). Therefore, most of the studies have been focused on microglia-to-astrocytes signaling in neurodegeneration and data regarding the influence of astrocytes on microglia activation are missing. Very recently, it was shown that neurotoxic astrocytes (termed A1 astrocytes by the authors) are observed in AD, PD, MS and ALS. This phenotype was shown to be induced by activated microglia through the release of Il-1α, TNF and C1q (Liddelow et al. 2017). In a manganese-mediated neurotoxicity model, activation of microglial NF-κB was demonstrated to be crucial to induce astrocyte reactivity, followed by the release of pro-inflammatory cytokines and chemokines (Kirkley et al. 2017). Moreover, soluble factors released upon

$A\beta_{25-35}$-mediated microglia activation stimulate Cx43-dependent release of ATP and glutamate that induce neuronal death via opening of the hemichannel Pannexin-1 (Panx1) (Orellana et al. 2011). Interestingly, this Aβ peptide was also able to induce increased surface levels of Cx43 and Panx1 in microglia (Orellana et al. 2011), highlighting an important cross-talk between microglia-astrocytes-neurons mediated by hemichannels. Nonetheless, once astrocytes are reactive they can also exacerbate microglial responses towards neurodegeneration. As partners in immune responses, astrocytes influence microglia activation status by the secretion of cytokines and chemokines. For instance, CCL2 was shown to induce microglia polarization towards the M1-phenotype in a CCR2-dependent manner *in vitro* (He et al. 2016a) and *in vivo* (Xu et al. 2017). A novel signaling pathway was recently described, consisting in the activation of NF-κB in astrocytes with consequent release of C3, as observed in AD mouse models. C3 is recognized by microglial C3aR and inhibits their phagocytic ability and clearance of Aβ, thus promoting a worsened disease scenario (Lian et al. 2016).

The major function of oligodendrocytes is to enwrap axons with myelin sheaths, which is essential for the conductance of neuronal action potentials and have the important ability to renew the multi-layered plasma membrane that form the myelin (Kabba et al. 2017; Peferoen et al. 2014a). Although not much is known regarding the cross-talk between microglia and oligodendrocytes in homeostatic conditions, a recent study showed that a specific microglia population exists in developing white matter regions in the adult brain, which was shown to contribute to the maintenance of oligodendrocyte progenitor cells (OPC) (Hagemeyer et al. 2017). Interestingly, M2-microglia derived factors were also shown to induce oligodendrogenesis (and neurogenesis) from neural stem/progenitor cells through activation of PPARγ pathway (Yuan et al. 2017), as well as to promote OPC differentiation during remyelination (Miron et al. 2013). In contrast, due to their high metabolic rate and energy demands, oligodendrocytes are extremely vulnerable to pro-inflammatory factors (mainly TNF-α) and ROS derived from activated microglia (Domingues et al. 2016; Peferoen et al. 2014a). This issue has been demonstrated after LPS challenge (Domingues et al. 2016), in SCI (Lee et al. 2015a) and in the mouse EAE (Yeo et al. 2012). While microglia activation influences the survival and differentiation of oligodendrocytes, these myelinating cells can also express CD200 what suggests their involvement in microglia vigilant function (Koning et al. 2009). On the other hand, under stress, oligodendrocytes can produce several chemokines (such as CXCL10, CCL2 and CCL5) and cytokines (including TNF, IL-6 and IL-8) that recruit microglia to the site of injury and induce their activation, as reviewed in Peferoen et al. (2014a). It is well known that communication between neurons and oligodendrocytes is mediated by exosomes that transfer metabolites, proteins and genetic material (Frühbeis et al. 2013). Interestingly, selective transfer of exosomes from

oligodendrocytes to microglia was also demonstrated, and indicated to occur by macropinocytosis (Fitzner et al. 2011).

The restricted and unique environment of the CNS is maintained by the BBB and BSCB. Endothelial cells linked by tight/adherence junctions are the key element enabling physical separation of blood circulation from CNS parenchyma. Pericytes, together with the basement membrane, astrocytes and microglia were shown to contribute to the barrier properties, being collectively denominated as neurovascular unit (Keaney and Campbell 2015). Once more, the interplay between microglia and endothelial cells has been mostly explored in the context of pathology (Dudvarski Stankovic et al. 2016). In fact, LPS-activated microglia increased the permeability of the BBB in a co-culture model (Sumi et al. 2009). Amongst the microglia-derived mediators that have the ability to open the BBB are ROS, MMP-9 and vascular endothelial growth factor (VEGF), which have been consistently reported (Dudvarski Stankovic et al. 2016). Moreover, microglia can also be recruited either by endothelial cells or by serum proteins, such as fibrinogen, that enters the brain upon BBB disruption (Davalos et al. 2012). Impaired BBB also facilitates the entrance of peripheral immune cells into the CNS parenchyma. Of notice, a recent study showed that cultured microglia exposed to serum, change their transcriptional program exhibiting increased proliferation and phagocytic ability (Bohlen et al. 2017), what suggests that these CNS-blood barriers have also an impact in maintaining microglia surveillance state.

Major cross-talk players between microglia and the neighborhood neurons, astrocytes and oligodendrocytes are depicted in Figure I.4.

2.3. Soluble factors *vs.* extracellular vesicles

The majority of studies concerning intercellular communication in the CNS have been focused either on the release of soluble factors that are recognized by specific receptors in adjacent cells, or on membrane-bound ligand-receptor interface, as described in the former sections. Although described in the 70s, cellular interplay by extracellular vesicles (EVs) in neurodegenerative conditions has only gained increased attention over the last years (Levy 2017; Thompson et al. 2016). Studies using cellular condition media (or in other words, the secretome) to explore cell-to-cell communication previously disregarded the existence and influence of EVs. Lately, the importance of EVs has become evident once they are considered not only determinants in intercellular cross talk, but also as mediators in disease-spreading and as tools for biomarker and therapeutic research (Brites and Fernandes 2016; Rufino-Ramos et al. 2017; Thompson et al. 2016).

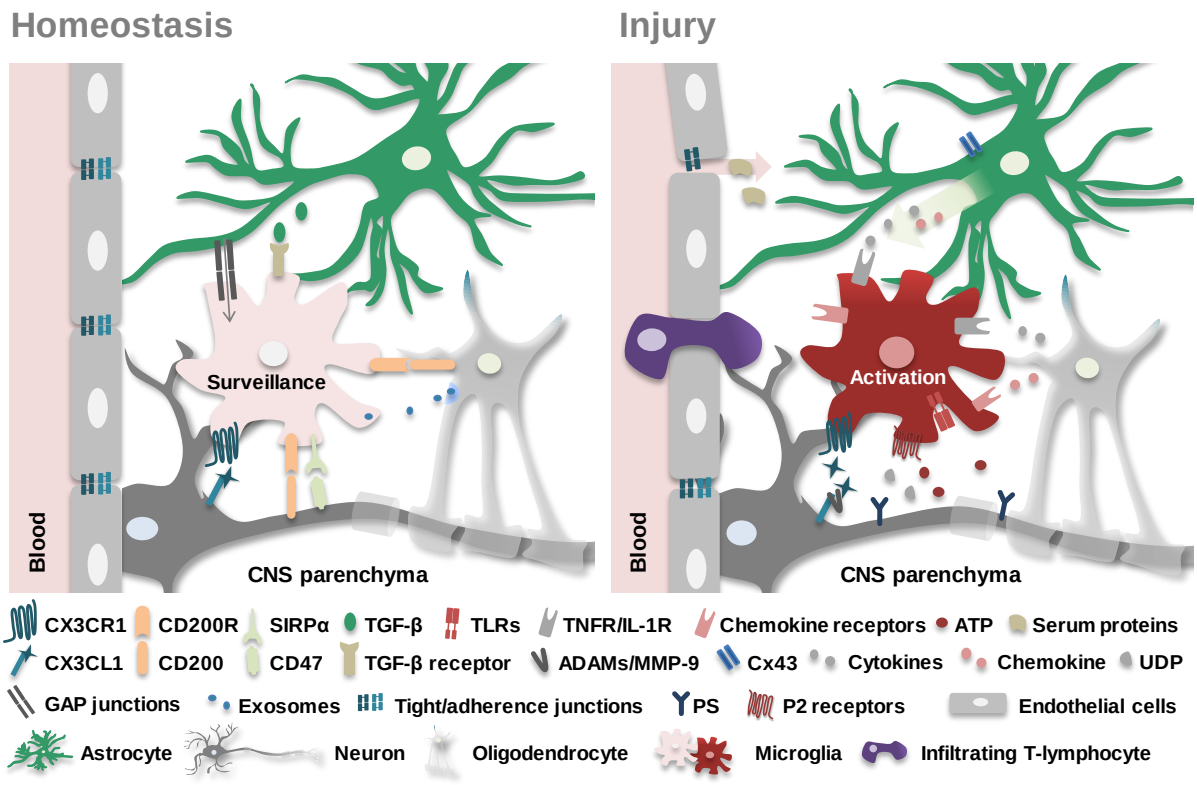

Figure I.4 - Intercellular communication regulates microglia responses in CNS homeostasis and injury. Under physiological conditions, interplay between neurons and glial cells are critically important to maintain microglia normal scavenging functions. The neuron-microglia axis CX3CL1-CX3CR1, CD200-CD200R and CD47-SIRPα are major contributors to restrain microglia activation. To note that CD200 can be expressed by oligodendrocytes, as well, and that microglia are able to internalize exosomes derived from these myelinating cells, considered to be important to maintain the normal CNS environment. Astrocytes produce TGF-β that upon binding to its microglial receptor promotes microglia ramified morphology and survival. Additionally, these glial cells are known to communicate via gap-junctions, which allow the direct passage of small molecules, such as ATP. During injury, neurons expose PS, release ATP, UDP and chemokines, and CX3CL1 is cleaved by ADAM10/17 and by MMP-9, resulting in its shedding from the membrane. All these molecules are recognized by microglia and induce a programmed response involving the activation of TLRs, P2 receptors and CX3CR1, together with phagocytosis, migration and secretion of inflammatory mediators. Damaged oligodendrocytes and activated astrocytes then release a number of cytokines and chemokines, which are able to activate microglia through additional TNFR/IL-1R. Finally, activation of microglia under stressful conditions may similarly derive from infiltrating T-lymphocytes and serum proteins that enter the CNS upon disruption of the BBB and/or the BSCB.
CX3CL1-CX3CR1, C-X3-C motif chemokine/receptor; CD, cluster of differentiation; CD200R, CD200 receptor; SIRPα, signaling regulatory protein alpha; TGF-β, transforming growth factor beta. PS, phosphatidylserine; MMP-9, matrix metalloproteinase 9; TLRs, toll-like receptors; TNFR/IL-1R, TNF and IL-1 receptors; BBB, blood-brain barrier; BSCB, blood-spinal cord barrier.

EVs are formed by a lipid bilayer surrounding a fluid-filled lumen that carries proteins, RNA, miRNAs, DNA and metabolites, sometimes reflecting the cell of origin. Almost all cells secrete EVs that have been categorized, according to their biophysical properties and biogenesis, as ectosomes or microvesicles, exosomes and apoptotic bodies. Apoptotic bodies have irregular shapes, vary between 50-5000 nm in diameter and are released from cells undergoing apoptosis with the main function of eliminating degradation products and cellular waste. Microvesicles and exosomes, although important for the elimination of unnecessary cellular components and toxic products from the cell (Xiao et al. 2017), actively

participate in the transfer of molecules between the donor cell and the recipient cell (Budnik et al. 2016; Kalra et al. 2017). Microvesicles are large vesicles (50-2000 nm) that are released directly from the plasma membrane by outward budding. Exosomes are very small, ranging between 40-150 nm in diameter and have an endocytic origin being released upon fusion of the multivesicular bodies (MVBs) with the plasma membrane (Kalra et al. 2017). Several reports suggest that exosomes have specific markers, allowing to distinguish them from microvesicles, but accumulating evidences indicate that their protein content highly overlap (Thompson et al. 2016). The combination of size, morphology and protein content analysis is, therefore, being used to more accurately characterize exosomes (Sheller et al. 2016). Biogenesis details, specific markers and functions of exosomes will be described in the next section.

Neurons, oligodendrocytes, astrocytes, microglia and endothelial cells are able to secrete EVs (Budnik et al. 2016; Dozio and Sanchez 2017). Although EV functions in the CNS have been explored in the context of neurodegenerative conditions, we must not forget that they have an important role in normal CNS physiology. Neurons release neurotransmitter receptors and miRNAs by EVs as a regulatory mechanism for excitability and synaptic plasticity, respectively (Budnik et al. 2016). Also, neuronal-to-astrocyte transfer of miR-124 in exosomes was shown to enhance excitatory amino acid transporter 2 (EAAT2), also known as glutamate transporter 1 (GLT-1) (Morel et al. 2013), which regulates the clearance of glutamate after synaptic transmission. Interestingly, EVs released by microglia were shown to mediate neuronal excitability by inducing the release of synaptic vesicles in presynaptic terminals (Antonucci et al. 2012). Oligodendrocytes-derived exosomes are loaded with myelin basic protein (MBP) and stress-related proteins, offering support to neurons in normal, as well as in stress conditions (Kramer-Albers et al. 2007). These exosomes are cleared by microglia in an immunological silent manner (Fitzner et al. 2011). Both astrocytes and microglia release microvesicles enriched in IL-1β upon ATP recognition through $P2X_7$ receptors (Bianco et al. 2009), and TNF-α was shown to induce the release of EVs from astrocytes (Wang et al. 2017a). Recently, a proteomic study evidenced that human brain endothelial cells release microvesicles and exosomes with different protein content, influencing distinct systems in the CNS (Dozio and Sanchez 2017). Under pathological circumstances, EVs have been mainly described as vehicles associated to the elimination of aggregated and misfolded proteins that additionally contribute to disease dissemination after uptake by distant recipient cells (Thompson et al. 2016).

2.3.1. Is there a role for exosomes in neurodegeneration?

Biogenesis of exosomes starts with the formation of endocytic vesicles from the plasma membrane, as depicted in Figure I.5. These early endosomes accumulate intraluminal vesicles (ILVs) through invagination of the endosome membrane originating the MVBs. This inward budding mechanism can occur via Endosomal Sorting Complexes Required for Transport (ESCRT)-dependent and independent pathways, in that the former is the most common. As the name itself suggests, these complexes also participate in cargo sorting, although this process is still largely unknown. Alternative pathways include the involvement of the lipids ceramide and phosphatidic acid, and tetraspanins (Hessvik and Llorente 2017; Kalra et al. 2017). After formation, the MVBs can fuse with lysosomes following to degradation, be recycled in the Golgi apparatus or proceed to exocytosis, releasing the ILVs upon fusion with the plasma membrane, which are thereafter called exosomes. Whereas exosomes release occurs physiologically within the CNS, stress and injury are known to influence exosome secretion and their content (Hessvik and Llorente 2017). Exosomal composition can reflect the cell of origin at some extends, but recent findings indicate that they are enriched in proteins related with their endosomal origin. These proteins have been considered as exosomal markers and include Alix and TSG101 (proteins of the ESCRT complexes), the tetraspanins CD9, CD63 and CD81, flotillin-1 (involved in membrane fusion and component of lipid rafts), MHC class I and II, and the heat-shock proteins HSP70 and HSP90. Exosomes are also enriched in cholesterol, sphingomyelin, ceramide and PS (Kalra et al. 2017; Thompson et al. 2016). Today, tracing the cellular origin of exosomes has become possible thanks to new technologies such as Multiplex proximity extension assay (Larssen et al. 2017). Most importantly is the possibility that the content of exosomes reflects what the cell is experiencing, what turns circulating exosomes as liquid biopsies and noninvasive biomarkers in early detection and diagnosis of neurodegenerative diseases.

Exosomal cargo is composed by miscellaneous proteins, lipids, RNA [small RNAs and messenger RNAs (mRNAs)]. Yet controversial, the transport of DNA and mitochondrial DNA was also reported. Although it is reasonable to believe that part of the cargo is randomly loaded in the cytosol that fills exosomal lumen, late studies have revealed some mechanisms by which specific proteins or miRNAs are internalized (Hessvik and Llorente 2017). Ubiquitination is recognized by ESCRT machinery and was reported to target proteins integrated in exosomal cargo (Cheng and Schorey 2016). Additionally, Villarroya-Beltri and colleagues (2013) showed that miRNAs, with a specific sequence motif (EXOmotif), were recognized by sumoylated heterogeneous nuclear ribonucleoprotein A2B1 (hnRNPA2B1), which determined their packaging into exosomes. Once in the extracellular space, exosomes can be internalized by different mechanisms, namely, membrane fusion, where the content of

exosomes is released into the cytosol, and endocytosis either by phagocytosis, macropinocytosis, clathrin-, caveolin- and lipid raft-mediated. The underlying mechanisms following internalization are yet to be clarified, but it is known that exosomes can fuse either with the endosomal membrane releasing their content or with lysosomes. For instance, the degradation of Aβ located on the surface of exosomes was referred to occur after their transported through the endocytic pathway to microglial lysosomes (Yuyama and Igarashi 2017). Anyway, the preferential uptake mechanism seems to depend on the recipient cell. In addition, exosomes can also induce receptor-mediated signaling transduction (Abels and Breakefield 2016; Mulcahy et al. 2014).

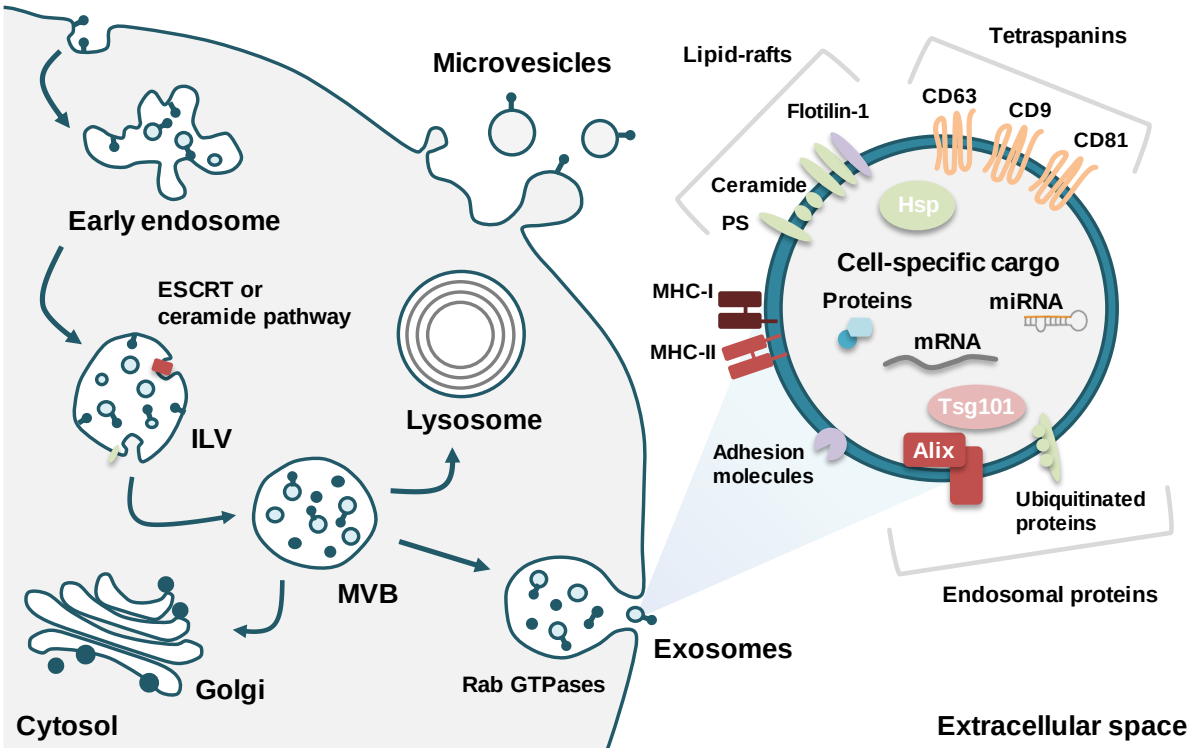

Figure I.5 - Exosome biogenesis and markers. Microvesicles result from the direct budding of the plasma membrane, ranging between 100-1000 nm in diameter. As part of the endocytic pathway, exosome biogenesis starts with the formation of the early endosome by invagination of the plasma membrane. Through the same process, the endosome accumulates intraluminal vesicles, which depend either on the ESCRT machinery or on the ceramide and phosphatidic acid or tetraspanins. Once the multivesicular body is completely formed it can follow three routes: proceed to the Golgi Apparatus for recycling, fuse with the lysosome for degradation, or fuse with cell membrane releasing the ~100 nm vesicles entitled exosomes. While still under investigation, this exocytic pathway is mediated by Rab GTPases. Whereas exosomal cargo includes cell-specific information (proteins, mRNAs, miRNAs and other non-coding RNAs), they also carry a set of proteins linked to their biogenesis. These include CD63, CD9, CD81 (tetraspanins), ceramide, flotilin-1 and phosphatidylserine (lipid-rafts), Alix, Tsg101 and ubiquitinated proteins (endosomal proteins), MHC-I and -II, Hsp and adhesion molecules.
ESCRT, Endosomal Sorting Complexes Required for Transport; mRNAs, messenger RNAs; CD, cluster of differentiation; MHC major histocompatibility complex class I and II; Hsp, heat shock proteins.

Exosomes have been implicated in a number of pathologies and important data have come from cancer investigation. Late studies have evidenced that exosomes contribute to disease dissemination by transporting mutant and misfolded proteins in a cell-to-cell basis or

even to distant areas where these proteins accumulate and cause damage (Levy 2017; Soria et al. 2017). In ALS, Grad and colleagues (2014b) have demonstrated that mutant SOD1 (mSOD1) and aggregated human wild type (WT) SOD1 are released from a motor neuron cell line (NSC-34) through exosomes and transmitted to naïve NSC-34 cells. It was additionally shown that TDP-43 is released from N2a and primary neurons via exosomes as a defensive mechanism of TDP-43 clearance, and brain-derived exosomes from patients revealed to induce nuclei-cytoplasm shuttling of TDP-43 in neurons (Iguchi et al. 2016), which is a hallmark of ALS-linked TDP-43 toxicity. With the same approach, Wang and coworkers (2017b) recently showed that Tau is transferred between neurons, and that Tau-containing exosomes isolated from the CSF of AD patients promote Tau aggregation in cultured neurons. N2a-shed exosomes also contain Aβ and exosomal proteins were identified in amyloid plaques of brain specimens from AD patients (Rajendran et al. 2006). Finally, exosomes were also shown to carry and propagate α-synuclein (Ngolab et al. 2017). Accumulation and aggregation of the protein were mainly observed in neurons.

MiRNAs are emerging as central exosomal cargo for their potential in modulating the function of recipient cells by regulating gene expression. In fact, studies have evidenced that horizontal transfer of miRNAs can modulate the function of recipient cells. For instance, Alexander and collaborators (2015) showed that miR-155 and miR-146a are transferred between immune cells *in vitro* and *in vivo*. MiR-155 potentiated the inflammatory response in recipient cells whereas miR-146a restrained activation. Additionally, exosomes from breast cancer cells (Chen et al. 2014) and glioblastoma cells (van der Vos et al. 2016) were able to confer chemoresistance to sensitive cells and microglia-phenotype alteration, respectively, which was suggested to be in part mediated by intercellular miRNA transfer.

3. Region-dependent diversity of microglia in the CNS

Early since the discovery of microglia by del Rio Hortega, microglia heterogeneity amongst brain areas were already suggested. Although some studies have shown regional differences, the specificities of microglia population and the physiological significance of such diversity across the CNS are still poorly understood. Lawson and colleagues (1990) described different morphologies comparing microglia from grey (radially branched) and white matter (longitudinal architecture). They additionally identified a round-shape microglia with short processes in areas where the BBB was lacking and associated with a higher level of basal activation (Olah et al. 2011), probably due to the interaction with serum proteins (Bohlen et al. 2017).

At the molecular level, it was demonstrated that microglial surface markers, including CD11b, CD40, CD45, CD80, CD86, CXCR3 and CCR9, were differentially expressed among

the striatum, hippocampus, cerebral cortex, cerebellum and spinal cord (de Haas et al. 2008). For example, CD11b was higher in spinal cord *vs.* cerebral cortex, and the hippocampus has much less CD80 expression than the cerebral cortex. *In vitro*, microglia obtained from different brain regions also evidenced dissimilar expression profiles of inflammatory mediators, either non-stimulated (Ren et al. 1999), or after LPS challenged (Kim et al. 2000), highlighting different susceptibilities to neuroinflammation-mediated damage. Indeed, ATP-stimulated microglia presented region-specific levels of neurotoxicity, being cortical and hippocampal the ones bearing stronger toxic effects (Lai et al. 2011). A recent genome wide study comparing microglia isolated from the cerebral cortex, hippocampus, striatum and cerebellum of adult mice have evidenced that region-dependent diversity mainly rely in metabolic and immune regulatory functions (Grabert et al. 2016). While microglia from all regions exhibit a $CD11^{+}F4/80^{+}CD45^{low}$ profile, as well as core signature genes (such as *Tmem119*, *Csf1r* and *Cx3cr1*), cortical and striatum-derived microglia had the transcriptional profile that mostly deviated from cerebellar microglia. Additionally, microglia obtained from the hippocampus and the cerebellum showed a more immune alert phenotype that differs from the classical and alternative polarization states. Expression of sensome proteins, associated with the sensing of endogenous ligands and microbes (Hickman et al. 2013), were increased in the cortex and striatum microglia when compared to the other regions.

Interestingly, unique microglial phenotypes were described in the cortex anchored at the initial segment of axons (Baalman et al. 2015), in the SVZ (Ribeiro Xavier et al. 2015) and in basal ganglia (De Biase et al. 2017). Accumulating evidence also point gender differences as a crucial contributor to microglia response diversity (Nissen 2017; Wolf et al. 2017), although researchers have only began to explore this issue.

Neurotransmitters have been hypothesized amongst the potential signals that determine the specific microglial behavior in each region. Indeed, the expression of neurotransmitters in specific neuronal populations as well as the expression of microglial neurotransmitter receptors differ across the CNS (Wolf et al. 2017). For instance, noradrenaline, but not dopamine, modulates microglia release of IL-6 and TNF-α after LPS stimulation (Färber et al. 2005). Altogether, because specific neuronal populations are affected in different neurodegenerative conditions, such as the dopaminergic neurons in PD or motor neurons in ALS, the specificities of microglia phenotype in each region may also be involved in the underlying disease-specific mechanisms.

3.1. Specificities of the spinal cord

Microglia processes are highly motile in the spinal cord white matter, illustrating their scavenging functions under normal conditions (Dibaj et al. 2010). Differences in microglia expression patterns between the brain and spinal cord, although very limited, have been reported in rodents. Taken together, spinal microglia was shown to express elevated levels of CD11b (de Haas et al. 2008; Li et al. 2016b), CD45, CD86 and CCR9, CD11c and MHC-II (Li et al. 2016b), *galectin-3* and *Mcp-1* (Nikodemova et al. 2014), and *Tnfa* (Crain and Watters 2016; Nikodemova et al. 2014), whereas *Bdnf*, *Il-10, Ifnbeta* (Crain and Watters 2016) and *Il-6* (Nikodemova et al. 2014) were similar to cortical microglia. The expression of *P2y12* was, in opposite, found to be decreased in spinal cord *vs.* cerebral cortex-derived microglia (Crain and Watters 2016), possibly reflecting a decreased ATP-mediated chemotactic ability. These findings suggest a more pro-inflammatory phenotype of microglia in the spinal cord, although dependent on specific mechanisms. Nonetheless, when exposed to LPS, brain-derived microglia were shown to release higher amounts of TNF-α, IL-1β and NO than spinal microglia. Li and coworkers (2016b) additionally showed that spinal and brain microglia respond differently to the anti-inflammatory minocycline in a chronic neuropathic pain model. Minocycline was able to attenuate spinal microglia response following spared nerve injury, but not of microglia from pre-frontal cortex, highlighting that microglia responses to damage are region-dependent.

Another important aspect potentially affecting microglia behavior resides in the intrinsic characteristics of BSCB. When compared to the BBB, the BSCB evidenced higher permeability to tracers and cytokines, and decreased expression of both tight (ZO1 and occluding) and adherens junctions (VE-cadherin and β-catenin) (Bartanusz et al. 2011; Reinhold and Rittner 2017). This vulnerability may add on the factors contributing to a higher basal activation of microglia at the spinal cord over that at the cortical region, and to easier infiltration of peripheral immune cells.

3.2. Pathologies involving microglia activation in the spinal cord

MS, SCI, neuropathic pain, ALS and motor neuron diseases are amongst the pathologies that affect the spinal cord and involve microglia activation. MS is a chronic demyelinating disorder driven by autoimmunity against myelin components. Intensive inflammation, axonal damage, gliosis and recruitment and activation of T-cells are key pathological hallmarks in focal demyelinated lesions, both in brain and spinal cord (Barateiro et al. 2015; Luo et al. 2017; Tiftikcioglu et al. 2017). In MS patients' samples, iNOS-expressing microglia (referred as M1-polarization) was found in both active and chronic lesions (Miron et al. 2013). Interestingly, accumulating evidence indicate a neuroprotective role for microglia in MS since

phagocytosis of neuronal and myelin debris are essential for remyelination (Domingues et al. 2016). Miron and colleagues (2013) showed that a transformation towards the M2 microglial phenotype during efficient remyelination was essential to oligodendrocyte differentiation. In a EAE mouse model, it was recently demonstrated that spinal microglia have a M1-profile (CD16/CD32) in the grey matter, whereas in the white one both M1 and M2 subtypes are observed (Shimizu et al. 2016). Also, treatment with nimodipine (a dihydropyridine known as an L-type calcium channel antagonist) induced spinal microglia apoptosis, increased remyelination and attenuated the clinical course of an EAE mouse model (Schampel et al. 2017).

More specific for the spinal cord, SCI has been largely associated with traumatic events, but it can also been developed due to tumors or infections, such as the Human Immunodeficiency Virus (HIV). Injury severity and location determine the symptoms that can vary between mild sensory/motor weakness, paraplegia or quadriplegia (Hirbec et al. 2017; Saghazadeh and Rezaei 2017). Microglia are the first responders upon injury and can exert neuroprotective or neurotoxic effects (David and Kroner 2011). Phagocytosis of cellular debris is referred as a pro-regenerative event, while production of IL-1β and TNF-α, which occurs 30 min after SCI in humans, or NO, account for a pro-inflammatory environment (David and Kroner 2011; Dibaj et al. 2010; Greenhalgh and David 2014; Yang et al. 2004). Using RNA-Seq and pathway analysis, a recent study showed that microglia/macrophages responses were time- but not severity-dependent. Upregulation of neuroprotective genes was observed in the first days post-injury, whereas both neurotoxic and neuroprotective genes were overexpressed alongside (Noristani et al. 2017). This inflammatory status is referred as secondary injury contributing to spread the initial damage to other spinal cord areas.

A growing body of evidence indicates that spinal microglia contribute to mechanisms leading to neuropathic pain. Briefly, this chronic condition arise from several nerve damage situations, including cancer, infection, trauma [such as SCI or peripheral nerve injury (PNI)], and diabetes, and is characterized by hyperexcitability of neurons at the dorsal horn of the spinal cord (indicated in Figure I.6). Spontaneous pain, hyperalgesia (increased pain perception of noxious stimuli), and tactile allodynia (pain hypersensitivity to normally innocuous stimuli), are the main symptoms (Tsuda 2016; Tsuda et al. 2017). Microglia activation in the dorsal horn occurs faster after PNI and directly contributes to pain hypersensitivity in models of neuropathic pain caused by PNI or diabetes (Narita et al. 2006; Pabreja et al. 2011). Research efforts have showed that the axis neuronal ATP - microglial $P2X_4$ receptor and CX3CL1-CX3CR1 are crucial to mediate microglia-induced pain (Tsuda et al. 2017; Zhang et al. 2017). Pharmacological blockade of $P2X_4$ receptor in the spinal cord reverted PNI-tactile allodynia and intrathecal delivery of $P2X_4$-stimulated microglia induces

allodynia in normal rats (Tsuda et al. 2003). CX3CL1-pain facilitation has been demonstrated by a number of studies and CX3CR1 knock-out reduces microglia activation, revert mechanical allodynia and attenuate pain hypersensitivity after spinal nerve damage (Clark et al. 2007; Gu et al. 2016; Staniland et al. 2010). Upon activation, microglia released factors disrupt the normal excitatory or inhibitory synaptic transmission in dorsal horn neurons, which result in excessive stimulation and pain symptoms. BDNF, TNF-α and IL-1β are among the factors mediating this effect (Tsuda et al. 2017).

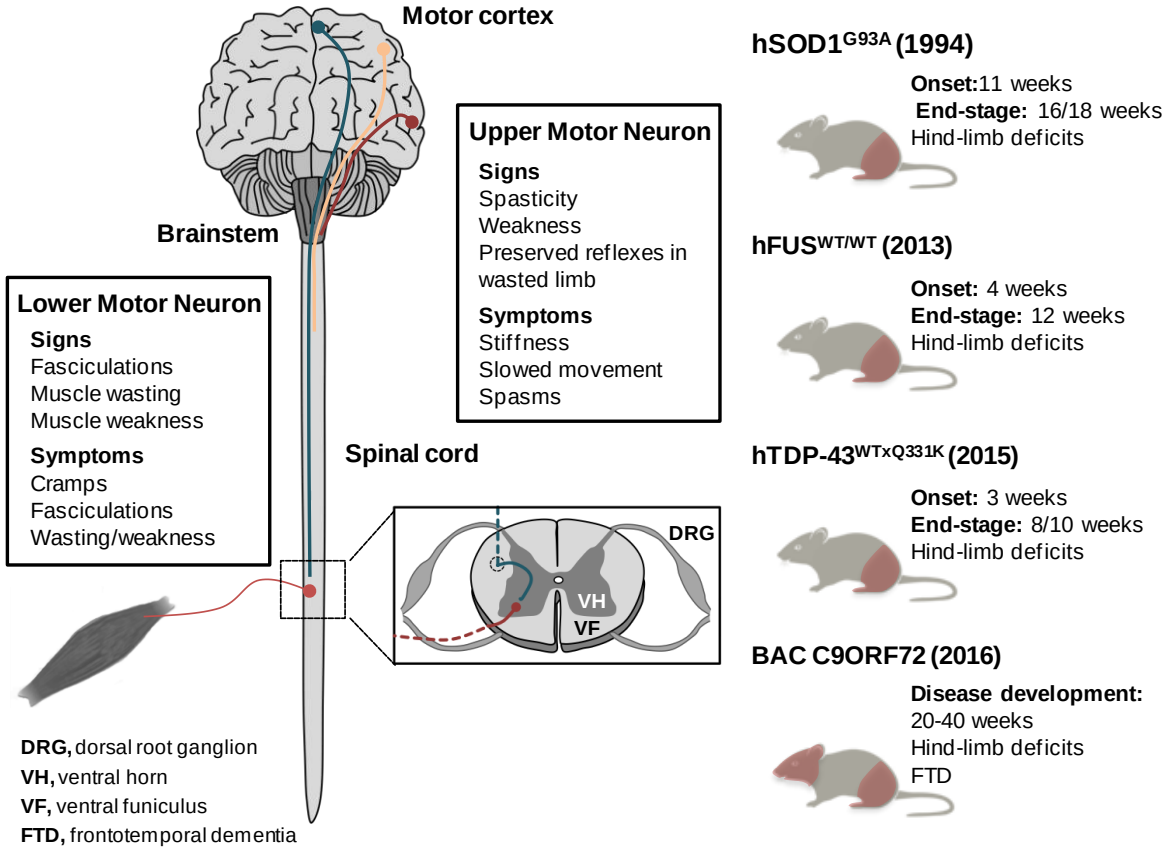

Figure I.6 - Corticospinal tract components affected in ALS and mouse models. ALS affects both upper motor neurons that project axons from the motor cortex to the brainstem and spinal cord and the lower motor neurons that connect the corticospinal tract to the muscles. The corticospinal tract crosses the spinal cord at its ventral side where the grey matter is designated as ventral horn and the white matter as ventral funiculus. The sensory spinal nerves cross the spinal cord at its dorsal side, where the cell bodies of the sensory neurons are accumulated in the DRGs. While distinct signs and symptoms result from degeneration of upper or lower motor neurons, ALS patients suffer from muscle weakness that starts in a specific region and then spreads throughout the body. Transgenic mice expressing the mutation G93A in the human protein SOD1 ($SOD1^{G93A}$) were developed in 1994 (Gurney et al. 1994) and have been the most studied ALS model. Recently, other models have been developed based on overexpression of human WT FUS ($FUS^{WT/WT}$) (Mitchell et al. 2012) and of human WT TDP-43 ($TDP\text{-}43^{WT}$) combined with mutant $TDP\text{-}34^{Q331K}$ (Mitchell et al. 2015), and on a repeated expansion of C9ORF72 (Liu et al. 2016b). These models reflect the most common mutations in ALS and the mice develop progressive disease resembling the human condition, with features specific for each mutation such as inclusions of the disease-causing protein.

SOD1, superoxide dismutase 1; FUS, fused in sarcoma; TDP-43, TAR DNA-binding protein; C9ORF72, chromosome 9 open reading frame 72; DRGs, dorsal root ganglions.

In opposite to the dorsal sensory network of the spinal cord, the ventral side controls the motor function. Upper motor neurons (UMN) extend their axons from the motor cortex into the brainstem and spinal cord where they contact with and stimulate the lower motor neurons (LMN) collectively forming the corticobulbar and corticospinal tracts. The last is characterized by large cell somas at the ventral horn while their processes widen into the peripheral nervous system to innervate the muscles, as schematically represented in Figure I.6. Motor neuron diseases, including spinal muscular atrophy (SMA) and ALS, are devastating and highly incapacitating disorders that also have an inflammatory component (Dharmadasa et al. 2017). As it will be further addressed, ALS progression is tightly associated with neuroinflammatory mechanisms with microglia directly contributing to motor neuron death (Frakes et al. 2014; Taylor et al. 2016), but there is a lack of research on this topic regarding other motor neuron disorders. For instance, the only studies focused on inflammation in SMA showed that inflammatory cytokines are elevated in SMA patients, and that microglia are activated in one SMA mouse model, but not in another more severe one (Deguise and Kothary 2017).

Overall, spinal microglia can exert different functions depending on the type of lesion or neurodegenerative process. While acute injury seems to promote both neurotoxic and neuroprotective/regenerative actions, chronic conditions are mainly associated with microglia-mediated neurodegeneration.

4. The role of microglia in Amyotrophic Lateral Sclerosis (ALS)

4.1. Overview on the etiology, epidemiology and clinical manifestation of ALS

ALS is a fast-progressing, neurodegenerative and lethal MND that was first described by the neurologist Jean-Martin Charcot in 1869. The pathological hallmark of ALS is the premature and selective death of UMN and LMN in the motor cortex, brainstem and spinal cord, which leads to muscle denervation and dysfunction (Boillée et al. 2006a). Importantly, whether ALS is in fact one disease, a syndrome or a spectrum of diseases is still a matter of debate (Al-Chalabi and Hardiman 2013; Dharmadasa et al. 2017; Grad et al. 2017). In the majority of cases considered as the “typical” ALS or just ALS, patients exhibit both UMN and LMN damage and, depending on where first symptoms occurred, designated as bulbar (facial, mouth/jaw and tongue muscles) or limb onset, which is the most common. Bulbar palsy associated to the localized involvement of the facial and mouth muscles, usually progresses towards UMN and LMN damage. Predominant UMN or LMN injury characterizes primary lateral sclerosis and progressive muscular atrophy, respectively (Dharmadasa et al. 2017; Grad et al. 2017).

ALS has a heterogeneous clinical presentation as the first symptoms depend on the location of the initial damage, which usually locates at the face, arms and legs, and rarely at the trunk and respiratory muscles. The discrete affected region at the onset spreads to neighboring areas and throughout the progression of the disease, patients usually suffer from general muscle atrophy and weakness (Figure I.6), muscle cramps and fasciculations (random and spontaneous twitching of muscle fibers), dysarthria (difficult speech control) and dysphagia (difficulty of swallowing). Ultimately, patients die by respiratory failure usually within 3-5 years from the first clinical manifestation (Kiernan et al. 2011). A reduced survival time is associated with older age at symptom onset, bulbar-onset and early involvement of respiratory muscles.

The mean age of onset of ALS is between 55-65 years, although some juvenile cases were also reported (Sheerin et al. 2014; Zou et al. 2012). Men are frequently more affected than women in a ratio of approximately 1.5-1. Worldwide ALS incidence and prevalence accounts for 2-3 and 6-8 per 100 000 individuals, respectively, although specific regions evidence higher estimates, such as Japan and the Pacific island Guam (Chiò et al. 2013). Nevertheless, the majority of studies have been performed in Europe and the United States of America (USA), and a new epidemiologic screening around the world is required. Nowadays, it is estimated that 700-800 people in Portugal suffer from ALS.

While the majority of ALS cases have unknown origin (classified as sporadic, sALS), in 5-10% cases of ALS it is caused by inherited genetic mutations, which are designated as familial ALS (fALS) and usually transmitted in an autossomal dominant fashion with high penetrance (Roggenbuck et al. 2016; Taylor et al. 2016). Mutations in SOD1, that account for 20% of the genetic forms, were the first reported and are the basis of the most studied *in vitro* and *in vivo* models of ALS (Gomes et al. 2008; Gurney 1994; Van Den Bosch 2011; Veyrat-Durebex et al. 2014). More recently, increased evidences suggest that RNA-binding proteins and alterations in RNA processing are powerful contributors to ALS pathogenesis (Ling et al. 2013). In fact, impaired RNA metabolism and processing were associated with mislocation of the nuclear TDP-43 or fused in sarcoma (FUS) in motor neurons, and were observed in both fALS and sALS patients (Kiernan et al. 2011; Taylor et al. 2016). A revolutionary finding in the ALS field was the presence of a non-coding GGGGCC hexanucleotide repeat in the first intron of the chromosome 9 open reading frame 72 (*C9ORF72*) gene (DeJesus-Hernandez et al. 2011; Renton et al. 2011) that accounts for about 40% of fALS and 7% of sALS (Majounie et al. 2012). Several other mutations are observed in ALS, including in the genes *HNRNPA1*, *SQSTM1*, *ANG* or *OPTN*, some of which are indicated in Table I.3. Interestingly, fALS-linked mutations, as well as misfolded SOD1, are also found in sALS patients (Bosco et al. 2010; Lattante et al. 2012), suggesting the

presence of common pathogenic mechanisms in both genetic and sporadic forms (Table I.3). In fact, fALS and sALS are clinically indistinguishable.

Of notice, the pathogenesis of frontotemporal dementia (FTD), which is characterized by neuronal death in frontal and temporal cortices triggering compromised judgment and executive skills, clearly overlaps with the one of ALS, not only at clinical, but also at the genetic level. C9ORF72 expansion is observed in 25% of familial FTD and in 88% of MND-FTD patients. Additionally, 50% of ALS patients present cognitive impairment, 15% of which have the symptoms of FTD (Dharmadasa et al. 2017; Grad et al. 2017; Majounie et al. 2012). Ubiquitinated TDP-43 inclusions are also a common feature linking ALS and FTD (Ling et al. 2013; Neumann et al. 2006).

Table I.3 - Genes involved in ALS cases

Gene	Protein	Function	% of fALS cases	First reported in fALS cases	Reported in sALS cases
SOD1	Superoxide dismutase 1	Superoxide dismutase	20%	(Rosen 1993)	(Gamez et al. 2006)
ANG	Angiogenin	Ribonuclease	<1%	(Greenway et al. 2006)	(Greenway et al. 2006)
TARDBP	TAR DNA-binding protein 43	RNA-binding protein	5%	(Sreedharan et al. 2008)	(Sreedharan et al. 2008)
FUS	Fused in sarcoma	RNA-binding protein	5%	(Vance et al. 2009)	(Zou et al. 2012)
OPTN	Optineurin	Autophagy adaptor	4%	(Maruyama et al. 2010)	(van Blitterswijk et al. 2012)
C9ORF72	Chromosome 9 open reading frame 72	Guanine nucleotide exchange factor?	~40%	(DeJesus-Hernandez et al. 2011)	(Renton et al. 2011)
UBQLN2	Ubiquilin 2	Autophagy adaptor	<1%	(Deng et al. 2011)	(Deng et al. 2011)
SQSTM1	Sequestosome 1	Autophagy adaptor	<1%	(Fecto et al. 2011)	(Fecto et al. 2011)
PFN1	Profilin 1	Actin-binding protein	<1%	(Wu et al. 2012a)	(Wu et al. 2012a)
HNRNPA1	hnRNP A1	RNA-binding protein	<1%	(Kim et al. 2013)	(Kim et al. 2013)
TBK1	Serine/threonine-protein kinase TBK1	Regulates autophagy and inflammation	?	(Freischmidt et al. 2015)	(Cirulli et al. 2015)

fALS, familiar ALS; sALS, sporadic ALS

Although the exact mechanism of disease pathogenesis remains unclear, ALS is recognized as a multifactorial disease comprising protein inclusions and altered molecular pathways within motor neurons but also involving inflammation and the activation of non-

neuronal cells, including astrocytes, microglia and oligodendrocytes. The mechanisms involved in motor neuron degeneration in ALS will be detailed in the following sections.

4.1.1. Diagnosis: focusing on the issue of biomarkers

Diagnostic delay is still an issue in ALS, as approximately an 11 month-period is usually required to ascertain a final ALS diagnosis. This delay has a huge impact on ALS patients as it limits appropriate health care, entrance at clinical trials and effectiveness of the available therapeutic agents (Nzwalo et al. 2014). Definite ALS diagnosis is still based on symptomatology and differential diagnosis according to the revised El Escoria criteria and the more recent Awaji criteria (updated in 2008 from the former) (De Carvalho et al. 2008). The Awaji criteria postulate the involvement of both UMN and LMN in 1 bulbar and 2 spinal regions or 3 spinal regions, as the former criteria. Additionally, it implies that neurophysiological recordings should be considered alongside with clinical information, and that fasciculation potentials are a crucial symptom (Costa et al. 2012; De Carvalho et al. 2017). Importantly, consultation with expert neurologists was indicated to reduce the delay in a definite diagnosis (Nzwalo et al. 2014). However, the discovery of novel biomarkers, mainly for the earlier stages of the disease, is an urgent need that depends on a better knowledge of ALS pathophysiological mechanisms.

Biomarkers constitute a measurable biological characteristic that reflect a biological or pathological condition and their discovery have been focused on body fluids (cerebrospinal fluid (CSF), blood, urine and saliva), due to their accessibility (Vu and Bowser 2017). Although the literature is not extensive, some potential biomarkers for ALS have been described, including neurofilament proteins, inflammatory mediators and miRNAs (Chen and Shang 2015; Vu and Bowser 2017). Neurofilaments are important constituents of motor neuron cytoskeleton that have been shown to accumulate during ALS pathogenesis. Upon motor neuron death, large amounts of neurofilaments are released to the CSF and blood. Several studies showed that both phosphorylated neurofilament heavy chain (pNFH) and neurofilament light chain (NFL) are elevated in the CSF and blood of ALS patients when compared to healthy or diseased controls, indicating their reliability as biomarkers for ALS (Boylan et al. 2013; Chen et al. 2016; Lu et al. 2015; Reijn et al. 2009). Interestingly, they have also been pointed out as indicators of prognosis. Higher levels in blood are associated with faster progression (Boylan et al. 2013; Lu et al. 2015). In addition, the combination of low levels of IL-10 and high levels of IL-6, granulocyte macrophage (GM)-CSF, IL-2, and IL-15 in the CSF distinguishes ALS from disease controls (Mitchell et al. 2009). Recently, the levels of TNFR1, TNF-α, IL-6, IL-1β, IL-8 and VEGF were also found increased in the blood of ALS patients comparing to controls (Hu et al. 2017).

The emerging role of miRNAs in different neurodegenerative diseases, including ALS, has highlighted their potential use as biomarkers. Although only a few studies have been performed, decreased CSF levels of thirteen miRNAs (for example, miR-115b-5p, miR-21-5p and miR-122-3p), together with increased miR-181-5p were found in sALS patients compared with healthy controls (Benigni et al. 2016). More recently, Waller and collaborators (2017) showed that miR-206 and miR-143-3p were increased and miR-374b-5p was decreased in the serum of ALS patients. While in the first study, the biological significance of the deregulated miRNAs requires further elucidation, in the last the authors suggest muscle denervation and degeneration as the cause.

Magnetic resonance imaging (MRI), functional MRI, magnetic resonance spectroscopy and positron emission tomography (PET) are among the neuroimaging techniques that have been considered for ALS diagnosis, due to their non-invasive approach (Chen and Shang 2015). In particular, novel PET targets and tracers have been developed to identify different pathological hallmarks, such as excitotoxicity and synaptic density, and a lot of effort has been dedicated to neuroinflammation (Tronel et al. 2017; Willekens et al. 2016). Specifically directed to microglia, the 18 kDa translocator protein (TSPO) is the most used microglial target in clinical use, although present in other myeloid cells as well, to which PET radioligands are being developed (Michell-Robinson et al. 2015). Interestingly, based on the ability to distinguish microglial TGF-β receptor from macrophages (Butovsky et al. 2014) it is expected that new PET radioligands for this surface target will be developed.

As previously referred, a promising strategy is also the use of exosomes as disease biomarkers, which has been showing positive outcomes in colorectal and lung cancer. More recently, researchers have begun to explore the content of exosomes as a biomarker for neurodegenerative conditions (Thompson et al. 2016). For example, proteomic analysis showed that exosome-associated syntetin 1 was abundant in samples from PD patients when compared to healthy controls (Tomlinson et al. 2015). One of the main advantages is the recognition of the producing cell by the expression of cell-specific proteins in the exosomes (Thompson et al. 2016).

4.2. Transgenic mouse models resembling a human condition

Based on the mutations found in fALS patients, several *in vivo* models have been generated. Genetic engineering of SOD1, TDP-43, FUS and C9ORF72 mutations has been conducted in mice, rats, zebrafish, fruitflies, canines and pigs [extensively reviewed in Picher-Martel et al. (2016)]. Because mice carrying SOD1 mutations have been the most extensively studied model in ALS, this section will be focused on SOD1-based pathology.

Clinical presentation of SOD1-ALS patients includes the most diverse well-described symptoms and it is poorly correlated with the specific mutation or the individuals within a family. Although the mean age of onset and disease progression rate also varies, patients with SOD1 mutations usually experience asymmetric weakness in one limb. Cognitive impairment is also rarely observed (Eisen et al. 2008; Millecamps et al. 2010). Different symptoms and progression rates can be detected when comparing fALS patients with distinct disease-causing proteins. SOD1 mutations determine later onset and longer lifespan than FUS mutations, the last being associated with the juvenile form of the disease. Whereas the affected region at onset in patients with SOD1 mutations is mainly the lower limbs, in TDP-43-ALS patients the first symptoms occur in the upper limbs. Patients with GGGGCC repeat expansion in C9ORF72 gene have the highest percentage of bulbar-onset and, together with FUS, have lower disease duration than other fALS-causing mutations (Millecamps et al. 2012; Millecamps et al. 2010).

The first mouse model carrying a SOD1 mutation was created in 1994 and expressed a substitution of a glycine over an alanine in position 93 (G93A) (Gurney et al. 1994), thereafter designated as *SOD1*^{G93A} mice. These mice develop progressive motor neuron disease recapitulating most of the clinical and neuropathological observations in patients. Motor deficits in Rotarod and Hangwire tests are observed around 3 months of age indicating hindlimb tremor and weakness. These first symptoms progress to hyper-reflexia and, due to motor neuron degeneration and muscle innervation, to paralysis and death after 4 months. Although SOD1 mutations in patients are associated with slow-progressing course, this mutation is associated with an early-onset and fast-progressing disease. Regarding pathogenic mechanisms, intracytoplasmic ubiquitinated SOD1 inclusions and gliosis are observed in mice *SOD1*^{G93A}, recapitulating the observations in SOD1-ALS patients (Hayashi et al. 2016; Kato et al. 2000).

More recently, three newly created mouse models for *FUS* (Mitchell et al. 2012), *TDP-43* (Mitchell et al. 2015) and *C9ORF72*-associated ALS (Liu et al. 2016b) were shown to develop progressive motor neuron disease and to reproduce the pathological hallmarks of the disease in each specific genotype. The creation of these novel ALS mouse models have increased the tools to explore the neuropathological mechanisms associated with motor neuron degeneration, which increases the hope for discovering novel biomarkers and targets, as well as new possibilities for testing new therapies.

4.3. Molecular pathways involved in motor neuron degeneration

Protein aggregation and formation of cytoplasmic inclusions are characteristic of motor neuron degeneration in ALS, which is transversal to fALS and sALS. SOD1 and FUS

inclusions are observed in patients with each specific disease-causing mutation (Rosen 1993; Vance et al. 2009). The repeated expansion in C9ORF72 gene can sequester RNA-binding proteins that accumulate in RNA foci and originate dipeptide repeats (DPR) through repeat-associated non-AUG (RAN) translation forming toxic inclusions (Taylor et al. 2016). Interestingly, TDP-43 aggregation is observed in almost all ALS cases (Ling et al. 2013). Although the mechanisms are not fully understood, insights into the toxicity associated with protein aggregation have been mostly investigated in SOD1 models.

SOD1 is a ubiquitous small antioxidant protein which catalyses the dismutation of superoxide radicals in hydrogen peroxide and oxygen. More than 170 mutations in SOD1 were already described in ALS cases (http://alsod.iop.kcl.ac.uk). Conformational instability and inappropriate folding leading to the formation of protein aggregates is indicated as the cause of SOD1-mediated toxicity (gain-of-function) (Pasinelli and Brown 2006). In fact, dismutase activity did not correlate with disease pathogenesis. Interestingly, a recent study identified non-native SOD1 trimers as the toxic species involved in motor neuron death (Proctor et al. 2016). SOD1 aggregation seems to be an early event in the disease pathogenesis and SOD-containing aggregates increase in abundance with disease progression (Bruijn et al. 1998). As shown in Figure I.7, several other interrelated mechanisms have been implicated in motor neuron atrophy in ALS, including oxidative stress (Mitsumoto et al. 2008; Shaw et al. 1995), mitochondrial dysfunction (Igoudjil et al. 2011; Sasaki and Iwata 2007; Vaz et al. 2015), ER stress (Atkin et al. 2008), impaired axonal transport and NF disorganization (De Vos et al. 2007), glutamate excitotoxicity (Spreux-Varoquaux et al. 2002; Vucic et al. 2008), impaired proteosome and autophagy (Kabashi et al. 2004; Tripathi et al. 2017), and Golgi fragmentation (Atkin et al. 2008). After the discovery of TDP-43 mutations and its presence in inclusions in about 90% of ALS patients, altered RNA metabolism, including biogenesis of miRNAs, gained a crucial attention (Paez-Colasante et al. 2015; Robberecht and Philips 2013). The majority of these mechanisms occur very early in ALS pathogenesis being observed before disease onset in mouse models.

A number of studies have been linking SOD1 accumulation with other disrupted mechanisms. For instance, SOD1 aggregates are known to sequester proteins such as the heat-shock proteins (Hsp) (Shinder et al. 2001), the poliubiquitine protein p62 (Gal et al. 2007) and the anti-apoptotic protein B-cell lymphoma 2 (BCL2) (Pasinelli et al. 2004), inducing reduced chaperone function, insufficient clearance of intracellular proteins and apoptotic-cell death, respectively. Mounting evidences showed that mSOD1 can accumulate at the intermembrane space and outer membrane of mitochondria causing vacuolation, alteration in morphology, mitochondrial dysfunction and degeneration (Igoudjil et al. 2011; Tafuri et al. 2015).

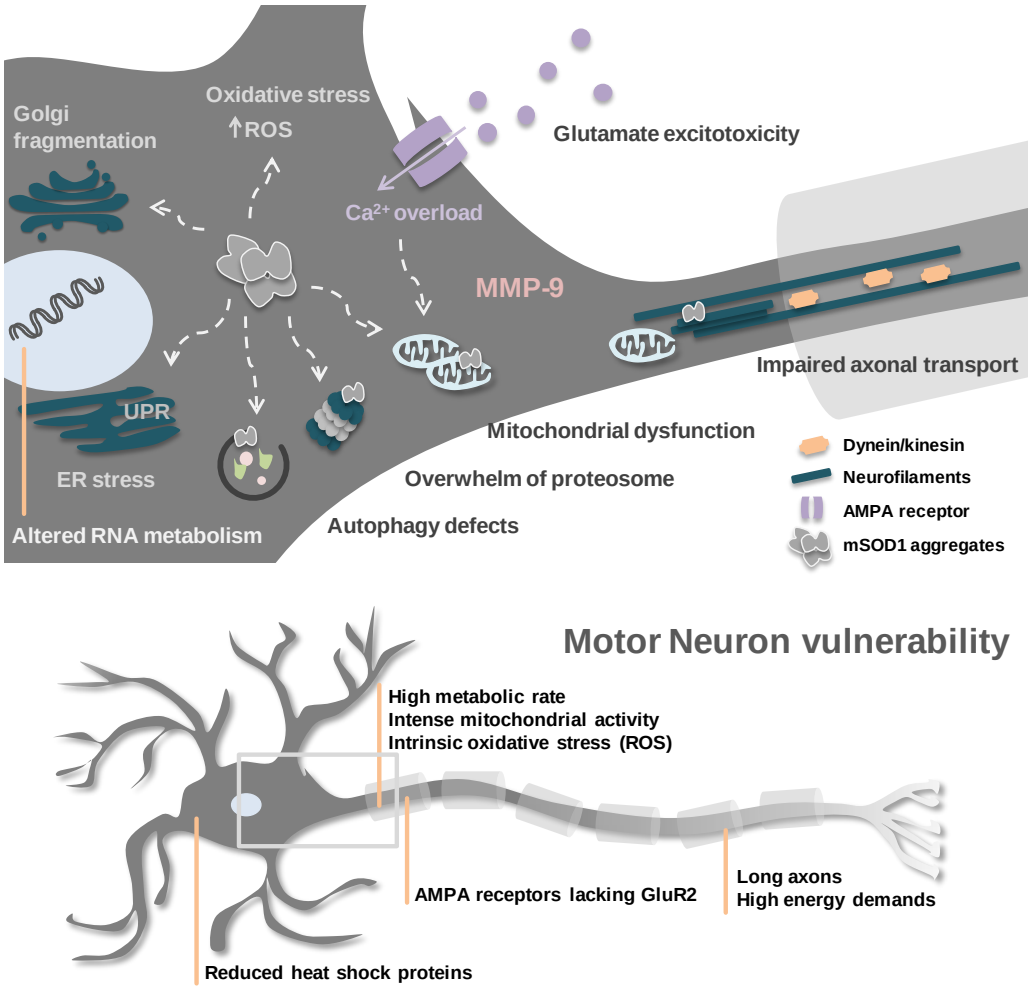

Figure I.7 - Molecular mechanisms involved in motor neurodegeneration in ALS. Mutated superoxide dismutase 1 (mSOD1) accumulation and aggregation promotes the disruption of several interrelated molecular pathways within motor neurons. UPR is elicited due to the formation of aggregates causing ER stress, together with overwhelming of the proteasome and autophagy defects. Golgi fragmentation and alterations of vesicular trafficking have been reported as well. Accumulation of mSOD1 also occurs in mitochondria promoting energy impairment, as well as increased production of ROS, thus contributing to oxidative stress in the motor neuron. Glutamate accumulation in the extracellular space can induce excitotoxicity with high Ca^{2+} entry, which further contribute to mitochondrial dysfunction. Impaired axonal transport is as well observed with the accumulation of neurofilaments, which may induce axonal retraction, and alterations in dynein- and kinesin-mediated transport. Although not directly related to mSOD1-mediated motor neuron injury, altered RNA metabolism is observed in different ALS models being a transversal mechanism of toxicity in motor neurons. Importantly, it was reported that the expression of MMP-9 is determinant for motor neuron death in ALS. Finally, special features of motor neurons may confer increased vulnerability to injury, namely the existence of high metabolic rate and intense mitochondria activity in their long axons with consequent intrinsic oxidative stress, the presence of AMPA receptors lacking the GluR2 subunit (impermeable to calcium ions entry), and reduced heat shock proteins which increases motor neuron susceptibility to protein misfolding and formation of aggregates.
UPR, unfolded protein response; ER, endoplasmic reticulum; ROS, reactive oxygen species; Ca^{2+}, calcium; MMP-9, matrix metalloproteinase-9; GluR2, glutamate receptor 2.

Three hypotheses have been proposed to describe the degeneration of both UMN and LMN in the corticospinal tracts: dying-back axonopathy, dying-forward and independent degeneration (Geevasinga et al. 2016; Nijssen et al. 2017). The dying-back phenomenon is well-known at the neuromuscular junction, where LMN axons are drawn back but no cell soma is lost in the anterior horn (Fischer et al. 2004). As motor neurons shrink, the

communication with the muscles is loss leading to muscle wasting and atrophy. A pathway linking motor neuron dying-back and SOD1 accumulation is reflected in the altered axonal transport due to mitochondrial dysfunction, which causes energy depletion and altered local protein synthesis at the pre-synaptic terminal (De Vos et al. 2007). The dying-forward hypothesis, on the other hand, describes that the early hyperexcitability of UMN before disease onset (Vucic et al. 2008) induces glutamate excitotoxicity-induced LMN degeneration. Independent and random degeneration of both UMN and LMN has also been suggested (Geevasinga et al. 2016).

Early studies have described apoptosis as the typical cell-death pathway by which motor neurons degenerate, which is illustrated by the activation of caspases 3, 7 and 9 and release of cytochrome *c* (Cyt *c*) (Guegan et al. 2001; Ilzecka 2011; Pasinelli and Brown 2006). With the increased knowledge on the diverse cell death mechanisms, it was recently showed that necroptosis is activated in motor neurons in both fALS and sALS models (Ito et al. 2016; Re et al. 2014), as indicated by high levels of receptor-interacting serine/threonine-protein kinase 1 (RIP1) and mixed lineage kinase domain-like (MLKL), which are markers of this caspase-independent programmed cell death. The mechanisms triggering each specific cell death pathway needs, however, further elucidation.

Despite extensive research effort, the selective vulnerability of motor neurons to mutations in ubiquitously expressed proteins remains mysterious. One hypothesis relies on specific motor neuron features that distinguish them from all the other CNS neurons, as depicted in Figure I.7. Interestingly, it was recently indicated that among the motor neuron population, some types of them seem to be more resistant to ALS-linked damage, such as the ones in the oculomotor system or in the fast-twitch fatigue-resistant (FR) motor neurons (Nijssen et al. 2017; Rozas et al. 2016). For example, Kaplan and colleagues (2014) showed that high MMP-9 expression in fast motor neurons was determinant to induce their degeneration in the *SOD1*^{G93A} model, where enhancement of ER stress was a key feature. Additionally, oculomotor neurons were shown to be more resistant to calcium-induced mitochondrial stress as they express the glutamate receptor 2 (GluR2) in AMPA receptors, a subunit that is lacking in motor neurons.

The fact that selective death of motor neurons begin focally and asymmetrically, and then progressively spreads to contiguous groups of motor neurons, suggest the existence of specific disseminating mechanisms. Prion-like mechanisms have been reported in SOD-linked ALS, meaning that a misfolded SOD1 protein can be transferred and is able to induce misfolding and aggregation in recipient cells (Grad et al. 2015). It was shown that mSOD1 can be actively secreted through a chromogranin chaperone-like process (Urushitani et al. 2006), or via exosomes, as above mentioned, either in the outer leaflet or in the lumen (Grad et al. 2014b). While SOD1 aggregates are taken up by microglia macropinocytosis,

exosomes were also observed in naïve NSC-34 cells, though the intake mechanism was not explored (Grad et al. 2014a; Silverman et al. 2016). This spreading mechanism was maintained through several passages of conditioned media incubation. Interestingly, overexpression of chromogranin A was shown to accelerate disease progression by increasing the amount of misfolded SOD1 in the extracellular environment (Ezzi et al. 2010). More recently, Ayers and colleagues (2016) showed that injection of spinal homogenates from paralyzed SOD1 mice into the sciatic nerve of adult *SOD1*$^{G85R\text{-}YFP}$ mice (develop later onset disease at 20 months) precipitated disease onset, and the injury was progressively propagated from the lumbar to the cervical spinal cord likewise the process in humans. Similar transmission mechanisms have been reported in TDP-43-ALS reinforcing the prion-like dissemination character of ALS pathogenesis (Grad et al. 2015; Silverman et al. 2016).

The well-described dissemination route of ALS also underlines an important role for glial cells that upon activation spread neuroinflammatory mediators to neighboring areas. In fact, ALS is a non-cell autonomous disease, where glial cells are actively involved in motor neuron injury, as it will be further addressed.

4.4. Non-cell autonomous disease: the role of glial cells

Since the demonstration that microglia and astrocytes were activated in post-mortem tissue of ALS patients, and in the spinal cord of ALS mice (Kawamata et al. 1992), the relevance of glial cell pathology has increased. Microglia activation was found in the motor cortex, the motor nuclei of the brainstem, along the corticospinal tract and in the ventral horn of the spinal cord (Kawamata et al. 1992) whereas astrogliosis was identified in both grey and white matter, in the ventral as well as the dorsal horn of the spinal cord, and in sites where the corticospinal tract enters the grey matter (Kushner et al. 1991; Nagy et al. 1994; Schiffer et al. 1996). Additionally, two independent studies evidenced that the expression of mSOD1 solely in motor neurons did not produce disease in transgenic mice (Lino et al. 2002; Pramatarova et al. 2001). Moreover, Clement and colleagues (2003) have demonstrated similar results by producing chimeric mice in which the expression of *SOD1*^{G93A} was selectively induced in motor neurons and in the surrounding glial cells. They showed that disease progressed slower when injured motor neurons were surrounded by healthy glia and, in contrast, signs of motor neuron damage were observed when microglia and astrocytes expressed mutant *SOD1*^{G93A}. However, it is still controversial whether glial cells have a role in disease onset or are just involved in exacerbating disease course. Indeed, mSOD1 gene excision from microglia (Boillée et al. 2006b) and selective reduction in astrocytes significantly delayed disease progression (Yamanaka et al. 2008a), while no changes were observed in disease onset. Surprisingly, two interesting studies showed that

ablation of proliferating microglia (Gowing et al. 2008) or astrocytes (Lepore et al. 2008a) did not affect motor neuron loss or disease progression in *SOD1*^{G93A} mice. These findings suggest that distinct populations of both glial cells may coexist and that proliferating glial cells may be engaged in a protective role. For instance, as previously mentioned, the recently described bipolar/rod-shaped microglia that are associated with neuroprotective properties are highly proliferative cells (Au and Ma 2017). Additionally, it was shown that microglia proliferation is beneficial after brain ischemia (Patel et al. 2013).

4.4.1. Astrocytes

Astrogliosis is a common hallmark of ALS and is observed in patients, as well as in mouse models (Vaz et al. 2016). *In vitro*, several lines of evidence indicate that astrocytes are toxic to motor neurons by releasing neurotoxic mediators. While the specific factors were not addressed, conditioned media from mouse *SOD1*^{G93A} astrocytes was shown to induce motor neuron excitability followed by death (Fritz et al. 2013). Pro-inflammatory mediators released from astrocytes derived from neural precursor cells of fALS and sALS patients also kill motor neurons (Haidet-Phillips et al. 2011). In addition, Meyer and colleagues (2014) have developed a method to convert adult human fibroblasts from fALS and sALS patients directly into astrocytes and were able to show that they were toxic when cocultured with motor neurons. More specifically, overexpression of NLRP3-inflammasome components (Johann et al. 2015), release of pro-nerve growth factor (NGF) (Ferraiuolo et al. 2011a), and reduced levels of GDNF and IGF-1 (Kaspar et al. 2003; Park et al. 2009), were indicated as factors involved in astrocyte-mediated motor neuron injury. Interestingly, neurotoxicity of sALS astrocytes was recently demonstrated *in vivo*. After transplantation into the spinal cord of adult WT mice, spinal neural progenitors from sALS patient iPSCs were able to be differentiated into astrocytes and colonized the entire spinal cord, inducing motor neuron deficits (Qian et al. 2017).

Diaz-Amarilla and colleagues (2011) have additionally characterized a population of astrocytes obtained from the spinal cord of symptomatic *SOD1*^{G93A} rats with extremely deleterious effects on motor neurons, which they designated as aberrant astrocytes. These astrocytes showed increased expression of S100B and Cx43 and lack of GLT-1. Interestingly, we recently observed that astrocytes obtained from the cortex of pre-symptomatic *SOD1*^{G93A} mice share similar features with this aberrant phenotype and are toxic to NSC-34 motor neurons, either expressing human SOD1^{WT} or SOD1^{G93A}, suggesting the neurotoxic potential of cortical astrocytes as well (unpublished data).

Most interesting, a recent study showed that reactive astrocytes obtained from stab-injury in the brain of adult WT mice induce protein aggregation and neurofilament inclusions, as

well as death of motor neurons at levels comparable with astrocytes obtained from adult *SOD1*^{G93A} mice (Tripathi et al. 2017). The study showed that TGF-β-induced autophagy defects were the underlying mechanism and that astrocytes caused toxicity regardless of genetic mutations. Interestingly, astrocyte-derived TGF-β was shown to accelerate disease in *SOD1*^{G93A} mice and to reduce microglial neuroprotective properties, including the production of IGF-1 (Endo et al. 2015).

One of the most relevant astrocyte-mediated motor neuron injuries is related to glutamate excitotoxicity. An early study in *SOD1*^{G93A} rats showed a strong reduction of GLT-1 in the spinal cord that started before motor neuron loss and progressively aggravated with the disease course (Howland et al. 2002). At the end-stage, a 90% reduction in GLT-1 was observed, which matched the loss verified in post-mortem spinal cord tissue from ALS patients (Rothstein et al. 1995). Importantly, astrocytes also participate in disease dissemination through the release of mSOD1, either by exosomes (Basso et al. 2013) or in a chromogranin-dependent pathway (Urushitani et al. 2006).

For all those findings, the interest in astrocytes as candidates for therapeutic strategies is increasing. As an example, transplantation of glial-restricted precursor cells in the spinal cord of *SOD1*^{G93A} rats demonstrated that these cells differentiated into GFAP-expressing astrocytes, rescued motor neuron injury and increased the survival rate of the animals (Lepore et al. 2008b). Benefits of the transplantation of astrocytes derived from stem cells are reviewed in Nicaise et al. (2015).

4.4.2. Oligodendrocytes

Less attention has been paid to the role of oligodendrocytes in ALS. Myelin abnormalities were found in pre-symptomatic SOD1 rats and aggravated in symptomatic stages. However, the contribution to disease is uncertain (Niebroj-Dobosz et al. 2007). Later, failure of oligodendrocyte metabolic support was suggested to contribute to motor neuron injury due to loss of the lactate transporter monocarboxylate transporter 1 (MCT1) (Kang et al. 2013; Lee et al. 2012b; Philips et al. 2013). This was observed in both ALS mouse models and patients (motor cortex and spinal cord). In addition, oligodendrocyte degeneration was observed in the gray matter of the spinal cord before disease onset and increased thereafter (Philips et al. 2013). Interestingly, grey matter demyelination was reported in patients (Kang et al. 2013). Removal of SOD1 from oligodendrocytes delayed disease onset and prolonged *SOD1*^{G37R} mice survival (Kang et al. 2013). Recently, Ferraiuolo and coworkers (2016) showed a direct neurotoxic effect of oligodendrocytes derived from iPSCs generated from fibroblasts of fALS and sALS patients. Oligodendrocyte-mediated motor neuron degeneration was caused by soluble and cell-contact mechanisms. Interestingly, knock-down of SOD1

rescued motor neurons when performed in progenitor cells, but not in differentiated oligodendrocytes from the different fALS and sALS patients, with the exception of C9ORF72 cases.

4.4.3. Peripheral immune cells infiltration

CNS infiltration of macrophages (Graves et al. 2004), monocytes (Zhang et al. 2005; Zondler et al. 2016) and T cells (Beers et al. 2011), but not B cells, was reported in ALS patients. While the percentage of T lymphocytes infiltrates are negligible at early disease stages, studies in ALS mice have indicated that T helper (CD4+) cells and T regulatory cells (Treg) are protective by inducing anti-inflammatory responses in microglia (Beers et al. 2008; Beers et al. 2011; Chiu et al. 2008). This effect was shown to be mediated, at least in part, by IL-4, which results in the symptomatic slow-phase of the disease. Accordingly, T cell depletion worsened disease progression. In contrast, modulating the inflammatory profile of monocytes reduced their infiltration, neuronal loss and prolonged mice lifespan (Butovsky et al. 2012). The role of peripheral immune cells in ALS is not completely understood. However, studying the functional phenotype of these circulating cells may serve as a biomarker of the disease, as indicated by recent studies showing abnormal profiles of both monocytes (Butovsky et al. 2012; Zondler et al. 2016) and T cells (Beers et al. 2017) from ALS patients.

An important aspect in peripheral immune cell infiltration relies in the permeability of the BBB and BSCB. Decreased expression of the endothelial tight/adherens junctions ZO-1, occludin and claudin-5 in presymptomatic *SOD1*^{G93A} mice indicate that vascular changes may precede motor neuron loss (Zhong et al. 2008). Garbuzova-Davis and coworkers additionally showed ultrastructural changes in both BBB and BSCB in sites of motor neuron loss in early and late symptomatic mice (Garbuzova-Davis et al. 2007a), being the last associated with vascular leakage of Evans blue (commonly used to evaluate barrier properties) (Garbuzova-Davis et al. 2007b). Disruption of the BSCB indicated by pericyte damage, IgG leakage and reduced tight and adherens junctions was later reported in patients by the same authors (Garbuzova-Davis et al. 2012). Although no correlation was so far studied, it is expected that the increase in BSCB permeability facilitates the infiltration of peripheral cells.

4.5. Microglia as central players in ALS

Several lines of evidence specify the involvement of microglia in motor neuron degeneration in ALS. PET scan imaging has evidenced the widespread of activated microglia in the brain of ALS patients (Corcia et al. 2013; Turner et al. 2004). Microglia activation in *SOD1*^{G93A} mice has been referred to occur before motor neuron degeneration and to

increase with disease progression till end-stage (Graber et al. 2010; Henkel et al. 2006). As previously referred, Boillée and colleagues (2006b) demonstrated that targeting *SOD1*^{G93A} specifically in microglia significantly slow disease progression in mice. Transplantation of bone marrow from WT mice into *SOD1*^{G93A}/*Pu.1*$^{-/-}$ mice (Beers et al. 2006) and into *SOD1*^{G93A} mice after microglia depletion with clodronate liposomes (Lee et al. 2012a), significantly decreased disease progression and prolonged mice lifespan.

In the following sections it will be discussed the phenotype of microglia in ALS, as well as the mechanisms of microglia activation and the mediators involved in cell-to-cell communication.

4.5.1. Phenotypic distinction along ALS progression

Microglial phenotypic distinction along ALS disease progression is not completely clarified. Primary *SOD1*^{G93A} microglia from 8-day-old mice have a pro-inflammatory and neurotoxic profile in culture (Xiao et al. 2007). In the presymptomatic stage (60 days) of *SOD1*^{G93A} mice, spinal microglia was indicated to express high levels of IL-10, which was associated with reduced innate immune responses to LPS (Gravel et al. 2016). Blocking IL-10 receptor precipitated clinical onset, while IL-10 overexpression delayed disease initiation and prolonged mice survival. Therefore, the authors suggested IL-10 expression as a protective mechanism to prevent disease development. A transformation from a M2-neuroprotective to a M1-neurotoxic microglial phenotype in the spinal cord of *SOD1*^{G93A} mice during disease progression has also been proposed (Beers et al. 2011; Liao et al. 2012). At the onset of disease, microglia express the M2-markers Ym1 and CD206 at comparable levels to WT microglia, but as disease progresses towards the end-stage, the expression of those markers decreases and NADPH oxidase 2 (NOX2) is upregulated (Figure I.8). Likewise, microglia isolated at the onset have neuroprotective effects while the M1-end-stage microglia kill motor neurons *in vitro* (Liao et al. 2012). Accordingly, other studies suggest the prevalence of M1-microglia in the symptomatic stage of *SOD1*^{G93A} mice (Beers et al. 2006; Frakes et al. 2014). Nonetheless, other evidences indicate that spinal *SOD1*^{G93A} microglia acutely isolated from the disease end-stage presented a distinctive phenotype when compared to M1 and M2 macrophages, or to LPS-stimulated microglia (Chiu et al. 2013). The authors additionally showed that mutant microglia coexpress neuroprotective and neurotoxic markers. Furthermore, Nikodemova and colleagues (2014) showed that at the onset, neither M1 nor M2 phenotypic markers change in microglia. Atypical phenotype with overexpression of VEGF, galectin3 and osteopontin and reduced M1/M2 markers, were associated with severe motor neuron degeneration in the spinal cord of *SOD1*^{G93A} rats at the end-stage. Interestingly, the authors showed that this phenotype does not respond to LPS, indicating its

impaired functionality and that it is not recapitulated by cortical microglia. While these last studies support the notion that microglia acquire a disease-specific phenotype, another report showed that increased number of Arg1-positive and iNOS-positive microglia throughout disease progression in *SOD1*^{G93A} mice (Lewis et al. 2014) is related with the coexistence of different phenotypes.

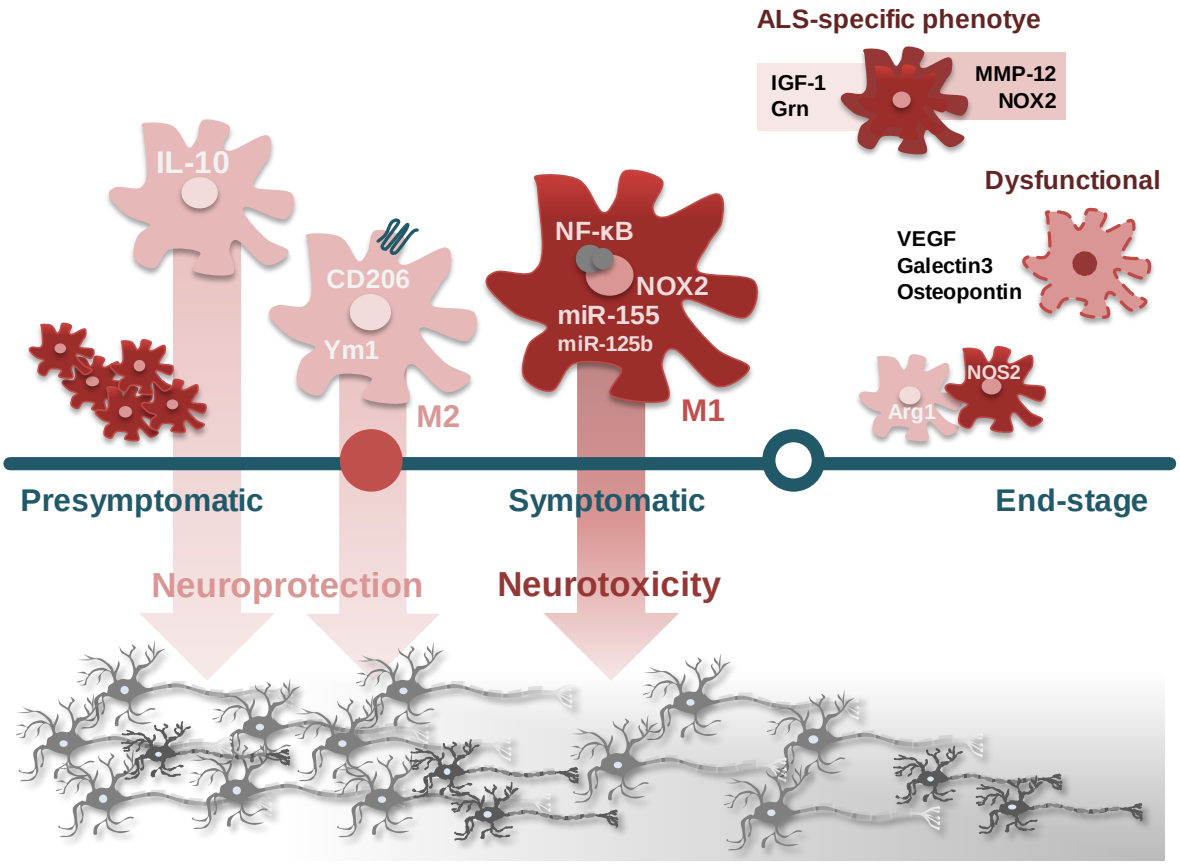

Figure I.8 - Microglia phenotypic transition along disease progression in ALS mice. At the presymptomatic stage, reactive and proliferative microglia have been observed. It was additionally demonstrated that at this stage, IL-10 overexpression in microglia is a protective mechanism delaying disease initiation. Once the symptoms appear (onset), microglia present a M2-phenotype characterized by the expression of CD206 and Ym-1. Both phenotypes were shown to confer neuroprotection. With the progression of the disease, microglia shift to a M1 pro-inflammatory state that induces toxicity towards motor neurons. NF-κB activation and upregulation of NOX2, miR-155 and miR-125b are indicated as mediators of microglia neurotoxicity. Close to the end-stage, independent studies show that microglia acquire multiple phenotypes, based on populations of microglia overexpressing Arg1 or NOS2, or a disease-specific status. A neurodegeneration-characteristic phenotype was reported for microglia expressing both anti- (IGF-1 and Grn) and pro-inflammatory (MMP-12 and NOX2) mediators. Finally, expression of VEGF, Galectin-3 and Osteopontin was associated with a dysfunctional microglia and related with severe motor neuron degeneration.
IL-10, interleukin-10; CD206, cluster of differentiation 206; NF-κB, nuclear factor-kappa B; NOX2, NADPH oxidase 2; miR, microRNA; Arg1, arginase 1; NOS2, nitric oxide synthase 2; IGF-1, insulin growth factor 1; Grn, progranulin; MMP-12, matrix metalloproteinase 12; VEGF, vascular endothelial growth factor.

Different studies have indicated that interaction with T cells participates in the regulation of microglia phenotype over the course of ALS (Beers et al. 2008; Chiu et al. 2008; Chiu et al. 2013). A curious finding was reported by Trias and collaborators (2013) on the change of microglia phenotype when collected from symptomatic mice into an astrocyte-like phenotype

(GFAP$^+$ and S100B$^+$), when cultured for two weeks. The authors proposed that a subpopulation of microglia may switch to an aberrant phenotype that contributes to disease progression.

Therefore, the role of microglia in ALS is still controversial and exploring microglial phenotype over disease course can bring new clues on the mechanisms that are being stimulated, allowing the development of disease stage-specific therapeutic strategies.

4.5.2. Neuroinflammatory pathways mediated by microglia

Damaged motor neurons seem to mediate the inflammatory response in a way dependent on the release of SOD1. In turn, microglia activation with extracellular SOD1^{G93A} induces motor neuron damage (Zhao et al. 2010). The authors showed that microglia recognition of mSOD1 is dependent on stimulation of TLR/CD14 receptors. In fact, TLR2 and TLR4, as well as RAGE, are elevated in the spinal cord of ALS patients (Casula et al. 2011), and *SOD1^{G93A}* mice lacking TLR4 have prolonged lifespan (Lee et al. 2015b). In addition, *in vitro* studies revealed that primary *SOD1^{G93A}* microglia show increased levels of TNF-α, ROS, NO and IL-6 compared with WT microglia, either unstimulated (Beers et al. 2006), or after stimulation with LPS (Liu et al. 2009; Xiao et al. 2007), and are more toxic to motor neurons.

Several neuroinflammation-related mediators have been found in ALS patients and in the spinal cord of mouse models. Although some anti-inflammatory cytokines, such as IL-4 and IL-10, were identified in the spinal cord of *SOD1^{G93A}* mice (Hensley et al. 2002), it is believed that a pro-inflammatory environment prevails in ALS. Increased expression of pro-inflammatory mediators, such as TNF-α, IL-1β, IL-6, cyclo-oxigenase-2 (COX2) and NOX2, were reported in ALS mice (Elliott 2001; Hensley et al. 2003; Hensley et al. 2002; Wu et al. 2006), as well as in ALS patients (Hu et al. 2017; Ono et al. 2001; Yiangou et al. 2006). MMP-9 and MMP-2 may account for the inflammatory mediators produced by microglia in ALS. High levels of MMP-9 were observed in CSF and skin of ALS patients (Fang et al. 2009), and in serum of symptomatic *SOD1^{G93A}* mice (Soon et al. 2010). Moreover, inhibition of MMP-9 activity (Lorenzl et al. 2006), or MMP-9 knock-out (Kiaei et al. 2007) in the *SOD1^{G93A}* mouse model, resulted in decreased motor neuron degeneration, improvement of motor function and prolonged mice survival. Despite the fact that HMGB1 is increased in the spinal cord of sporadic patients, its contribution to the inflammatory environment in ALS is unclear. Lo Coco (2007) showed that HMGB1 is mainly located at the nucleus of astrocytes, but even more of microglia in the spinal cord of *SOD1^{G93A}* mice. It was additionally suggested that the decrease of HMGB1 levels occurring in motor neurons along disease progression may result from its release to the extracellular media, where it can act as an alarmin. Moreover, motor neurons with SOD1 seem to be more susceptible to Fas/FADD/caspase 8 apoptosis pathway, as reported by Raoul and colleagues (2002). Relatively to FasL, also

known as the death receptor signal, it was found increased in the transgenic mice spinal cord (Hensley et al. 2002).

Crucial determinants of microglia-mediated motor neuron injury were reported. Frakes and colleagues (2014) showed that inhibiting NF-κB activation specifically in microglia rescued motor neurons in a coculture system and extended *SOD1*^{G93A} mice survival. Further supporting its role, NF-κB activation in WT microglia promoted motor neuron injury. Additionally, miR-155 targeting was shown to restore microglia homeostatic phenotypic signature and attenuated disease progression in *SOD1*^{G93A} mice (Butovsky et al. 2015). Importantly, upregulation of miR-155 was observed in the spinal cord of rodent models, as well as in both fALS and sALS patients (Butovsky et al. 2015; Butovsky et al. 2012; Koval et al. 2013). Upregulation of miR-155 before disease onset in *SOD1*^{G93A} mice (Butovsky et al. 2012), was also observed in the 3xTg AD mouse model (Guedes et al. 2014). Other miRNAs linked to neuroinflammation were also reported in ALS. These include upregulation of miR-146a in ALS patients (Koval et al. 2013) and of miR-125b in *SOD1*^{G93A} microglia (Parisi et al. 2013). A recent study showed that miR-125b targets A20 in *SOD1*^{G93A} microglia being involved in the regulation of NF-κB activation (Parisi et al. 2016). Data on inhibition of miR-125b supports motor neuron survival.

Microglial migratory and phagocytic ability have been poorly addressed in ALS. Two independent studies evidenced opposite results regarding microglia chemotaxis towards MCP-1. While Yamasaki and collaborators (2010) showed that primary *SOD1*^{G93A} microglia migrated less that non transgenic ones, although migration towards ATP was equivalent, no differences were obtained by Sargsyan et al. (2011). Phagocytosis in ALS is not well characterized, as well. Phagocytic microglia was found aggregated near motor neurons at the presymptomatic stage of a rat model of ALS (Sanagi et al. 2010). Another study using primary cortical *SOD1*^{G93A} microglia demonstrated that mutant cells have impaired ability to phagocyte neuronal debris, especially those expressing SOD1^{G93A} (Sargsyan et al. 2011). A rare variant in *TREM2* was lately described as a risk factor for the development of sporadic ALS (Cady et al. 2014), further suggesting compromised microglial phagocytic ability in ALS pathogenesis.

As a multifactorial disease, involving not only motor neuron injury, but also glial cell activation, ALS is potentially tightly related with deregulation of intercellular communication. However, despite the factors mediating motor neuron loss, changes in the motor neuron-microglia cross-talk axis are largely unexplored. Actually, it was only reported that inhibition of CX3CR1 worsened disease progression in mice (Cardona et al. 2006b), and that a variant in CX3CR1 gene in patients was correlated with a fast disease course (Lopez-Lopez et al. 2014). The interplay between microglia and astrocytes is also poorly understood and controversial reports support that microgliosis can either precede astrogliosis or vice versa

(Graber et al. 2010; Yamanaka et al. 2008a; Yang et al. 2010). A recent study further indicates that TGF-β produced by astrocytes inhibits microglia activation and their neuroprotective properties in the spinal cord of *SOD1*^{G93A} mice, while a microglial population expressing M1-phenotype markers seemed to remain unchanged (Endo et al. 2015). Besides suggesting the presence of multiple microglia subsets, with potential opposing functions, such study showed a direct detrimental effect of astrocytes on microglia behavior, as well.

Whereas several studies have been focused on determinants of microglia-mediated motor neuron death, almost nothing is known about microglia activation prior to disease onset. One may expect that early motor neuron changes, such as the above mentioned cortical hyperexcitability or ER alterations can be perceived by microglia inducing a, so far unknown, premature response.

4.6. Therapies under development

ALS is an extremely severe disease with no cure and attempts to find a novel therapeutic agent are imperative since the most common riluzole therapeutics, only slightly prolongs patients survival for a few months (Vucic et al. 2014). Riluzole is a benzothiazole derivative and has been proven to ameliorate glutamate excitotoxicity through different mechanisms including inhibition of pre-synaptic release of glutamate and inactivation of neuron sodium channels that reduce glutamate transmission. However, a different property seems to be associated with riluzole neuroprotection effects, as other anti-glutamate agents were not effective when tested in clinical trials (Ferraiuolo et al. 2011b). Together with riluzole, ALS patients' treatment includes control of the symptoms in order to improve their quality of life. Physiotherapy for weakness and disability, speech therapy and communication aids for dysarthria and analgesia for skin pressure pain due to immobility are some examples (Vucic et al. 2014). Additionally, non-invasive ventilation has been crucial in ALS welfare as it greatly improves quality of life and, more importantly, extends patient survival for up to 13 months (Dharmadasa et al. 2017). In May, this year, the U.S. Food and Drug Administration (FDA) approved a new drug to treat ALS, Radicava (edaravone), tested in Japan and in use there since 2015, bringing new hope for people living with ALS (https://www.fda.gov/newsevents/newsroom/pressannouncements/ucm557102.htm). The drug is thought to relief from oxidative stress effects, but has several side effects that include headaches, bruising and gait problems among the most common (https://alsnewstoday.com/2017/05/18/things-to-know-about-the-new-als-drug-radicava/).

Potential therapeutic approaches are intended to target the altered mechanisms observed in ALS pathogenesis and include protein homeostasis regulators, such as

chaperones and autophagy inducers, anti-oxidant and anti-apoptotic drugs, anti-inflammatory mediators and neurotrophic factors (Carlesi et al. 2011). Therapies targeting neuroinflammation have been popular and a number of drugs are currently being tested in clinical trials (Crisafulli et al. 2017). Masitinib, a tyrosine kinase inhibitor in Phase III clinical trial, is a promising product that already received the orphan drug designation by the FDA and a conditional marketing authorization application from the European Medicines Agency (EMA).

Another recent therapeutical proposal relies in miRNA-based therapies that have been growing in interest due to their wide range of action (Rupaimoole and Slack 2017). This has been commonly developed in cancer but less in ALS. Nevertheless, a miRNA-based strategy is being developed by miRagen Therapeutics to target miR-155 in ALS (MRG-107). Particularly important in the delivery of this small RNA molecule is the potential of exosomes as delivering vehicles. While offering protection against degradation, exosomes have the advantage of being non-immunogenic, in opposite to other vehicles like liposomes, for instance (Aryani and Denecke 2016). Sensitivity to target specific cells and passage across BBB and BSCB represent additional benefits of exosomes. Nevertheless, the use of exosomes as therapeutically carriers is still in its infancy and a number of issues needs further clarification, such as exosome loading capacity, dosage and biodistribution after systemic administration (Sarko and McKinney 2017). Remarkably, the adeno-associated virus serotype 9 (AAV9) was shown to efficiently transduce neonatal motor neurons and adult astrocytes following a peripheral injection, offering a novel CNS-specific delivery system (Foust et al. 2009). AAV9 carrying SOD1-shRNA was shown to reduce the levels of SOD1 in the spinal cord of mSOD1 mice promoting delayed onset and slowing disease progression (Foust et al. 2013).

Cell replacement therapies have also been explored. Indeed astrocyte and microglia precursor cell transplantation in the spinal cord of *SOD1*^{G93A} mice was shown to extend survival (Lee et al. 2012a; Lepore et al. 2008b). As reviewed in Thomsen et al. (2014b), a few clinical trials have been conducted using different cell transplantation approaches that include spinal cord injections of NSC and intrathecal/intramuscular injections of mesenchymal stem cells (MSC). A new horizon in personalized medicine arose with the exploitation of iPSCs for drug screening and engineered cells transplantation. As reviewed in Jaiswal (2017), we are one step closer to the use iPSCs in clinical practice in ALS since protocols for iPSCs-derivation into motor neurons have been developed and administration in rodent models tested. Cervical and dual-targeted intraspinal transplantation of neural stem cells in ALS patients were recently published and revealed to be feasible and well-tolerated (Feldman et al. 2014; Glass et al. 2016). Consensus points reflecting the design of phase II/III clinical trials were also published (Atassi et al. 2016). Recently, a combined stem cell

and gene therapy approach was approved by FDA and financed by the ALS Association in that stem cells releasing GDNF will be placed directly on only one side of the body, and muscle strength will be recorded together with safety outcomes (http://www.alsa.org/news/media/press-releases/fda-approves-clinical-trial-102416.html).

So far we may then conclude, based on the failure of several compounds and processes to effectively delay ALS progression and due to the multifactorial character of the disease, that therapeutic strategies should be designed to include several combined targets, as highlighted by the recent study of Frakes and colleagues (2017). They showed that targeting both astrocytes and microglia in *SOD1*^{G93A} mice could have a synergistic effect in sustaining mice survival for longer time than the modulation of one cell type alone.

5. Global Aims

Microgliosis and astrogliosis are typically observed in symptomatic ALS mice, as well as in ALS patients. However the underlying mechanisms of glial activation along disease progression, and changes occurring prior to disease onset, are still not fully understood. The players involved in the intercellular cross-talk, though largely unknown, are fundamental to fully understand functions and dysfunctions of glial cells and how they influence the fate of motor neurons. In this way, the global aim of the present thesis is to understand the determinants of microglia activation and astrocytes reactivity and their contribution to ALS disease initiation and progression. As experimental models we will use the mouse microglial cell line N9, the NSC-34 motor neurons transfected with human $SOD1^{G93A}$, and the *SOD1*^{G93A} mouse model. The ALS mice model will be the source for the isolation of microglia and astrocytes from the spinal cord of pups at 7 postnatal days, as well as for studying the course of disease by collecting spinal cord tissue at the pre-symptomatic (4-6 weeks-old) and symptomatic (12-14 weeks-old) stages. By studying stage-specific mechanisms, not only it is intended to explore novel promising biomarkers, including those for early ALS stages, but also to identify a set of therapeutic targets more directed to the specific environment associated with each stage of the disease, allowing the development of combined medicines to most effectively prevent neuroinflammation and neurodegeneration in ALS disease progression. Specific aims are to:

(i) Characterize the functions and markers involved in N9 microglia polarization towards the classical M1-phenotype after lipopolysaccharide (LPS) treatment, together with the content of their derived exosomes in inflammatory microRNA material (inflamma-miR), to later assess response differences of N9-microglial cells overexpressing $SOD1^{G93A}$ to LPS and exposed to exosomes released by NSC-34 motor neurons expressing $SOD1^{G93A}$ (mSOD1 motor neurons) (aim (ii));

(ii) Evaluate the cargo and the effect of exosomes derived from mSOD1 motor neurons on the phenotype of N9 microglial cells by identifying the induced inflammatory pathways and inflamma-miR profile changes, relatively to non-transfected NSC-34 cells;

(iii) Determine differences in glial- and inflammatory-related markers and cross-talk players in the spinal cord of *SOD1*^{G93A} mice at the pre- and symptomatic stages *vs.*wild type animals, to identify ALS stage-specific biomarkers and potential targets;

(iv) Investigate differences in the polarization features of microglia isolated from the spinal cord of the *SOD1*^{G93A} pups after short- and long-term cultures, as compared with matched wild type controls, and changes in their activation profile when co-incubated with astrocytes isolated from the same animals.

Chapter II

EXPLORING NEW INFLAMMATORY BIOMARKERS AND PATHWAYS DURING LPS-INDUCED M1 POLARIZATION

Carolina Cunha[1], Cátia Gomes[1], Ana Rita Vaz[1,2], Dora Brites[1,2]

[1]Neuron Glia Biology in Health and Disease Group, Research Institute for Medicines (iMed.ULisboa), Faculty of Pharmacy, Universidade de Lisboa, Avenida Professor Gama Pinto, 1640-003 Lisbon, Portugal

[2]Department of Biochemistry and Human Biology, Faculty of Pharmacy, Universidade de Lisboa, Lisbon, Portugal

***Mediators Inflamm*. (2016) 2016:6986175**

Abstract

Identification of mediators triggering microglia activation and transference of noncoding microRNA (miRNA) into exosomes are critical to dissect the mechanisms underlying neurodegeneration. We used lipopolysaccharide- (LPS-) induced N9 microglia activation to explore new biomarkers/signaling pathways and to identify inflammatory miRNA (inflamma-miR) in cells and their derived exosomes. Upregulation of iNOS and MHC-II (M1-markers) and downregulation of arginase 1, FIZZ1 (M2-markers), and CX3CR1 (M0/M2 polarization) confirmed the switch of N9 LPS-treated cells into the M1 phenotype, as described for macrophages/microglia. Cells showed increased proliferation, activated TLR4/TLR2/NF-κB pathway, and enhanced phagocytosis, further corroborated by upregulated MFG-E8. We found NLRP3-inflammasome activation in these cells, probably accounting for the increased extracellular content of the cytokine HMGB1 and of the MMP-9 we have observed. We demonstrate for the first time that the inflamma-miR profiling (upregulated miR-155 and miR-146a plus downregulated miR-124) in M1 polarized N9 cells, noticed by others in activated macrophages/microglia, was replicated in their derived exosomes, likely regulating the inflammatory response of recipient cells and dissemination processes. Data show that LPS-treated N9 cells behave like M1 polarized microglia/macrophages, while providing new targets for drug discovery. In particular, the study yields novel insights into the exosomal circulating miRNA during neuroinflammation important for emerging therapeutic approaches targeting microglia activation.

1. Introduction

Microglia are a unique cell population within the central nervous system (CNS) as they descend from myeloid origin and are commonly recognized as the resident immune cells in the brain (Vilhardt 2005). They constitute about 10-20% of glial cell population and are continuously monitoring the surrounding environment, acting as sensors of CNS homeostasis (Davalos et al. 2005; Nimmerjahn et al. 2005). Microglia rapidly change their morphology, gene expression, and functional performance upon any threat to tissue homeostasis, acquiring an activated phenotype, which is an adaptive process specific for each stimulus and CNS region (McKimmie et al. 2006). Accumulating evidence supports their involvement in synaptic development and remodeling (Perry and O'Connor 2010), emphasizing that microglial functions are extended beyond immune-defense mechanisms. Although microglial cells are first protectors of brain homeostasis, in case of prolonged or chronic stimulation they may become deleterious to the neuronal population. Indeed, exacerbated stages of neurotoxicity can progress to pathological conditions including neurodegenerative disorders such as Alzheimer's disease or Parkinson's disease (Graeber and Streit 2010), where microglia actively contributes to neuroinflammation and neuronal degeneration (Brites and Vaz 2014).

Despite the diversity of microglia responses, their activation has been characterized by a recognized number of phenotypes classically described for macrophages (Fernandes et al. 2014). The surveillant/nonpolarized phenotype, also known as M0, describes alert but not activated microglia which are continuously screening the environment (Ohsawa and Kohsaka 2011). The almost exclusive microglial fractalkine receptor, CX3C chemokine receptor 1 (CX3CR1), is highly expressed in M0 phenotype (Sheridan and Murphy 2013) but, besides the maintenance of microglia surveillance, CX3CR1/fractalkine cross talk is also important in promoting migration of activated cells (Cardona et al. 2006b). The M1 phenotype or classical activated microglia can be induced by lipopolysaccharide (LPS) or interferon-gamma (IFN-γ) with increased production of proinflammatory cytokines, chemokines, matrix metalloproteinases (MMPs), as well as reactive oxygen and nitrosative species (ROS and RNS, resp.), among others (Durafourt et al. 2012). M1 microglia is associated with a neurotoxic phenotype with enhanced major histocompatibility complex class II (MHC-II), inducible nitric oxide synthase (iNOS/NOS2), and interleukin-1β (IL-1β) markers. The alternative M2 phenotype that is related to the damage resolution (Chhor et al. 2013) may include several subtypes (Brites and Vaz 2014) and is induced by IL-4, IL-10, and transforming growth factor-β (TGF-β). Arginase 1 (arg1), found in inflammatory zone 1 (FIZZ1), and Ym1 are recognized markers of M2 polarization (Liu et al. 2012). However,

although the expression of these markers is used to differentiate microglia phenotypes, there is still much to learn about the determinants of microglia specific functional polarization.

Stimulation of the toll-like receptors (TLRs) signaling cascade is known to trigger the translocation of nuclear factor kappa B (NF-κB) into the nucleus and the expression of proinflammatory genes (Zhu et al. 2014), involving the activation of the inflammasome. However, its activation in the context of microglia neurotoxic potential remains unknown. Inflammasome mediators comprise NOD-like receptor family, pyrin domain containing 3 (NLRP3) and caspase-1 responsible for the cleavage of IL-18 and IL-1β proforms (Walsh et al. 2014). Recently, it was shown that the release of the alarmin high mobility group box 1 (HMGB1) is mediated by the NLRP3 inflammasome activation (Lu et al. 2013) and constitutes a signal to activate microglia (Park et al. 2004), though the regulation process is still unclear.

Together with the release of inflammatory mediators, microglia migration and phagocytosis are part of the cell response to injury. Protein milk fat globule-EGF factor 8 (MFG-E8) was shown to recognize phosphatidylserine (PS) in the apoptotic neurons, thus enabling microglial phagocytosis (Hanayama et al. 2002). Nevertheless, its specific regulation in different challenging situations remains unknown.

The majority of these inflammatory pathways have been identified along diverse studies performed with macrophage/microglia primary cultures. Due to such culture time consumption and reduced yield for the experimental assays, all the collected information on microglia inflammatory mediators is fragmented. Therefore, we here embraced the assessment of an integrated study on the several inflammatory signaling pathways leading to the upregulation of microglia M1 polarization biomarkers and downregulation of those related to M2 subtypes in the microglial N9 cells upon LPS treatment. N9 cells were generated by immortalization of embryonic primary cultures from the ventral mesencephalon and cerebral cortex of ICR/CD1 mice using oncogenic murine retroviruses carrying the v-myc or the v-mil oncogenes of the avian retrovirus MH2 (Righi et al. 1989b). These cells have been preferentially used due to the simplicity and ease of manipulation, but only a limited number of inflammatory mediators and genes were identified in N9 cells, despite responding similarly to LPS as primary microglial cells derived from the same mouse strain (Nikodemova and Watters 2011).

MicroRNAs (miRNAs) have recently emerged as key regulators of inflammation and as mediators of macrophage/microglia polarization (Freilich et al. 2013). Actually the inflamma-miRs, miR-155, and miR-146a have been related to the microglia polarization into M1. While the first enhances the proinflammatory response, the second acts as a negative regulator (He et al. 2014) being essential in halting excessive inflammation. Oppositely, miR-124, miR-21, and miR-145 are associated with an anti-inflammatory response repressing the M1

phenotype polarization (Ponomarev et al. 2013). However, it is accepted that such microglia phenotype regulation is quite complex and miR-146a, as an example, may be increased during M1 microglia polarization being also overexpressed in dystrophic/senescent macrophages (Jiang et al. 2012), whereas miR-124 has been identified in surveillant microglia, as well as in M2 microglia (Veremeyko et al. 2013). Another issue that has been recently addressed is the particular importance of the exosomes for sustained inflammation. Exosomes are small vesicles (~100 nm) formed through the endocytic process and released upon multivesicle bodies fusion with the plasma membrane (Aryani and Denecke 2016; Brites and Fernandes 2016). They have been associated with intercellular communication, even at long distances, by direct transfer of mRNA, proteins, and miRNAs, the last being essential for regulating gene expression in the recipient cells.

Since the pathways underlying the switch of microglia towards the M1 phenotype are not fully understood, we first characterized the polarization of N9 microglial cells into the M1 subtype upon LPS exposure, based on macrophage/microglia M1 and M2 biomarkers, and consequent microglia innate functions, such as phagocytosis and chemotaxis. Much attention has been lately given on microglia-dependent inflammasome activation (Burm et al. 2015; Gustin et al. 2015), but no data are available on LPS-treated microglia, which is the reason why we assessed the inflammasome multiprotein complex in our model. Once miRNAs are emerging as potent fine-tuners of neuroinflammation (Ksiazek-Winiarek et al. 2013) and indicated to regulate the inflammatory response when transported in exosomes from primary bone marrow-derived dendritic cells (Alexander et al. 2015), we decided to assess their representation in the LPS-polarized cells and in their derived exosomes to extend our knowledge on such issue, still scarcely explored in microglia primary cultures and unknown in N9 cells. Actually, exosomal miRNAs are currently being extensively studied as biomarkers of disease and the understanding on how they are loaded into exosomes and delivered to specific recipient cells may help in developing therapeutic approaches to modulate innate cell function. Here, we have further clarified microglia inflammatory mediators and targets that once modulated may restrict microglia activation in neurodegenerative disorders, like Alzheimer's disease and amyotrophic lateral sclerosis.

2. Materials and Methods

2.1. N9 Cell Culture and Treatment

N9 cell line was a gift from Teresa Pais (Institute of Molecular Medicine, Universidade de Lisboa, Portugal). Cells (8.3×10^4 cells/cm^2) were plated on uncoated 12- or 6-well tissue culture plates (Orange Scientific, Braine-l'Alleud, Belgium) in culture medium [RPMI media supplemented with fetal bovine serum (FBS) (10%) and L-glutamine (1%) and with the

antibiotic penicillin/streptomycin (1%)] and were grown to confluence before experiments. No bacterial contaminations were observed in any experiment. To induce N9 cells reactivity we used 300 ng/mL of lipopolysaccharide (LPS, *E. coli* O111:B4, 437627, Calbiochem, Darmstadt, Germany) diluted in basal media for 24 h, as described by Cui and colleagues (2002). Response of LPS-treated cells was compared with nontreated microglia (control).

2.2. Determination of Cell Death

Phycoerythrin-conjugated annexin V (V-PE) and 7-aminoactinomycin-D (7-AAD) mixture (Guava Nexin® Reagent, #4500-0450, Millipore, Billerica, MA, USA) were used to determine the percentage of viable, early-apoptotic, and late-apoptotic/necrotic cells by flow cytometry. After incubation, adherent microglia were collected by trypsinization and added to the cells present in the incubation media. After centrifugation, the pellet of cells was resuspended in PBS containing 1% of bovine serum albumin (BSA), stained with Guava Nexin Reagent according to manufacturer's instruction, and analyzed on a Guava easyCyte 5HT flow cytometer (Guava Nexin Software module, Millipore), as usual in our lab (Barateiro et al. 2012). Two readings were performed for each sample.

2.3. Quantitative RT-PCR

After incubation, cellular media were removed and cells were collected with TRIzol® (Life Tecnologies, Carlsbad, CA, USA) using a cell scrapper as implemented in the lab (Barateiro et al. 2013). Total RNA was then extracted from N9 cells using TRIzol reagent method according to manufacturer's instructions and quantified using NanodropND-100 Spectrophotometer (NanoDrop Technologies, Wilmington, DE, USA). Conversion into cDNA was performed with RevertAid H Minus First Strand cDNA Synthesis Kit (Thermo Scientific, Waltham, MA, USA). Quantitative RT-PCR (qRT-PCR) was performed by using β-actin as an endogenous control to normalize the expression level. The sequences used for primers are represented in Supplementary Table II.1. qRT-PCR was accomplished on a 7300 Real-Time PCR System (Applied Biosystems, Life Technologies) using a SYBR Green qPCR Master Mix (Thermo Scientific). The qRT-PCR was performed in 96-well plates with each sample performed in triplicate, and no-template control was included for each amplification. qRT-PCR was achieved under optimized conditions: 52ºC for 2 min followed by 95ºC for 10 min and finally 40 cycles at 95ºC for 0.15 min and 62ºC for 1 min. In order to verify the specificity of the amplification, a melt-curve analysis was performed, immediately after the amplification protocol. Nonspecific products of PCR were not found in any case. Relative mRNA concentrations were calculated using the ΔΔCT equation. For miRNA analysis, conversion of cDNA was achieved with the universal cDNA Synthesis Kit (Exiqon, Vedbaek, Denmark) as

described by Cardoso et al. (2012), following manufacturer's recommendations. The miRCURY LNA™ Universal RT miRNA PCR system (Exiqon) was used in combination with predesigned primers (Exiqon), represented in Supplementary Table II.1 (Supplementary Data), using SNORD110 as reference gene. The reaction conditions consisted of polymerase activation/denaturation and well-factor determination at 95ºC for 10 min, followed by 50 amplification cycles at 95ºC for 10 s and 60ºC for 1 min (ramp-rate 1.6ºC/s). Relative mRNA concentrations were calculated using the ΔΔCT equation. Two readings were performed for each sample.

2.4. Western Blot Analysis

After incubation, cellular media were removed and cells collected with Cell Lysis Buffer (Cell Signaling, Beverly, MA, USA) plus 1 mM phenylmethylsulfonyl fluoride (PMSF, Sigma) as usual in our lab (Fernandes et al. 2006). Briefly, total cell extracts were lysed for 5 minutes on ice with shaking, collected with cell scrapper, and sonicated for 20 secs. The lysate was then centrifuged at 14,000g for 10 min at 4ºC, and the supernatants were collected and stored at -80ºC. Nuclear extracts were prepared as usual in our lab (Fernandes et al. 2006). Protein content in the extracellular media was obtained by precipitation using trichloroacetic acid in 10% (v/v) of acetone solution. After a centrifugation of 15,000g for 10 min at 4ºC, the pellet was washed in acetone containing 10 mM dithiothreitol resuspended in lysis buffer and stored at -80ºC. Protein concentration in total and nuclear extracts, as well as in extracellular medium, was determined using a protein assay kit (Bio-Rad, Hercules, CA, USA) according to manufacturer's specifications. Then, equal amounts of protein were subject to SDS-PAGE and transferred to a nitrocellulose membrane. After blocking with 5% (w/v) nonfat milk solution, membranes were incubated with primary antibodies (Supplementary Material, Table II.2) diluted in 5% (w/v) BSA overnight at 4ºC, followed by the secondary antibodies goat anti-rabbit HRP-linked (1 : 5000, sc-2004, Santa Cruz Biotechnology®, CA, USA) and goat anti-mouse HRP-linked (1 : 5000, sc-2005, Santa Cruz Biotechnology) diluted in blocking solution. Chemiluminescence detection was performed by using LumiGLO® reagent (Cell Signaling) and bands were visualized in the ChemiDoc™ XRS System (Bio-Rad). The relative intensities of protein bands were analyzed using the Image Lab™ analysis software (Bio-Rad). One single reading was performed for each sample.

2.5. Immunocytochemistry

For immunofluorescence detection, N9 cells were fixed with freshly prepared 4% (w/v) paraformaldehyde in PBS and a standard immunocytochemical technique was performed as previously indicated (Fernandes et al. 2006). Briefly, cells were incubated overnight at 4ºC

with the primary antibodies: rabbit anti-Iba1 (1:250, 019-19741, Wako, Wako Pure Chemical Industries Ltd., Osaka, Japan), rabbit anti-NF-κB (1 : 500 or 1 : 200 for nuclear extracts, sc-372, Santa Cruz Biotechnology), and goat anti-Ki-67 (1 : 50, Santa Cruz Biotechnology, sc-7846). The secondary antibodies incubated for 2 h at room temperature were goat anti-rabbit Alexa Fluor 488, goat anti-rabbit Alexa Fluor 594, and rabbit anti-goat 594 (1:1000, Invitrogen Corporation™, Carlsbad, CA, USA). Cell nuclei were stained with Hoechst 33258 dye (blue, Sigma-Aldrich). Fluorescence was visualized using an AxioCam HR camera adapted to an AxioScope A1® microscope (Zeiss, Germany). Merged images of UV and fluorescence of ten random microscopic fields were acquired per sample by using Zen 2012 (blue edition, Zeiss) software. Original magnifications used were 400 and 630x.

For morphological characterization of N9 microglia, we used the particle measurement analysis in ImageJ (1.47v, NIH, USA) to automatically measure the 2D area, perimeter, and Feret's diameter of single microglia cells after Iba-1 immunostaining, which are considered valuable additional parameters to evaluate the shape of microglia (Kurpius et al. 2006). As indicated in Supplementary Figure II.1, we observed that ramified N9 microglia presented lower number of ramifications in comparison to primary cultured microglia (Supplementary Figure II.1B) obtained from mice cortex (Caldeira et al. 2014). Nevertheless, we were able to observe different N9 microglia morphologies that included round/oval shape (Supplementary Figure II.1B), ramified with 2 or 3 processes (Supplementary Figure II.1C-D), and amoeboid shape, either completely devoid of ramifications or with thicker and shorter branches (Supplementary Figure II.1D-E). Translocation of NF-κB from the cytoplasm to the nucleus was determined by the quantification of the number of NF-κB-positive nuclei and normalized to the total number of cells. For evaluation of the proliferation ability of microglia, we quantified the number of cells showing Ki-67 expression in the nucleus. Ki-67 is present in the nucleus during all phases of the cell cycle while being absent in the resting stage (G0).

2.6. Quantification of Nitrite Levels

NO levels were estimated by assessing the concentration of nitrites (NO_2), the stable end-product from NO metabolism, in culture media by the Griess method, as we published (Silva et al. 2011). Briefly, extracellular media free from cellular debris were mixed with Griess reagent in 96-well tissue culture plates for 10 min in the dark, at RT. The absorbance at 540 nm was determined using a microplate reader. A calibration curve was used for each assay. All samples were measured in duplicate and the mean value was used. Two readings were performed for each sample.

2.7. Gelatin Zymography

MMP-9 and MMP-2 activities were determined in the N9 extracellular media by performing a SDS-PAGE zymography in 0.1% gelatin-10% acrylamide gels, under nonreducing conditions, as previously described (Silva et al. 2010). After electrophoresis, the gels were washed for 1 h with 2.5% Triton-X-100 in 50 mM Tris pH 7.4 containing 5 mM $CaCl_2$ and 1 μM $ZnCl_2$, to remove SDS and to renature the MMP species in the gel. To induce gelatin lysis, the gels were incubated at 37ºC in the developing buffer (50 mM Tris pH 7.4, 5 mM $CaCl_2$, 1 μM $ZnCl_2$) overnight. For enzyme activity analysis, the gels were stained with 0.5% Coomassie Brilliant Blue R-250 (Sigma-Aldrich) and destained in 30% ethanol/10% acetic acid/H_2O (v/v). Gelatinase activity, detected as a white band on a blue background, was measured using computerized image analysis (Image Lab, Bio-Rad). One reading was performed for each sample.

2.8. Caspase-1 Activity Assay

Activity of caspase-1 was determined by a colorimetric method (Calbiochem, Darmstadt, Germany) as published by us (Fernandes et al. 2007). Briefly, cells were harvested, washed with ice-cold PBS, and lysed for 30 min on ice in the lysis buffer. The activity of caspase-1 was assessed in cell lysates by enzymatic cleavage of chromophore pNA from the substrate, according to manufacturer's instructions. The proteolytic reaction was carried out in protease assay buffer containing 2 mM Ac-YVAD-pNA. Following incubation of the reaction mixtures, the formation of pNA was measured at λ = 405 nm with a reference filter of 620 nm. One reading was performed for each sample.

2.9. Microglial Phagocytosis Assay

To evaluate the phagocytic ability of N9 microglia, cells were incubated with 0.0025% (w/w) fluorescent latex beads, diameter 1 μm, for 75 min at 37ºC and fixed with freshly prepared 4% (w/v) paraformaldehyde in PBS. N9 cells were immunostained with rabbit anti-Iba1 (1:250, 019-19741, Wako), and nuclei were counterstained with Hoechst 33258 dye (blue). UV and fluorescence images of ten random microscopic fields (original magnification: 400x) were acquired per sample by using Zen 2012 (blue edition, Zeiss) software. Total phagocytic cells and the number of ingested beads per cell were counted with ImageJ software to determine the percentage of phagocytic cells and the mean number of ingested beads per cell (Silva et al. 2010).

2.10. Cell Migration Assay

Cell migration assay was performed in a 48-well microchemotaxis chamber (Boyden Chamber, Neuro Probe, Gaithersburg, MD, USA) as we published (Caldeira et al. 2014). Briefly, N9 cells were resuspended in serum-free RPMI and 50 µL of cell suspension was placed into each top well (2-4 × 10^4 cells per well). The bottom wells were filled with serum-free RPMI (basal medium) alone, or with ATP (10 µM), and LPS (300 ng/mL) diluted in basal medium. Microglial cells were allowed to migrate for 6 h through a polycarbonate track-etch membrane with polyvinylpyrrolidone (PVP) (Neuro Probe) towards the solution in the bottom wells. Afterwards, the membrane was removed and the bottom side fixed with cold methanol. Cells were stained with 10% Giemsa in PBS (w/v), freshly prepared and filtered. The number of total cells was counted in ten microscopic fields with ImageJ software (original magnification: 100x) acquired to observe the complete well using Leica IM50 software and Leica DFC490 camera (Leica Microsystems, Wetzlar, Germany), adapted to an AxioSkope HBO50 microscope (Zeiss). For each experiment, at least three wells per condition were acquired.

2.11. Exosome Isolation

Exosomes were obtained from the extracellular media of N9 cells either from control or from LPS-stimulated cells, according to Wang et al. (2010), with minor modifications. Briefly, 20 ml of extracellular media was centrifuged at 1,000g for 10 min to remove dead cells and debris followed by another centrifugation at 16,000g for 60 min, to separate microvesicles (size ~1000 nm). The recovered supernatant was passed through a 0.2 µm filter to remove suspended particles and further centrifuged in the Ultra L-XP100 centrifuge (Beckman Coulter Inc., California, USA) at 100,000g for 120 min. This pellet fraction (exosomes, size ~100 nm) was resuspended in PBS and centrifuged again at 100,000g for 120 min. The final pellet containing exosomes was resuspended in lysis buffer and RNA inside exosomes was extracted using miRCURY Isolation Kit-Cell (Exiqon), according to manufacturer's instructions. Briefly, after lysis of the exosomes, the RNA was absorbed to a silica matrix, washed with the recommended buffers, and eluted with 20 µL of the supplied elution buffer by centrifugation. The synthesis of cDNA and qRT-PCR was performed as mentioned above.

2.12. Dynamic Light-Scattering (DLS) Measurements

Size measurements were made at 25ºC with a Zetasizer Nano S DLS apparatus (Malvern Instruments, Worcestershire, UK). After the ultracentrifugation procedure abovementioned, each sample was diluted in PBS and was read three times in the Zeta Sizer Nano S (Zen 1600) to evaluate the diameter of the collected particles. A histogram of the percentage of

particles with specific diameters was calculated using DTS (nano) 7.03 software (Malvern Instruments). Data represent an average of 3 measurements for each sample.

2.13. Statistical Analysis

The results of at least four independent experiments are expressed as mean ± s.e.m. Comparisons between LPS-treated N9 cells and nontreated cells (control) in all experiments were made via two-tailed Student's *t*-test or unpaired *t*-test with Welch's correction, depending on whether variances were equal or different, respectively. Comparison of more than two groups, namely, in the morphological characterization, chemotaxis assay, and phagocytosis tests, was done by one-way ANOVA followed by multiple comparisons Bonferroni post hoc correction using GraphPad Prism 5 (GraphPad Software, San Diego, CA, USA). Values of $p < 0.05$ were considered statistically significant and those of $p < 0.01$ and $p < 0.001$ highly significant.

3. Results

3.1. LPS-Treated N9 Microglia Acquire a M1 Phenotype, with Upregulation of Specific M1-Markers, with Main Amoeboid Morphology and Increased Proliferation Rate

Despite the great plasticity of microglial responses, the different subsets of microglia activation have been characterized by the expression of specific markers, as previously referred. Moreover, in addition to the well-known proinflammatory response mediated by TLR/NF-kB pathway, microglia activation may also imply the alteration of the gene expression profile not only by inducing the transcription of specific genes but also by downregulating nonrequired functions. We have explored the mRNA expression of M1 and M2 markers, as well as the fractalkine receptor CX3CR1 in N9 microglia exposed to LPS, not fully documented in previous studies. As shown in Figure II.1, incubation of N9 microglia with LPS led to increased expression of the M1-markers *Nos2* and *Mhc-II*, while promoting the downregulation of the M2-markers *arg1* and *Fizz1* (Figure II.1A). Expression of both mRNA and protein levels of CX3CR1 were found diminished by LPS exposure (Figures II.1B, C), indicating a reduced prevalence of cells with surveillant/anti-inflammatory properties, thus favoring a major representation of M1 polarized microglial cells.

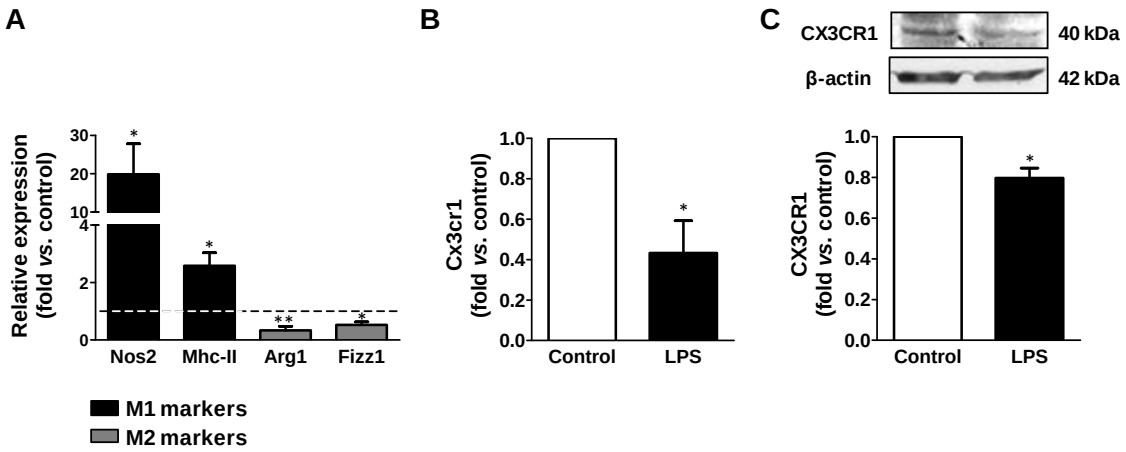

Figure II.1 - Lipopolysaccharide (LPS) polarizes N9 microglia into M1 rather than M2 phenotype. Expression of genes [inducible nitric oxide synthase (*Nos2*), major histocompatibility complex class II (*Mhc-II*), arginase 1 (*Arg1*), found in inflammatory zone 1 (*Fizz1*) (A), and CX3C chemokine receptor 1 (*Cx3cr1*)] (B) was determined by qRT-PCR (each sample was evaluated in duplicate). Markers of classically (M1) and alternatively activated (M2) microglia are indicated in black and gray, respectively. CX3CR1 protein levels were assessed by Western blot analysis (C). Comparisons between LPS-treated N9 cells and nontreated cells (control) were made via two-tailed Student's *t*-test. Results are mean ± s.e.m. from five (A, C) or six (B) independent experiments. Results from Western blot (C) were performed in duplicate. *p < 0.05 and **p < 0.01 versus nontreated cells (control, assumed value of 1, dashed line).

Morphological changes and increased cell density have been indicated for microgliosis (Streit et al. 1999). Although insufficient to characterize microglial functional behavior, these parameters are still useful to illustrate microglia activation. Therefore, we have additionally performed a morphological characterization by immunocytochemistry using the microglia specific marker Iba1, together with cell area, perimeter, and Feret's diameter (Kurpius et al. 2006). As depicted in Figure II.2, our results showed that N9 microglia change from a round/oval or ramified morphology to an amoeboid shape, presenting either a complete absence of ramifications or the presence of thicker and shorter branches, in about 75% of the cells ($p < 0.001$) incubated with LPS (Figures II.2A, B). We have previously shown that reactive isolated primary microglial cultures also show a similar morphology (Caldeira et al. 2014). Accordingly, area, perimeter, and Feret's diameter were increased in LPS-treated cells (Figures II.2C-E). In order to evaluate cell density, we evaluated the *Cd11b* expression and the number of cells presenting nuclear Ki-67 expression. We observed an increased *Cd11b* expression (Figure II.2F) and a higher number of Ki-67-positive nuclei (Figures II.2G, H) in LPS-stimulated cells as compared with control samples. Now, considering the cellular viability of N9 microglia after LPS exposure, we found that the number of viable cells was decreased (from 84% in control to 67% in LPS-treated N9 cells, $p < 0.01$, Table II.1), as a consequence of the increased number of microglia showing early-apoptotic features.

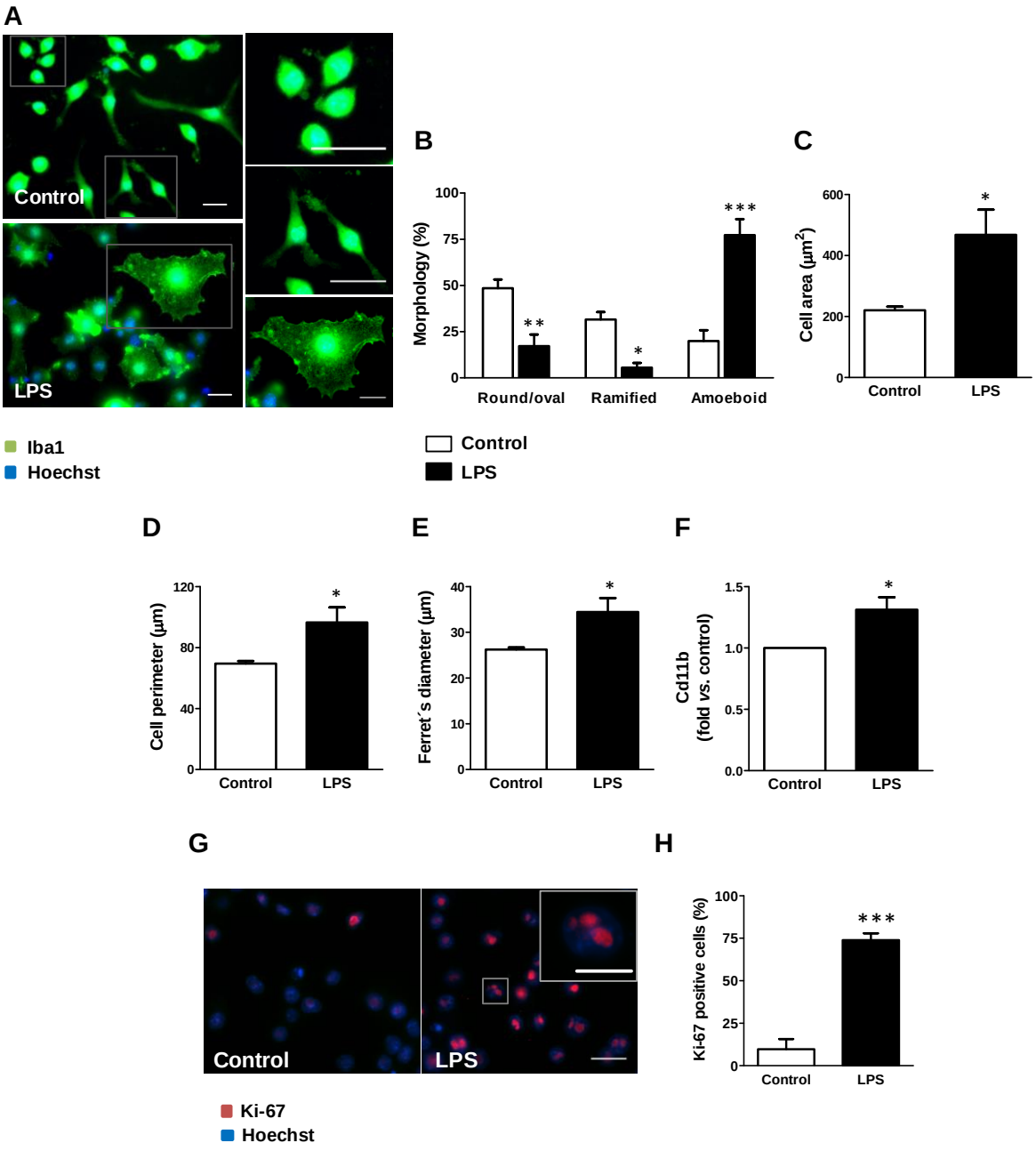

Figure II.2 - M1 polarized N9 microglia display amoeboid morphology, together with increased cell area, perimeter, and Feret's diameter, while showing increased proliferation rate based on the high representation of CD11b and Ki-67 positive cells. Morphological analysis and detection of Ki-67 in the nucleus were performed by immunocytochemistry using anti-Iba1 and anti-Ki-67, respectively, as indicated in Materials and Methods. For morphology, representative results of one experiment are shown (A) and quantified as the percentage of cells with different morphologies, namely, round/oval, ramified, and amoeboid (B). Evaluation of cell area (C), perimeter (D), and Feret's diameter (E) was performed using the computer program ImageJ. *Cd11b* expression was assessed by qRT-PCR (F). Representative results of Ki-67 immunostaining are shown (G) and expressed as the percentage of Ki-67 positive cells versus total number of cells (H). Results are mean ± s.e.m. from four independent experiments, except for *Cd11b* expression (f), where five experiments were performed. Comparison of more than two groups (B) was done by one-way ANOVA followed by multiple comparisons Bonferroni post hoc correction. Comparisons between lipopolysaccharide-treated (LPS-treated) N9 cells and nontreated cells (control) were made via two-tailed Student's *t*-test (F, G) or unpaired *t*-test with Welch's correction (c, d, e). *p < 0.05, **p < 0.01, and ***p < 0.001 versus nontreated cells (control). Scale bar represents 20 µm (and 10 µm in the close-up shown inset in G).

Table II.1 - N9 microglia exposed to LPS show increased cell death as indicated by Guava Nexin® assay

	Viable cells (%)	Early apoptosis (%)	Late apoptosis/Necrosis (%)
Control	84 ± 8.3	10.6 ± 4.2	5.0 ± 3.0
LPS	66.9 ± 4.5*	23.3 ± 7.6*	10.3 ± 5.0*

Phycoerythrin-conjugated annexin V (V-PE) and 7-aminoactinomycin D (7-AAD) (Guava Nexin® Reagent, #4500-0450, Millipore) were used to determine the percentage of viable, early-apoptotic and late-apoptotic/necrotic cells by flow cytometry. After incubation, cells were trypsinized, added to extracellular media and then stained with annexin V-PE and 7-AAD. Samples were analysed on a Guava easyCyte 5HT flow cytometer (Guava Nexin® Software module, Millipore). Three distinct populations of cells were identified: viable cells (annexin V-PE and 7-AAD negative), early apoptotic cells (annexin V-PE positive and 7-AAD negative), and late stages of apoptosis/necrosis (annexin V-PE and 7-AAD positive). *$p < 0.05$ versus nontreated cells (Control).

3.2. M1 Polarized N9 Microglia Show Reduced Migration Ability Towards Chemoattractants but Display Increased Phagocytosis and MFG-E8 Expression

After confirming the typical features of microglia M1 polarization in N9 cells, we wondered whether LPS was able to modify their migration ability. For that, we have performed a chemotaxis assay using the Boyden Chamber, and migration of LPS-treated and nontreated microglia was tested towards well-known chemoattractants, such as ATP (10 μM) (Davalos et al. 2005; Ohsawa and Kohsaka 2011) and LPS (300 ng/mL) (Mashimo et al. 2008). Nontreated N9 cells were highly responsive to ATP chemoattraction (~2-fold increase, $p < 0.001$) in comparison to those freely migrating to the basal medium and to the LPS-treated cells that were revealed to become unresponsive (Figure II.3). To note, however, is that LPS-treated cells showed the same migration ability as nontreated microglia towards the basal medium. LPS revealed a lower chemoattractive capacity when compared to that of ATP ($p < 0.001$) and, as observed for ATP, the LPS-treated cells also showed a reduced mobility as compared to cells that were not exposed to LPS stimulus.

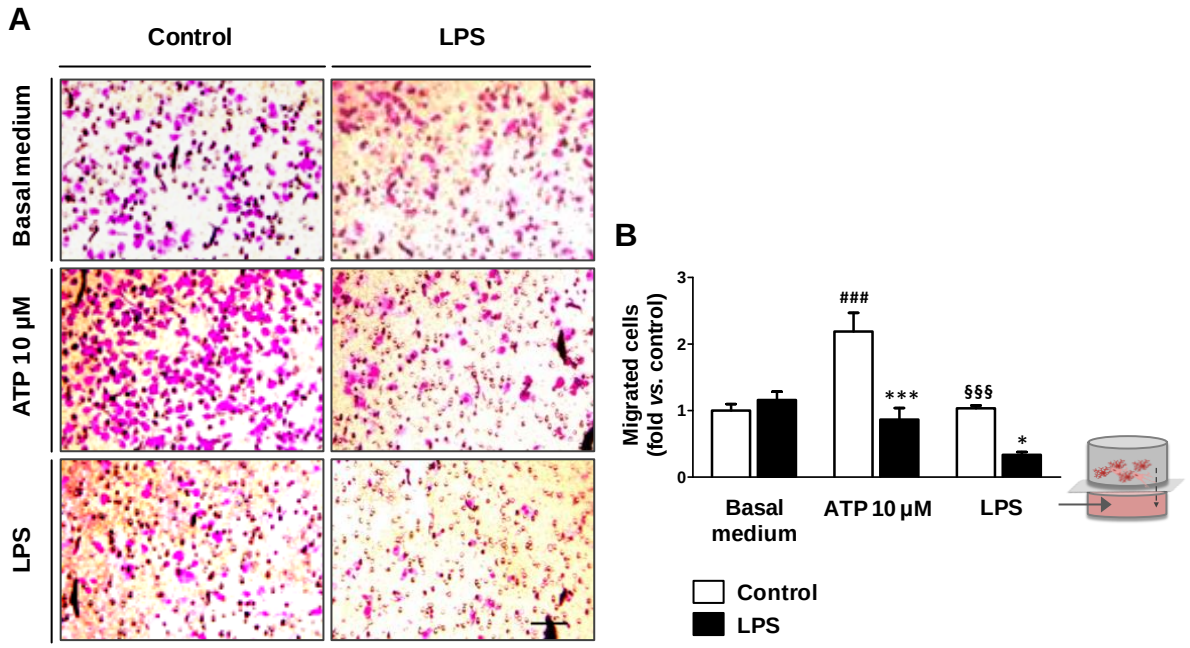

Figure II.3 - M1 polarized N9 microglia have reduced ability to migrate towards ATP and lipopolysaccharide (LPS). Migration was assessed using a Boyden Chamber. Nontreated (control) and LPS-stimulated microglia were allowed to migrate for 6 h to basal medium (basal migration), ATP at 10 µM and LPS at 300 ng/mL. Representative results of one experiment are shown (A). The total number of cells per well was counted and the results were expressed as fold versus control (basal migration) (B). Results are mean ± s.e.m. from four independent experiments. Comparison was done by one-way ANOVA followed by multiple comparisons Bonferroni post hoc correction. *$p < 0.05$ and ***$p < 0.001$ versus respective control; $^{###}p < 0.001$ versus basal migration in controls; and $^{§§§}p < 0.001$ versus migration of control cells to ATP. Scale bar represents 100 µm.

When analyzing the phagocytic properties of microglia, essential for clearance of debris and elimination of pathogenic organisms (Napoli and Neumann 2009), the treatment with LPS reduced the number of cells showing no intracellular beads ($p < 0.05$), while increasing those with more than 6 ingested beads ($p < 0.05$) (Figures II.4A, B). In addition, we were able to observe, for the first time in this model, that 24 h incubation with LPS induces the expression and release of MFG-E8 from N9 cells (~1.5- and ~2-fold, respectively, $p < 0.01$), as indicated by Western blot analysis of total extracts and extracellular media (Figures II.4C, D). We may then assume that LPS-treated cells intensify their phagocytic ability as a defensive mechanism despite their increased immobility.

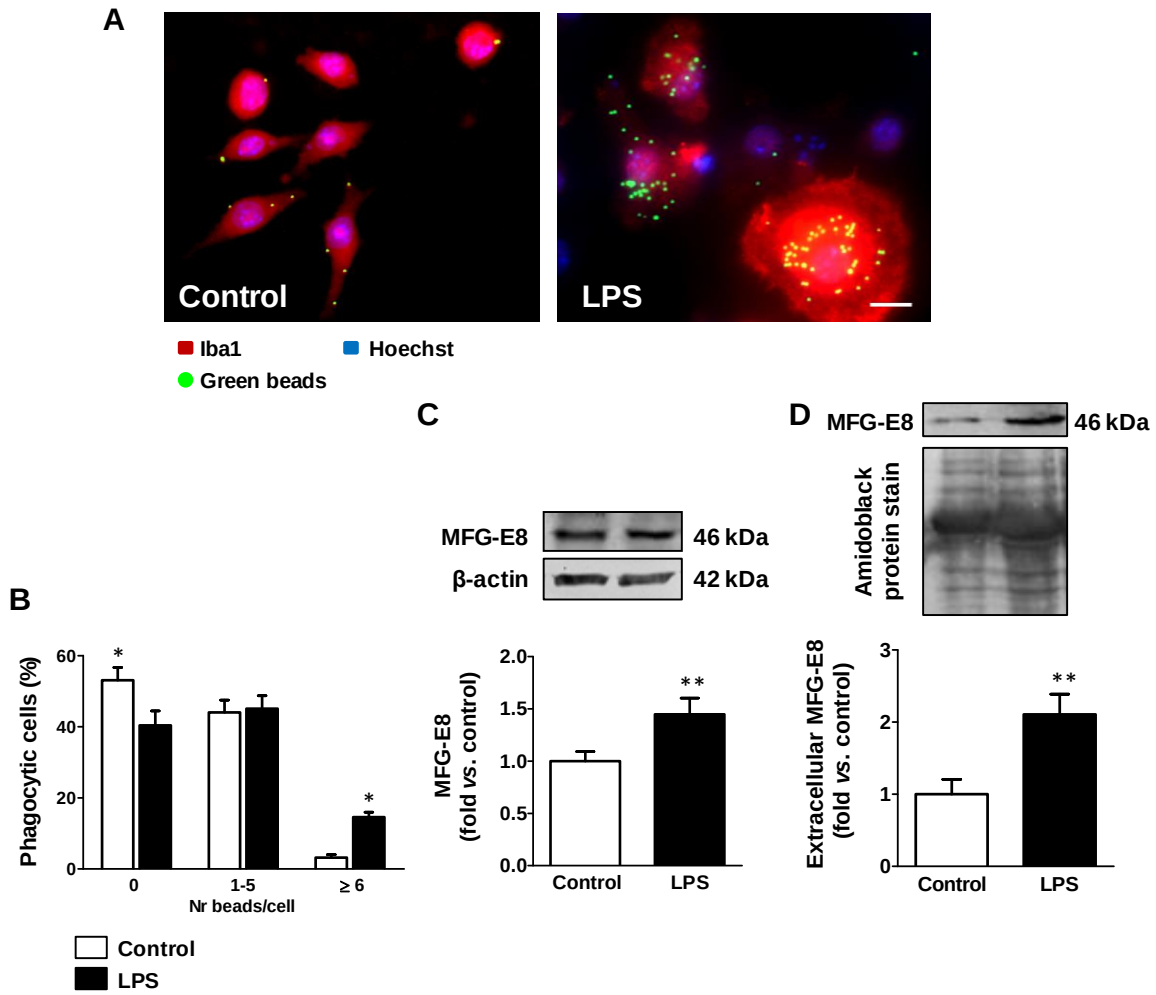

Figure II.4 - M1 polarized N9 microglia show enhanced phagocytic ability and milk fat globule-EGF factor 8 (MFG-E8) upregulated expression. Representative results of one experiment are shown for the phagocytosis of latex beads (A) and results are expressed as the percentage of cells engulfing specific numbers of ingested beads versus total number of cells (B). MFG-E8 expression and release were assessed by Western blot analysis ((C) and (D), resp.). Results are mean ± s.e.m. from five (B) or six (C, D) independent experiments, performed in duplicate. Comparison of more than two groups (B) was done by one-way ANOVA followed by multiple comparisons Bonferroni post hoc correction. Comparisons between lipopolysaccharide- (LPS-) treated N9 cells and nontreated cells (control) were made via two-tailed Student's *t*-test (C, D). *p < 0.05 and **p < 0.01 versus nontreated cells (control). Scale bar represents 20 μm.

3.3. M1 Polarization of Microglia is Mediated by Activation of the Inflammatory TLR2/TLR4/NF-κB/Inflammasome Signaling Cascade and Release of HMGB1

By investigating the signaling pathway mediated by TLR/NF-κB activation, we found that TLR4 was translocated to the membrane of microglial cells incubated with LPS, as demonstrated by an increased expression of the glycosylated form ($p < 0.01$, Figure II.5A). We also noticed an increased expression of TLR2 ($p < 0.05$, Figure II.5B). Consequently, NF-κB was translocated into the nucleus, as demonstrated by the ~2-fold increase in protein expression in the nuclear fraction ($p < 0.05$, Figure II.5C) and by the elevated staining of LPS-treated N9 microglia nuclei when compared to control samples (Figures II.5D, E). NF-κB

transactivation was also demonstrated in reactive microglia primary cultures (Caldeira et al. 2014) and to be implicated in inflammasome activation (Bauernfeind et al. 2009; Liu et al. 2014) that is associated with the maturation of the microglial proinflammatory cytokines IL-1β and IL-18 by caspase-1 (Lee et al. 2013; Walsh et al. 2014). Hence, the next step was to evaluate the cascade of such events in the N9 microglia exposed to LPS. As depicted in Figure II.5, LPS significantly enhanced the expression of *Nlrp3* inflammasome (Figure II.5F, $p < 0.001$) as well as of *Il-1beta* (Figure II.5G, $p < 0.05$) and *IL-18* (Figure II.5H, $p < 0.05$) in N9 cells. The activation of inflammasome was also observed by treating N9 cells (Falcão et al. 2017), immortalized microglia (Halle et al. 2008), and cultured primary microglia (our unpublished data) with amyloid-beta peptide. Moreover, the high caspase-1 activity we observed (Figure II.5I, $p < 0.01$) further indicates an increased capacity to mediate the cleavage of IL-1β and IL-18 pro-forms (Lee et al. 2013).

M1 polarized microglia is also related to the generation of other inflammatory mediators, such as ROS and MMPs (Chhor et al. 2013; Durafourt et al. 2012). Actually, we found elevated levels of MMP-9 (~3-fold, $p < 0.01$), but not of MMP-2 (Figures II.6A, B), which may derive from the observed NF-κB activation (Figures II.5C, E) demonstrated to be a regulator of MMP-9 gene expression, but not of MMP-2 (Fanjul-Fernández et al. 2010). NO is considered a signaling molecule and a proinflammatory mediator, as well. Our studies showed that the concentration of nitrites, indirectly indicating the level of NO, was likewise markedly enhanced in the extracellular medium (Figure II.6C).

Proinflammatory effects of LPS were shown to be enhanced by the endogenous danger signal molecule HMGB1 released by necrotic cells (Gao et al. 2011). The majority of the studies have reported HMGB1 effects on macrophages and microglia activation (Kim et al. 2006; Park et al. 2004), but only a few report its increased expression in activated microglia, both in the postischemic brain (Kim et al. 2008) and in the reactive primary microglia cultures (Caldeira et al. 2014). In addition, we recently found more than a 2-fold increase in both gene and protein expression of HMGB1 in N9 cells treated with 1 μM amyloid-beta peptide (Falcão et al. 2017). Therefore, we examined the pattern of cellular and extracellular distribution of HMGB1 in our inflammatory N9 cells. Surprisingly, we observed a reduced HMGB1 protein expression in cell lysates of microglia activated by LPS and in nuclear extracts (Figures II.6D, E). However, once HMGB1 was shown to be massively released into the extracellular environment in pathological conditions (Kim et al. 2006), we decided to evaluate its presence in cellular supernatants. In accordance with this, HMGB1 was found to accumulate in culture medium after incubating N9 microglial cells with LPS for 24 h (~2-fold increase, $p < 0.05$), as depicted in Figure II.6F. These results indicate that HMGB1 is rapidly released into the extracellular space after LPS-induced microglial activation.

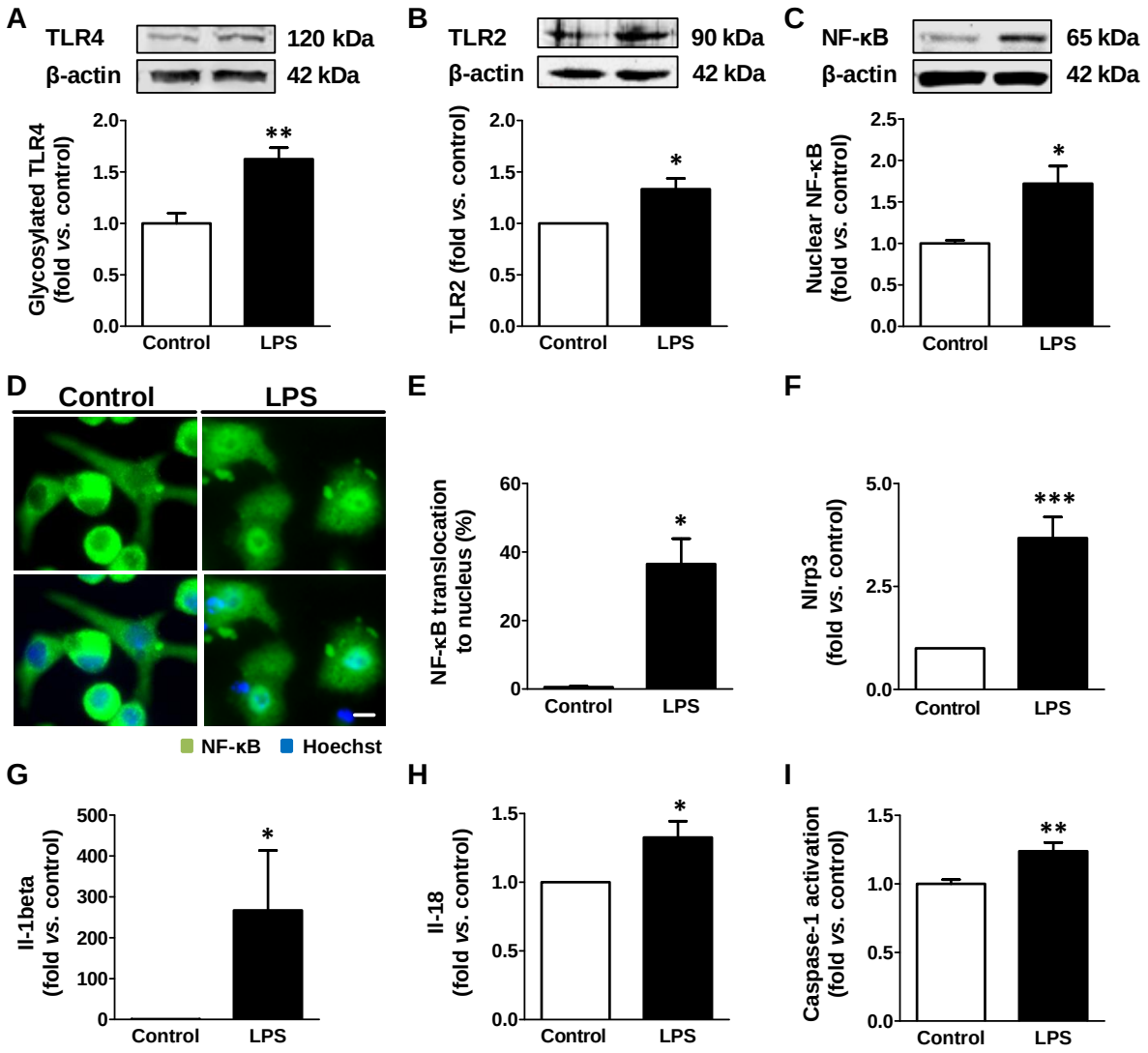

Figure II.5 - M1 polarized N9 microglia evidence activation of TLR4/TLR2/NF-κB signaling pathway and of inflammasome complex. Protein expression of glycosylated toll-like receptor 4 (TLR4) (A) and TLR2 (B) was evaluated by Western blot analysis. Translocation of nuclear factor kappa B (NF-κB) to the nucleus is represented by considering the Western blot analysis of nuclear expression (C). To observe NF-κB cellular localization, immunocytochemistry against anti-NF-κB was performed as indicated in Materials and Methods and representative results are shown (D) and presented as the percentage of cells with nuclear staining versus total number of cells (E). NOD-like receptor family, pyrin domain containing 3 *(Nlrp3)*, interleukin- *(IL-) 1beta,* and *IL-18* expression were measured by qRT-PCR ((F), (G), and (H), resp.). Detection of caspase-1 activation was achieved by a colorimetric assay, as described in Materials and Methods (I). Results are mean ± s.e.m. from six (A, C), five (F, G, H), four (B), or three (E, I) independent experiments; (C) and (I) were performed in duplicate. Comparisons between lipopolysaccharide- (LPS-) treated N9 cells and nontreated cells (control) were made via two-tailed Student's *t*-test for all the parameters, except for (C, E), where unpaired *t*-test with Welch's correction was applied. *p < 0.05, **p < 0.01, and ***p < 0.001 versus nontreated cells (control). Scale bar represents 20 μm.

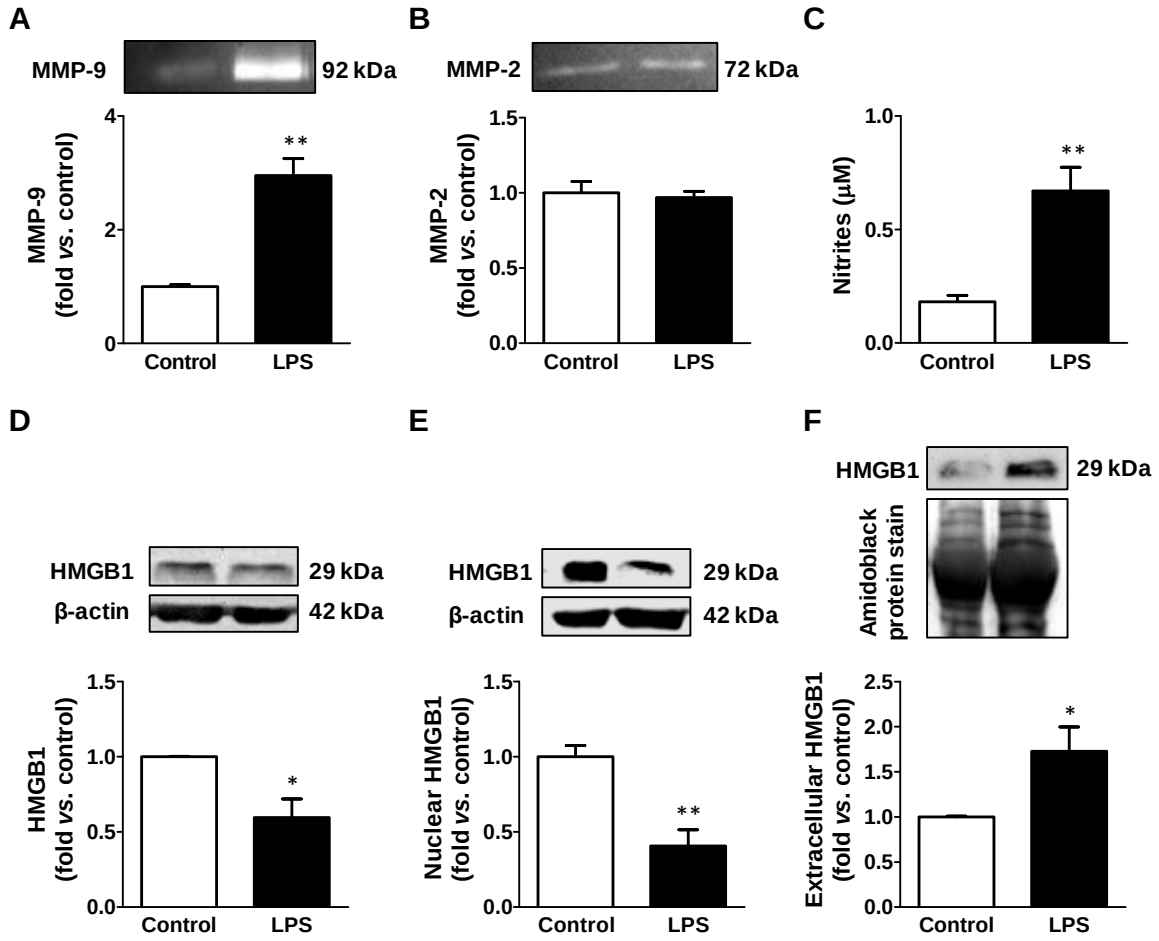

Figure II.6 - M1 polarized N9 microglia have low intracellular content of HMGB1 and increased secretion of MMP-9, NO, and HMGB1 to the cell milieu. Extracellular medium was assessed for matrix metalloproteinase-9 (MMP-9) (A) and MMP-2 (B) activities by the gelatin zymography assay and results were expressed as fold versus nontreated cells (control). Nitrites that reflect nitric oxide (NO) production were assessed by the Griess reaction followed by Microplate Reader for Absorbance Assays (C). High mobility group box 1 (HMGB1) expression was determined in total extracts (D), nuclear fraction (E), and extracellular media (F) by Western blot analysis. Results are mean ± s.e.m. from six (A, B, D, E) or four (C, F) independent experiments. Nitrites measurement (C) was performed in duplicate. Comparisons between lipopolysaccharide- (LPS-) treated N9 cells and nontreated cells (control) were made via two-tailed Student's *t*-test (E) or unpaired *t*-test with Welch's correction (A, C, D, F). *$p < 0.05$ and **$p < 0.01$ versus nontreated cells (control).

3.4. Differential Expression of Inflamma-miRs in M1 Polarized N9 Microglia by LPS Is Recapitulated in Cell-Derived Exosomes

To identify miRNA subtypes subsequent to N9 cell polarization by LPS we evaluated the expression of specific inflammatory miRNAs associated with microglia activation, namely, mmu-miR-155-5p (miR-155), related to M1 phenotype, hsa-miR-146a-5p (miR-146a) linked to repair, and resolution and hsa-miR-124-3p (miR-124), expressed in surveillant and anti-inflammatory microglia. Such inflamma-miRs were previously identified in reactive cultured microglia (Caldeira et al. 2014) and both miR-155 and miR-146a found to be elevated in N9 cells upon treatment with amyloid-beta peptide (Falcão et al. 2017).

As displayed in Figure II.7, microglia stimulation with LPS induced an elevated expression of miR-155 (~6-fold, $p < 0.01$) and of miR-146a (2-fold, $p < 0.05$), while promoting the downregulation of miR-124 expression (0.4-fold, $p < 0.05$). These data support the acquisition of a M1 phenotype in microglia activated by LPS with the loss of their neuroprotective properties and sustained upregulation of proinflammatory features by the miR-155 regulation networks. Intriguingly, the overexpression of miR-146a may constitute a mechanism of regulating the inflammatory response (Wu et al. 2015a), exemplifying the complexity of the M1/M2/M0 landscape. In addition, we found that N9 cells were able to release exosomes of approximately 160 nm diameter, as determined by DLS analysis (Figure II.7B). We observed that these extracellular vesicles carried the same miRNAs of the M1 polarized cell, demonstrating that such exosomes recapitulate the miRNA cargo of the cell of origin. Moreover, since miR-124 was only detectable in nonstimulated N9 cells (control), we may hypothesize that miR-155 and miR-146a are the most implicated in promoting the phenotypic conversion of adjacent cells.

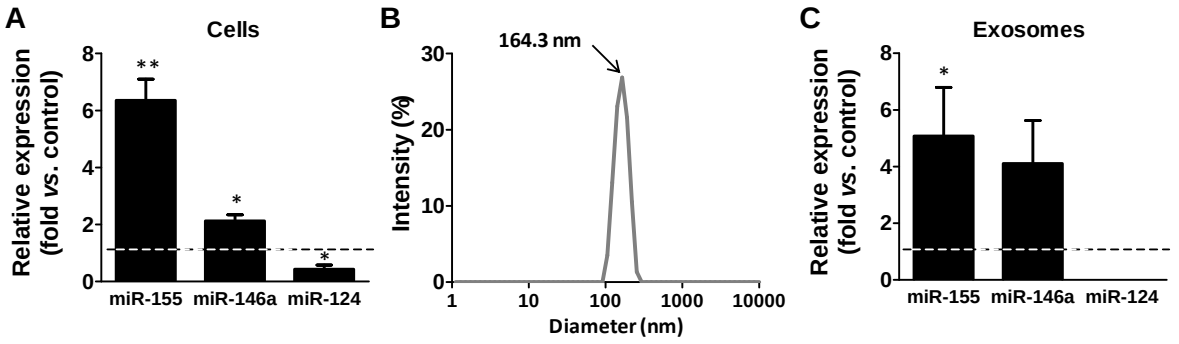

Figure II.7 - M1 polarized N9 microglia display upregulated levels of miR-155 and miR-146a, as well as downregulated miR-124, which are recapitulated in cell-derived exosomes. N9 cells were collected after incubation with lipopolysaccharide (LPS) and miR-155, miR-146a, and miR-124 expression were evaluated by qRT-PCR, both in cells (A) and in exosomes (C). Results are mean ± s.e.m. from five independent experiments. Comparisons between LPS-treated N9 cells and nontreated cells (control) were made via two-tailed Student's *t*-test. *$p < 0.05$ and **$p < 0.01$ versus nontreated cells (control). Vesicles isolated from the extracellular media of N9 cells were characterized in terms of their size by dynamic light scattering (B).

4. Discussion

In this study, we have profiled N9 microglia activation upon LPS stimulation at cellular, functional, and molecular levels, by considering either gene or protein expression of inflammatory/anti-inflammatory associated markers. In addition, we not only characterized the different faces of microglial response associated with the M1 polarization but also explored the involvement of new inflammatory players. Data support LPS-induced microglia M1 phenotype with the activation of the inflammatory cascade mediated by TLR/NF-κB signaling pathway in N9 cells. More interestingly, we provide new evidence indicating

decreased migration ability but increased phagocytosis with the involvement of MFG-E8 production and release. In addition, our study is innovative in evidencing that LPS triggers the upregulation of the NLRP3 inflammasome complex in N9 cells and leads HMGB1 release to the extracellular medium together with that of MMP-9. For the first time we obtained upregulation of miR-155 and miR-146, along with a reduced expression of miR-124 in the N9 cells treated with LPS, as previously observed in macrophages/microglia M1 polarized cells (Ponomarev et al. 2013), and we showed that a similar representative profile occurs in exosomes isolated from LPS-treated N9 cells supernatants.

N9 cell line has been widely used in the evaluation of microglial functions in different conditions, as an alternative to primary cell cultures, due to increased yield and homogeneity of cells in culture. More importantly, no differences were found between N9 cells and microglia primary cultures relative to the activation of inflammatory mediators by LPS (Nikodemova and Watters 2011). Previous separated studies evidenced an assembly of effects induced by LPS that included NF-κB activation (Zhao et al. 2011), amoeboid morphology with process retraction (Lu et al. 2010; Zhang et al. 2012a), release of proinflammatory mediators (McKimmie et al. 2006; Zhang et al. 2012a), low migratory capacity (Cui et al. 2002), and increased phagocytic ability (Bruce-Keller et al. 2000). Nevertheless, there is still limited information concerning the activation pattern of these cells and the combined events implicated in the phenotypic transition towards M1 polarization, which are mandatory when intrinsic characteristics of microglia are to be explored and therapeutic agents to be tested. Moreover, no inflammasome activated complex was ever described, nor were inflamma-miR profiling and exosome cargo identified. In addition, only our data report the increased expression of HMGB1 in amyloid-beta peptide-treated N9 cells (Falcão et al. 2017), as well as its nucleocytoplasmic shuttling and further release in LPS-treated cells, as we describe in this study. We first settled that our N9 microglia predominantly switched to the M1 subtype in the presence of LPS, as described for macrophages and microglia primary cultures (Chhor et al. 2013; Durafourt et al. 2012). Using established markers that allow the differentiation between M1 and M2 activated cells [for review see (Fernandes et al. 2014)], we observed that the M1-markers *Nos2* and *Mhc-II* were upregulated while the M2-markers *Arg1* and *Fizz1* were downregulated after LPS exposure. In conformity, we also observed downregulation of CX3CR1, a condition identified in M1 monocyte-macrophages (Shechter et al. 2013) and in primary microglia exposed to LPS (Boddeke et al. 1999). Moreover, low CX3CR1 is associated with marked neuronal loss after systemic inflammation (Cardona et al. 2006b) and facilitates sepsis-induced immunosuppression resulting from monocyte inability to recognize CX3CL1 and kill pathogenic microorganisms (Pachot et al. 2008). Therefore, the decrease of CX3CR1 in our model may relate to the persistent microglia activation.

The increased number of amoeboid N9 microglia and the reduction of ramified cells are features of microglia activation and were observed after treatment with LPS (Lu et al. 2010; Zhang et al. 2012a). Increased proliferation rate of microglia by LPS, as we obtained in N9 cells based on the nuclear appearance of the Ki-67 marker and upregulation of *Cd11b* expression, was previously noticed in BV2-stimulated microglia (Jose et al. 2014). Nevertheless, *in vivo* data do not sustain the presence of proliferating microglia during systemic inflammation (Chen et al. 2012), though it was evidenced during ischemia (Li et al. 2013).

The ability of microglia to sense distant signals and be attracted to them, a function designated by chemotaxis, is orchestrated by multiple chemotactic compounds released at the site of damage, either by injured cells or by pathogenic organisms. As claimed by others (Davalos et al. 2005), ATP showed to be a chemotactic agent and promoted the migration of N9 microglia, a property that was however reduced after LPS treatment, probably as a consequence of the diminished processes that compromise the migratory capacity towards a chemoattractant signal (Ohsawa and Kohsaka 2011). Indeed, cell migration to lesion sites is faster than morphological changes associated with microglia activation, in which purines such as ATP can no longer attract and may even repel them (Orr et al. 2009). Such alterations may relate to changing of surface markers such as P2Y12 upon LPS exposure (Haynes et al. 2006). In fact, P2Y receptors were previously associated with microglia chemotactic function to ATP (Honda et al. 2001). Reduced ability to migrate towards LPS was also a feature of our M1 polarized N9 cells, although there is some controversy on the ability of LPS to induce or inhibit migration (Lively and Schlichter 2013; Mashimo et al. 2008; Scheiblich et al. 2014), since it may depend on LPS concentration and on mediators released by the activated microglia near the site of injury (Babcock et al. 2003).

Phagocytosis is another microglial function that is extremely important to their neuroprotective properties, required not only for synaptic plasticity but also for clearance of cellular debris and elimination of pathogenic organisms (Napoli and Neumann 2009). Our results indicate that LPS increases N9 microglia phagocytosis, as previously described for LPS-treated BV2 cells, as well as primary cultures of microglia and macrophages (Majerova et al. 2014). *In vivo* studies showed that LPS administration increases microglia phagocytosis of viable neurons during development, inflammation, and neuropathology, a property denominated as phagoptosis (Fricker et al. 2012). A new finding was the increased expression of the phagocytosis-associated protein MFG-E8, together with its release, when the N9 cells were treated with LPS. There are still controversial data concerning the protective/noxious role of MFG-E8. On one hand, MFG-E8 has been associated with microglia anti-inflammatory properties, as demonstrated by Spittau et al. (2014), when the cells were stimulated by TGF-β, in the MGF-E8$^{-/-}$ mice showing an increased

proinflammatory response (Hanayama et al. 2002), as well as in the septic mouse presenting downregulation of MFG-E8 levels (Komura et al. 2009). On the other hand, Liu and colleagues (2013b) have demonstrated that MFG-E8 overexpression occurred concomitantly with TNF-α and IL-1β upregulation. Thus, given the increased expression of intracellular and released MFG-E8 found in our model, we hypothesize that MFG-E8 upregulation is typical of M1 polarized microglia.

Considering the inflammatory signaling cascades, the activation of TLR4/2-NF-κB pathway is consistent with the proinflammatory response triggered by LPS (Zhang et al. 2012a; Zhao et al. 2011). The role of inflammasome is poorly understood in microglia activation pattern. Our data show for the first time that expression of NLRP3, IL-1β, and IL-18 mRNA increases by LPS exposure and may relate to the activation of caspase-1. Bauernfeind and colleagues (2009) proposed that NF-κB induces mRNA expression of NLRP3, which is further required for the formation of inflammasome complexes. Others have reported the activation of NLRP3 complexes and recruitment of caspase-1, together with IL-18/IL-1β release, in primary microglia (Hanamsagar et al. 2011) and in macrophages (Lee et al. 2013) stimulated by infection-associated agents. Our results are also consistent with works in the BV-2 cell line and in rat primary microglia reporting that microglia exposed to LPS show increased generation of redox molecules (NO) and iNOS activation (Zhang et al. 2012a; Zhao et al. 2011), as well as enhanced MMP-9 expression (Lively and Schlichter 2013) and activity (Lee and Kim 2011). Most interesting, TLR2-dependent NO expression was shown to be necessary for microglial MMP-9 expression (Bai et al. 2014). Although it has been shown that MMP-2 may be also involved in glial cell activation (Cho et al. 2006) and our recent studies indicate increased release of MMP-2 into the extracellular media in microglia treated with amyloid-beta peptide (unpublished results), we did not observe any variation between LPS-stimulated and nonstimulated cells (control) in terms ofMMP-2 release. This difference between the results found for MMP-9 and MMP-2 may be explained by the existence of specific binding sites for NF-κB in MMP-9, which are lacking in MMP-2 promoter region, as reported by Fanjul-Fernández et al. (2010).

We next explored the expression of the alarmin HMGB1 in the context of inflammation in our culture model, since it has been described to be a signal released to the extracellular environment that leads to inflammatory mechanisms through the activation of RAGE and TLR2/TLR4 receptors (Park et al. 2004). We are the first to report that the decrease in its nuclear and cytoplasmic content in N9 microglia after the LPS stimulus is most likely due to its substantial release to the cell supernatants. Actually, HMGB1 is released from the cells after translocation from the nucleus to the cytoplasm (Wu et al. 2012b), indicating that secretion of HMGB1 may be associated with inflammasome complex activation (Lu et al. 2013).

The influence of miRNA in microglia-mediated immune response was recently reviewed (Guedes et al. 2013) and abnormal expression of inflamma-miRs showed them to contribute to chronic proinflammatory status and to be a significant mortality risk factor (Cãtaña et al. 2015). MiRNAs are small noncoding RNA molecules that are 18–25 nucleotides in length involved in the regulation of gene expression. Main inflammatory miRNAs are miR-155, miR-21, miR146a/b, and miR-124 (Quinn and O'Neill 2011). We found upregulation of miR-155 and miR-146, together with a reduced expression of miR-124, in N9 microglia upon LPS exposure. This pattern corroborates the increased representation of polarized M1 microglial N9 by LPS over the M2 polarization, as described by several authors (Cardoso et al. 2012; Ponomarev et al. 2013). Freilich and colleagues (2013) found a similar expression profile in primary cultured microglia upon a short-time incubation with LPS (4 h). Targets of miR-155 are the suppressor of cytokine signaling 1 (SOCS1), CCAAT/enhancer-binding protein alpha (C/EBPα), and Smad2 (Cardoso et al. 2012; Ponomarev et al. 2013) which are important players in anti-inflammatory response. As such, increased expression of miR-155 potentiates inflammation and sustains microglia activation and resulting neurotoxicity. We have also demonstrated here that incubation with LPS promotes upregulation of miR-146a in N9 microglia. It is possible that such effect results from the TLR2/TLR4 activation, as described for BV-2 and EOC 13.31 cell lines (Saba et al. 2012). Others indicate that miR-146a regulates NF-κB signaling pathway by directly targeting IRAK1 and tumor-necrosis-factor-receptor-associated factor 6 (TRAF6), proteins involved in the transduction pathway of NF-κB transactivation by immune stimulation (Taganov et al. 2006). However, in our model, the upregulation of miR-146a at 24 h incubation with LPS was not able to suppress inflammatory response. This inability was similarly observed when 72 h treatment was assayed (data not shown). Interestingly increased expression of miR-146a may be related to LPS tolerance, previously observed in monocytes and suggested to act as a tuning mechanism to prevent an overstimulated inflammatory state (Nahid et al. 2009). In what concerns miR-124, known to promote microglia quiescence (Ponomarev et al. 2011), it was revealed to switch cell polarization from M1 to the M2 phenotype (Willemen et al. 2012) in various subsets of monocyte cells and microglia (Veremeyko et al. 2013). This finding indicates that the decreased expression of miR-124 that we found in our model is consistent with the phenotype M1 preponderance. Our data also indicate that the expression profile of inflamma-miRs in exosomes recapitulates the one found in the cells, which suggests that M1 polarized microglia is able to directly transport miRNAs to an adjacent cell and modulate its phenotype, besides the release of soluble inflammatory signals. As a consequence, the proinflammatory environment observed in many neurotoxic situations may be sustained through the transfer of the microglia phenotype associated miRNAs from cells into exosomes.

5. Conclusions

Overall, the present data integrate an ensemble of signaling cascades related to the M1 path activation of N9 microglial cells, together with innovative data pointing to inflammasome complex activation, downregulation of the neuronal fractalkine receptor CX3CR1, and reduction of miR-124 upon incubation with LPS. New findings also include the LPS-induced increase in the expression of MFG-E8, miR-155, and miR-146a, together with raised secretion of HMGB1 and MMP-9, as schematically represented in Figure II.8. Our study firstly identified that the delivery of miR-155 from microglia to adjacent cells may be mediated by exosomes, as previously observed for dendritic cells in response to endotoxin (Alexander et al. 2015). Our model of LPS-induced M1 polarization of N9 cells, by exploring new molecules and pathways implicated in such activation, enhanced our understanding on the neurodegenerative processes associated with microglia inflammation, while identifying promising biomarkers to be used in neurological disorders, in particular exosomes and their cargo in miR-155. Finally, our study further suggests that targeting NLRP3 inflammasome, HMGB1 signaling, and miR-155 transfer to exosomes may be suitable therapeutic approach to restrain neuroinflammation in disorders whereby microglia activation has a critical role.

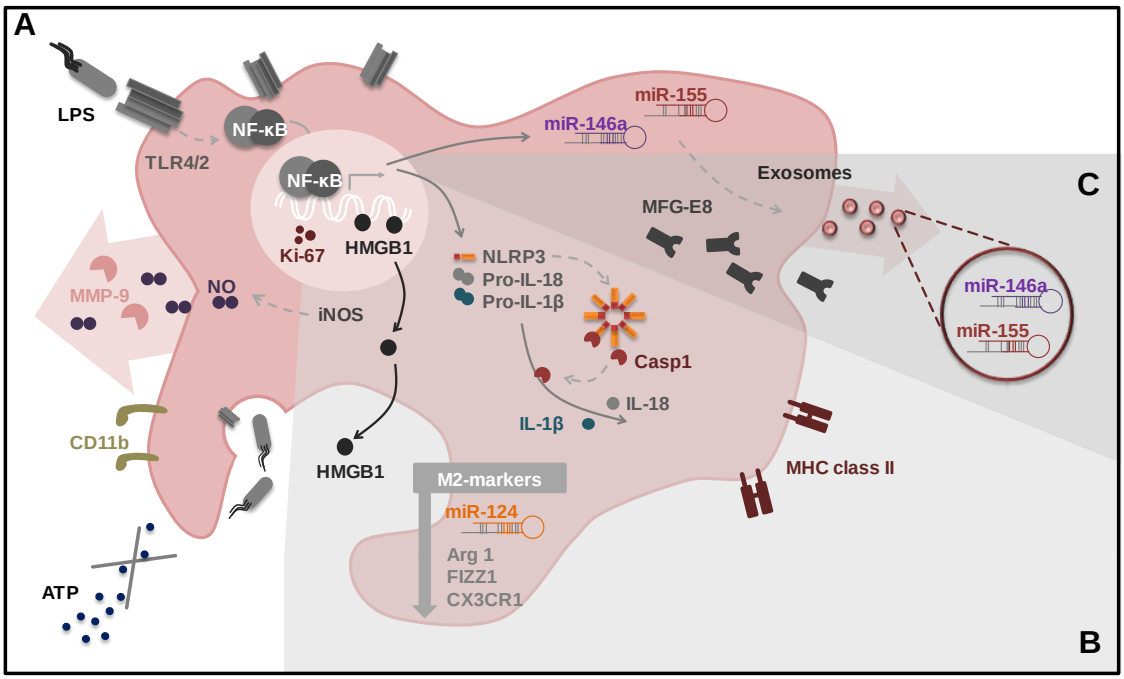

Figure II.8 - Schematic representation of inflammatory players implicated in lipopolysaccharide- (LPS-) induced M1 polarization of N9 microglial cells and of exosome upregulated microRNAs. (A) We first studied functions and pathways commonly described for microglia classical activation. We observed that LPS causes a moderate degree of apoptosis in the N9 cells and a switch from the ramified to an amoeboid cell shape. LPS-stimulated cells lose the ability to migrate towards ATP but show increased phagocytic ability, as revealed by the elevated number of latex beads ingested. LPS also triggers microglia proliferation as indicated by the increased number of *Cd11b* positive cells and Ki-67 stained nuclei. Inflammatory events are mediated through the signaling pathway involving the toll-like receptor 4 (TLR4)/TLR2 and nuclear factor kappa B (NF-κB) in LPS-treated N9 microglia and implicate the upregulation of microRNA-155 (miR-155) and miR-146a as well as the release of nitric oxide (NO) and matrix metalloproteinase-9 (MMP-9) to the extracellular milieu. (B) Our study provided new evidence that N9 cells treated with LPS have increased expression of inflammasome complex comprehending the upregulation of interleukin- *(IL-)1beta*, *IL-18,* and NOD-like receptor family pyrin domain containing 3 *(Nlrp3)*, together with enhanced caspase-1 activation. Increased expression of *Nos2* and major histocompatibility complex class II *(Mhc-II)* (markers of M1 polarization or classically activated microglia), in conjunction with decreased expression of arginase 1 *(Arg1)*, found in inflammatory zone 1 *(Fizz1),* miR-124 (markers of M2 polarization or alternatively activated microglia), and reduced CX3C chemokine receptor 1 (CX3CR1) expression corroborate the acquisition of a prevalent M1 phenotype in microglial cells exposed to LPS. (C) Finally, we described for the first time that increased MFG-E8 expression and release are induced in M1 polarized microglia and that miRs expression profile is recapitulated in cell-derived exosomes, further supporting M1 polarization in LPS-treated N9 cells and dissemination of inflammatory mediators by extracellular vesicles.

Acknowledgments

This work was funded by the Project PTDC/SAUFAR/118787/2010 (to Dora Brites) and, in part, by iMed.ULisboa (UID/DTP/04138/2013) from Fundação para a Ciência e a Tecnologia (FCT) and Santa Casa da Misericórdia de Lisboa, Portugal. Ana Rita Vaz holds a postdoctoral research fellowship (SFRH/BPD/76590/2011) and Carolina Cunha and Cátia Gomes are recipients of Ph.D. fellowships (SFRH/BD/91316/2012 and SFRH/BD/102718/2014, resp.), all from FCT.

6. Supplementary Material

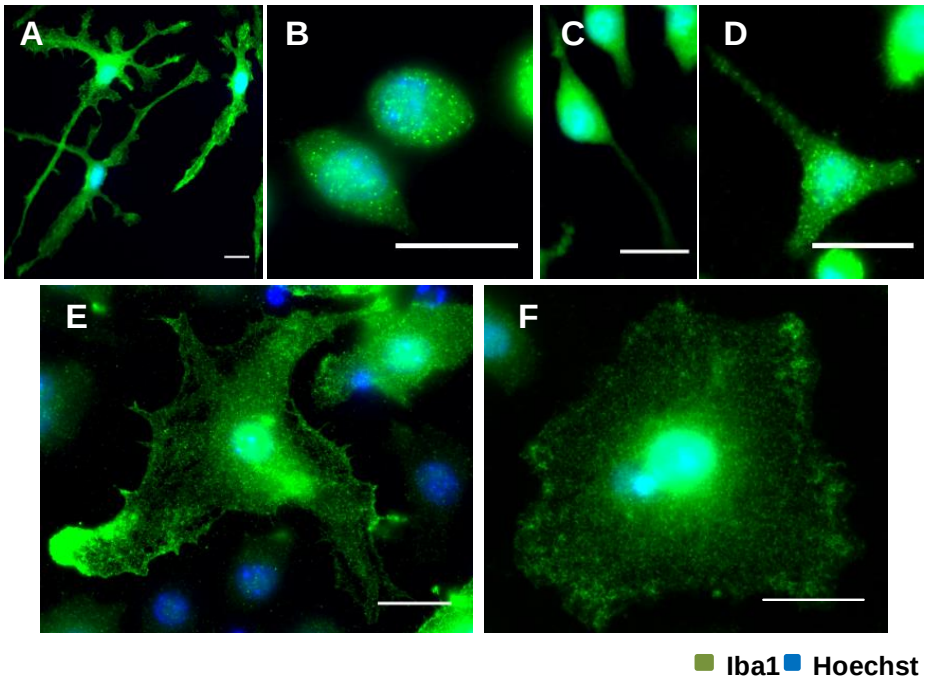

Supplementary Figure II.1 - N9 microglial cells show lower number and length of ramifications than primary cultured microglia from mice cortical brain and a combination of distinct morphologies. Morphological analysis was performed by immunocytochemistry using anti-Iba1, as indicated in methods. Nuclei were stained with Hoechst (blue fluorescence). Primary cultures of microglia isolated from mice cortical brain were stained with Iba-1 and used for comparative purpose (A). Different morphologies observed in N9 cells included round/oval (B), ramified with two (C) or three (D) ramifications, amoeboid with thicker branches (D) and amoeboid with absent ramifications (E). Representative results of one experiment are shown and scale bar represents 20 µm.

Supplementary Table II.1 - List of primers used in qRT-PCR

Gene	Forward Primer Sequence	Reverse Primer Sequence
beta-actin	5'-GTCCCGGCATGTGCAA-3'	5'-AGGATCTTCATGAGGTAGT-3'
Nos2	5'-ACCCACATCTGGCAGAATGAG-3'	5'-AGCCATGACCTTTCGCATTAG-3'
Mhc-II	5'-TGGGCACCATCTTCATCATTC-3'	5'- GGTCACCCAGCACACCACTT-3'
Arg1	5'-CTTGGCTTGCTTCGGAACTC-3'	5'-GGAGAAGGCGTTTGCTTAGTTC-3'
Fizz1	5'-GCCAGGTCCTGGAACCTTTC-3'	5'-GGAGCAGGGAGATGCAGATGAG-3'
Cx3cr1	5'-TCGTCTTCACGTTCGGTCTG-3'	5'-CTCAAGGCCAGGTTCAGGAG-3'
Cd11b	5'-CAGATCAACAATGTGACCGTATGGG-3'	5'-CATCATGTCCTTGTACTGCCGCTTG-3'
Nlrp3	5'-TGCTCTTCACTGCTATCAAGCCCT-3'	5'-ACAAGCCTTTGCTCCAGACCCTAT3'
Il-1beta	5'-CAGGCTCCGAGATGAACAAC-3'	5'-GGTGGAGAGCTTTCAGCTCATA-3'
Il-18	5'-TGGTTCCATGCTTTCTGGACTCCT-3'	5'-TTCCTGGGCCAAGAGGAAGTG-3'

miRNA	Target Sequence
mmu-miR-155-5p	5'-UUAAUGCUAAUUGUGAUAGGGGU-3'
hsa-miR-146a-5p	5'-UGAGAACUGAAUUCCAUGGGUU-3'
hsa-miR-124-3p	5'-UAAGGCACGCGGUGAAUGCC-3'

Supplementary Table II.2 - List of primary antibodies used in Western Blot

Primary antibody	Species	Reference	Dilution
β-actin	mouse	A5441, Sigma-Aldrich, St. Louis, MO, USA	1:5000
CX3CR1	rabbit	sc-30030, Santa Cruz Biotechnology®, CA, USA	1:100
MFG-E8	rabbit	sc-33546, Santa Cruz Biotechnology®, CA, USA	1:175
TLR4	mouse	sc-10741, Santa Cruz Biotechnology®, CA, USA	1:100
TLR2	rabbit	sc-10739, Santa Cruz Biotechnology®, CA, USA	1:100
NF-κB	rabbit	sc-372, Santa Cruz Biotechnology®, CA, USA	1:500 (or 1:200 for nuclear extracts)
HMGB1	mouse	651402, BioLegend,San Diego, CA, USA	1:200

Chapter III

EXOSOMES FROM NSC-34 CELLS TRANSFECTED WITH HSOD1-G93A ARE ENRICHED IN MIR-124 AND DRIVE ALTERATIONS IN MICROGLIA PHENOTYPE

Sara Pinto[1†], Carolina Cunha[1†], Marta Barbosa[1], Ana Rita Vaz[1,2], Dora Brites[1,2]

[1]Neuron Glia Biology in Health and Disease Group, Research Institute for Medicines (iMed.ULisboa), Faculty of Pharmacy, Universidade de Lisboa, Avenida Professor Gama Pinto, 1640-003 Lisbon, Portugal

[2]Department of Biochemistry and Human Biology, Faculty of Pharmacy, Universidade de Lisboa, Lisbon, Portugal

[†]These authors have contributed equally to this work.
Carolina Cunha has implemented the isolation and characterization of exosomes as well as the analysis of microRNAs expression in both NSC-34 cells and their derived exosomes. Carolina also supervised the laboratorial work of Sara Pinto.

***Front Neurosci*. (2017) 11:273**

Abstract

Amyotrophic lateral sclerosis (ALS) is a fatal adult-onset neurodegenerative disorder affecting motor neurons (MNs). Evidences indicate that ALS is a non-cell autonomous disease in which glial cells participate in both disease onset and progression. Exosomal transfer of mutant copper-zinc superoxide dismutase 1 (mSOD1) from cell-to-cell was suggested to contribute to disease dissemination. Data from our group and others showed that exosomes from activated cells contain inflammatory-related MicroRNAs (inflamma-miRNAs) that recapitulate the donor cell. While glia-derived exosomes and their effects in neurons have been addressed by several studies, only a few investigated the influence of motor neuron (MN)-derived exosomes in other cell function, the aim of the present study. We assessed a set of inflamma-miRs in NSC-34 MN-like cells transfected with mutant SOD1(G93A) and extended the study into their derived exosomes (mSOD1 exosomes). Then, the effects produced by mSOD1 exosomes in the activation and polarization of the recipient N9 microglial cells were investigated. Exosomes in coculture with N9 microglia and NSC-34 cells [either transfected with either wild-type (wt) human SOD1 or mutant SOD1(G93A)] showed to be transferred into N9 cells. Increased miR-124 expression was found in mSOD1 NSC-34 cells and in their derived exosomes. Incubation of mSOD1 exosomes with N9 cells determined a sustained 50% reduction in the cell phagocytic ability. It also caused a persistent NF-κB activation and an acute generation of NO, MMP-2, and MMP-9 activation, as well as upregulation of IL-1β, TNF-α, MHC-II, and iNOS gene expression, suggestive of induced M1 polarization. Marked elevation of IL-10, Arginase 1, TREM2, RAGE, and TLR4 mRNA levels, together with increased miR-124, miR-146a, and miR-155, at 24h incubation, suggest the switch to mixed M1 and M2 subpopulations in the exosome-treated N9 microglial cells. Exosomes from mSOD1 NSC-34 MNs also enhanced the number of senescent-like positive N9 cells. Data suggest that miR-124 is translocated from the mSOD1 MNs to exosomes, which determine early and late phenotypic alterations in the recipient N9-microglial cells. In conclusion, modulation of the inflammatory-associated miR-124, in mSOD1 NSC-34 MNs, with potential benefits in the cargo of their exosomes may reveal a promising therapeutic strategy in halting microglia activation and associated effects in MN degeneration.

Keywords: amyotrophic lateral sclerosis, microglia polarization, microglia surface receptors, inflamma-microRNA, motor neurons (MNs), MN-derived exosomes, mutant SOD1

1. Introduction

Since the beginning of the last decade, exosomes, and their role in the central nervous system (CNS), namely in the pathophysiology of neurodegenerative diseases such as amyotrophic lateral sclerosis (ALS), have been of increased interest in the science community. Indeed, autophagy and release of extracellular vesicles (such as exosomes and microvesicles) have been pointed to be involved in the secretion of harmful/damaged proteins and RNAs to alleviate intracellular stress conditions and sustaining cell homeostasis (Baixauli et al. 2014). Once exosomes represent a new way of long distance transfer of biological molecules into other cells, they are believed to be key players in disease dissemination, as well as a powerful tool for delivering medicines (Aryani and Denecke 2016; Budnik et al. 2016). Exosomes and microvesicles or ectosomes, originated from endosomal, and plasma membrane, respectively, contain proteins, lipids, soluble factors, mRNAs and microRNAs (miRNAs) (Brites and Fernandes 2016).

In familial ALS (fALS), transfer of misfolded and mutant copper-zinc superoxide dismutase 1 (mSOD1) from cell-to-cell was evidenced to be mediated by exosomes (Silverman et al. 2016). Among the several potential pathogenic genes in fALS and sporadic cases (sALS), the most frequent are C9orf72 (40% of fALS and 5-6% of sALS cases) and SOD1 (20% of fALS and 3% of sALS cases) (Krüger et al. 2016). This fatal and progressive neurodegenerative disease affects motor neurons (MNs) in the spinal cord and motor cortex. However, neuroinflammation and peripheral immune system activation were shown to accompany ALS neurodegeneration (Zondler et al. 2017). The underlying mechanisms are still unknown, but seem to involve multiple neural cell dysfunctional processes and complex multisystem deregulation, what turns difficult the identification of specific targets and the development of successful therapies. Lately, the interplay between MNs and glial cells mediated by exosomes was suggested to be crucial in the disease outcome and progression. Actually, it was shown that astrocyte-derived exosomes may transfer mSOD1 to MNs contributing to neurodegeneration and disease spread (Basso et al. 2013). More recently, it was demonstrated that both mSOD1 and misfolded wild-type (wt) SOD1 from NSC-34 MN-like cells are transferred on the surface of exosomes and delivered to neighboring MN cells by macropinocytosis (Grad et al. 2014b).

While glia-derived extracellular vesicles and their load effects in neurons have been recently evaluated as a novel form of communication in the brain (Basso and Bonetto 2016; Schiera et al. 2015), only a few studies have investigated the influence of MN-derived exosomes in other cell function. Such studies have demonstrated how exosomes shuttle proteins from neurons to muscle cells. Indeed, the transfer of Synaptotagmin 4 (Syt4), a membrane trafficking protein implicated in the retrograde signal, from presynaptic

compartments to postsynaptic muscle cells, was evidenced to be mediated by exosomes (Korkut et al. 2013). Other studies showed that extracellular vesicles from muscle have significant effects on the survival and neurite outgrowth of NSC-34 MN-like cells (Madison et al. 2014). In addition, exosome transfer of amyloid-β (Aβ) peptide from neurons to microglia revealed to be facilitated by phosphatidylserine recognition and to be followed by transportation to lysosomes and degradation, thus decreasing the extracellular levels of Aβ (Yuyama et al. 2012). Macropinocytosis may also be involved in the internalization of exosomes by a subset of microglia, as recently observed for exosomes secreted by oligodendrocytes, in an immunologically “silent” manner (Fitzner et al. 2011). Microglia was reported to have reduced neuroprotective properties and increased neurotoxic potential in ALS, and diverse microglia subpopulations were shown to coexist (Brites and Vaz 2014; Gerber et al. 2012). It was considered that microglia display the M2 anti-inflammatory phenotype at the early stages of the disease, switching to the M1 classically activated subtype as the disease progresses (Zhao et al. 2013). It was also suggested that microglia acquire a unique phenotype in ALS, not directly related with M1 or M2 polarization, and show an impaired function at the end-stage of ALS disease (Chiu et al. 2013; Nikodemova et al. 2014). Understanding the underlying conditions triggering different microglia phenotype profiling may help in the development of novel therapeutic strategies directed to specific ALS disease stages. Emerging data indicate that activation of microglia into the M1 subtype is associated with the increased expression of inflammation-related miRNAs (inflamma-miRs), secretion of proinflammatory cytokines and alarmins, such as the high mobility group box protein 1 (HMGB1), and release of exosomes (Brites and Fernandes 2016; Cunha et al. 2016; Falcão et al. 2017). Several microglial receptors have been implicated in the generation of an inflammatory response, like the Receptor for Advanced Glycation Endproducts (RAGE) by binding HMGB1 or the toll-like receptor-4 (TLR4) by binding lipopolysaccharide (LPS) and Aβ peptide. Others, in promoting phagocytosis and inhibiting the production of inflammatory mediators, such as the triggering receptor expressed by myeloid cells 2 (TREM2) (Doens and Fernandez 2014). Such receptors were shown to play important roles in microglial activation status.

Recent evidences showed that endogenous miR-155 and miR-146a, two critical miRNAs in regulating inflammation, are present in exosomes and pass between immune cells, such as dendritic cells, intervening in the cellular inflammatory response (Alexander et al. 2015). MiRNAs are a subset of non-coding RNAs that may inhibit mRNA translation, cause mRNA degradation or even switch from repression to activation depending on cell cycle stages (Kye and Goncalves Ido 2014; Li et al. 2015). Presynaptic alterations were shown to correlate with increased miR-124 and miR-142, which regulate Rab3a expression in motor nerves providing the basis for impaired synaptic function in neuromuscular disorders (Zhu et al.

2013). Dysregulation of miRNA expression and function in ALS also include elevation of miR-155 in either the rodent ALS model or in the spinal cord tissue of both fALS and sALS patients (Koval et al. 2013). In this study it was demonstrated that inhibition of miR-155 extended the survival of animals. Consistent with these results, ablation of miR-155 in the SOD1 mouse recovered microglia function and attenuated the disease (Butovsky et al. 2015). In this context, the anti-miR-155 MRG-107 compound is being developed with the proposal of reducing neuroinflammation in ALS patients (http://www.alsa.org/news/media/press-releases/miragen-therapeutics-060216.html).

Despite the current knowledge on the role of exosomes from NSC-34 MNs overexpressing human SOD1 mutated in G93A in cell-to-cell transfer of mSOD1 toxicity, it was never investigated how the uptake of such exosomes by receptor cells, such as microglia, may contribute to their activation and/or loss of function. In this study we hypothesized that exosomes can transfer specific inflammatory-related miRNAs as signaling cues for N9-microglia stimulation. Here we evaluated: (i) a specific set of inflamma-miRs in mSOD1 NSC-34 like MNs (mutated in G93A) and in their derived exosomes; (ii) the preferential cell distribution of mSOD1 MN-derived labeled exosomes in a coculture system of NSC-34 MNs and N9 microglial cells; and (iii) alterations in microglia polarization and function by interaction with mSOD1 MN-derived exosomes. Increased content in miR-124 was found in mSOD1 NSC-34 MN-derived exosomes. In the coculture system of MNs and N9 microglial cells, exosomes were preferentially internalized by N9 cells. The results obtained demonstrate that exosomes from mSOD1 MNs induce early activation of inflammatory signaling pathways and delayed increased expression of miR-124, miR-146a, and miR-155, together with mixed M1 and M2 phenotypic markers. In addition, exosomes caused microglia dysfunction evidenced by the loss of phagocytic ability and increased number of senescent-like cells. Data highlight that increased level of miR-124 in circulating exosomes may reveal a good biomarker of MN degeneration in ALS and that its modulation may have benefits in halting exosomal-inflamma-miRs dissemination and induced effects on microglia activation and dysfunction.

2. Material and Methods

2.1. NSC-34 Cell Culture

We used mouse MN-like NSC-34 cells stably expressing wt and mSOD1, which were a kind gift from Júlia Costa (ITQB, Universidade Nova de Lisboa, Portugal). Mouse NSC-34 is a hybrid cell line produced by the fusion of MNs from the spinal cord embryos with N18TG2 neuroblastoma cells (Cashman et al. 1992) that exhibit properties of MNs after differentiation and maturation protocols. Thus, NSC-34 cells were grown in proliferation media [Dulbecco's

modified Eagle's medium (DMEM) high glucose with glutamine, w/o pyruvate, supplemented with 10% of fetal bovine serum (FBS) and 1% of Penicillin/Streptomycin] and selection was made with Geneticin 418 sulfate (G418) at 0.5 mg/ml (Vaz et al. 2015). Medium was changed every 2-3 days. Culture plates were coated with Poly-D-Lysine (10 µg/ml) before plating the cells. Cells were seeded at a concentration of 5×10^4 cells/ml and maintained at 37ºC in a humidified atmosphere of 5% CO_2. After 48 h in proliferation medium, differentiation was induced by changing medium for DMEM-F12 plus 1% of FBS-exosome depleted, 1% of non-essential amino acids (NEAA), 1% of Penicillin/Streptomycin and 0.5 mg/ml of G418, as indicated by Cho et al. (2011). Cells were maintained in culture with differentiation medium for 4 days *in vitro* (DIV) to induce SOD1 accumulation (Vaz et al. 2015). DMEM, DMEM-F12, FBS, Penicillin/Streptomycin, and NEAA were purchased from Biochrom AG (Berlin, Germany). G418 was obtained from Gibco/Calbiochem (Darmstadt, Germany), and Poly-D-Lysine and RPMI were from Sigma-Aldrich (St. Louis, MO, USA).

2.2. Exosome Isolation and Characterization

Exosomes were isolated from the extracellular media of wt and mSOD1 NSC-34 cells, as currently in use in our lab (Cunha et al. 2016). Briefly, the culture media (20 ml) of the NSC-34 cells differentiated for 4 DIVs was centrifuged at 1,000 g for 10 min to remove cell debris. Then, the supernatant was transferred to another tube and centrifuged again at 16,000 g for 60 min, to separate microvesicles (size ~1,000 nm). The recovered supernatant was subsequently filtered in a 0.22 µm pore filter, and further centrifuged in the Ultra L-XP100 centrifuge (Beckman Coulter Inc., California, USA) at 100,000 g for 120 min to pellet exosomes (size ~100 nm). The pellet of exosomes was then resuspended in phosphate-buffered saline (PBS) and centrifuged one last time at 100,000 g for 120 min, in order to wash the pellet. All centrifugations were performed at 4ºC. Characterization of exosomes in terms of size and concentration was performed by Nanoparticle tracking analysis (NTA) using the Nanosight, model LM10-HSBF (Malvern, UK) and the NTA software version 3.1. Transmission electron microscopy (TEM) technique used the Jeol JEM 1400 Transmission Electron Microscope (Peabody, MA, USA). Western blot analysis was performed as usual in our lab (Vaz et al. 2015) to evaluate the expression of alix, flotillin-1 and CD63 by using 20 µg of total protein and specific antibodies (mouse anti-Alix, Cell Signaling, #2171; mouse anti-flotillin-1, BD Biosciences, #6108; goat anti-CD63, Santa Cruz Biotechnology®, #sc-31214). Normalization was made by using Amido Black staining as loading control. To evaluate total RNA and microRNA, the final pellet containing exosomes was resuspended in lysis buffer, and exosomal RNA extracted with the miRCURY Isolation Kit-Cell (Exiqon), as described below.

2.3. N9 Cell Culture

Mouse microglial N9 cell line, a popular retroviral-immortalized cell line resulting from the immortalization of microglia isolated from the cortex of CD1 mouse embryos (Righi et al. 1989a), was a gift from Teresa Pais (Institute Gulbenkian de Ciência, Oeiras, Portugal). This cell line shows diverse features similar to microglia in primary cultures, such as migration, phagocytosis and inflammation-related features (Fleisher-Berkovich et al. 2010). Indeed, N9 cells were shown to respond similarly to primary microglial cells derived from the same mouse strain, when treated with LPS (Nikodemova and Watters 2011), as recently demonstrated by us (Cunha et al. 2016). Cells were cultured in Roswell Park Memorial Institute (RPMI) medium supplemented with 10% of FBS, 1% of L-glutamine (Biochrom AG) and 1% of Penicillin/Streptomycin. Cells were seeded at a concentration of 1×10^5 cells/ml and maintained at 37ºC in a humidified atmosphere of 5% CO_2.

2.4. Coculturing of NSC-34 with N9 Microglial Cells, Exosomal Labeling, and Assessment of Preferential Exosome Cellular Distribution

NSC-34 cells differentiated for 4 DIV were cocultured with N9 cells in RPMI medium for 24 h, at 37ºC in a humidified atmosphere of 5% CO_2. We used the normal proportion of microglia and neurons in the CNS (ratio 1:1) (Silva et al. 2011). In the coculture model, the N9 microglial cells were plated in coverslips with paraffin wax feet, as described by Phatnani et al. (2013). The coverslips containing microglia were placed inverted over the layer of wt or mSOD1 NSC-34 MNs and maintained separated from such layer by the paraffin spots, thus avoiding direct contact between the two types of cells. Cells were plated in the same proportion (1:1) and maintained in coculture for 24 h. At the end of incubation, exosomes in the supernatant of NSC-34 (wt or mSOD1) with N9 cocultures were isolated as described above. To obtain PKH67 labeled fluorescent exosomes, the isolated exosomes were resuspended in PBS and mixed with an equal volume of PKH67 probe solution for 5 min at room temperature, using the PKH67 Fluorescent Cell Linker Kit (#MINI67, Sigma-Aldrich), as described by Dutta et al. (2014). Then, isolated exosomes were resuspended in RPMI medium and added either to N9 cells + wt NSC-34 MNs, or to N9 cells + mSOD1 NSC-34-MNs, using the above described cocultured system, for an additional period of 24 h and in a ratio of 1:1 (v/v). After incubation, NSC-34 MNs and N9 microglia were collected separately, and fixed with 4% (w/v) paraformaldehyde in PBS and cell nuclei were stained with Hoechst 33258 dye. UV and fluorescence images (original magnification: 630X) were acquired per sample by using Zen 2012 (blue edition, Zeiss) software.

2.5. Interaction of Exosomes from wt and mSOD1 NSC-34 MNs with N9 Microglia

N9 cells were plated for 24 h before incubation with exosomes from wt and mSOD1 NSC-34 MNs, at a concentration of 1 × 10^5 cells/ml. Exosomes from NSC-34 cells were resuspended in RPMI medium and incubated in N9 microglial cells, using a fixed ratio of 1:1. To assess exosome internalization by N9 cells, exosomes were labeled with PKH67, as previously described. To evaluate the effects produced by exosomes on N9 microglia, we incubated the cells in RPMI medium in the absence (control), or in the presence of exosomes, either from wt NSC-34 MNs, or from mSOD1 NSC-34 MNs. N9 microglia responses were evaluated at 2, 4, and 24 h. These different time-points of incubation were accomplished to evaluate the effects produced by an early (2 and 4 h) and a lasting (24h) period of exosome interaction with naïve N9 microglia. At the end of each incubation period, medium free of cellular debris was collected to assess the released soluble factors. Attached cells were: (i) fixed for 20 min with freshly prepared 4% (w/v) paraformaldehyde in PBS for immunocytochemical studies or to detect PKH67 labeled fluorescent exosomes; (ii) fixed with Fixing Solution for cellular senescence assays; (iii) used to extract total RNA using TRIzol® reagent, according to the manufacturer's instructions; or (iv) collected in Cell Lysis Buffer (Cell Signaling Beverly, MA, USA) plus 1 mM phenylmethylsulfonyl fluoride (PMSF, Sigma) for western blot analysis.

2.6. N9 Microglia Phagocytosis Assay

To evaluate the phagocytic ability of N9 microglia, cells were incubated with 0.0025% (v/v) fluorescent latex beads (#L1030, Sigma-Aldrich), diameter 1 µm, for 75 min at 37ºC. For immunofluorescence detection, N9 cells were fixed for 20 min with freshly prepared 4% (w/v) paraformaldehyde in PBS and a immunocytochemical technique was performed as usually in our lab for microglial cells (Caldeira et al. 2014; Cunha et al. 2016). N9 microglia were immunostained with rabbit anti-ionized calcium-binding adaptor molecule 1 (Iba1) (1:250, #019-19741, Wako), and nuclei were counterstained with Hoechst 33258 dye (blue). UV and fluorescence images of ten random microscopic fields (original magnification: 400X) were acquired per sample using an AxioCam HR camera adapted to an AxioScope A1® microscope (Zeiss, Germany), and Zen 2012 (blue edition, Zeiss) software. The number of cells with ingested beads and total cells were counted using ImageJ software to determine the percentage of phagocytosing cells (Silva et al. 2010).

2.7. Determination of Senescent-Like Positive N9 Microglia

Activity of senescence-associated beta-galactosidase (SA-β-gal) was determined as a biomarker of microglia-like senescence by using the Cellular Senescence Assay Kit

(#KAA002RF, Merck Millipore, Darmstadt, Germany), according to the manufacturer's instructions. Nuclei were counterstained with hematoxylin (Merck). The number of total cells was counted in 10 microscopic fields with ImageJ software (original magnification: 400X) acquired to observe the complete well using Leica IM50 software and Leica DFC490 camera (Leica Microsystems, Wetzlar, Germany), adapted to an AxioSkope HBO50 microscope (Zeiss). The number of turquoise stained microglia (SA-β-gal-positive cells) was counted to determine the amount of senescent cells relatively to the total cell number (percentage) (Caldeira et al. 2014).

2.8. Detection of NF-κB Activation

For immunofluorescence detection of nuclear factor-kappa B (NF-κB) translocation, cells were fixed as above and a standard immunocytochemical technique (Fernandes et al. 2006) was carried out using a rabbit anti-p65 NF-κB subunit antibody (1:200, #sc-372, Santa Cruz Biotechnology®, CA, USA). N9 microglial nuclei were stained with Hoechst 33258 dye. UV and fluorescence images of ten random microscopic fields (original magnification: 400X) were acquired as indicated for phagocytosis assay. NF-κB positive cells were identified by the ratio between the mean gray value of the nucleus and the mean gray value of the whole cell, using ImageJ software. A threshold was defined for each individual experiment and cells above that value were considered positive for NF-κB. Positive cells and total cells were counted to determine the percentage of NF-κB positive nuclei.

2.9. Quantification of Nitrite Levels

Levels of nitric oxide (NO) were estimated by measuring the concentration of nitrites (NO_2), a product of NO metabolism, in the extracellular media of N9 cells incubated in the absence, or in the presence of exosomes released by wt and mSOD1 NSC-34 cells. Extracellular media, free from cellular debris, were mixed with Griess reagent [1% (w/v) sulfanilamide in 5% H_3PO_4 and 0.1% (w/v) N-1 naphtylethylenediamine, all from Sigma-Aldrich, in a proportion of 1:1 (v/v)] in 96-well tissue culture plates for 10 min in the dark, at room temperature, as we published (Vaz et al. 2015). The absorbance at 540 nm was determined using a microplate reader. A calibration curve was used for each assay. All samples were measured in duplicate.

2.10. Assessment of Gelatinases (MMP-2 and MMP-9) by Gelatin Zymography

Activities of MMP-9 and MMP-2 were determined in the N9 extracellular media after incubation in the absence and in the presence of exosomes released by wt and mSOD1 NSC-34 cells by performing a SDS-PAGE zymography in 0.1% gelatin-10% acrylamide gels,

under non-reducing conditions, as usual in our lab (Silva et al. 2010). Briefly, after electrophoresis, the gels were washed for 1 h in a solution containing 2.5% Triton-X-100 to remove SDS and to renature the MMP species in the gel and then incubated at 37ºC to induce gelatin lysis (buffer: 50 mM Tris pH 7.4, 5 mM $CaCl_2$, 1 μM $ZnCl_2$) overnight. Gels were then stained with 0.5% Coomassie Brilliant Blue R-250 (Sigma-Aldrich) and destained in 30% ethanol/10% acetic acid/H2O (v/v). Gelatinase activity, detected as a white band on a blue background, was measured using computerized image analysis (Image Lab™, Bio-Rad).

2.11. Quantitative Real Time-PCR

Total RNA was extracted from exosome-treated N9 microglia using TRIzol® (LifeTechnologies, Carlsbad, CA, USA), according to manufacturer's instructions. Total RNA was quantified using Nanodrop ND-100 Spectrophotometer (NanoDrop Technologies, Wilmington, DE, USA) and conversion to cDNA was performed with SensiFAST™ cDNA synthesis (#BIO-65054, BIOLINE, London, UK). Quantitative RT-PCR (qRT-PCR) was performed on a 7300 Real Time PCR System (Applied Biosystems) using a SensiFAST™ SYBR® (Hi-ROX, #BIO-92002/S, BIOLINE). qRT-PCR was accomplished under optimized conditions: 50ºC for 2 min and 95ºC also for 2 min, followed by 40 cycles at 95ºC for 5 s and 62ºC for 30 s. In order to verify the specificity of the amplification, a melt-curve analysis was performed, immediately after the amplification protocol. Non-specific products of PCR were not found in any case. Results were normalized to β-actin and expressed as fold change. The sequences used for primers are represented in Supplementary Table II.1 (Supplementary Material). Relative miRNA concentrations were calculated using the ΔΔCT equation. RNA inside exosomes was extracted using mercury Isolation Kit - Cell (#300110, Exiqon, Vedbaek, Denmark). For miRNA analysis, conversion of cDNA was achieved with the universal cDNA Synthesis Kit (#203301, Exiqon), as described by Cardoso et al. (2012) and currently implemented in our lab (Caldeira et al. 2014; Cunha et al. 2016), following manufacturer's recommendations. The miRCURY LNA™ Universal RT miRNA PCR system (#203403, Exiqon) was used in combination with predesigned primers (Exiqon), represented in Supplementary Table III.1 (Supplementary Material), using SNORD110 as reference gene. The reaction conditions consisted of polymerase activation/denaturation and well-factor determination at 95ºC for 10 min, followed by 50 amplification cycles at 95ºC for 10 s and 60ºC for 1 min (ramp-rate 1.6ºC/s). Relative miRNA concentrations were calculated using the ΔΔCT equation. All samples were measured in duplicate.

2.12. Western Blot

Cells were collected in Cell Lysis Buffer, as usual in our lab (Vaz et al. 2015). Briefly, total cell extracts were lysed for 5 min on ice with shaking, collected with cell scrapper, and sonicated for 20 s. The lysate was then centrifuged at 14,000 g for 10 min at 4ºC, and the supernatants were collected and stored at -80ºC. Protein concentration was determined using a protein assay kit (Bio-Rad, Hercules, CA, USA) according to manufacturer's specifications. Then, equal amounts of protein were subjected to SDS-PAGE and transferred to a nitrocellulose membrane. After blocking with 5% (w/v) nonfat milk solution, membranes were incubated with primary antibody mouse anti-HMGB1 (1:200, from Biolegend) diluted in 5% (w/v) BSA overnight at 4ºC, followed by the secondary antibody goat anti-mouse HRP-linked (1:5,000, sc-2005, Santa Cruz Biotechnology®) diluted in blocking solution. Chemiluminescence detection was performed by using LumiGLO® reagent (Cell Signaling) and bands were visualized in the ChemiDoc™ XRS System (Bio-Rad). The relative intensities of protein bands were analyzed using the Image Lab™ analysis software (Bio-Rad).

2.13. Statistical Analysis

Results of at least seven independent experiments were expressed as mean ± SEM. Comparisons between the different parameters evaluated in wt and mSOD1 NSC-34 MNs were made via one-tailed Student's *t*-test for equal or unequal variance, as appropriate. In addition, we have performed unpaired *t*-test with Welch's correction when the variances were different between 2 groups. Comparison of more than two groups was done by one-way ANOVA followed by multiple comparisons Bonferroni *post-hoc* correction using GraphPad Prism5 (GraphPad Software, San Diego, CA, USA). *P*-values of 0.05 were considered statistically significant.

3. Results

3.1. mSOD1 NSC-34 MNs and Their Derived Exosomes Show Increased Levels of miR-124

Lately, miRNAs are emerging as potent fine-tuners of neuroinflammation and reported to be dysregulated in ALS (Butovsky et al. 2015; Koval et al. 2013). However, the contribution of individual miRNAs to neurodegeneration and neuroinflammation in ALS disease remains to be elucidated. We decided to investigate alterations on specific inflamma-miRs in the mSOD1 NSC-34 MNs and in their derived exosomes, using for comparison wt cells and their correspondent exosomes.

Cellular differentiation was induced and exosomes were isolated from extracellular media after 4 DIV, to induce SOD1 accumulation, as previously reported (Vaz et al. 2015). Recent data from our group, obtained by dynamic light scattering and TEM, indicated that the nanoparticle size of exosomes in the extracellular media of NSC-34 cells was approximately of ~140 nm (Vaz et al. 2016). We have additionally performed a more detailed characterization by NTA analysis, having observed an average diameter size of ~130 nm and a concentration of ~5.3 × 10^8 particles/ml (Figures III.1A, B), independently of being originated from wt or mSOD1 NSC-34 MNs. Western blot analysis showed the presence of exosomal marker proteins, namely Alix, Flotillin-1, and the tetraspanin CD63 in lysates obtained after the exosomal isolation procedure (Figure III.1C). In addition, exosomes isolated from wt and mSOD1 cells exhibited the characteristic cup-shape morphology by TEM (Figure III.1D). It is important to refer that similar total RNA concentrations were found for exosomes isolated from wt or mSOD1 cells (Figure III.1E). When compared to their wt counterpart, the mSOD1 MNs revealed an increased cargo in miR-124 (Figure III.1F), which is the predominant miRNA in the brain, namely in neurons (Sun et al. 2015). No detectable amounts of miR-146a or miR-155 were found in either of them.

Since exosomes are known to contain miRNAs that can be transferred into recipient cells causing changes in their functionality (Alexander et al. 2015; Valadi et al. 2007), we decided to evaluate the miRNA expression in the MN-derived exosomes. Interestingly, exosomes from mSOD1 MNs evidenced to be enriched in miR-124, recapitulating their cells of origin, and again no expression of miR-146a or miR-155 was detected in either type of exosomes.

3.2. Exosomes from wt and mSOD1 NSC-34 Donor Cells Are Similarly Disseminated in the Recipient N9 Microglia, and When Added to NSC-34+N9 Cocultures They Preferentially Distribute in N9 Microglial Cells

NSC-34 cells were demonstrated to uptake extracellular vesicles from a muscle cell line (C2C12) (Madison et al. 2014) and toxic exosomes were shown to be transferred from mSOD1 astrocytes to MNs (Basso et al. 2013). To determine whether exosomes released from mSOD1 and wt NSC-34 cells after 24 h incubation were similarly transferred into N9 microglial cells, we fluorescently labeled exosomes with PKH67, as previously described (Figure III.2A). No differences were found in such distribution. To further understand whether mixed exosomes in the supernatant of NSC-34(wt)+N9 and of NSC-34(mSOD1)+N9 cocultures were preferentially captured by MNs or by N9 microglia, we isolated exosomes from the culture medium, labeled them with PKH67, incubated the exosomes with matched NSC-34(wt)+N9 and NSC-34(mSOD1)+N9 cocultures, and assessed the distribution of PKH67-labeled exosomes in either one of the cells. In Figure III.2B, it is clearly shown that

N9 microglia are the preferential recipient cells for the mixed exosomes released from both donor cell types. Indeed, intracytoplasmic green exosomes are only visible in N9 microglia, indicating that these cells are more likely to incorporate and to be functionally influenced by exosomes, as compared to NSC-34 MNs.

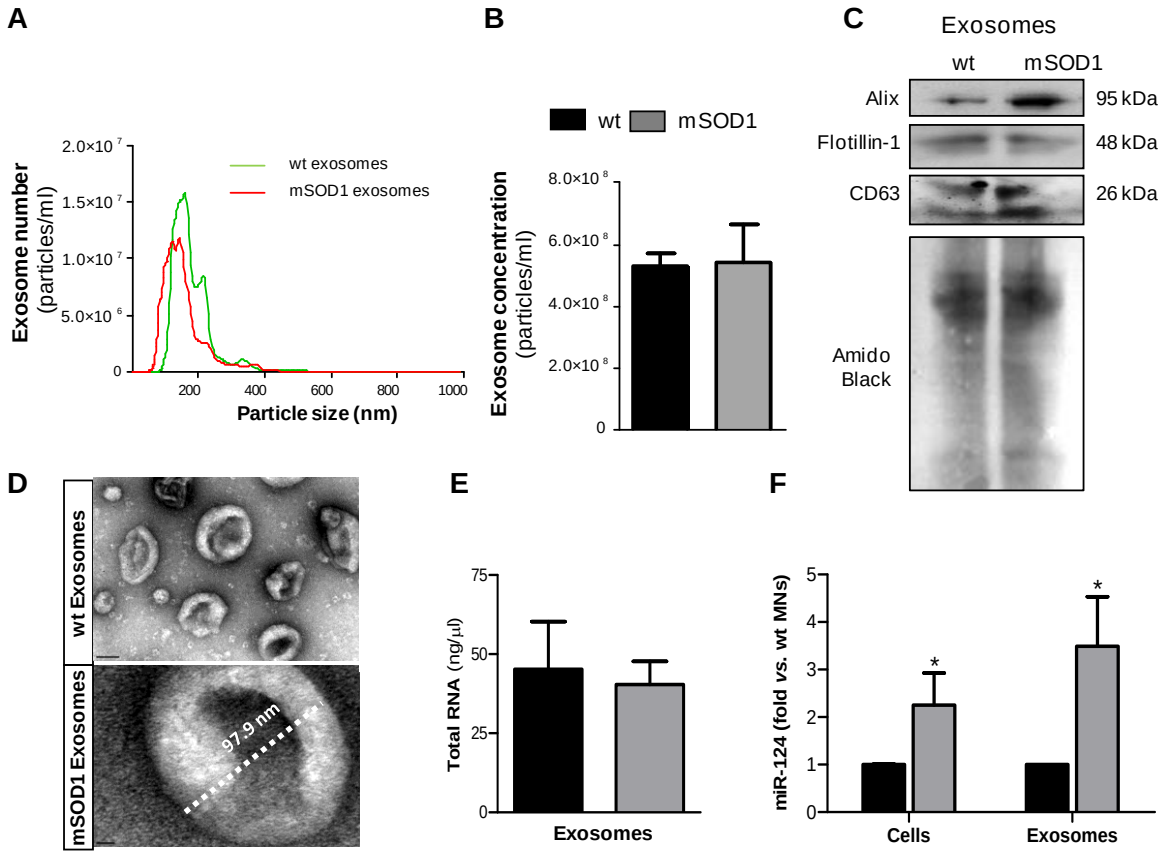

Figure III.1 - Exosomes released by wild-type (wt) SOD1 NSC-34 motor neurons (MNs) and by those mutated in G93A (mSOD1) show similar number, size and total RNA content, but only mSOD1 NSC-34-derived exosomes display elevated expression of microRNA (miR)-124, thus recapitulating the donor cell. Exosomes were isolated from the extracellular media of NSC-34 cells, either human wild-type SOD1 (wt MNs) or mutated in G93A (mSOD1 MNs), after 4 days *in vitro* differentiation, as described in methods. (A,B) Evaluation of the nanoparticles (exosomes) size and density by NTA indicates that the majority of vesicles from MNs have diameter ~130 nm, with no differences between wt and mSOD1 NSC-34 MNs in terms of particle concentration. (C) Western blot analysis indicates the presence of common exosome markers (Alix, Flotillin-1, and CD63). (D) Representative images obtained by transmission electron microscopy (TEM) of exosomes are depicted evidencing cup shape morphology and protein clusters. (E,F) RNA was extracted from cells and exosomes to evaluated microRNA (miRNA) expression. Quantification of total RNA (E) revealed no differences between samples from wt and mSOD1 NSC-34 MNs, while (F) miRNA profile show an increase only in miR-124 in both mSOD1 cells and in their derived exosomes. Results are mean (± SEM) from at least five independent experiments. Differences between mSOD1 NSC-34 MNs and wt NSC-34 MNs in cells and exosomes were obtained by the two-tailed Student's *t*-test with Welch's correction. *p < 0.05 vs. respective wt MNs (Control). Scale bar represents 100 nm in exosomes from wt NSC-34 MNs and 10 nm in mSOD1 NSC-34 MNs.

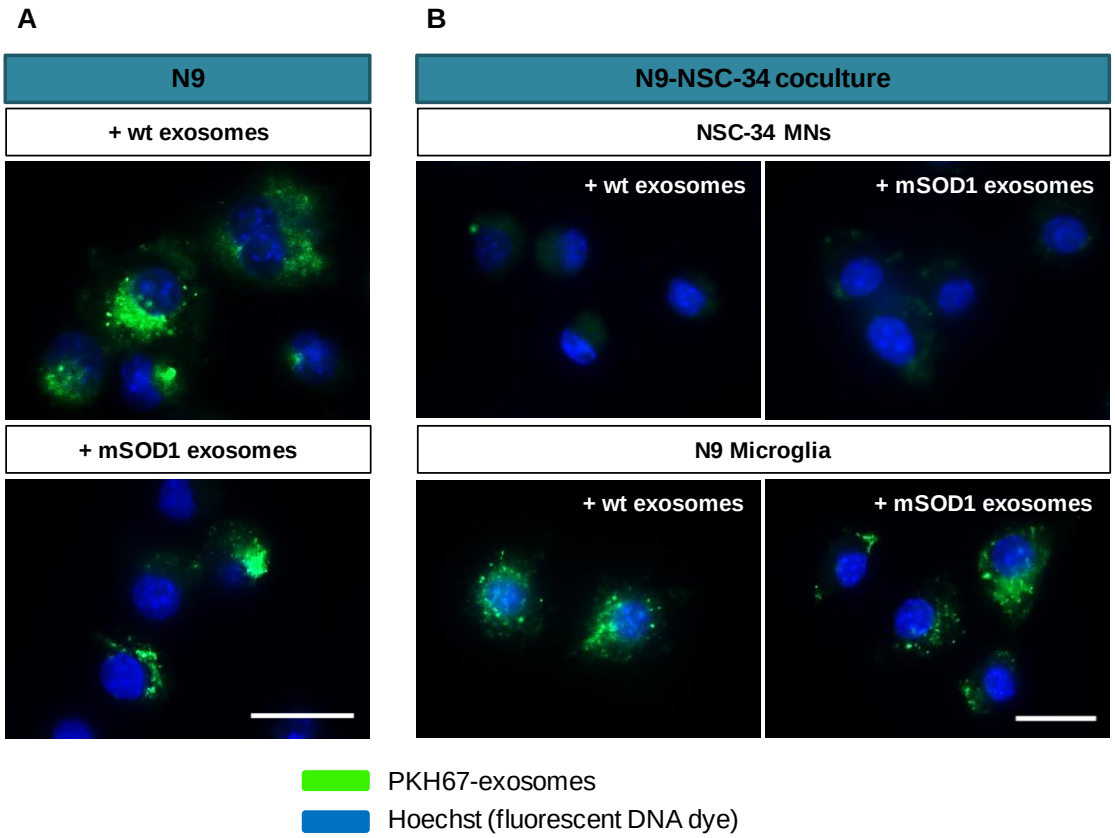

Figure III.2 - Exosomes from NSC-34 motor neurons (MNs), either wild-type (wt) or mutated in G93A (mSOD1) are equally distributed in N9 microglia, which also revealed to be the preferential recipient cells for exosomes derived from MNs+N9 cocultures. (A) Exosomes were isolated from NSC-34 MNs (wt and mSOD1), stained with the PKH67 Fluorescent Cell Linker Kit (in green) and incubated with N9 microglial cells for 24 h, and representative results of one experiment show the distribution of NSC-34-derived exosomes in monocultured N9 cells. (B) In parallel studies, exosomes were isolated from NSC-34 and N9 cells cocultures, stained as before and incubated for 24 h in a fresh NSC-34+N9 coculture and representative results of one experiment indicate the preferential distribution of exosomes in N9 microglia, as compared with NSC-34 MNs, when in the coculture system. Nuclei were stained with Hoechst dye (in blue). Scale bar represents 20 μm.

3.3. Increased HMGB1 Gene Expression in mSOD1 NSC-34 MNs May Contribute to Its Enhanced Nuclear Expression in the N9 Microglia When Cocultured with Such Cells

HMGB1 is a ubiquitous nuclear protein that is increasingly expressed and released by injured neurons and activated microglia (Brites and Vaz 2014; Cunha et al. 2016; Gao et al. 2011). To evaluate whether mSOD1 MNs that were shown to be dysfunctional (Vaz et al. 2015) expressed increased HMGB1 and influenced the expression of HMGB1 in N9 microglia, we assessed its expression levels in both wt and mSOD1 NSC-34 MNs, as well as in N9 microglia when in coculture with NSC-34 MNs, in the absence and in the presence of a surcharge of exosomes isolated from the coculture supernatant (Figure III.3).

We observed up-regulated HMGB1 gene and protein expression in mSOD1 NSC-34 MNs, as compared to wt cells (Figures III.3A, B). To note, however, that the exosomes *per se* did not produce noticeable alterations in the N9 microglia HMGB1 gene expression in the absence of mSOD1 NSC-34 MNs (data not shown). The decrease observed in N9 microglia

at 24 h incubation with mSOD1 exosomes (Figure III.3C), suggests either degradation/cleavage of the protein or its release into the cell supernatant. In addition, although not significant, we observed a slight elevation in HMGB1 mRNA levels in the N9 microglia exposed to mSOD1 NSC-34 MNs. Significant increase in the HMGB1 gene expression was, however, obtained in N9 cells cocultured with mSOD1 MNs (without cell contact) surcharged with exosomes isolated from a 24 h matching coculture system (Figure III.3D, $p < 0.05$), emphasizing secretome relevance in the signaling mechanisms underlying HMGB1-induced microglial activation. Therefore, we next decided to evaluate if the internalization of wt and mSOD1 NSC-34 MN-derived exosomes in N9 microglia caused changes in the cell dynamic properties and function, determined by specific cell polarization phenotypes.

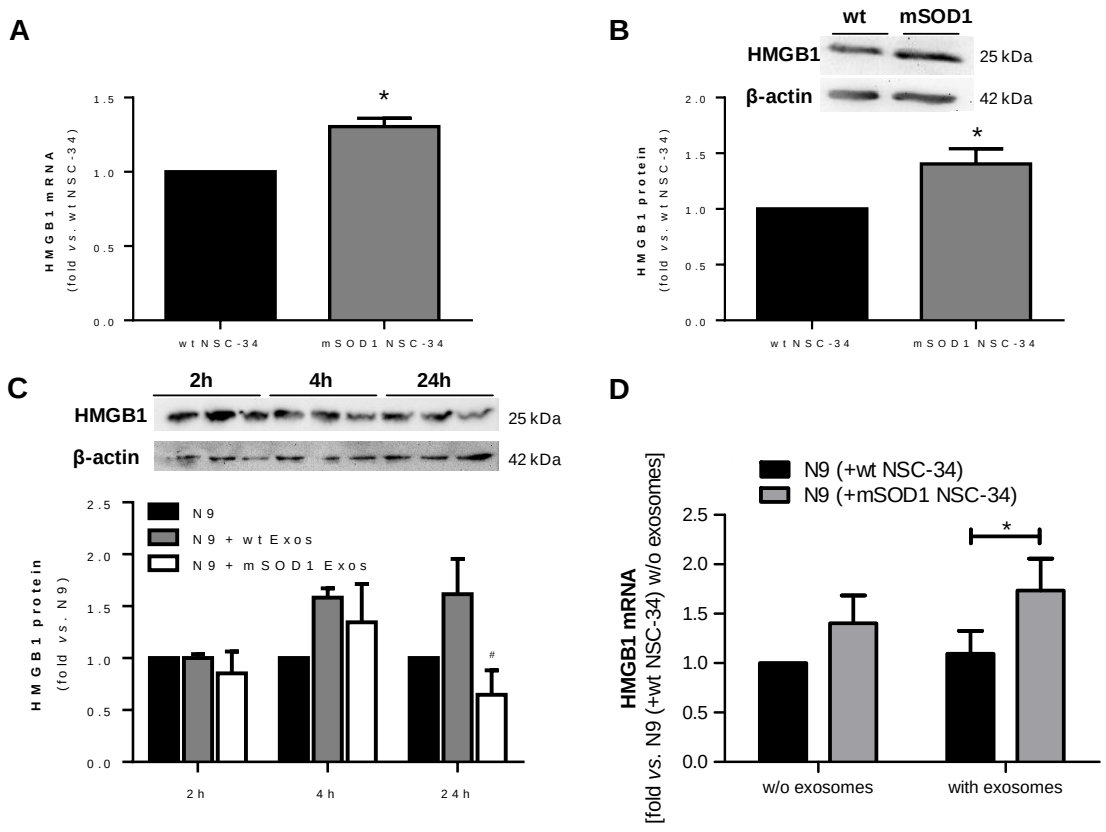

Figure III.3 - HMGB1 upregulation is only observed in mSOD1 NSC-34 motor neurons (MNs) and in N9 microglia cocultured with MNs after surcharge with exosomes isolated from the coculture supernatants, mainly if containing mSOD1 MN-derived exosomes. High mobility group box 1 (HMGB1) gene (A) and protein (B) expression was evaluated by qRT-PCR and Western Blot, respectively, in NSC-34 cells expressing either human wild-type SOD1 (wt MNs), or mutated in G93A (mSOD1 MNs), after 4 days *in vitro*. HMGB1 protein was also evaluated in (C) N9 cells-microglia incubated for 2, 4, and 24 h with exosomes (Exos) from wild-type (wt) NSC-34 MNs and mSOD1 NSC-34 MNs (N9+wt Exos and N9+mSOD1 Exos, respectively) or in (D) N9 cocultured with either wt or mSOD1 MNs, incubated or not with exosomes isolated from the media of a matched NSC-34-N9 coculture experiment, as indicated in methods. Results are mean (± SEM) from at least four independent experiments and are expressed as fold change vs. respective wt MNs. Differences between mSOD1 NSC-34 MNs and wt NSC-34 MNs were obtained by two-tailed Student's *t*-test with Welch's correction (A,B). Differences between the three different groups at each time point were obtained by one-way ANOVA followed by Bonferroni *post-hoc* correction (C,D) *$p < 0.05$ vs. respective wt NSC-34 MNs. $^{\#}p < 0.05$ vs. treatment with exosomes from wt NSC-34 MNs.

3.4. Exosomes Released by mSOD1 NSC-34 MNs Lead to Persistent NF-kB Activation and Early Production of Inflammatory Mediators in the Recipient N9 Microglia

The proinflammatory transcription factor NF-κB has been shown to activate numerous molecules and factors, and to be critical in the regulation of neuroinflammation-associated disease pathogenesis, (Shih et al. 2015). Thus, we evaluated whether mSOD1 exosomes were able to activate NF-κB in N9 cells, a process implicated in MN death in ALS (Frakes et al. 2014).

We observed that although a slight effect was produced by exosomes derived from wt NSC-34 MNs on the NF-κB translocation into the nucleus, only those from mSOD1 NSC-34 MNs activated significantly and persistently (from 2 to 24 h incubation) the NF-κB signaling pathway (Figures III.4A, B). This early and lasting NF-κB activation (Sen and Smale 2010) suggest that distinct sets of genes are activated in N9 microglia upon interaction with exosomes released from ALS NSC-34 MNs.

We and others have previously shown that NO is a key player in MN degeneration in ALS (Drechsel et al. 2012; Vaz et al. 2015) and that increased generation of redox molecules (NO) and iNOS activation occurs in M1 polarized N9 microglia (Cunha et al. 2016). Increased NO production was observed after 2 h of incubation with exosomes only from mSOD1 MNs (Figure III.4C). Such effect disappeared after 4 h incubation and even an inhibitory effect was produced by MN-derived exosomes at 24 h of incubation.

Activation of MMPs is another marker of neuroinflammation and elevation of MMP-9 and MMP-2 expression was observed in the spinal cord of SOD1G93A mice (Fang et al. 2009). Exosomes revealed to induce the MMP-2 activation whenever released from wt or mSOD1 MNs (Figure III.4D). Intriguingly, only those from mSOD1 NSC-34 MNs were able to activate MMP-9 (Figure III.4E), in accordance with our prior data showing such activation in mSOD1 NSC-34 MNs (Vaz et al. 2015). However, similarly to NO, this increase ceased over time, returning to basal levels.

Finally, we observed that the expression of the proinflammatory cytokines TNF-α and IL-1β was significantly upregulated and maintained until 4 h interaction, differently from the above mentioned inflammatory mediators, in cells exposed to exosomes from mSOD1 NSC-34 MNs, also disappearing after 24 h incubation (Figures III.4F, G).

Based on these data we may assume that exosomes from the mSOD1 NSC-34 MNs transiently switch N9 microglia into a M1 polarized cell (Chhor et al. 2013; Durafourt et al. 2012). Since early or late NF-κB activation was shown to induce different sets of genes, by respectively encoding TNF-α, IL-8, MMP-9, or cell surface receptors, adhesion molecules and signal adapters (Tian et al. 2005), we next evaluated the effects produced on the expression of cell surface receptors.

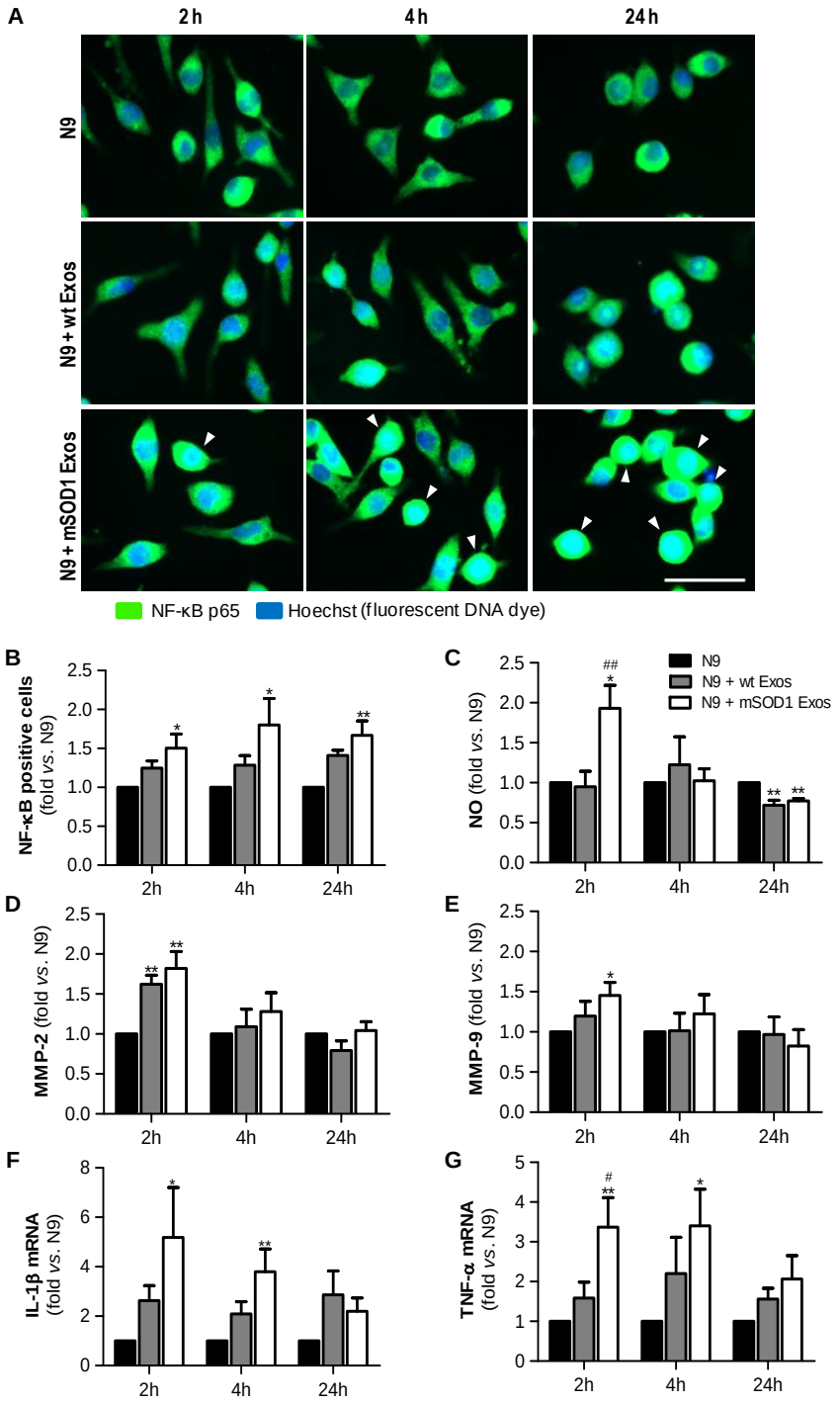

Figure III.4 - Exosomes derived from NSC-34 motor neurons (MNs) mutated in G93A (mSOD1) lead to sustained NF-kB activation and acute production of inflammatory mediators in the recipient N9 microglia. N9 cells were incubated for 2, 4, and 24 h with exosomes (Exos) from wild-type (wt) NSC-34 MNs and mSOD1 NSC-34 MNs (N9+wt Exos and N9+mSOD1 Exos, respectively), as indicated in methods. Non-treated cells were considered as control. (A) Representative results of nuclear factor kappa B (NF-κB) translocation into the nucleus and (B) number of NF-κB positive cells after interaction of exosomes with microglia. (C) Nitric oxide (NO) production was assessed by Griess reaction. (D,E) Activation of metalloproteinases (MMP)-9 and MMP-2, respectively, was assessed by gelatin zymography assay. (F,G) Relative tumor necrosis factor-α (TNF-α) and interleukin-1β (IL-1β) mRNA levels, respectively, were determined by qRT-PCR in total RNA. The fluorescence intensity of cells was quantified using the ImageJ software. Results are mean (± SEM) from at least seven independent experiments and are expressed as fold change relatively to non-treated N9 microglia. Differences between the three different groups at each time point were obtained by one-way ANOVA followed by Bonferroni *post-hoc* correction. *$p < 0.05$ and **$p < 0.01$ vs. non-treated cells; $^{\#\#}p < 0.01$ vs. treatment with exosomes from wt NSC-34 MNs. Scale bar represents 40 µm.

3.5. Exosomes from mSOD1 NSC-34 MNs Lead to a Delayed Upregulation of Receptors Involved in N9 Microglia Response to Stimuli

To determine whether late NF-κB activation in microglia treated with mSOD1 exosomes was associated with the increased expression of membrane surface receptors, like TREM2, RAGE, and TLR4, we evaluated their gene expression levels in a time-dependent manner. Indeed, microglia was shown to express multiple receptors able to efficiently respond to external stimuli (Pocock and Kettenmann 2007).

TREM2 receptor has been identified as a potential regulator of the microglial phenotype (Stefano et al. 2009) and found elevated in the spinal cord of ALS patients and SOD1G93A mice (Cady et al. 2014). As depicted in Figure III.5A, increased expression of TREM2 gene in N9 microglia was evident after 24 h incubation with both wt NSC-34 MNs and mSOD1 MNs-derived exosomes, although some fluctuations were observed overtime. TREM2 overexpression has been related with suppression of neuroinflammation and microglia M2 polarization associated with increased phagocytic ability (Jiang et al. 2016; Painter et al. 2015).

RAGE is also a receptor found elevated in association with mSOD1 (Shibata et al. 2002). In the present study, it is clear its net elevation only in the N9 microglia treated for 24 h with exosomes from mSOD1 MNs (Figure III.5B, $p < 0.05$ vs. wt NSC-34 MNs, and $p < 0.01$ vs. non-treated N9 microglia).

Besides RAGE, elevation of TLR4 was also identified in the spinal cord of sALS patients, mainly in glial cells (Casula et al. 2011). Both receptors play an important role in the regulation of innate and adaptive immunity during neuroinflammation. RAGE was recently indicated as enhancing TLR responses through binding and internalization of RNA (Bertheloot et al. 2016). Therefore, it was not surprising to find the same pattern of increased gene expression of TLR4 only in cells incubated for 24h with exosomes released by mSOD1 NSC-34 MNs (Figure III.5C).

At this point, our data indicate that exosomes from mSOD1 NSC-34 MNs determine an early inflammatory response on N9 microglia, which by releasing inflammatory mediators trigger the activation of RAGE/TLR signaling mechanisms and a second delayed stage of activation.

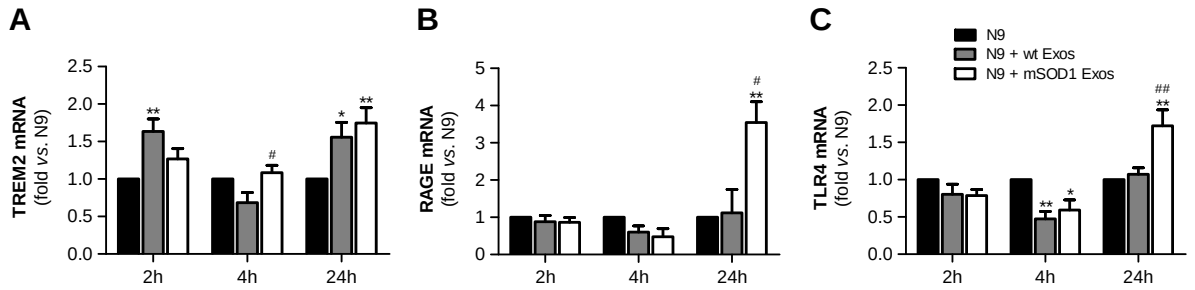

Figure III.5 - Exosomes from NSC-34 motor neurons (MNs) mutated in G93A (mSOD1) lead to delayed upregulation of the receptors TREM2, RAGE and TLR4 in N9 microglia. N9 cells were incubated for 2, 4, and 24 h with exosomes (Exos) from wild-type (wt) NSC-34 MNs and mSOD1 NSC-34 MNs (N9+wt Exos and N9+mSOD1 Exos, respectively), as indicated in methods. Non-treated cells were considered as control. Gene expression of (A) triggering receptor expressed on myeloid cells 2 (TREM2), (B) Receptor for Advanced Glycation Endproducts (RAGE) and (C) Toll-like receptor-4 (TLR4) was determined by qRT-PCR in total RNA. Results are mean (± SEM) from at least five independent experiments and are expressed as fold change relatively to non-treated N9 microglia. Differences between the three different groups at each time point were obtained by one-way ANOVA followed by Bonferroni *post-hoc* correction. *$p < 0.05$ and **$p < 0.01$ vs. non-treated cells; $^{\#}p < 0.05$ and $^{\#\#}p < 0.01$ vs. treatment with exosomes from wt NSC-34 MNs.

3.6. Exosomes from SOD1 NSC-34 MNs Induce an Early M1 Polarization and Heterogeneous (M1/M2) Microglia Subclasses at Lasting Times

In order to fully understand the effect of mSOD1 NSC-34-derived exosomes in N9-microglia phenotypic diversity, we searched for pro- and anti-inflammatory markers expressed in M1 and M2 microglial phenotypes (Brites and Vaz 2014; Cunha et al. 2016; Freilich et al. 2013), respectively.

Data showed that exosomes from mSOD1 NSC-34 cells trigger upregulation of the M1-associated markers iNOS and MHC-II after 2 and 4 h incubation, but not after 24 h interaction (Figures III.6A, B), suggesting that N9 microglial cells switch their polarization after continued interaction with the mSOD1 exosomes. Attenuated immune response with reduced MHC-II levels was observed at 24 h incubation, indicating that later, after activation, N9 microglial cells may downregulate MHC-II synthesis, as observed for dendritic cells (Villadangos et al. 2001). Indeed, the gene expression of M2-related markers, such as IL-10 and Arginase 1 (Figures III.6C, D), was found substantially enhanced at this time after treatment with mSOD1 exosomes.

To study the role of exosomal miR-124, and other cargo contents, in producing microglia dynamic changes we evaluated the expression of two anti-inflammatory miRNAs (miR-146a and miR-124) and the proinflammatory miR-155, a recognized inducer of the M1 polarization found increased in ALS patients and models (Butovsky et al. 2015; Koval et al. 2013; Liu and Abraham 2013) in N9 microglial cells after the transfer of mSOD1 exosomes.

We observed that a prompt reduction of calming miRNAs by NSC-34 MN-derived exosomes (Figures III.7A, B-2 h incubation) was followed by a marked and moderate selective elevation of miR-124 and miR-155, respectively, by mSOD1 exosomes (Figures

III.7A, C-24 h incubation). Surprisingly, both wt and mSOD1 exosomes produced a delayed increase in miR-146a expression.

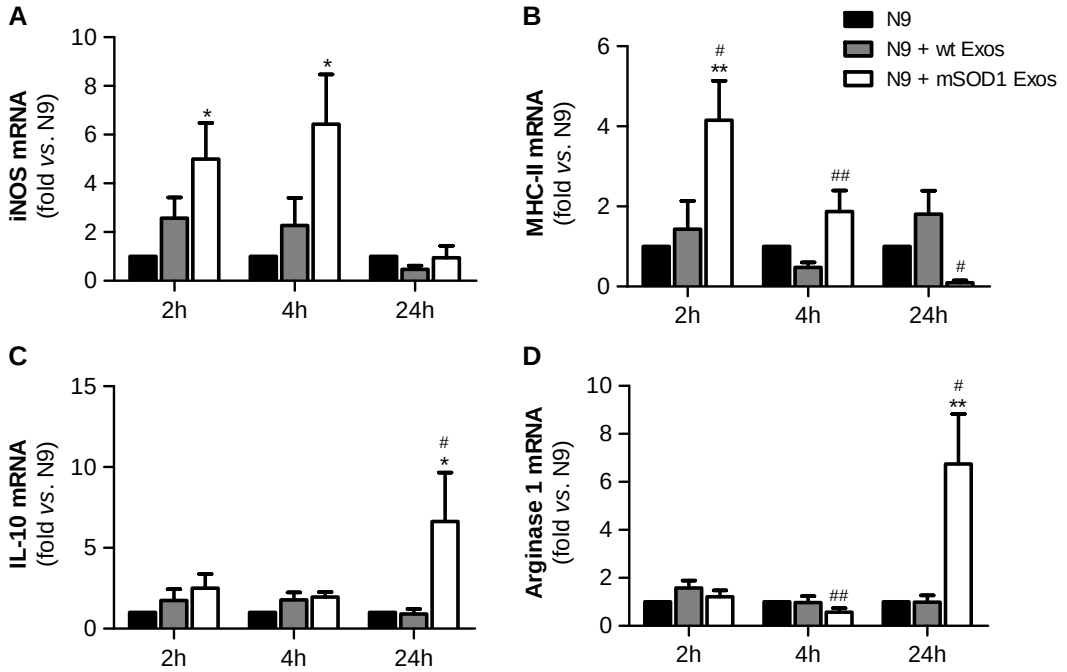

Figure III.6 - Exosomes from NSC-34 motor neurons (MNs) mutated in G93A (mSOD1) trigger early upregulation of M1- and late expression of M2-markers in N9 microglia. N9 microglia cells were incubated for 2, 4, and 24 h with exosomes (Exos) from wild-type (wt) NSC-34 MNs and mSOD1 NSC-34 MNs (N9+wt Exos and N9+mSOD1 Exos, respectively), as indicated in methods. Non-treated cells were considered as control. Relative mRNA levels of (A) inducible form of nitric oxide synthase (iNOS), (B) major histocompatibility complex-class-II (MHC-II), (C) interleukin-10 (IL-10), and (D) arginase-1 were determined by qRT-PCR in total RNA. Results are mean (± SEM) from at least eight independent experiments and are expressed as fold change relatively to non-treated N9 microglia. Differences between the three different groups at each time point were obtained by one-way ANOVA followed by Bonferroni *post-hoc* correction. *$p < 0.05$ and **$p < 0.01$ vs. non-treated cells; $^{\#}p < 0.05$ and $^{\#\#}p < 0.01$ vs. treatment with exosomes from wt NSC-34 MNs.

The immediate decrease in the N9 microglial miR-124 and miR-146 upon interaction with exosomes, indicative of M1 (proinflammatory) in opposite to M2 (alternative) microglia subtype, may justify the acute upregulation of inflammatory mediators previously observed (Figures III.4, III.6) for both wt (not significant) and mSOD1 NSC-34 MN-derived exosomes (at least $p < 0.05$). In contrast, the marked elevation of miR-124 at 24 h incubation in the N9 microglia treated with mSOD1 exosomes may derive, at least in part, from its increased content in MNs and in their derived exosomes that are collected by the cells, thus skewing M1 to M2a polarization (Veremeyko et al. 2013).

The upregulation of both calming and inflammatory miRNAs at 24 h, subsequent to the transfer of mSOD1 exosomes into the N9 cells, is indicative of induction of different polarized microglia subtypes, representing heterogeneous classes of activated N9 microglia, including both M1/M2 phenotypes. Influence of these diverse and simultaneous states on the variable rate of ALS progression surely deserves further investigation.

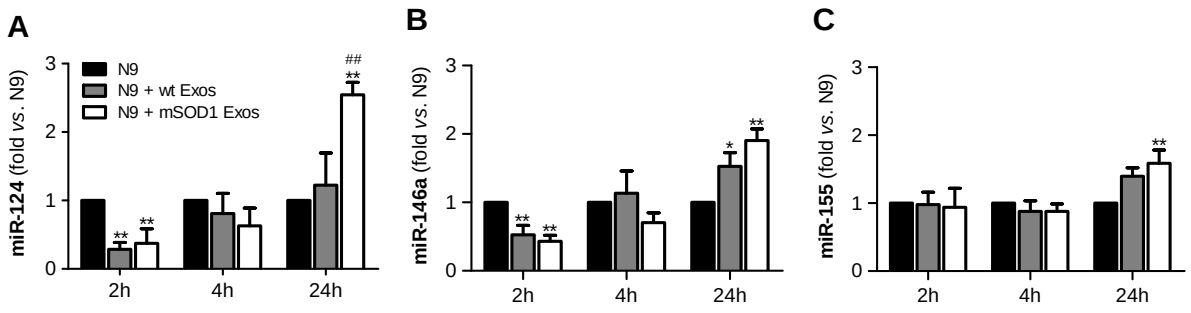

Figure III.7 - Early decreased expression of calming microRNAs (miR-124 and miR-146a) is indicative of N9 microglia M1 phenotype, but their increase together with that of miR-155 suggests the coexistence of multiple activated phenotypes at 24 h. N9 microglial cells were incubated for 2, 4, and 24 h with exosomes (Exos) from wild-type (wt) NSC-34 MNs and mSOD1 NSC-34 MNs (N9+wt Exos and N9+mSOD1 Exos, respectively), as indicated in methods. Non-treated cells were considered as control. (A–C) Relative miR-124, miR-146a, and miR-155 levels were determined by qRT-PCR in total RNA. Results are mean (± SEM) from eight independent experiments and are expressed as fold changes relatively to non-treated microglia. Differences between the three different groups at each time point were obtained by one-way ANOVA followed by Bonferroni *post-hoc* correction. *$p < 0.05$ and **$p < 0.01$ vs. non-treated cells; $^{\#\#}p < 0.01$ vs. treatment with exosomes from wt NSC-34 MNs.

3.7. Exosomes from mSOD1 NSC-34 MNs Induce Loss of N9 Microglia Phagocytic Ability and Cellular Senescence

After identifying that exosomes released by mSOD1 NSC-34 MNs induce phenotypical alterations, we asked whether the N9 microglial cells were disturbed in one of their most relevant neuroprotective functions, the phagocytic ability. Also based on the elevation of miR-146a at 24 h incubation produced by both sorts of exosomes in the N9 microglial expression, we questioned if increased cell senescence was produced. Actually, miR-146a was already suggested as a marker of a senescence-associated proinflammatory status (Caldeira et al. 2014; Olivieri et al. 2013). As depicted in Figure III.8, we observed a sudden and sustained decreased in the number of engulfed beads by N9 microglia upon interaction with mSOD1 exosomes, not noticed with those from wt NSC-34 MNs. Increased release of cytokines at 2 and 4 h incubation followed by upregulation of TLR4 after treatment with mSOD1 exosomes for 24 h, may account to this compromised N9 microglia function. We have previously used the quantitative assay of SA-β-gal activity to evaluate the increase in the number of senescent-like microglia (Caldeira et al. 2014), as similarly proposed by other Authors (Debacq-Chainiaux et al. 2009). Results revealed that the percentage of positively stained cells increased after 24 h of incubation with exosomes from mSOD1 MNs, when compared with non-treated cells (Supplementary data, Supplementary Figure III.1). Therefore, and despite of causing less than 10% enhancement in the number of senescent-like N9 microglia, such occurrence may additionally contribute to microglia impaired function. Overall these findings suggest that besides inducing microglia M1/M2 activation, exosomes from

mSOD1 NSC-34 MNs also generate harmful effects by triggering the loss of microglia protective functions.

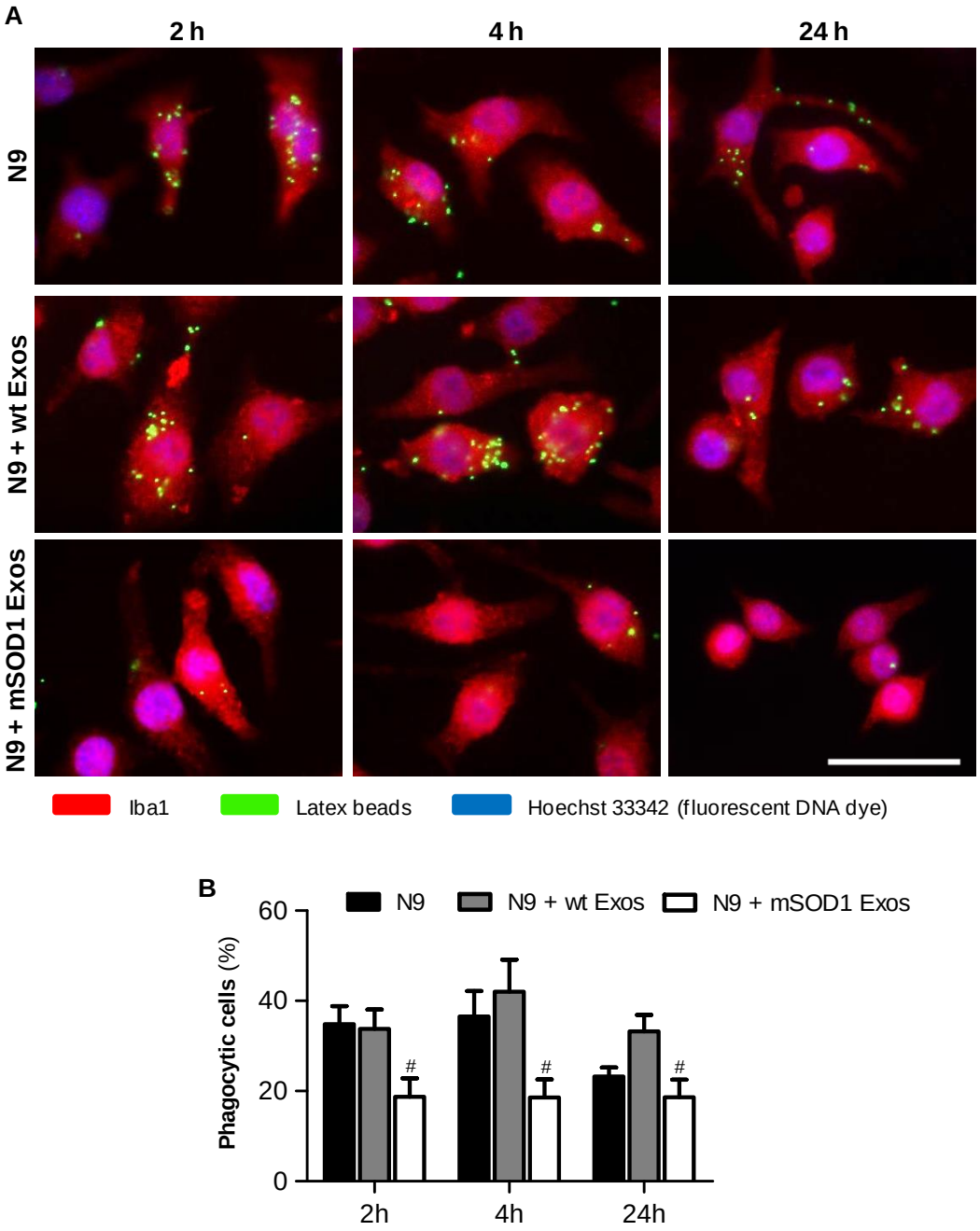

Figure III.8 - Exosomes from NSC-34 motor neurons (MNs) mutated in G93A (mSOD1) determine a sustained and marked decrease in the N9 microglia phagocytic ability. N9 microglial cells were incubated for 2, 4, and 24 h with exosomes (Exos) from wild-type (wt) NSC-34 MNs and mSOD1 NSC-34 MNs (N9+wt Exos and N9+mSOD1 Exos, respectively), as indicated in methods. Non-treated cells were considered as control. (A) Representative results of one experiment, showing engulfed latex beads (in green) by the Iba1 stained (in red) microglia with nuclei labeled by Hoechst dye (in blue). (B) Results are expressed as percentage of cells, relatively to the total number of microglia, showing ingested beads. Results are mean (± SEM) from eight independent experiments. Differences between the three different groups at each time point were obtained by one-way ANOVA followed by Bonferroni *post-hoc* correction. $^{\#}p < 0.05$ vs. exosomes from wt MNs. Scale bar represents 40 µm.

4. Discussion

Understanding the role of exosomes, either in physiological or in pathological conditions, as well as their involvement in the spreading of disease, is essential for a complete comprehension of the intra and extracellular signaling events involved in ALS and as clues for the development of more effective therapeutic strategies in this pathology. Exosomes are nowadays considered as mediators of neuroinflammation (Gupta and Pulliam 2014). We are the first in elucidating the effects of stably transfected mSOD1 NSC-34 MN-derived exosomes on the N9 microglia activation profile and on its functional properties. Previous studies demonstrated that toxic exosomes are transferred from mSOD1 astrocytes to MNs (Basso et al. 2013) and that exosomes-dependent and -independent mechanisms are involved in mSOD1 propagation (Grad et al. 2014a). It was lately hypothesized that extracellular vesicles are mainly released from live cells and from cells in the early dying process. It was proposed that within the recipient cell, the misfolded SOD1 species can template the misfolding of normally folded wt SOD1 (Silverman et al. 2016). In this work we established that exosomes derived from mSOD1 NSC-34 cells are enriched in miR-124 and responsible for N9 microglia activation and loss of function.

MiRNAs are genome encoded, short, non-protein coding RNA molecules that are expressed throughout the brain operating as fine tuners of post-transcriptional intricate events and involved in neuronal function and dysfunction (Im and Kenny 2012; Saba and Schratt 2010). Indeed, miRNAs are known to be crucial for neuronal differentiation and miR-124 was indicated to regulate hundreds of genes and to counteract astrocyte-specific route (Neo et al. 2014). When miR-124 is down-regulated, it triggers defective neuronal survival and reduced axonal outgrowth (Sanuki et al. 2011). Thus, overexpression of miR-124 was shown to be related with neuronal differentiation in neuroblastoma cell lines and embryonic stem cells (Krichevsky et al. 2006; Makeyev et al. 2007), and to contribute to neurite outgrowth (Yu et al. 2008), and neurogenesis (Visvanathan et al. 2007). MiR-124 was also found expressed in a subset of sensory neurons and suggested to have different functions and/or targets (Makeyev et al. 2007).

We evaluated the expression of specific inflamma-miRs in the mSOD1 NSC-34 cells. In contrast with the undetectable amounts of miR-146a and miR-155, we observed an upregulation of miR-124 in the mSOD1 NSC-34 MNs. Moreover, and similarly to the presence of miR-124a found in secreted exosomes from primary cortical neurons (Morel et al. 2013), we noticed that exosomes from mSOD1 NSC-34 MNs collected by ultracentrifugation were enriched in miR-124, as well. Those Authors additionally documented that such exosomes were internalized by astrocytes where they modulated the astroglial glutamate transporter GLT-1. Here, we have observed that the exosomes released

from NSC-34 MNs when incubated with N9 microglia and NSC-34 MNs, were preferentially collected by N9 microglia instead of being transferred into NSC-34 MNs. Previous studies have also evidenced the selective transfer of exosomes from oligodendrocytes to microglia (Fitzner et al. 2011). Interestingly, elevation of miR-124 in nerve terminals was associated to a decreased neurotransmitter release at the neuromuscular junction (Kye and Goncalves Ido 2014), probably accounting to their dysfunction. Moreover, miR-124 upregulation was also demonstrated to be connected to a decreased capacity of cells to repair DNA strand breaks (Chen et al. 2015) and to be increased by stressful conditions (Sun et al. 2015). Clearly, the harmful or beneficial effects of miR-124 upregulation in ALS require further investigation, namely in terms of its transfer to microglia. Although with unknown biological significance in the periphery, its specific brain localization and presence in serum exosomes after acute ischemic stroke (Ji et al. 2016) is indicative of its promising potential as a biomarker of brain damage.

Spreading mechanisms are likely to underlie ALS disease progression based on the propensity of mutant SOD1 to misfold, on conditions that accelerate aggregation of wt SOD1 and on the interplay between affected neurons and their neighboring glial cells (Maniecka and Polymenidou 2015). SOD1 cell-to-cell transmission may occur via both exosome-dependent and exosome-independent routes (Grad et al. 2014b). Indeed, these Authors demonstrated that NSC-34 cells stably transfected with mutant SOD1 release neurotoxic species of SOD1 that are transferred to naïve cells by macropinocytosis via conditioned medium transfer, either associated with exosomes (relatively efficient), or as protein-only aggregates. Interestingly, previous studies have shown that extracellular aggregated mSOD1 incubated for 24 h with microglia lead to increased ROS production and TNF-α release, and that the aggregates were internalized after 1 h incubation with minimal degradation after 24 h (Roberts et al. 2013). Since we observed that the exosomes released from NSC-34 MNs, when incubated with N9 microglia and NSC-34 MNs, were selectively transferred into N9 microglia, we decided to evaluate the temporal progression of the mechanisms leading to microglia activation by the mSOD1 MN-derived exosomes.

Previous studies in the spinal cord of SOD1G93A mice suggest that HMGB1 is not involved as a primary event in the MN death and that no changes occur relatively to its subcellular distribution in glial cells (Lo Coco et al. 2007). Further studies documented that increased expression of HMGB1, TLR4, and RAGE in reactive glial cells is observed in both gray (ventral horn) and white matter of the spinal cord from sALS patients (Casula et al. 2011). These Authors identified an elevated HMGB1 signal in the cytoplasm of glial cells and suggested that its release may be associated to the perpetuation of inflammation and necrosis of surrounding neurons due to inflammasome activation and secretion of proinflammatory cytokines, such as IL-1β and IL-18 (Baroja-Mazo et al. 2014; Lu et al. 2013).

Recently, it was additionally showed that HMGB1 is a critical pathogenic molecule leading to neurite degeneration and innate immune activation during Alzheimer's disease pathology (Fujita et al. 2016; Venegas and Heneka 2017). Little is known about HMGB1 production and release by microglial cells, although we have shown that activated N9-microglia is able to secrete HMGB1 in response to the LPS-proinflammatory stimulus (Cunha et al. 2016) and to Aβ interaction (Falcão et al. 2017). HMGB1 also interacts with RAGE and TLR4, therefore extending the inflammatory cascade, while also promotes autophagy in detriment of apoptosis (Shen et al. 2013). Our results document an increased HMGB1 mRNA and protein levels in the mSOD1 NSC-34 MNs and in the N9 microglia cocultured with mSOD1 NSC-34 MNs in the presence of exosomes isolated from the extracellular media of such cultures, but not when N9 microglia is incubated with exosomes in the absence of NSC-34 MNs, suggesting that HMGB1 is released to the extracellular media after a prolonged incubation. Thus, we hypothesize that NSC-34 MN-derived soluble HMGB1 is necessary to induce N9 microglial HMGB1 enhanced expression, or that it is a consequence of a sustained microglial inflammatory status, after the release of proinflammatory cytokines and activation of RAGE and TLR4 receptors (Casula et al. 2011; Yu et al. 2006). Besides its delayed kinetic release, HMGB1-mediated production of proinflammatory cytokines requires the presence of these receptors, which we found to only be upregulated after 24h of mSOD1 NSC-34 MN-derived exosomes interaction with naïve N9 microglia. The active secretion of HMGB1 into the extracellular milieu was documented to only begin 8–12 h after ligation to TLRs (Andersson and Tracey 2011). In addition, previous studies indicated that the cytokine is a downstream and late mediator of inflammation that is released up to 1 week after admittance of patients with sepsis (Sunden-Cullberg et al. 2005).

TLR4 has been indicated to be involved in the pathological mechanisms of ALS disease, and blocking TLR4 with an antagonist extended the survival of the mSOD1 mice model (Lee et al. 2015b). Recent evidences point out that the expression of RAGE is higher in the spinal cord of mSOD1 mouse model of ALS as compared with the wt one, and that pharmacological blockade of RAGE delays the progression of ALS and prolongs life span (Juranek et al. 2016). Here, we show for the first time that the expression of N9 microglial TLR4 and RAGE are enhanced in the N9 microglial cells upon the acceptance of exosomes from the mSOD1 NSC-34 MNs reinforcing the pathogenicity of such extracellular vesicles in ALS. In fact, protein levels of RAGE and its ligand HMGB1 were indicated to be elevated in ALS patients (Juranek et al. 2015).

TREM2 is another microglial receptor leading to downstream signaling cascades activation. It is implicated in multiple microglial transcriptional programs causing microglial phenotypes that do not fit the conventional M1/M2 paradigm and cell expansion (Poliani et al. 2015). TREM2 is thought to increase phagocytic activity and to suppress cytokine production

(Chiu et al. 2013), while TREM2 p.R47H variant revealed to be a potent risk factor for sALS (Cady et al. 2014). Our data evidenced that exosomes *per se* induce a moderate, although significant late TREM2 gene upregulation. Controversial effects of increased expression of TREM2 protein were correlated with either apoptosis and decreased synaptic communication in Alzheimer's disease (AD) patient samples (Lue et al. 2015), or with an increased microglia ability to phagocytose, to inhibit Aβ proinflammatory responses and to rescue spatial cognitive impairment in the AD mouse model (Jiang et al. 2014). Therefore, potential benefits and harmful consequences of TREM2 upregulation require a further understanding on the still obscure microglia activation stages and their specific consequences on astrocytes and neurons.

Microglia were shown to induce MN death via the classical NF-κB pathway in ALS. Indeed, while NF-κB activation in astrocytes did not confer neuroprotection, its abolishment in microglia facilitated MN survival (Frakes et al. 2014). Based on this assumption we may conclude that the activation of the NF-κB pathway by the mutated exosomes add on microglia neurotoxicity toward MNs in ALS. The sustained NF-κB activation was paralleled by a loss in the phagocytic ability exclusively in N9 microglia exposed to mSOD1 exosomes. Previous studies demonstrated that TLR signaling inhibits the phagocytosis of apoptotic cells through NF-κB activation in microglia/macrophages (Deng et al. 2013; Feng et al. 2011) and that exosomes trigger the NF-κB signaling pathway (Bretz et al. 2013; Matsumoto et al. 2005). In the present study, such effect was mostly seen with mSOD1 exosomes, and the duration intended as determinant of different cellular responses (Bonnay et al. 2014): early release of proinflammatory mediators and late upregulation of cell surface receptors.

Neuroinflammation is a major component of ALS pathology, with activation and proliferation of microglia observed at sites of MN injury (Boillée et al. 2006b). Our results show a marked increase of NO levels and MMP-2 and MMP-9 activation, upon a short exposure to exosomes from mSOD1 NSC-34 MNs. The increase in NO levels only occurred in cells exposed to mSOD1 exosomes, indicating their role as promoters of microglial oxidative stress. Extracellular mSOD1 activation of microglia was shown to be mediated through the CD14/TLR pathway, leading to activation of NF-κB, followed by upregulation of iNOS and release of NO from these cells (Zhao et al. 2010). Our data indicate a similar microglia activation triggered by mSOD1 exosomes from NSC-34 MNs, what is consentaneous with the TLR-dependent signaling pathways already proposed for exosomes (Bretz et al. 2013).

Elevation of MMP-9 activity was found primarily in ALS associated NSC-34 MNs (Lim et al. 1996; Vaz et al. 2015). MMP-9 and MMP-2 secretion was suggested to be shed as membrane vesicle-associated components and to have a role in synaptic plasticity (Sbai et al. 2008; Taraboletti et al. 2002). Once ALS MNs release increased amounts of MMP-9 (Vaz

et al. 2015), it may be hypothesized that increased levels of both MMPs in exosomes account for their subsequent release from the activated microglia. Accordingly, the expression of proinflammatory cytokines like TNF-α and IL-1β was also early upregulated in N9 microglia exposed to mSOD1 exosomes, and probably associated with the acute translocation of NF-κB to the nucleus and induction of genes involved in the production of proinflammatory mediators (Ghosh et al. 1998). Because activation of NF-κB in microglia was shown to induce gliosis and MN death, we may assume that exosomes from ALS NSC-34 MNs may have a role in neuroinflammation and neurodegeneration associated to ALS onset and progression (Frakes et al. 2014).

M1/macrophages/microglia have been associated to MN degeneration and ALS disease progression (Hooten et al. 2015; Lee et al. 2016), although a 50% reduction on reactive and proliferating microglia was initially shown to not influence neuronal damage (Gowing et al. 2008). Using established markers that allow the differentiation between M1 and M2 activated cells (Brites and Vaz 2014), we observed that the M1-markers iNOS and MHC-II were early upregulated after transfer of mSOD1 exosomes into N9 microglial cells compatible with M1 polarization. Interestingly, we observed a delayed up-regulation of the M2-associated markers (Arginase 1 and IL-10) in N9 cells exposed for 24 h to exosomes from mSOD1 NSC-34 MNs, while levels of iNOS remained unchanged and MHC-II were even downregulated. This profile, together with sustained NF-κB activation and RAGE/TLR4/TREM2 upregulation at longer time-points suggest a switch of microglia phenotype from a classic M1 activated phenotype to a mixture of microglia subtypes that include M2 polarized cells. The precise harmful and still obscure role of microglia in ALS remains to be fully clarified, but may reside in the increased levels of miR-155 in the cell. Actually, Butovsky et al. (2015) found that miR-155 was overexpressed in the mSOD1 mouse, as well as in fALS and sALS patients, and that its targeting restored the dysfunctional microglia and attenuated disease progression in the mouse model. Other miRNAs besides miR-155 were also found upregulated in ALS microglia, such as miR-146b, miR-22, and miR-125b, thus strengthening the impact that miRNAs may have in modulating inflammatory genes and pathogenic mechanisms (Parisi et al. 2013).

Lately, exosomes released from activated cells were shown to contain inflammatory miRNAs, such as miR-146a, miR-155, and miR-21 among others (Alexander et al. 2015; Xu et al. 2014). We recently evidenced that miR-155 and miR-146a are increased in exosomes from LPS-induced M1 polarization of N9 microglia (Cunha et al. 2016). Other Authors (Alexander et al. 2015) also observed that these same miRNAs are released from dendritic cells within exosomes, pass between immune cells, negatively influencing (miR-146a) or promoting (miR-155) endotoxin-induced inflammation in mice. Therefore, we decided to evaluate the miRNAs associated with the modulation of the immune response (inflamma-

miR), namely miR-155, miR-146a, and miR-124. Other miRNAs not indicated as directly implicated in microglia polarization were not considered in the present study. Our results identified their overall overexpression after 24 h incubation of the mSOD1 exosomes with N9 microglia. Therefore, we hypothesize that different microglia subpopulations may coexist with distinct roles that may include from neuroprotection to neurotoxic properties. The elevation of miR-155 is associated with RAGE overexpression and microglia M1 activation, while determine neurogenic deficits (Onyeagucha et al. 2013; Woodbury et al. 2015). In respect to miR-124 it was shown to promote microglia quiescence by diminishing M1 polarization and enhancing M2 phenotype (Liu and Abraham 2013; Ponomarev et al. 2011), in particular the M2c microglia subset (Veremeyko et al. 2013). However, it is also a trigger of microglia functional maturity, at least during CNS development, where microglia evidence a reduced cellular motility and phagocytic ability (Svahn et al. 2016). Finally, miR-146a overexpression is found in M1, M2a, M2c, and senescent microglia subsets (Cobos Jimenez et al. 2014; Jiang et al. 2012). Our results further enhance the knowledge of the dysregulated miRNAs in ALS reinforcing miR-155 (Roberts et al. 2013), but also miR-146a and miR-124 among the most highly expressed in the microglia after internalization of mSOD1 NSC-34 MN-derived exosomes.

Here, we show that besides early and late activation processes and sustained activation of the NF-κB pathway, mSOD1 exosomes also trigger a substantial loss of the N9 microglia phagocytic ability, subsequently accompanied by an increased proportion of senescent-like microglia. Beneficial or detrimental consequences of microglial phagocytosis in tissue repair is a matter of controversy (Fu et al. 2014), but it has been claimed to be essential in the clearance of cellular debris, as well as in pathogenic organisms (Kloss et al. 2001; Nakamura et al. 1999). While the release of proinflammatory mediators is accepted as having a role in damage resolution, and chronic microglia activation as being associated with ageing and neurodegenerative diseases, much less attention has been paid to microglial phagocytosis, and to when such ability is reduced. Decreased phagocytic ability was demonstrated for senescent microglia in aging and in Alzheimer's disease models (Caldeira et al. 2014; Hickman et al. 2008; Zhu et al. 2011). While M1 microglia are often associated with acute inflammatory stimulus, M2 cells play a key role in tissue regeneration, promote phagocytosis and are designated as being protective. However, the distinction into M1/M2 subtypes is lately considered to be a simplification as represents the extreme states (Goldmann and Prinz 2013). Actually, M2 (non-M1) activation state is considered to involve heterogeneous and functionally distinct macrophages/microglia (Roszer 2015). Recent studies state that delayed cell clearance critically affects the dynamics of phagocytosis and suggest evaluation of phagocytic efficiency in neurological disorders (Abiega et al. 2016).

Taken together, the results obtained in this work indicate that exosomes released from mSOD1 NSC-34 MNs are enriched in miR-124 and are preferentially internalized by N9 microglia, causing a specific pattern of cell activation determined by early and late NF-κB and lasting decrease of the phagocytic ability. Acute response determines the increased production of proinflammatory mediators and cytokines. In such conditions microglia was shown to induce the formation of A1 reactive astrocytes with neurotoxic properties (Liddelow et al. 2017). Delayed activation is associated with enhanced expression of cell surface receptors and of miR-155, miR-146a, and miR-124. Therefore, exosomes from mSOD1 NSC-34 MNs initially polarize N9 microglia into the M1 proinflammatory phenotype, which may further enhance neuroinflammation and MN degeneration, together with a reduced ability to repair and maintain cellular homeostasis. However, with time, mSOD1 exosomes trigger different stages of activation leading to a miscellaneous population constituted by microglia expressing markers of M1, M2, and senescent states. In conclusion, exosomes released by the mSOD1 NSC-34 MNs have the potential to determine specific microglia subsets compatible with the previously assigned neurodegeneration-specific gene-expression profile found in the spinal cord microglia (Chiu et al. 2013). Despite the upregulation of the phagocytosis-related TREM2, TLR4 and RAGE surface receptors, microglia show a decreased ability to phagocytose and propensity to cell senescence upon exosome interaction, thus favoring the involvement of mSOD1 exosomes in the ALS onset and progression, whose precise mechanism of action requires additional studies.

Acknowledgments

This work was funded by the Research Grant of the Santa Casa Scientific Research Program on ALS, by Santa Casa da Misericórdia de Lisboa (SCML), Portugal (Project ELA-2015-002, to DB) and, in part, by the EU Joint Programme - Neurodegenerative Disease Research (JPND) MADGIC project and Fundação para a Ciência e Tecnologia (FCT), Lisboa, Portugal (JPco-fuND/0003/2015 to DB and UID/DTP/04138/2013 to iMed.ULisboa). AV holds a postdoctoral research fellowship (SFRH/BPD/76590/2011) and CC is recipient of a PhD fellowship (SFRH/BD/91316/2012), all from FCT. MB is recipient of a Research Grant from SCML. The funding organization had no role in study design, data collection and analysis, decision to publish, or preparation of the manuscript. We thank Prof. José Paulo Farinha and Dr. Tânia Ribeiro for NTA analysis in Nanosight, model LM10-HSBF at Institute of Nanoscience and Nanotechnology, Instituto Superior Técnico, University of Lisbon.

5. Supplementary Material

Supplementary Table III.1 - List of primer sequences used in qRT-PCR

	Gene	Sequence (5'-3')
A	*TNF-α*	5'-TACTGAACTTCGGGGTGATTGGTCC-3' (fwr)
		5'-CAGCCTTGTCCCTTGAAGAGAACC-3' (rev)
	IL-1β	5'-CAGGCTCCGAGATGAACAAC-3' (fwr)
		5'-GGTGGAGAGCTTTCAGCTCATA-3' (rev)
	HMGB1	5'-CTCAGAGAGGTGGAAGACCATGT-3' (fwr)
		5'-GGGATGTAGGTTTTCATTTCTCTTTC-3' (rev)
	RAGE	5'-CTGGTGGGACTGTGACCTTG-3' (fwr)
		5'-TCTGCCTGTCATTCCTAGCTC-3' (rev)
	TREM2	5'-AGCTACCCGCTACTGCAAAG-3'(fwr)
		5'-TCACTGCCAGGGGGTCTAAG-3' (rev)
	TLR4	5'-ACCTGGCTGGTTTACACGTC-3' (fwr)
		5'-GTGCCAGAGACATTGCAGAA-3' (rev)
	Arginase 1	5'-CTTGGCTTGCTTCGGAACTC-3' (fwr)
		5'-GGAGAAGGCGTTTGCTTAGTTC-3' (rev)
	IL-10	5'-ATG CTG CCT GCT CTT ACT GA-3' (fwr)
		5'-GCA GCT CTA GGA GCA TGT GG-3' (rev)
	iNOS	5'-ACCCACATCTGGCAGAATGAG-3' (fwr)
		5'-AGCCATGACCTTTCGCATTAG-3' (rev)
	MHC-II	5'-TGGGCACCATCTTCATCATTC-3' (fwr)
		5'-GGTCACCCAGCACACCACTT-3' (rev)
	β-actin	5'-GCTCCGGCATGTGCAA-3' (fwr)
		5'-AGGATCTTCATGAGGTAGT-3' (rev)

	microRNA	Sequence (5'-3')
B	miR-124	5'-UAAGGCACGCGGUGAAUGCC-3'
	miR-146a	5'-UGAGAACUGAAUUCCAUGGGUU-3'
	miR-155	5'-CTCAGAGAGGTGGAAGACCATGT-3'
	SNORD110	Reference gene

(A) Primers used in gene expression. **(B)** Primers used in microRNA expression.

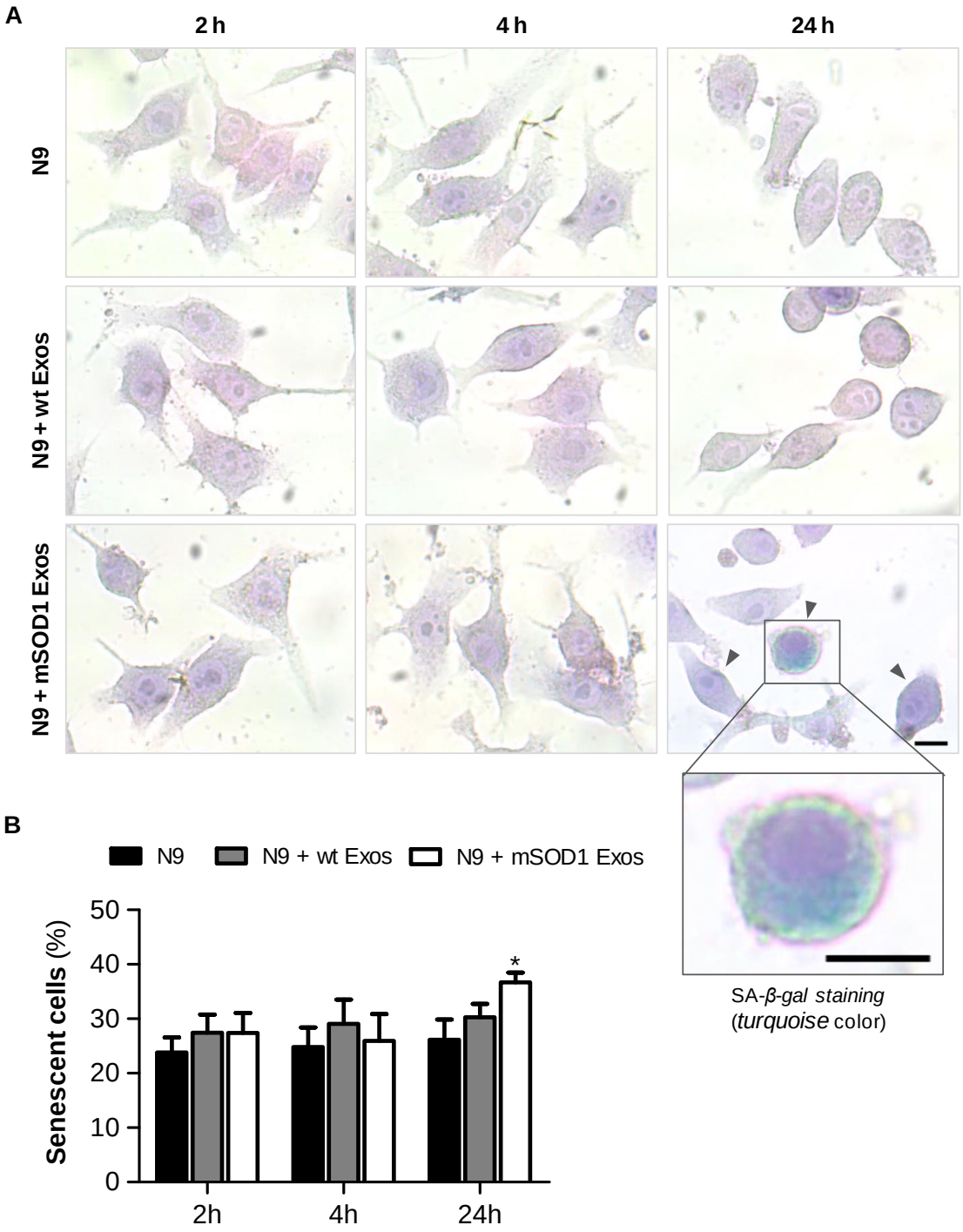

Supplementary Figure III.1 - Increased number of senescence-associated beta-galactosidase (SA-β-gal) expressing cells follows the exposure of N9 microglial cells to exosomes from mSOD1 NSC-34 MNs. N9 microglial cells were incubated for 2, 4, and 24 h with exosomes (Exos) from wild-type (wt) NSC-34 MNs and mSOD1 NSC-34 MNs (MG+wt Exos and MG+mSOD1 Exos, respectively), as indicated in methods. Non-treated cells were considered as control. (A) Representative results of one experiment show senescent-like cells (SA-b-gal staining). (B) Results are expressed as the percentage of SA-β-gal positive cells (turquoise staining) relatively to the total number of microglia. Results are mean (± SEM) from at least five independent experiments. Differences between the three different groups at each time point were obtained by one-way ANOVA followed by Bonferroni *post-hoc* correction. *p < 0.05 vs. non-treated cells. Scale bar represents 40 μm.

Chapter IV

DOWNREGULATED GLIA INTERPLAY AND INCREASED MIRNA-155 AS PROMISING MARKERS TO TRACK ALS AT AN EARLY STAGE

Carolina Cunha[1], Catarina Santos[1], Cátia Gomes[1], Adelaide Fernandes[1,2], Alexandra Marçal Correia[3], Ana Maria Sebastião[4,5], Ana Rita Vaz[1,2], Dora Brites[1,2]

[1]Neuron Glia Biology in Health and Disease Group, Research Institute for Medicines (iMed.ULisboa), Faculty of Pharmacy, Universidade de Lisboa, Avenida Professor Gama Pinto, 1640-003 Lisbon, Portugal

[2]Department of Biochemistry and Human Biology, Faculty of Pharmacy, Universidade de Lisboa, Lisbon, Portugal

[3]Museu Nacional de História Natural e da Ciência, Universidade de Lisboa, Lisbon, Portugal

[4]Instituto de Farmacologia e Neurociências, Faculdade de Medicina, Universidade de Lisboa, Lisboa, Portugal

[5]Instituto de Medicina Molecular, Faculdade de Medicina, Universidade de Lisboa, Lisboa, Portugal

Mol Neurobiol. **(2017) [Epub ahead of print]**

Abstract

Amyotrophic lateral sclerosis (ALS) is a fatal neurodegenerative disease of unknown cause. Absence of specific targets and biomarkers compromise the development of new therapeutic strategies and of innovative tools to stratify patients and assess their responses to treatment. Here, we investigate changes in neuroprotective-neuroinflammatory actions in the spinal cord of *SOD1*^{G93A} mice, at presymptomatic and symptomatic stages to identify stage-specific biomarkers and potential targets. Results showed that in the presymptomatic stage, there are alterations in both astrocytes and microglia, which comprise decreased expression of GFAP and S100B and upregulation of GLT-1, as well as reduced expression of CD11b, M2-phenotype markers, and a set of inflammatory mediators. Reduced levels of Connexin-43, Pannexin-1, CCL21, and CX3CL1 further indicate the existence of a compromised intercellular communication. In contrast, in the symptomatic stage, increased markers of inflammation became evident, such as NF-κB/Nlrp3-inflammasome, Iba1, pro-inflammatory cytokines, and M1-polarizion markers, together with a decreased expression of M2-phenotypic markers. We also observed upregulation of the CX3CL1-CX3CR1 axis, Connexin-43, Pannexin-1, and of microRNAs (miR)-124, miR-125b, miR-146a and miR-21. Reduced motor neuron number and presence of reactive astrocytes with decreased GFAP, GLT-1, and GLAST further characterized this inflammatory stage. Interestingly, upregulation of miR-155 and downregulation of MFG-E8 appear as consistent biomarkers of both presymptomatic and symptomatic stages. We hypothesize that downregulated cellular interplay at the early stages may represent neuroprotective mechanisms against inflammation, SOD1 aggregation, and ALS onset. The present study identified a set of inflamma-miRNAs, NLRP3-inflammasome, HMGB1, CX3CL1-CX3CR1, Connexin-43, and Pannexin-1 as emerging candidates and promising pharmacological targets that may represent potential neuroprotective strategies in ALS therapy.

Keywords: Inflamma-miRNAs, Transgenic *SOD1*^{G93A} mice, Presymptomatic and symptomatic stages, Astrocytes and microglia function, Motor neuron-glia communication, ALS biomarkers

1. Introduction

Neurodegenerative processes usually begin years before clinical manifestations (Benatar and Wuu 2012). This issue was never clarified in amyotrophic lateral sclerosis (ALS) and knowledge on the biochemical alterations preceding clinical symptoms would help on preventive therapeutic approaches. Presymptomatic ALS studies may rely on people presenting genetic risk factors or animal models. The *SOD1*^{G93A} mouse is the most widely used model to investigate ALS disease mechanisms. In such model, we may evaluate early stages of disease onset and mechanisms leading to the spread of misfolded/aggregated superoxide dismutase 1 (SOD1). Previous studies established the presymptomatic stage at 4-6 weeks old and the symptomatic phase at 12-14 weeks (Nascimento et al. 2014; Rocha et al. 2013). Although only a few studies focused on changes before symptom onset, a recent report revealed an early loss of adenosine A1 and A2A receptor cross-talk at the neuromuscular junction as contributing to excitotoxicity (Nascimento et al. 2015). Another study linked the overexpression of interleukin (IL)-10 by microglia in the presymptomatic phase to a disease onset delay (Gravel et al. 2016). Nevertheless, the underlying mechanisms involved were not addressed. In addition, there is no sensitive biomarker of the presymptomatic stage that may help on the development of new drugs (Tefera et al. 2016). Moreover, since promising therapeutic approaches in the ALS *SOD1*^{G93A} mice merely showed efficacy when performed in the presymptomatic stage (Apolloni et al. 2016), the missing biomarkers are considered a crucial issue. Increased neurofilament levels were found in serum and cerebrospinal fluid (CSF) of ALS patients at symptomatic stage, but not before (Gaiottino et al. 2013). Therefore, prospective studies use the progression rate of symptoms to address the final outcome of the disease (Chio et al. 2002; Turner and Al-Chalabi 2002). With the growing interest in the early diagnosis in family members at risk of developing ALS, it is of outmost relevance to identify early sensitive biomarkers that may help on genetic counseling, while identifying areas for further research (Benatar et al. 2016).

Neuroinflammation and glial cell activation were shown to contribute to motor neuron (MN) degeneration in ALS (Brites and Vaz 2014; Turner et al. 2004). Activation of toll-like receptors (TLRs), nuclear factor kappa B (NF-κB), NOD-like receptor family pyrin domain containing 3 (NLRP3)-inflammasome, upregulation of proinflammatory cytokines and high mobility group box 1 (HMGB1), together with microRNA (miR)-155 and miR-146a, were only found during disease progression and end stages in both animal models and samples from ALS patients (Campos-Melo et al. 2013; Casula et al. 2011; Hensley et al. 2002; Johann et al. 2015; Koval et al. 2013; Lee et al. 2015b; Lo Coco et al. 2007). Intriguingly, inhibition of miR-155 in the *SOD1*^{G93A} mice significantly prolonged survival (Butovsky et al. 2015; Koval et al. 2013), and therapeutics targeting miR-155 are being presently developed (ALSA 2017).

Nevertheless, the potential of miR-155 as an early-stage biomarker in the spinal cord (SC) of ALS mice and its consistency along disease stages was not fully addressed yet. Moreover, the stage-specificity of other inflammatory-related microRNAs (inflamma-miRs) in ALS also requires further investigation.

The present paper intends to improve our understanding about alterations on the expression of common inflammatory-related markers at the presymptomatic stage and to establish how they differ from those found at the symptomatic stage, using the SC of the ALS *SOD1*^{G93A} mouse model. Such information can provide valid tools to recognize early ALS disease and to identify targets for developing new medicines. We thus define alterations in genes and proteins related to astrocyte and microglia reactivity and dysfunction, deactivation/activation of neuroinflammation-associated signaling pathways, and deregulated microglia-MN communication, as well as stage-specific inflamma-miRNAs, including miR-155, at both presymptomatic and symptomatic stages.

2. Methods

2.1. Animals

Transgenic B6SJL-TgN (SOD1G93A)1Gur/J males (Jackson Laboratory, no. 002726) overexpressing the human SOD1 (hSOD1) gene carrying a glycine to alanine point mutation at residue 93 (G93A) (*SOD1*^{G93A}) (Gurney et al. 1994) and B6SJLF1/J non-transgenic, wild-type (WT) females were purchased from The Jackson Laboratory (Bar Harbor, ME, USA). Maintenance and handling took place at Instituto de Medicina Molecular animal house facilities, where a colony was established. Mice were maintained on a background B6SJL by breeding *SOD1*^{G93A} transgenic males with non-transgenic females. Males were crossed with non-transgenic females because transgenic females are infertile. Experiments were conducted in two age groups: 4-6- and 12-14-week-old animals, corresponding to the presymptomatic and symptomatic phases of the disease, respectively. Such age groups in the *SOD1*^{G93A} mice were previously established by other authors based on the Rotarod test (Rocha et al. 2013). In brief, mice were placed on the rod at the lowest rotation speed (4 rpm) where they had to maintain for at least 120 s. In the testing day, mice were assessed at 5 and 10 rpm, for a maximum of 300 s each speed. The latency to fall was recorded and three trials were performed per speed with 5-min rest between each one. This transgenic mouse strain (ref. no. 002726) provided by Jackson Laboratories have an abbreviated life span (50% survive at 128.9±9.1 days) when compared with the C57BL/6J background (50% survive at 157.1±9.3 days). Both males and females were used since no gender influences over the intrinsic features of neuromuscular transmission were detected in this transgenic mice strain (Nascimento et al. 2015). Transgenic *SOD1*^{G93A} mice were compared to aged-

matched WT mice. The ear tissue extracted during the tagging procedure was then used in PCR for mice genotyping. All animals were housed 4-5 animals/cage, under 12 h light/12 h dark cycle, and received food and water ad libitum.

The present study was performed in accordance with the European Community guidelines (Directives 86/609/EU and 2010/63/EU, Recommendation 2007/526/CE, European Convention for the Protection of Vertebrate Animals used for Experimental or Other Scientific Purposes ETS 123/Appendix A) and Portuguese Laws on Animal Care (Decreto-Lei 129/92, Portaria 1005/92, Portaria466/95, Decreto-Lei 197/96, Portaria 1131/97). All the protocols used in this study were approved by the Portuguese National Authority (General Direction of Veterinary) and the Ethics Committee of the Instituto de Medicina Molecular of the Faculty of Medicine, Universidade de Lisboa, Lisbon, Portugal. All animal procedures were approved by the Institutional Animal Care and Use Committee and studies were conducted in accordance with the United States Public Health Service's Policy on Humane Care and Use of Laboratory Animals. Every effort was made to minimize the number of animals used and their suffering.

2.2. Tissue Slices and Homogenates

Mice were deeply anesthetized with sodium pentobarbital (60 mg/kg, i.p.). For quantitative real-time reverse transcription polymerase chain reaction (qRT-PCR) or Western blot (WB), mice were perfused with 0.1 M PBS at pH 7.4 and lumbar SC dissected and rapidly frozen at -80 °C. For histological and immunohistochemistry studies, mice were perfused with a fixative containing 4% paraformaldehyde in PBS and fixed lumbar SC were removed, post-fixed with the same fixative for 24 h at 4 °C and then preserved in 30% sucrose solution. Transversal 20-µm thick sections were serially cut with the cryostat Leica CM1850 (UV Leica; Wetzlar, Germany).

2.3. Histological Analysis

For neuronal Nissl bodies assessment, tissue sections were rinsed with 2% acetic acid for 5 min, and then stained for 10 min with 1% cresyl violet (Sigma-Aldrich, St. Louis, MO, USA), as usual in our laboratory (Cardoso et al. 2015). After rinsing in distilled water, sections were differentiated in 0.75% acetic acid and rinsed again in distilled water. For hematoxylin-eosin (H&E) staining, tissue sections were stained for 10 min with hematoxylin, extensively washed with tap water, differentiated with 1% HCl and rinsed again in tap water. After that, sections were counterstained with eosin during 2 min, dehydrated within a series of ethanol (70, 95, and 100%) and xylene baths and mounted with DPX (Merck Millipore Corporation,

Darmstadt, Germany). Images were acquired with a bright-field microscope (Zeiss, model AxioSkop HBO50) with an integrated digital camera (Zeiss, model Axiocam 105 color).

2.4. Immunohistochemistry

Frozen lumbar SC sections (20-µm thick cryosections) were collected on Superfrost Plus glass slides (Thermo Scientific, Waltham, MA, USA) and stored at -20 °C. After defrosting, each section was covered for 10 min with 0.3 M glycine followed by blocking solution (2% FBS in TBS-Triton 10%) for 1 h at room temperature (RT). After that, samples were incubated for 24 h with the primary antibodies (indicated in supplementary Table IV.1) at 4°C. In the next day, the sections were incubated for 1 h at RT with secondary antibodies anti-mouse-Alexa Fluor 594 (1:200, A11005, Invitrogen Corporation, Carlsbad, CA, USA) or anti-rabbit-Alexa Fluor 488 (1:200, A11008, Invitrogen). Then, SC sections were stained with DAPI dye diluted in PBS (0.1 µg/ml) for 5 min. After that, sections were washed twice and sequentially dehydrated with ethanol (50, 70, 96, and 100%) and xylene baths, each during 5 min, and mounted in DPX on a microscope slide. Finally, fluorescence images of the ventral horn and funiculus of the lumbar SC were acquired per sample using a fluorescence microscope (AxioSkope, Zeiss, Germany) with an integrated digital camera (Zeiss, model Axiocam HRm).

2.5. Western Blot

Total protein isolation from organic phases of TRizol-chloroform lumbar SC was performed by using TRIzol® Reagent (LifeTechnologies) as previously described (Simões et al. 2013). Then, protein expression was performed by Western blot analysis as usual in our laboratory (Fernandes et al. 2006). The protein extracts were separated on sodium dodecyl sulfate-polyacrylamide gel electrophoresis (SDS-PAGE) and transferred to a nitrocellulose membrane. The membranes were blocked with 5% non-fat milk in TBS-T (0.1% Tween-20) and incubated overnight at 4 °C with specific primary antibodies (indicated in Supplementary Table IV.1). Finally, membranes were washed and incubated with anti-rabbit (1:5000, sc-2004, Santa Cruz Biotechnology, CA, USA), anti-mouse (1:5000, sc-2005, Santa Cruz Biotechnology) or anti-goat (1:4000, sc-2768, Santa Cruz Biotechnology) secondary antibodies conjugated with horseradish peroxidase for 1 h at RT. The chemiluminescent detection was performed after membrane incubation with LumiGLO® (Cell Signaling, Beverly, MA, USA). The relative intensities of protein bands were analyzed using the Image LabTM analysis software, after scanning with ChemiDocXRS, both from Bio-Rad Laboratories (Hercules, CA, USA). Results were normalized to β-actin and expressed as fold change. A

total of 2-3 mice per group (randomly chosen) were used and data normalized to the average of aged matched WT mice for each electrophoresis gel.

2.6. Quantitative RT-PCR

Total RNA was extracted from lumbar SC tissue using TRIzol® Reagent (Life Technologies; Carlsbad, CA, USA), as usual in our laboratory. Total RNA was quantified using Nanodrop ND-100 Spectrophotometer (NanoDrop Technologies; Wilmington, DE, USA) and conversion to complementary DNA (cDNA) was performed with SensiFAST™ cDNA synthesis (BIO-65054, BIOLINE, London, UK). Quantitative RT-PCR (qRT-PCR) was performed to evaluate messenger RNA (mRNA) expression of the genes indicated in Supplementary Table IV.2, using β-actin as an endogenous control to normalize the gene expression levels. qRT-PCR was performed on a 7300 Real-Time PCR System (Applied Biosystems) using a SensiFAST™ SYBR® (Hi-ROX, BIO-92002/S, BIOLINE). qRT-PCR was performed under optimized conditions: 50°C for 2 min and 95°C also for 2 min, followed by 40 cycles at 95°C for 5 s and 62°C for 30 s. In order to verify the specificity of the amplification, a melt-curve analysis was performed, immediately after the amplification protocol. Non-specific products of PCR were not found in any case. Results were normalized to β-actin. Expression of miRNAs was also performed by qRT-PCR. Here, total RNA was extracted from the lumbar SC as indicated above and, after RNA quantification, cDNA conversion was performed with the universal cDNA Synthesis Kit (Exiqon, Vedbaek Denmark), as described by Caldeira et al. (2014), using 5 ng of total RNA according to the following protocol: 60 min at 42°C followed by heat-inactivation of the reverse transcriptase for 5 min at 95°C. For miRNA quantification, the miRCURY LNA™ Universal RT microRNA PCR system (Exiqon) was used in combination with the predesigned primers (Exiqon) for mmu-miR-155-5p (miR-155, 5′-UUAAUGCUAAUUGUGAUAGGGGU-3′), hsa-miR-124-3p (miR-124, 5′-UAAGGCACGCGGUGAAUGCC-3′), hsa-miR-146a-5p (miR-146a 5′-UGAGAACUGAAUUCCAUGGGUU-3′), hsa-miR-21-5p (miR-21, 5′ -UAGCUUAUCAGA CUGAUGUUGA-3′), hsa-miR-125b- 5p (miR-125b, 5′-UCCCUGAGACCCUAACUUGUGA-3′) and SNORD110 (reference gene). The reaction conditions consisted of polymerase activation/denaturation and well-factor determination at 95°C for 10 min, followed by 50 amplification cycles at 95°C for 10 s and 60°C for 1 min (ramp-rate of 1.6°/s). In both cases, relative mRNA/miRNA concentrations were calculated using the ΔΔCT equation and results were represented as fold change. A total of 2-3 mice per group (randomly chosen) were used and data normalized to the average of aged-matched WT mice for each multi-well PCR plate.

2.7. Statistical Analysis

Results were expressed as mean + SEM. Differences between WT and *SOD1*^{G93A} mice in each stage were determined by unpaired student t test. Welch's correction was applied when variances between groups were significantly different. Two-way ANOVA followed by Bonferroni's multiple comparisons post hoc correction was used for analysis involving presymptomatic and symptomatic *SOD1*^{G93A} mice and aged-matched WT. Statistical analysis was performed using GraphPad Prism 5 (GraphPad Software; San Diego, CA, USA). Values of $p < 0.05$ were considered statistically significant.

3. Results

3.1. Comparative Histological, Gene, and Protein Profiling in the *SOD1*^{G93A} Mice, Before and After Disease Onset

Results obtained in the 4-6- and 12-14-week-old *SOD1*^{G93A} mice were compared with the 4-6-week-old WT mice, using the two-way ANOVA analysis.

Before evaluating the specific gene and protein profiling of the *SOD1*^{G93A} mice in the presymptomatic and in symptomatic stages, we assessed SOD1 expression, as well as MNs and glial cell representation in the ventral horn of mice SC (Figure IV.1A) along disease progression. Expression of hSOD1 at both pre and symptomatic stages was obtained by WB (Figure IV.1B) and by immunohistochemical analysis (Figure IV.1C). As expected, we observed higher levels of SOD1 in the transgenic mice than in the WT animal. Reduced number of MNs was only found in the symptomatic *SOD1*^{G93A} mice, as shown by reduced Cresyl violet staining and immunoreactivity against the neuronal nuclei (NeuN) protein (Figure IV.1C). WB analysis further demonstrated a 0.5-fold decreased protein expression ($p < 0.05$) of NeuN (Figure IV.1D). Pyknotic basophilic necrotic/apoptotic MNs were additionally identified by H&E staining at the symptomatic stage of the *SOD1*^{G93A} mice, together with an increased number of glial cells (Figure IV.1C). In parallel, we observed an increased expression of the proliferation marker Ki67 (Figure IV.1E) only in the symptomatic *SOD1*^{G93A} mice, which may be associated with gliosis in accordance with recent observations obtained for LPS-stimulated microglia (Cunha et al. 2016). Next, we assessed gene and protein expression differences (Table IV.1).

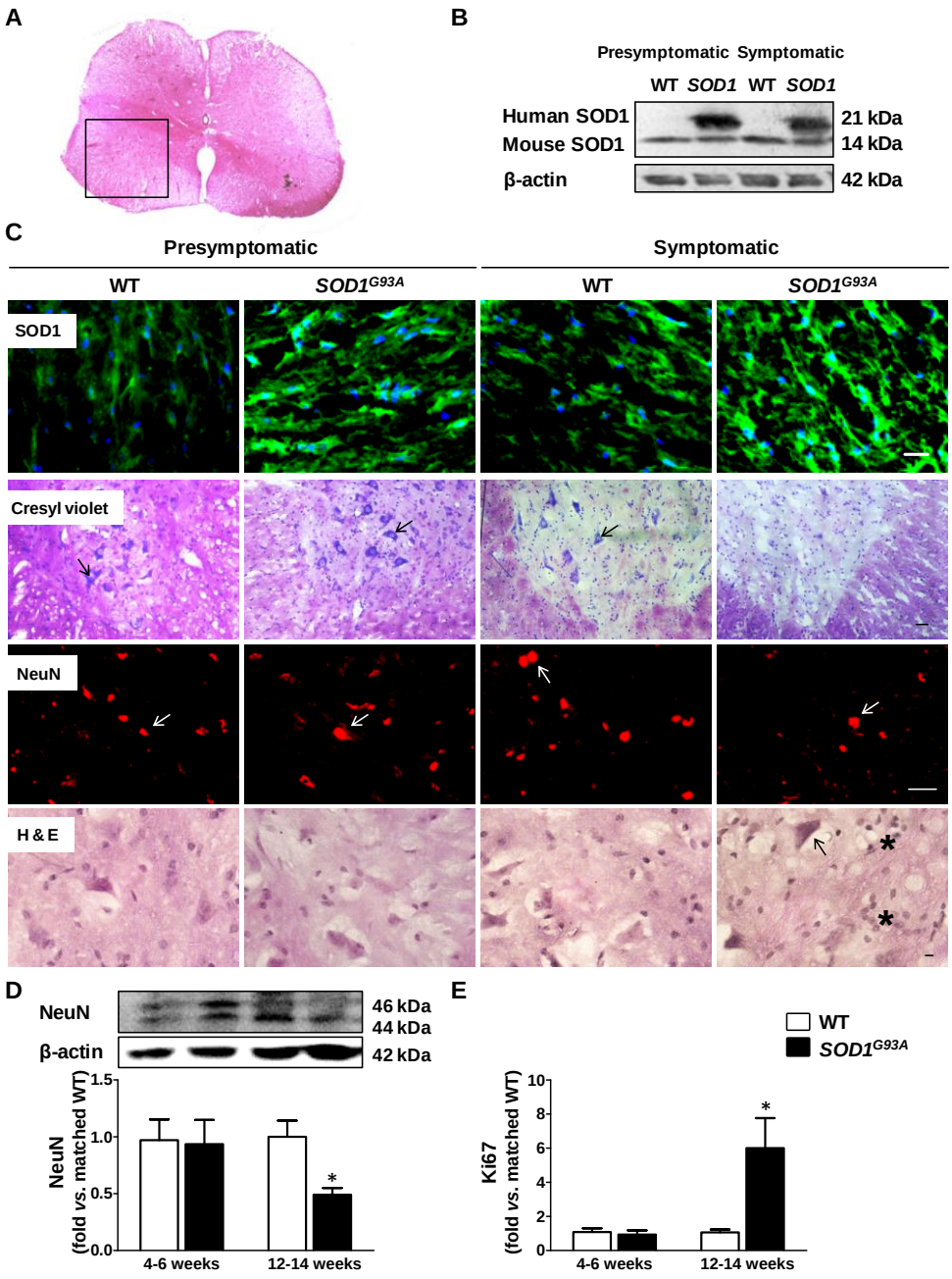

Figure IV.1 - Increased glial cell density and loss of motor neurons are only observed in symptomatic *SOD1*^{G93A} mice. (A) Lumbar spinal cord (SC) tissue sample of a WT mice at the presymptomatic stage stained with hematoxylin and eosin (H&E), where it is indicated the ventral horn and ventral funiculus (square) portions used in the present study. Analysis was performed as indicated in "Methods." (B) Representative image of the detection of human and mouse SOD1 expression in the SC collected from the wild type (WT) and *SOD1*^{G93A} mice at presymptomatic and symptomatic stages evidencing the increased expression of the mutant SOD1. β-actin was used as a loading control. (C) Representative images of presymptomatic and symptomatic stages of the *SOD1*^{G93A} mice, and corresponding WT samples, obtained by immunohistochemical staining of SOD1 expression with enhanced expression in the transgenic animal by Cresyl violet staining for the Nissl substance in the cytoplasm of motor neurons (arrows), and by NeuN immunostaining for the nucleus of neurons (arrows), highlighting the loss of motor neurons at the symptomatic stage, and by hematoxylin and eosin (H&E) staining showing the hyperchromatic (darkly stained) basophilic pyknotic neuron (arrow) and the increased number of glial cells (asterisks) in the symptomatic stage. Scale bar represents 80 μm for Cresyl violet staining and 20 μm for all the others. (D) Identification and quantification of NeuN expression corroborating motor neuron degeneration (results are mean + SEM, n = 6-9 mice per group). (E) Ki67 expression assessed by qRT-PCR highlights increased cell proliferation at the symptomatic stage. Results are mean + SEM (*p < 0.05 vs. WT mice, n = 5-6 mice per group, two-way ANOVA followed by Bonferroni's multiple comparisons post hoc test).

In the presymptomatic stage, we observed an upregulation of miR-155, with downregulation of the suppressor of cytokine signaling 1 (SOCS1) expression, considered to be its direct target (Pathak et al. 2015). Decrease of neuronal *Ccl21*, a microglial activating chemokine (de Jong et al. 2005), together with the M2 genes *Arg1*, *Fizz1* and *Cd206*, and non-elevated M1-markers, plus the reduced milk fat globule-EGF factor 8 (MFG-E8) protein expression, are suggestive that M1- or M2-polarized microglia are not predominant and that neuroprotective phenotypes may be decreased.

In contrast, in the symptomatic stage, we observed NF-κB activation, upregulation of all the inflamma-miRs, as well as of the genes *S100b*, *Cd11b*, *Mhc-II*, *Cebpa*, *Cd80*, *Tgfb1*, *Cd206*, *Autotaxin*, *Nlrp3*, *IL-1b*, *Tnfa*, *Il-10*, *Cx43*, *Cx3cr1*, and *Cx3cl1*, together with the ionized calcium-binding adapter molecule 1 (Iba1), HMGB1, CX3CL1, and CX3CR1 proteins, collectively indicating astrocytosis, microgliosis, and neuroinflammation. Sustained increase of miR-155, as well as of increased expression of the anti-inflammatory associated markers *Socs1*, together with *Arg1* subexpression, reinforce the existence of a neuroinflammatory status after disease onset. In addition, reduced GFAP expression is indicative of astrocyte aberrancy (Diaz-Amarilla et al. 2011). To better differentiate changes in the expression of genes and proteins before (presymptomatic in-depth signature) and after disease onset (symptomatic in-depth signature), we separately analyzed gene and protein markers, inflammatory mediators, and inflamma-miRs expression in 4-6-week-old and in 12-14-week-old *SOD1*^{G93A} mice, respectively, in order to better define stage-specific alterations.

Table IV.1 - Assessment of global differences for gene and protein expression between presymptomatic and symptomatic stages by two-way ANOVA analysis followed by Bonferroni´s multiple comparisons test.

MARKERS	Presymptomatic stage		Symptomatic stage	
	WT	*SOD1^{G93A}*	WT	*SOD1^{G93A}*
GENE				
Microglia and astrocyte				
S100b	1.05 ± 0.15	0.56 ± 0.16	1.46 ± 0.47	**5.06 ± 2.33***
Cd11b	1.09 ± 0.16	0.52 ± 0.08	1.73 ± 0.63	**3.87 ± 1.04***
Nos2	1.03 ± 0.11	0.89 ± 0.33	1.00 ± 0.39	0.55 ± 0.19
Mhc-II	1.11 ± 0.22	0.58 ± 0.20	0.73 ± 0.15	**3.24 ± 0.86*****
Cebpa	1.08 ± 0.19	0.65 ± 0.15	1.10 ± 0.23	**5.03 ± 1.95***
Cd80	1.08 ± 0.17	1.18 ± 0.46	0.41 ± 0.07	**1.77 ± 0.49***
Arg1	1.06 ± 0.17	**0.32 ± 0.07****	0.76 ± 0.20	**0.21 ± 0.04***
Fizz1	1.08 ± 0.18	**0.26 ± 0.07***	0.74 ± 0.27	0.37 ± 0.16
Socs1	1.10 ± 0.21	**0.44 ± 0.09***	0.82 ± 0.22	**0.22 ± 0.06***
Tgfb1	1.19 ± 0.24	0.34 ± 0.08	1.10 ± 0.19	**5.28 ± 1.93****
Cd206	1.12 ± 0.23	0.61 ± 0.12	0.65 ± 0.17	**1.50 ± 0.33***
Autotaxin	1.11 ± 0.22	0.76 ± 0.27	0.58 ± 0.14	**2.09 ± 0.35****
Inflammasome				
Nlrp3	1.03 ± 0.14	0.36 ± 0.13	0.71 ± 0.39	**1.84 ± 0.44***
Il-1b	1.13 ± 0.22	0.68 ± 0.21	1.11 ± 0.53	**4.42 ± 1.29****
Il-18	1.24 ± 0.28	0.85 ± 0.30	0.86 ± 0.36	1.83 ± 0.66
Cytokines				
Tnfa	1.19 ± 0.30	0.47 ± 0.05	2.49 ± 0.89	**6.67 ± 1.17****
Il-6	1.13 ± 0.24	0.52 ± 0.08	1.55 ± 0.46	1.69 ± 0.49
Il-10	1.06 ± 0.16	0.94 ± 0.18	1.08 ± 0.19	**9.87 ± 2.96*****
Intercellular communication				
Cx43	1.03 ± 0.11	0.58 ± 0.10	0.41 ± 0.07	**1.69 ± 0.42****
Panx1	1.02 ± 0.09	0.59 ± 0.05	1.14 ± 0.19	1.43 ± 0.24
Ccl21	1.28 ± 0.38	**0.31 ± 0.06***	0.53 ± 0.29	0.56 ± 0.14
Ccr7	1.12 ± 0.22	2.08 ± 0.40	1.91 ± 0.54	2.95 ± 0.87
Cx3cr1	1.06 ± 0.16	0.63 ± 0.21	0.58 ± 0.12	**3.82 ± 1.66****
Cx3cl1	1.11 ± 0.22	0.38 ± 0.15	0.56 ± 0.18	**2.74 ± 1.25***
microRNAs				
mmu-miR-155-5p	1.01 ± 0.08	**2.18 ± 0.33***	1.11 ± 0.37	**2.76 ± 0.21*****
hsa-miR-125b-5p	1.00 ± 0.05	1.34 ± 0.25	0.88 ± 0.25	**1.96 ± 0.16****
hsa-miR-146a-5p	1.06 ± 0.17	0.90 ± 0.10	0.81 ± 0.20	**3.48 ± 0.78****
hsa-miR-21-5p	1.06 ± 0.17	1.47 ± 0.38	1.17 ± 0.34	**10.55 ± 3.03****
hsa-miR-124-3p	1.17 ± 0.32	1.35 ± 0.30	0.54 ± 0.08	**1.50 ± 0.20***
PROTEIN				
Microglia and astrocyte markers				
S100B	1.00 ± 0.34	0.59 ± 0.20	0.59 ± 0.20	1.16 ± 0.30
GFAP	1.00 ± 0.17	0.52 ± 0.10	1.26 ± 0.16	**0.65 ± 0.14***
GLT-1	1.00 ± 0.10	1.59 ± 0.22	2.48 ± 0.57	1.44 ± 0.42
GLAST	1.00 ± 0.10	1.21 ± 0.26	3.05 ± 1.54	2.33 ± 0.69
Iba1	1.00 ± 0.10	1.40 ± 0.10	1.08 ± 0.09	**2.30 ± 0.53***
TLR/ NF-κB pathway				
TLR2	1.00 ± 0.14	1.20 ± 0.32	1.91 ± 0.40	**0.94 ± 0.09***
TLR4	1.00 ± 0.13	0.80 ± 0.18	1.39 ± 0.47	0.53 ± 0.09
NF-κB	1.00 ± 0.14	1.19 ± 0.29	1.06 ± 0.21	**2.25 ± 0.40***
pNF-κB	1.00 ± 0.15	0.65 ± 0.27	0.70 ± 0.05	1.54 ± 0.63
HMGB1	1.00 ± 0.13	0.89 ± 0.15	1.21 ± 0.24	**1.41 ± 0.22***
Intercellular communication				
MFG-E8	1.00 ± 0.19	**0.50 ± 0.11***	1.00 ± 0.14	0.53 ± 0.10
CX3CR1	1.00 ± 0.17	1.14 ± 0.30	1.11 ± 0.21	**2.97 ± 1.05***
CX3CL1 membrane-bound	1.00 ± 0.14	0.52 ± 0.05	1.74 ± 0.26	**2.72 ± 0.47***
CX3CL1 soluble	1.00 ± 0.17	1.35 ± 0.28	1.72 ± 0.34	**2.85 ± 0.35***

Data is expressed as fold change vs. 4-6 weeks old mice (MEAN ± SEM). *p < 0.05, **p < 0.01 and ***p < 0.01 vs. matched WT animals.

3.2. Presymptomatic In-depth Gene and Protein Signature

Results were obtained in 4-6-week-old *SOD1^{G93A}* mice using aged-matched WT mice as controls.

3.2.1. Gene and Protein Expression Associated with Glial Cell Reactivity are Downregulated or Unchanged in the Presymptomatic Stage

Strong reactive astrogliosis surrounding MNs has been described in ALS patients and animal models (Vargas and Johnson 2010). However, information on whether this astrogliosis precede or follows MN degeneration is not completely clarified. In the present study, we found a reduced expression of *S100b* (0.5-fold, Figure IV.2A), not significantly translated in the protein levels (Figure IV.2B, C), together with a downregulation of GFAP (Figure IV.2D). Interestingly, when evaluating the glutamate transporters, a 1.6-fold increase in glutamate transporter GLT-1, but not in GLAST (Figure IV.2D) was obtained, which may be a protective response against the increased extracellular glutamate, considered to be a common feature in ALS. As for microgliosis, also considered a hallmark in ALS, we observed that, despite an enhanced Iba1 expression (Figure IV.2D, E), *Cd11b* was decreased (0.5-fold, Figure IV.2F) and no changes were evident in the autotaxin gene expression (Figure IV.2G), a protein that protects microglia from oxidative stress (Awada et al. 2012). Interestingly, all markers of M2-polarized microglia (*Cd206*, *Arg1*, *Fizz1*, *Socs1*, and *Tgfb1*) were similarly reduced and those associated to the M1 phenotype were either unchanged (*Cd80* or *Nos2*), or showed a diminished trend (*Mhc-II* and *Cebpa*) (Figure IV.2H). Based on the low expression of such markers we hypothesize that no prevalent M1 or M2 phenotypes are present, what is in agreement with the concept that a unique microglial phenotype signature exists in ALS (Chiu et al. 2013).

3.2.2. Decreased *Nlrp3*, *Tnfa*, and *Il-6* Suggests a Repressed Inflammatory Status in the Presymptomatic Stage

No changes were noticed in the classical inflammatory TLR2/TLR4/NF-κB pathway (Figure IV.3A). Attesting a downregulation of inflammatory markers in the presymptomatic stage, decrease of the *Nlrp3-inflammasome*, as well as of cytokines *Il-1beta*, *Il-6* and *Tnfa*, but not of *Il-18* and *Il-10*, was obtained (Figure IV.3B). These results, associated with an unaltered alarmin HMGB1 expression (Figure IV.3C), reinforce the absence of an inflammatory SC milieu at the presymptomatic stage.

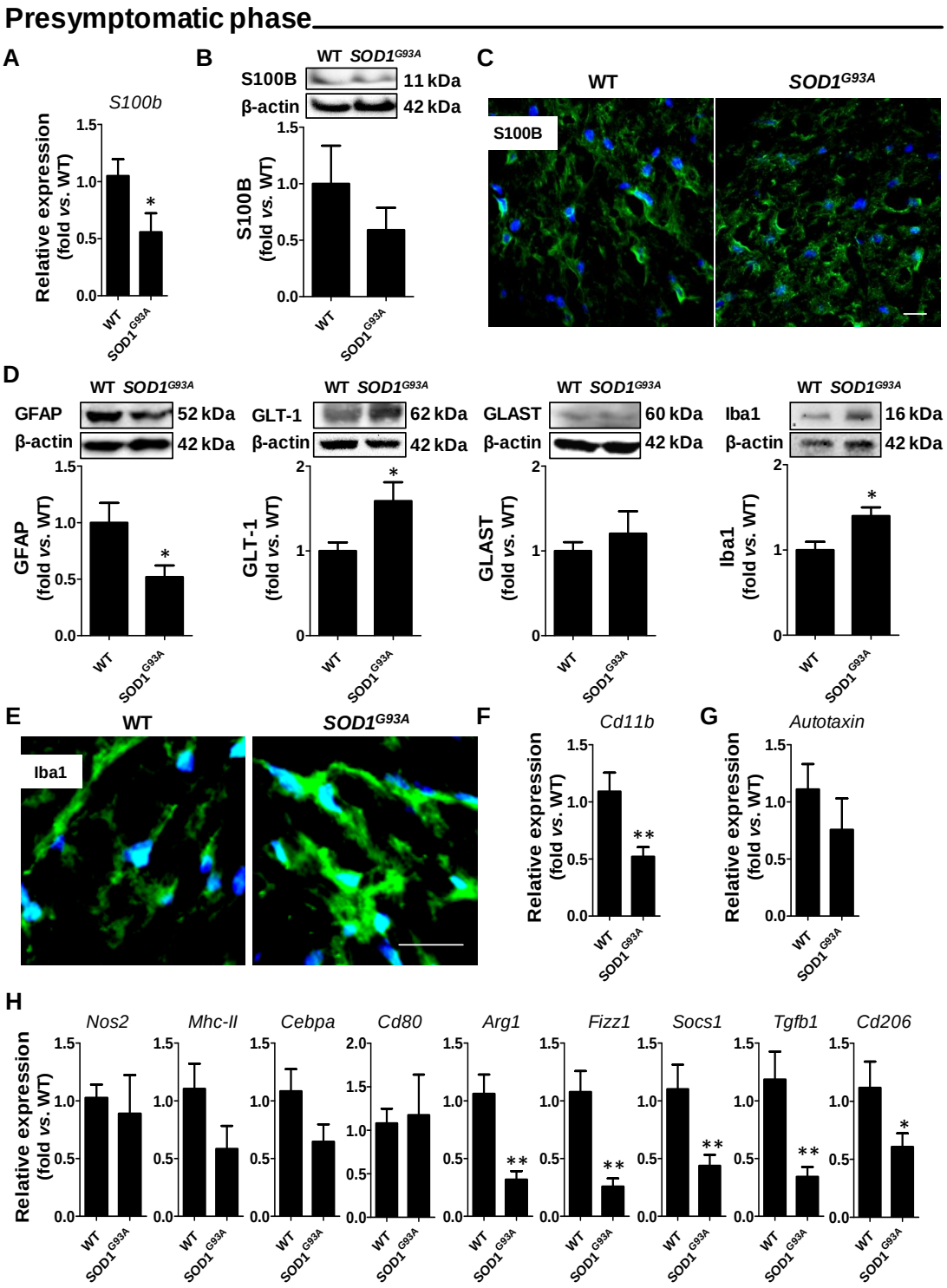

Figure IV.2 - Microglial and astrocytic functions are downregulated in the presymptomatic *SOD1^{G93A}* mice. Samples of the spinal cord tissue were processed as indicated in "Methods." (A) *S100b* quantification by qRT-PCR. (B) Western blot analysis of S100B. (C) Representative images of the S100B detection by immunohistochemistry using anti-S100B in the ventral funiculus of the spinal cord. (D) Western blot analysis of GFAP, glutamate transporters GLT-1/GLAST, and Iba1. (E) Representative images of Iba1 detection by immunohistochemistry using anti-Iba1 in the ventral funiculus of the spinal cord. (F) *Cd11b* evaluation by qRT-PCR. g *Autotaxin* quantification by qRT-PCR. (H) Expression of markers used for the characterization of microglia phenotypes assessed by qRT-PCR. *Nos2*, *Mhc-II*, *Cebpa*, and *Cd80* are M1-phenotype markers while *Arg1*, *Fizz1*, *Socs1*, *Tgfb1*, and *Cd206* are markers of M2-polarized cells. Results are mean + SEM (*p < 0.05, **p < 0.01 vs. WT mice, n = 4-8 mice per group, unpaired Student's *t*-test). (C, E) Scale bar represents 20 µm.

3.2.3. MiR-155 Is Upregulated in the Presymptomatic Stage of *SOD1^{G93A}* Mice

Several inflamma-miRs, such as miR-155, miR-21, miR-146a, miR-125b, and miR-124, have been associated with different phenotypes and functions of microglia, which may differentially account for neuroinflammation in ALS (Brites and Vaz 2014). We observed that among all of them, only miR-155 was significantly upregulated (Figure IV.3D). This finding indicates that miR-155 upregulation occurs earlier, before disease onset, and in the absence of other common pro-inflammatory specific markers. In such case, we may consider that its presence, instead of being associated with a neuroinflammatory status, may have an anti-inflammatory role to restrain the disease progression in this presymptomatic stage, as suggested for other pathological conditions (Li et al. 2016a).

3.2.4. Impaired Cell-to-Cell Communication May Compromise Normal Tissue Homeostasis Before Disease Onset

Intercellular communication is essential for microenvironment homeostasis maintenance. We first observed that expression of glial Connexin-43 (Cx43) and Pannexin-1 (Panx1) hemichannel proteins, known to play a role in gap junctional intercellular communication, was inhibited in the presymptomatic stage (~0.6-fold, Figure IV.4A). Also decreased was the MFG-E8 protein (0.5-fold, Figure IV.4B) known to participate in a wide variety of cellular interactions (Raymond et al. 2009) and particularly important in microglia phagocytosis of apoptotic neurons, pathway that is induced upon recognition of phosphatidylserine (Liu et al. 2013b). When we explored differences on the ligand-signaling network *Ccl21-Ccr7* and *Cx3cl1-Cx3cr1* systems, as important players in the communication between damaged neurons and microglia, decreased levels of neuronal chemokines were observed (Figure IV.4C, D). In addition, as depicted in Figure IV.4E, we differentiated membrane from soluble forms of FKN (respectively, 95 and 76 kDa bands) (Sheridan and Murphy 2013; Suzuki et al. 2011) by WB analysis, having observed that only the membrane fraction of Cx3cl1 (95 kDa) accounted for the reduced signaling trafficking. Nevertheless, no changes were detected in their microglial receptors, although a decreased trend was evidenced in the case of the CX3CR1 receptor (Figure IV.4C-F). Overall, these data suggest that astrocyte-astrocyte/neuron and neuron-microglia communication is impaired in the *SOD1^{G93A}* mice before symptom onset and corroborate the microglia irresponsiveness status.

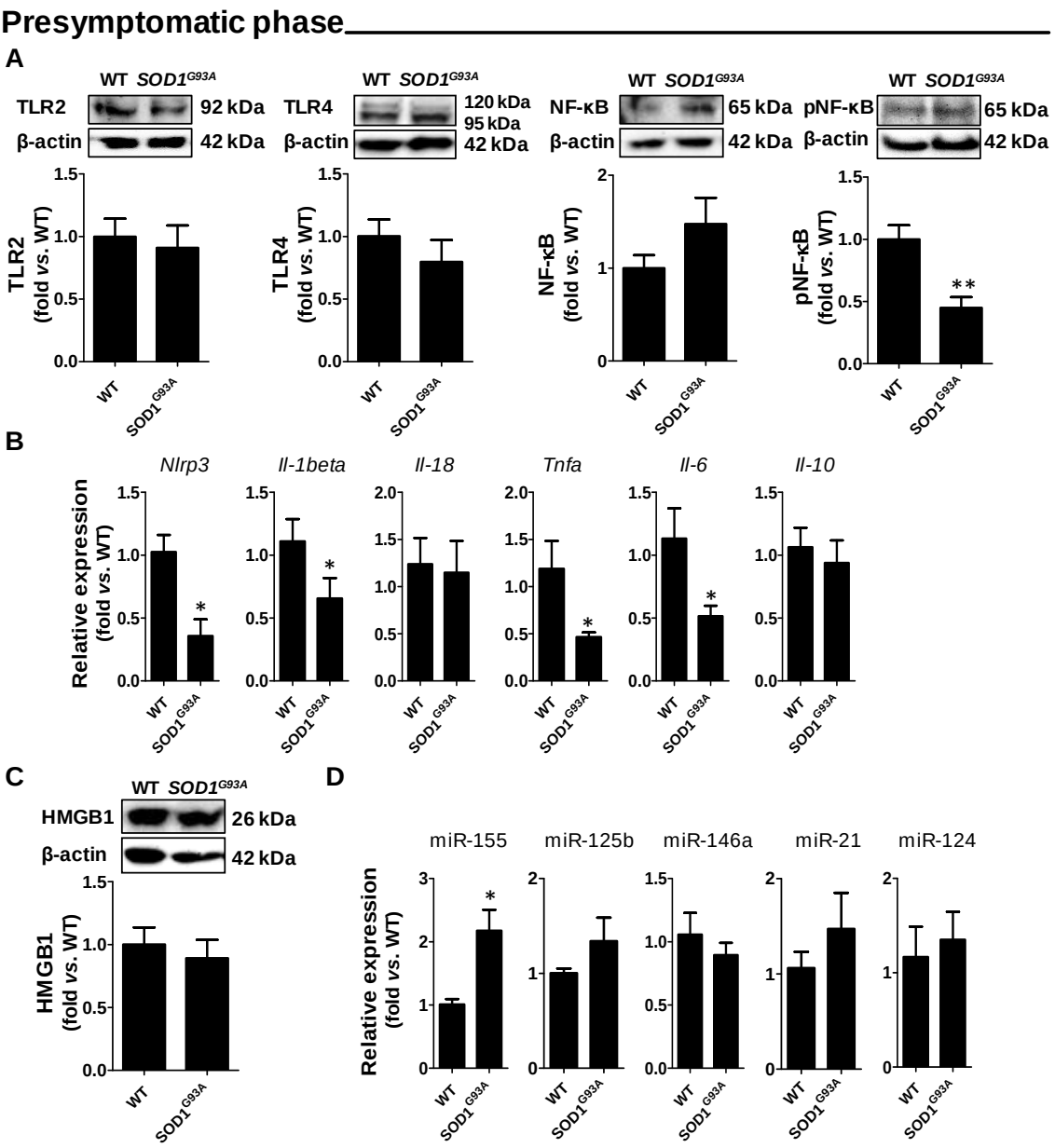

Figure IV.3 - Unaltered TLR/NF-κB signaling pathway courses with decreased Nlrp3 expression and miR-155 upregulation in the asymptomatic *SOD1^{G93A}* mice. Samples of the spinal cord tissue were processed as indicated in "Methods." (A) Western blot analysis of TLR2, TLR4, NF-κB, and pNF-κB. (B) Expression of Nlrp3, *Il-1beta*, *Il-18*, *Tnfa*, *Il-6*, and *Il-10* assessed by qRT-PCR. (C) Western blot analysis of HMGB1.d Profile of the inflammatory-related miR-155, miR-125b, miR-146a, miR-21, and miR-124 assessed by qRT-PCR. Results are mean + SEM (*p < 0.05 vs. WT mice, n = 5-8 mice per group, unpaired Student's *t*-test).

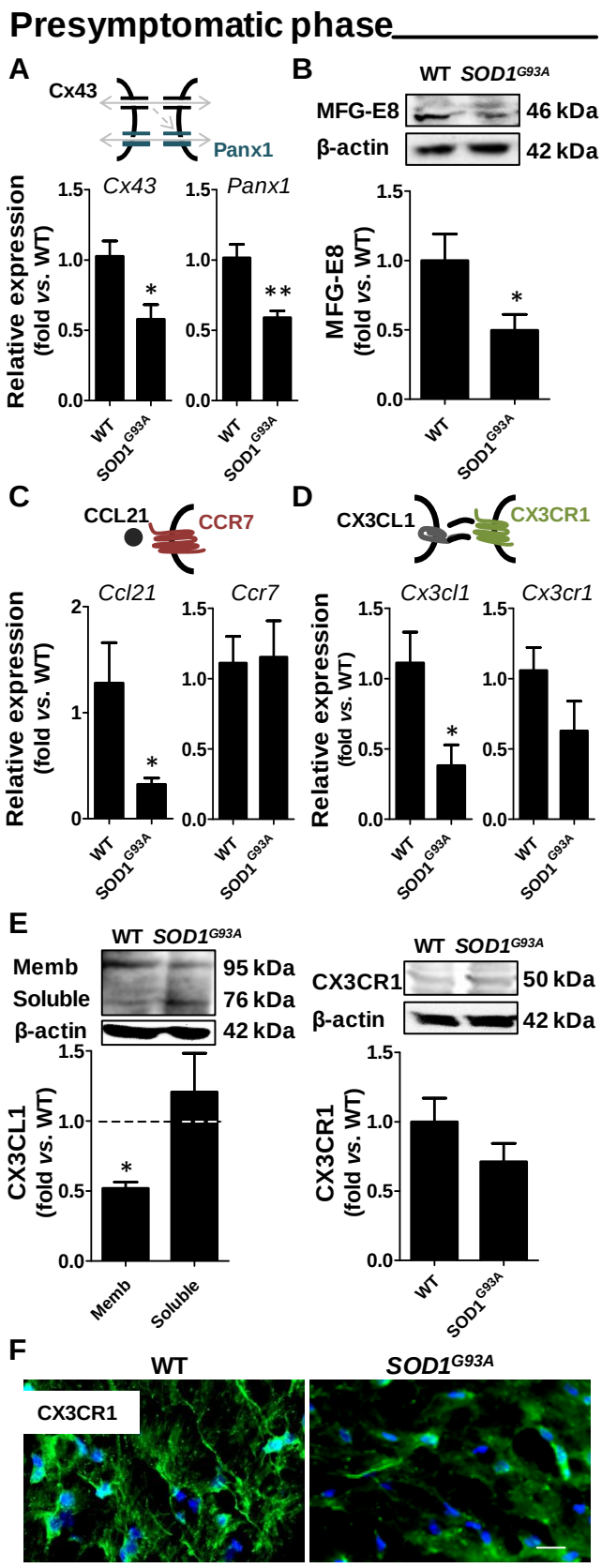

Figure IV.4 - Intercellular communication is impaired in the presymptomatic *SOD1*^{G93A} mice. Samples of the spinal cord tissue were processed as indicated in "Methods." (A) *Cx43* and *Panx1* expression assessed by qRT-PCR. (B) Western blot analysis of MFG-E8. (C) *Ccl21* and *Ccr7* expression assessed by qRT-PCR. (D) *Cx3cl1* and *Cx3cr1* expression assessed by qRT-PCR. (E) Western blot analysis of CX3CR1, and of membrane-bound and soluble CX3CL1 forms. Dashed line represents WT values. Results are mean + SEM (*p < 0.05 vs. WT mice, n = 5-11 mice per group, unpaired Student's *t*-test). (F) Representative immunofluorescent images of CX3CR1 are shown. Scale bar represents 20 µm.

3.3. Symptomatic In-depth Gene and Protein Signature

Results were obtained in 12-14-week-old *SOD1^{G93A}* mice using aged-matched WT mice as control.

3.3.1. Atypical Reactive Astrocytes and Heterogeneous Microglia Phenotypes Characterize the Symptomatic Stage in the *SOD1^{G93A}* Mice Model

In the symptomatic stage, we observed a clear increase in S100B gene and protein expression (Figure IV.5A-C), accompanied by a decreased GFAP expression, and reduced expression of GLT-1 and GLAST proteins (Figure IV.5D), which have been described as features of aberrant astrocytes with neurotoxic potential in a specific population of cells isolated from the SC of the transgenic mSOD1 rats (Diaz-Amarilla et al. 2011). Now, considering the existence of Iba1/*Cd11b*-activated microglia (Figure IV.5E-F), as well as autotaxin-increased expression (Figure IV.5G), enhanced *Cd80*, *Mhc-II*, and *Cebpa* gene expression, and decreased *Arg1* and *Socs1* (Figure IV.5H), we hypothesize that microglia may be preferentially polarized into the M1 phenotype during the symptomatic phase, despite the inexistence of alterations in *Nos2* and *Fizz1* expression levels. To consider, however, that other myeloid cells may also be present in the SC at this stage and account for such observations (Butovsky et al. 2012). Nonetheless, we also found increased *Cd206* and *Tgfb1*, which are indicative of M2 polarization. Therefore, the presence of multiple polarized microglial subtypes, together with prevalent proinflammatory subclasses, reinforces the atypical signature nature of the symptomatic stage and of its associated microglial cells.

3.3.2. NF-κB/*NLRP3-Inflammasome*, HMGB1, and Inflamma-miRs are Upregulated in the Symptomatic Stage of *SOD1^{G93A}* Mice

TLR2- and TLR4-mediated signals may either determine attenuation or augmentation of inflammatory responses depending on the stimuli (Oak et al. 2006). Our results demonstrate that both TLR2 and TLR4 are decreased in the symptomatic *SOD1^{G93A}* mice (Figure IV.6A), though we also have observed an increase in Tlr2 gene expression (data not shown). However, upregulated inflammatory signaling pathways involving NF-κB and its active phosphorylated form (pNF-κB) (Figure IV.6A), increased *Nlrp3*, *Il-1beta* and *Tnfa* expression (Figure IV.6B), as well as elevated HMGB1 cellular content (Figure IV.6C), are indicative of an increased inflammatory status in the SC of the *SOD1^{G93A}* mice at the symptomatic stage. Compensatory mechanisms involving the increased expression of Il-10, as we noticed in our model, was previously indicated as an adaptive immune escape mechanism that if inhibited increase the survival of the ALS mice (Gravel et al. 2016). Again, no changes were observed

for *Il-18* likewise the Presymptomatic stage, which were now accompanied by an unaltered *Il-6* expression, as well (Figure IV.6B).

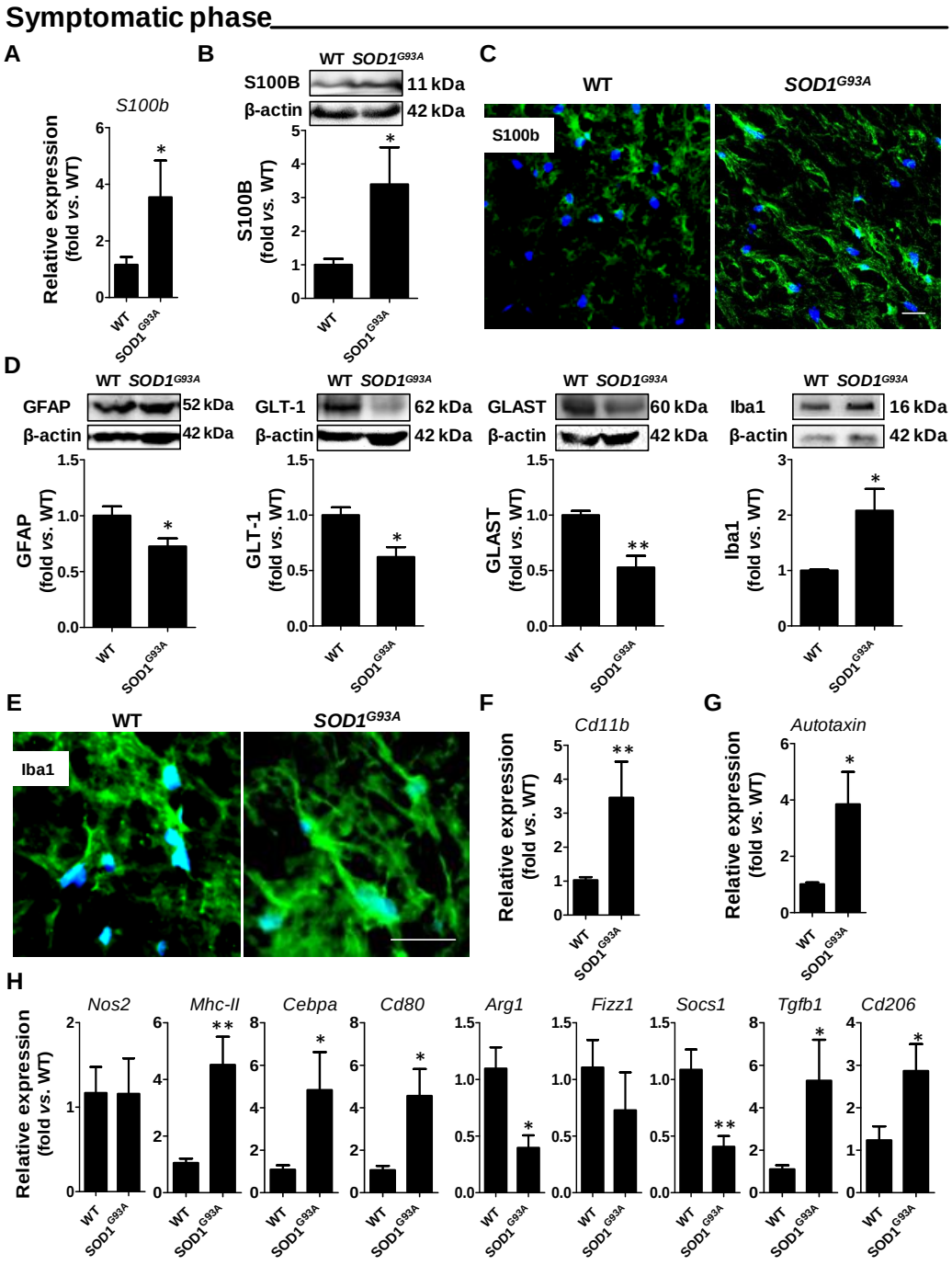

Figure IV.5 - Reactive and dysfunctional astrocytes coexist with multiple activated microglia subtypes in the symptomatic *SOD1*^{G93A} mice. Samples of the spinal cord tissue were processed as indicated in "Methods." (A) *S100b* quantification by qRT-PCR. (B) Western blot analysis of S100B. (C) Representative images of the S100B detection by immunohistochemistry using anti-S100B in the ventral funiculus of the spinal cord. (D) Western blot analysis of GFAP, glutamate transporters GLT-1/GLAST and Iba1. (E) Representative images of Iba1 detection by immunohistochemistry using anti-Iba1 in the ventral funiculus of the spinal cord. (F) *Cd11b* quantification by qRT-PCR. (G) *Autotaxin* quantification by qRT-PCR. (H) Expression of markers used for the characterization of microglia phenotypes assessed by qRT-PCR. *Nos2*, *Mhc-II*, *Cebpa* and *Cd80* are M1-phenotype markers while *Arg1*, *Fizz1*, *Socs1*, *Tgfb1*, and *Cd206* are markers of M2-polarized cells. Results are mean + SEM (*p < 0.05, **p < 0.01 vs. WT mice, n = 6 mice per group, unpaired Student's *t*-test). (C, E) Scale bar represents 20 μm.

Interestingly, in what concerns the inflamma-miRs, we found that the increase of miR-155 was a sustained feature, but at this time complemented with miR-125b, miR-146a, miR-21, and miR-124 elevated expression, some with calming and others with stressful consequences (Figure IV.6D). Actually, miR-155 and miR-125b are associated with pro-inflammatory responses and NF-κB activation (Cunha et al. 2016; Ponomarev et al. 2013; Volonté et al. 2015). With respect to miR-146a and miR-21, also produced after NF-κB activation, they act as feedback negative regulators to restrain microglia activation (Ponomarev et al. 2013; Saba et al. 2012). MiR-124, the most abundant miRNA in the brain and often produced by neurons, is known to contribute to pathological conditions, while also influences microglia to adopt either a surveilling state or an anti-inflammatory phenotype (Ponomarev et al. 2011; Ponomarev et al. 2013). Thus, considering each miRNA-specific function, the profile of inflamma-miRs we observed suggests a strong dysregulation of different inflammatory pathways determining diverse microglia activation subsets and a great complexity of pathophysiological events launched by the multifactorial ALS disease. New evidences actually suggest that microglia polarization is a continuum between pro- and anti-inflammatory states and also that microglia may present phenotypes with overlapping features between the typical M1 and M2 phenotypes (Limatola and Ransohoff 2014).

3.3.3. Upregulated Cell-to-Cell Communication in the Symptomatic Phase May Represent a Coordinated Cellular Response to Tissue Damage

In opposite to the downregulated astrocyte-astrocyte/neuron and neuron-microglia cross-talk identified in the Presymptomatic phase, the increased expression of *Cx43*, *Panx1*, *Ccl21*, and *Cx3cl1* (Figure IV.7) can be a set of organized mechanisms to augment secondary messengers and signals for tissue regeneration. Elevated CX3CL1-CX3CR1 gene and protein signaling axis between neurons and microglia, recently evidenced to downregulate phagocytic clearance (Zabel et al. 2016), was manifest at this time. Interestingly, the more pronounced elevation in the soluble fraction of CX3CL1 (76 kDa) than that in the membrane-bound fraction (95 kDA) sustains an increased proteolytic cleavage and release. As shown in Figure IV.7B, the reduced MFG-E8 expression, previously observed in the Presymptomatic stage, reinforces that MFG-E8-mediated phagocytosis is compromised in *SOD1*^{G93A} mice throughout the disease and attests its relevance as a promising sustained novel target and biomarker for ALS. Collectively, these findings help to further understand the ALS pathophysiological mechanisms and additionally demonstrate their complexity, while identifying new potential therapeutic drug targets.

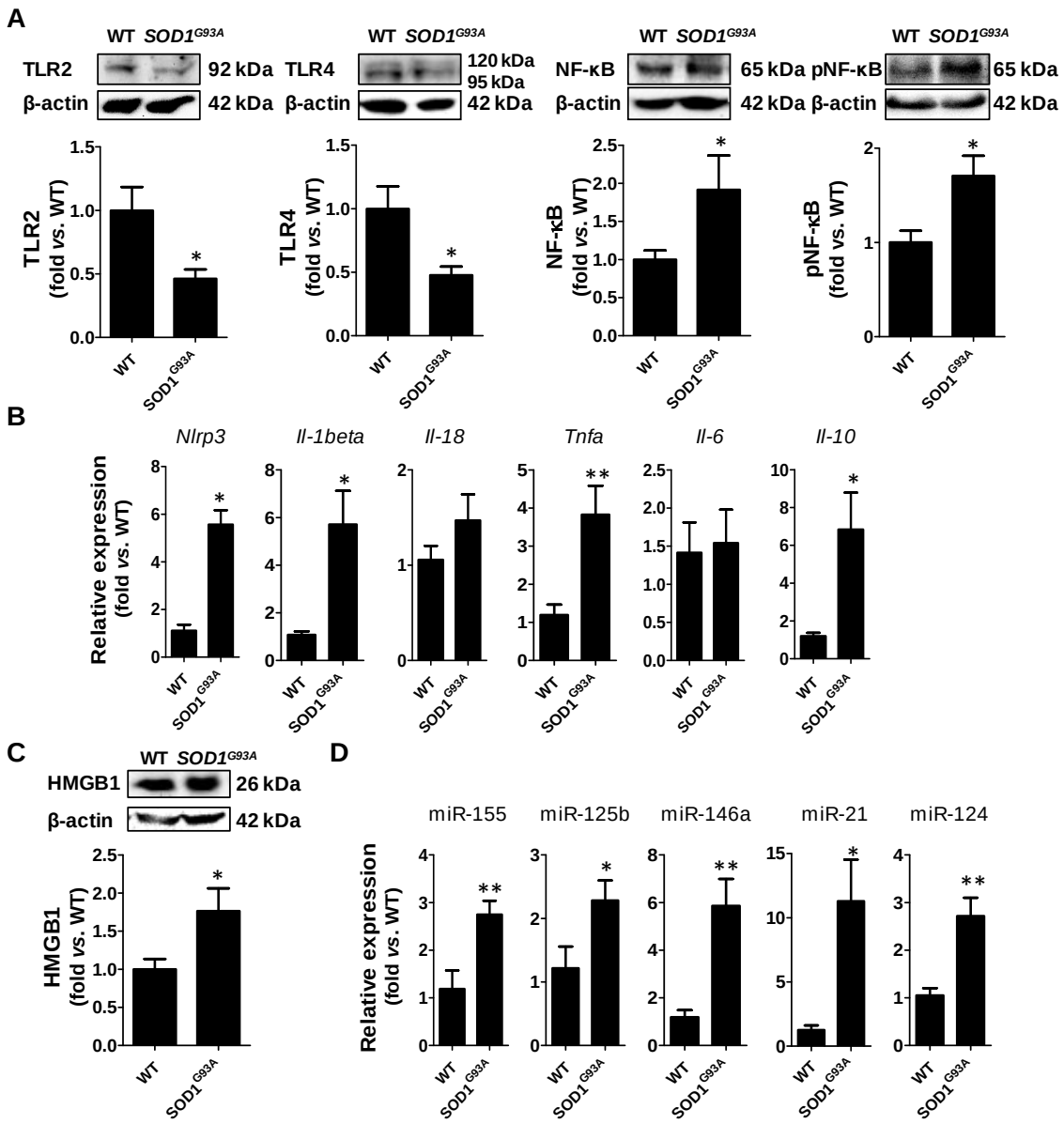

Figure IV.6 - TLR/NF-κB signaling pathway activation courses with *Nlrp3* stimulation and miR-155 upregulation in the *SOD1^{G93A}* mice after symptom onset. Samples of the spinal cord tissue were processed as indicated in "Methods." (A) Western blot analysis of TLR2, TLR4, NF-κB and pNF-κB. (B) Expression of *Nlrp3*, *Il-1beta*, *Il-18*, *Tnfa*, *Il-6*, and *Il-10* assessed by qRT-PCR. (C) Western blot analysis of HMGB1. (D) Profile of the inflammatory-related miR-155, miR-125b, miR-146a, miR-21, and miR-124 determined by qRT-PCR. Results are mean + SEM (*p < 0.05, **p < 0.01 vs. WT mice, n = 5-9 mice per group, unpaired Student's *t*-test).

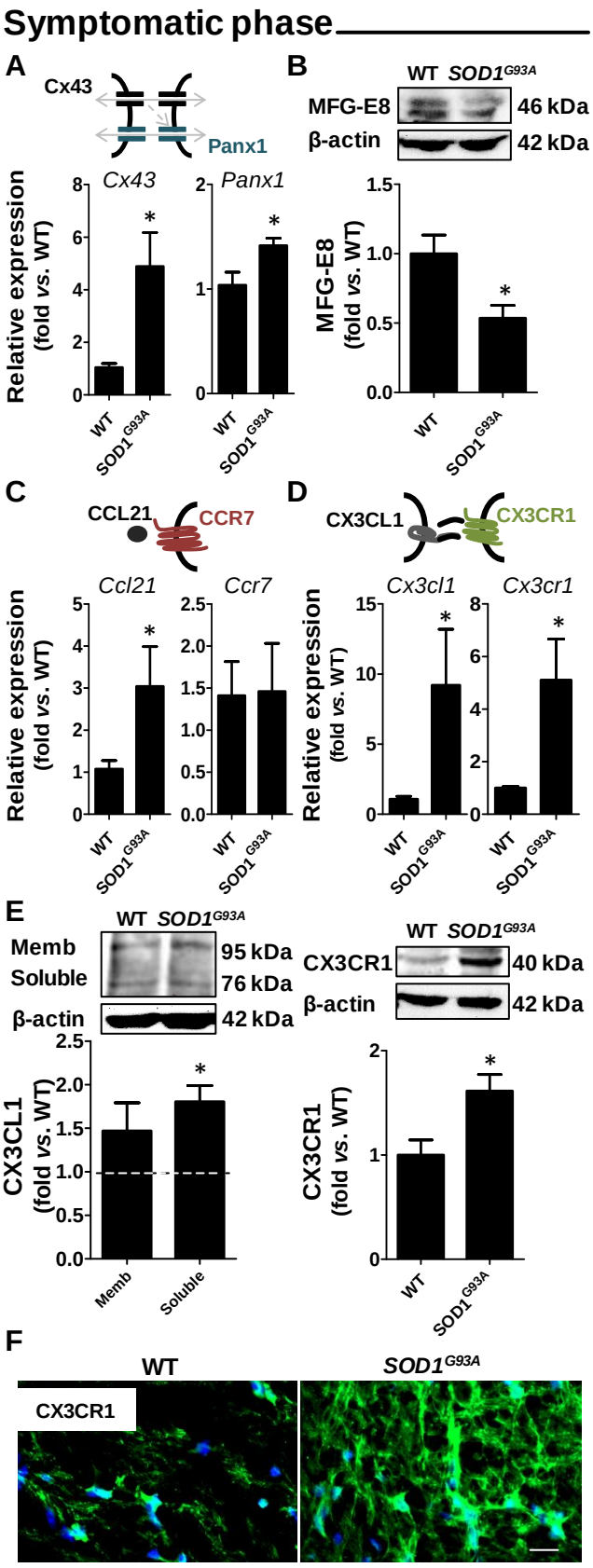

Figure IV.7 - Interplay between motor neurons and glial cells is enhanced in the symptomatic *SOD1*^{G93A} mice. Samples of the spinal cord tissue were processed as indicated in "Methods." (A) *Cx43* and *Panx1* expression assessed by qRT-PCR. (B) Western blot analysis of MFG-E8. (C) *Ccl21* and *Ccr7* expression assessed by qRT-PCR. (D) *Cx3cl1* and *Cx3cr1* expression assessed by qRT-PCR. (E) Western blot analysis of CX3CR1, and of membrane-bound and soluble CX3CL1 forms. Results are expressed as mean + SEM from at least 5 experiments. Dashed line represents WT levels. Results are mean + SEM (*p < 0.05 vs. WT mice, n = 6-11 mice per group, unpaired Student's *t*-test). (F) Representative immunofluorescent images of CX3CR1 are shown. Scale bar represents 20 μm.

4. Discussion

Intensive research efforts have increased the knowledge on the mechanisms underlying MN degeneration in ALS. However, there is still limited information on the early determinants and specificities at presymptomatic and symptomatic stages. This is particularly important given the lack of effective biomarkers not only for early diagnosis of ALS but also for monitoring disease progression rate (Vu and Bowser 2017). Additionally, due to multifactorial effectors in ALS and their intricate mechanisms, clinical trials constantly fail to validate novel therapeutic strategies, requiring the discovery of new targets and innovative therapies. We show that gene and protein profiling diverge from the presymptomatic to the symptomatic stage. While a subexpression of glial-associated genes and proteins occurs early before disease onset in the SC of *SOD1*^{G93A} mice, probably compromising cellular interplay, increased expression of inflammatory mediators coexist with neurodegeneration, microglia predominant M1 phenotype and overregulated cell-to-cell communication, after disease onset. Intriguingly, the presence of different microglia phenotypes and the activation of several regulatory mechanisms at promoting tissue regeneration seem to simultaneously coexist. Most important, this study uncovers miR-155 overexpression and MFG-E8 downregulation as key players prior to disease onset and along disease progression.

Involvement of miR-155 in both familial and sporadic ALS patients was recently demonstrated, and miR-155 targeting in microglia was shown to restore normal cell function (Butovsky et al. 2015; Koval et al. 2013). A previous study showed that miR-155 was upregulated at 60 days old *SOD1*^{G93A} mice in both SC-derived CD39^{+} microglia and in splenic Ly6C monocytes (Butovsky et al. 2012). Our data further showed that overexpression of miR-155 in the SC is even detectable at earlier time periods, in the present case at 4-6 weeks. Upregulation of miR-155 was shown to contribute to microglia-mediated immune response and neuroinflammation, as well as to promote genome instability by affecting several DNA repair factors (Cardoso et al. 2012; Czochor et al. 2016; Guedes et al. 2014). Interestingly, there are later evidences demonstrating its benefits in preventing the elevation of pro-inflammatory cytokines (Li et al. 2016a; Yuan et al. 2016). Our results suggest miR-155 as a candidate to orchestrate the direct downregulation of SOCS1 and, by targeting of C/EBPβ and Smad2, the downregulation of arginase-1 (Arg1) and transforming growth factor beta (TGF-β), respectively (Cardoso et al. 2012; Volonté et al. 2015). However, this is not consistent with the absence of inflammatory responses, usually considered to course with the elevation of miR-155. One may hypothesize that miR-155 upregulation is due to the lack of CX3CL1 inhibitory input from neurons, essential for microglia surveilling phenotype (Cardona et al. 2006b). In addition, the protective and anti-inflammatory role of miR-155 was recently suggested in the model of atherosclerosis-associated chronic inflammation (Li et al.

2016a). These findings bring some controversy about its role in neuroinflammation. Furthermore, although the targets are unknown, Butovsky and collaborators (2015) showed that miR-155 interferes with microglia phagocytosis, which may be reflected in MFG-E8 downregulation in both disease stages. MFG-E8 recognizes phosphatidylserine on the outer membrane leaflet of apoptotic cells, such as neurons, and works as a bridge to attach microglia to such cells, thus triggering signaling cascade pathways that stimulate the process of destroying the dying cell (Liu et al. 2013b). So far, there was no evidence of MFG-E8 involvement in ALS. *In vitro* studies showed that activated microglia upregulate MFG-E8, thus promoting the phagocytosis of viable neurons (Fricker et al. 2012), which occurs with the production of pro-inflammatory cytokines (Liu et al. 2013b). However, MFG-E8 knock-out was also shown to enhance pro-inflammatory responses *in vivo* (Hanayama et al. 2002). The outcome of the observed decrease in MFG-E8 may then rely on impaired phagocytosis of apoptotic cells by dysfunctional microglia, reason why MFG-E8-driven therapies might be considered. Actually, MFG-E8 upregulation has already shown to resolve inflammation in other pathologies (Das et al. 2016).

In the symptomatic stage, the heterogeneous activated microglia may trigger the elevation of all inflamma-miRs, some of them already identified in ALS rodents and patients (Koval et al. 2013). In particular, miR-125b was shown to be increased in cortical *SOD1*^{G93A} microglia promoting tumor necrosis factor alpha (TNF-α) expression (Parisi et al. 2016) that together with miR-155 switch microglia towards the M1-phenotype (Cunha et al. 2016). Given that miR-21 and miR-146a control microglia inflammatory reactivity, their upregulation may restrict neuroinflammatory effectors, justifying the TLR downregulation we observed (He et al. 2014). The elevation of miR-124, known as having calming effects on microglia (Ponomarev et al. 2011), has been also shown to be expressed by stressed neurons and to be linked to neurodegeneration (Sun et al. 2015). Actually, we observed a marked upregulation of miR-124 in the MN-like cell line (NSC-34 cells) expressing *SOD1*^{G93A} (Pinto et al. 2017). Therefore, the elevation of miR-124 may be more closely related with the existence of neurodegeneration than with a surveilling microglia phenotype.

Because ALS is mainly a sporadic disease, and since presymptomatic changes can only be assessed in people with genetic risk of developing ALS, studies have been limited to rodent ALS models. Regardless the data from Thomsen et al. (2014a) showing MN loss in the SC before disease onset, we were unable to find such neurodegeneration in our *SOD1*^{G93A} presymptomatic mice. Nevertheless, some pathogenic mechanisms, such hyperexcitability, were displayed in young age (Kuo et al. 2004; Vucic et al. 2008). We show for the first time that a subexpressed glia-associated genes and proteins in the SC of presymptomatic *SOD1*^{G93A} mice may act as a defensive signaling mechanism network against ALS onset and MN degeneration. Consistent downregulation was found for GFAP

and MFG-E8 proteins, and for *S100b*, *Cd11b*, *Arg1*, *Fizz1*, *Socs1*, *Tgfb1*, *Cd206*, *Cd80*, *Nlrp3*, *Il-1beta*, *Il-6*, *Tnfa*, *Cx43*, *Panx1*, *Ccl21*, *Cx3cl1* genes, attesting the depressed activation of both astrocytes and microglia at the preonset phase. A distinct adaptive shift in microglial phenotypes at preclinical stage, with microglia evidencing an anti-inflammatory phenotype and attenuated innate immune TLR2 response to lipopolysaccharide insult, was recently documented (Gravel et al. 2016). Nevertheless, and contrasting with data obtained by these authors, we did not identify any elevation of IL-10 that could be attributed to microglia, at least at the gene expression level. In contrast, marked elevation of IL-10 gene expression was observed in the symptomatic mice. Overall, we propose that preonset compensatory control of SOD1-associated homeostatic imbalance, with depressed glial function responses precede the inflammatory emergence associated to ALS clinical symptoms. This is not without precedent, since it was recently reported a transcriptional downregulation of highly insoluble proteins in Alzheimer's disease as mitigating aberrant protein aggregation (Ciryam et al. 2016).

Previous reports emphasize the existence of incongruence on microglia phenotypes and neurotoxic effects in ALS (Brites and Vaz 2014). The neurodegenerative-specific microglia phenotype differing from M1 and M2 polarized microglia subtypes, when acutely isolated from the *SOD1*^{G93A} mice model (Chiu et al. 2013), is in line with mixed microglia populations, as suggested by the M2-CD206/TGF-β increased expression, aside the prevalent proinflammatory phenotype. In addition, expression of inflamma-miRs reinforces the presence of distinct phenotypes. In fact, miR-146a upregulation is associated with senescent cells, including the senescent microglia (Caldeira et al. 2014), suggesting that together with neuroinflammatory miR-155-/miR-125b-expressing microglia, a senescent/dysfunctional population of cells may also coexist. Together, such phenotypes are believed to have deleterious effects and accelerate disease propagation (Boillée et al. 2006b; Frakes et al. 2014; Nikodemova et al. 2014). Downstream signaling cascades activating NF-κB and NLRP3-inflammasome are induced in the symptomatic stage, comprehending the cytokines IL-1β and TNF-α and the alarmin HMGB1, as previously reported in ALS patients (Casula et al. 2011; Johann et al. 2015). While the NF-κB activation has been attributed to microglia and described as a major pathological determinant in the *SOD1*^{G93A} mice (Frakes et al. 2014), NLRP3-inflammasome was found mainly expressed in astrocytes (Johann et al. 2015), suggesting the crucial involvement of microglia astrocyte interactive mechanisms.

Aberrant and neurotoxic astrocytes showing decreased GFAP, GLT-1, and GLAST, as well as increased Cx43 and S100B levels, were identified in symptomatic *SOD1*^{G93A} rats (Diaz-Amarilla et al. 2011), adding on the ALS complexity. Besides our matching results in the mouse model, we for the first time assessed homeostatic signature alterations after symptom onset. The upregulation of Cx43-Panx1 and CX3CL1-CX3CR1 axes, together with

increased CCL21 levels, reinforce the multifactorial nature of the symptomatic-associated mechanisms. The direct transfer of small molecules, including the important second messenger Ca^{2+} through Cx43 and Panx1, regulate different aspects of neuron-astrocyte-microglia interplay. Pro-inflammatory mediators stimulate hemichannels to open, what may lead to neuronal death through different mechanisms (Montero and Orellana 2015). As Orellana et al. (2011) proposed, Aβ-activated microglia secrete pro-inflammatory cytokines that stimulate the release of glutamate and ATP through astrocytic Cx43 which, in turn, induces activation of neuronal Panx1 and associated neurodegeneration. Thus, the observed dysregulated expression pattern of Cx43/Panx1 in *SOD1^{G93A}* mice suggests that, before symptom onset, homeostatic control through hemichannels is hindered, whereas later upregulation of both hemichannels by glial cells may account to MN degeneration. In addition, since overexpression of the chemokine CCL21 induces massive brain inflammation in mice (Chen et al. 2002), we hypothesize that the upregulation of Cx43/Panx1 and CCL21 may be a key factor for glial activation and myeloid cell recruitment, then ultimately contributing to disease propagation into unaffected areas. The interface between CX3CL1 and CX3CR1 is, however, far more controversial since the outcome of the interaction is extremely context-dependent (Wolf et al. 2013). Despite the fact that deletion of CX3CR1 was shown to induce a worsened disease progression in *SOD1^{G93A}* mice (Cardona et al. 2006b), CX3CR1 inhibition halted microglia activation induced by Aβ1-40 fibrils *in vivo* (Wu et al. 2013). A recent study in a cohort of sporadic ALS patients has shown that the presence of a less functional variant of CX3CR1determines a reduced survival time (Lopez-Lopez et al. 2014). Nonetheless, CX3CL1 cleavage is an early event in neuronal death induced by an excitotoxic stimulus (Chapman et al. 2000), and soluble CX3CL1 was shown to induce the expression of microglial IL-1β (Wolf et al. 2013), indicating that upon release of CX3CL1, microglia response may encompass toxic features. Finally, although upregulation of autotaxin was found in other neuroinflammatory diseases (Zahednasab et al. 2014), our findings are innovative in establishing autotaxin as an ALS-associated inflammatory marker in the *SOD1^{G93A}* mice.

Overall, we provide new evidences on the mechanisms underlying both pre and symptomatic stages of ALS. The remarkable depressed glia functionality and reduced cell-to-cell communication in the preonset stage opens new clues on potential mechanisms at preventing the lethal fate of MNs. As early potential targets and biomarkers, we identified the upregulation of miR-155 and the downregulation of MFG-E8. Upregulation of miR-155 in monocytes from ALS mouse model and patients was previously found (Butovsky et al. 2012), and benefits on its targeting already reported (Butovsky et al. 2015). However, no references were made for the existence of elevated expression of miR-155 in the SC of *SOD1^{G93A}* mouse model at such early presymptomatic stage. After disease onset, astrocytes acquire

proliferative/reactive properties, and microglia predominantly switch to a proinflammatory state, with both cells displaying neurotoxic properties and contributing to an insidious scenario. We further show that other microglia phenotypes may coexist after disease onset and course with some defensive mechanisms as the disease progresses. Such findings outline that combined therapies may be more effective at delaying ALS progression, and that by pushing the balance towards neuroprotection, through acting in different cellular processes, may enhance the appearance of successful therapeutic approaches for ALS. Among them, our data specify NLRP3-inflammasome, HMGB1, miR-155/miR-125b, shed CX3CL1, and hemichannels Cx43/Panx1, as promising targets to be repressed, and outline MFG-E8 and M2-microglia subtypes to be upregulated, when designing molecular interventions with pleiotropic functionality for ALS-associated neuroinflammation.

Acknowledgements

This work was funded by the Research Grant of the Santa Casa Scientific Research Program on ALS, by Santa Casa da Misericórdia de Lisboa (SCML), Portugal, Project Ref. ELA-2015-002 (to DB), by the project PTDC/SAU-FAR/118787/2010 (to D.B.) and, in part, by iMed.ULisboa (UID/DTP/04138/2013) from Fundação para a Ciência e a Tecnologia (FCT). A.R.V. holds a postdoctoral research fellowship (SFRH/BPD/76590/2011), and C.C. and C.G. are recipients of PhD fellowships (SFRH/BD/91316/2012 and SFRH/BD/102718/2014, respectively), all from FCT. The funding organization had no role in study design, data collection and analysis, decision to publish, or preparation of the manuscript. We thank to Dr. Rui Gomes (Instituto de Medicina Molecular, Faculdade de Medicina de Lisboa, Universidade de Lisboa, Portugal) for genotyping mice.

5. Supplementary Material

Supplementary Table IV.1 - List of primary antibodies used in IHC and WB.

Primary antibody	Species	Reference	Dilution in IHC	Dilution in WB
SOD1	Rabbit	sc-11407, Santa Cruz Biotechnology	1:50	1:500
NeuN	Mouse	MAB377, Millipore	1:100	1:100
S100B	Rabbit	Ab52642, Abcam, Cambridge, UK	1:200	1:1000
GFAP	Rabbit	G9269, Sigma-Aldrich	-	1:500
GLT-1	Rabbit	Ab41621, AbCam, Cambridge, UK	-	1:200
GLAST	Rabbit	Ab416, AbCam, Cambridge, UK	-	1:200
Iba1	Rabbit	Wako 019-19741, Wako Pure Chemical Industries Ltd, Osaka, Japan	1:250	1:500
TLR4	Mouse	sc-10741, Santa Cruz Biotechnology	-	1:100
TLR2	Rabbit	sc-10739, Santa Cruz Biotechnology	-	1:100
NF-kB p65	Rabbit	sc-372, Santa Cruz Biotechnology	-	1:500
NF-kB p65 phospho S536	Rabbit	Ab131109, Abcam	-	1:500
HMGB1	Mouse	651402, BioLegend; San Diego, CA, USA	-	1:200
MFG-E8	Rabbit	sc-33546, Santa Cruz Biotechnology	-	1:100
CX3CL1	Goat	sc-7227, Santa Cruz Biotechnology	-	1:50
CX3CR1	Rabbit	Ab8021, Abcam	1:100	1:500
β-actin	Mouse	A5441, Sigma-Aldrich	-	1:5000

Supplementary Table IV.2 - List of primer sequences used for mRNA analysis.

Gene	Sequence (5'-3')/Source
Ki-67	5'-CAGTACTCGGAATGCAGCAA-3' (fwr)
	5'-CAGTCTTCAGGGGCTCTGTC-3' (rev)
S100b	5'-GAGAGAGGGTGACAAGCACAA-3' (fwr)
	5'-GGCCATAAACTCCTGGAAGTC-3' (rev)
Cd11b	5'-CAGATCAACAATGTGACCGTATGGG-3' (fwr)
	5'-CATCATGTCCTTGTACTGCCGCTTG-3' (rev)
Nos2	5'-ACCCACATCTGGCAGAATGAG-3' (fwr)

	5’-AGCCATGACCTTTCGCATTAG-3’ (rev)
Mhc-II	5’-TGGGCACCATCTTCATCATTC-3’ (fwr)
	5’-GGTCACCCAGCACACCACTT-3’ (rev)
Cebpa	5’-AGCTTACAACAGGCCAGGTTTC-3’ (fwr)
	5’-CGGCTGGCGACATACAGTAC-3’ (rev)
Arg1	5’-CTTGGCTTGCTTCGGAACTC-3’ (fwr)
	5’-GGAGAAGGCGTTTGCTTAGTTC-3’ (rev)
Fizz1	5’-GCCAGGTCCTGGAACCTTTC-3’ (fwr)
	5’-GGAGCAGGGAGATGCAGATGAG-3’ (rev)
Socs1	5’-CACCTTCTTGGTGCGCG-3’ (fwr)
	5’-AAGCCATCTTCACGCTGAGC-3’ (rev)
Tgfb1	5’-CAGAGCTGCGCTTGCAGAG-3’ (fwr)
	5’-GTCAGCAGCCGGTTACCAAG3’ (rev)
Nlrp3	5’-TGCTCTTCACTGCTATCAAGCCCT-3’ (fwr)
	5’-ACAAGCCTTTGCTCCAGACCCTAT-3’ (rev)
Il-18	5’-TGGTTCCATGCTTTCTGGACTCCT-3’ (fwr)
	5’-TTCCTGGGCCAAGAGGAAGTG-3’ (rev)
Il-1beta	5’-CAGGCTCCGAGATGAACAAC-3’ (fwr)
	5’-GGTGGAGAGCTTTCAGCTCATA-3’ (rev)
Cx43	5’-ACAGCGGTTGAGTCAGCTTG-3’ (fwr)
	5’-GAGAGATGGGGAAGGACTTGT-3’ (rev)
Panx1	5’-TGTGGCTGCACAAGTTCTTC-3' (fwr)
	5’-ACAGACTCTGCCCCACATTC-3’(rev)
Ccl21	5’-CAGGACTGCTGCCTTAAGTA-3’ (fwr)
	5’-GCACATAGCTCAGGCTTAGA-3’ (rev)
Ccr7	5’-CATGGACCCAGGTGTGCTTC-3’ (fwr)
	5’-TCAGTATCACCAGCCCGTTG-3’ (ver)
Cx3cl1	5’-CTCACGAATCCCAGTGGCTT-3’ (fwr)
	5’-TTTCTCCTTCGGGTCAGCAC-3’ (rev)
Cx3cr1	5’-TCGTCTTCACGTTCGGTCTG-3’ (fwr)
	5’-CTCAAGGCCAGGTTCAGGAG-3’ (rev)
Cd80	5’-ACTAGTTTCTCTTTTTCAGGTTGTG-3’ (fwr)
	5’-GAGCCAATGGAGCTTAGGCA-3’ (rev)
Cd206	5’-GTGGAGTGATGGAACCCCAG-3’ (fwr)
	5’-CTGTCCGCCCAGTATCCATC-3’ (rev)
b-actin	5’-GCTCCGGCATGTGCAA-3’ (fwr)
	5’-AGGATCTTCATGAGGTAGT-3’ (rev)

Chapter V

SOD1^{G93A} SPINAL MICROGLIA SWITCH FROM PRO-INFLAMMATORY TO HETEROGENEOUS PHENOTYPES WITH *IN VITRO* AGING AND CROSS-TALK WITH PAIRED REACTIVE ASTROCYTES

Carolina Cunha[1], Cátia Gomes[1], Ana Rita Vaz[1,2], Dora Brites[1,2]

[1]Neuron Glia Biology in Health and Disease Group, Research Institute for Medicines (iMed.ULisboa), Faculty of Pharmacy, Universidade de Lisboa, Avenida Professor Gama Pinto, 1640-003 Lisbon, Portugal

[2]Department of Biochemistry and Human Biology, Faculty of Pharmacy, Universidade de Lisboa, Lisbon, Portugal

(To be submitted)

Abstract

Neuroinflammation is a recognized hallmark of amyotrophic lateral sclerosis (ALS). While recent studies show specific microglia-induced motor neuron injury pathways, microglial phenotypic dynamics along disease course are largely unknown. Here, we isolated microglia from the spinal cord of *SOD1*^{G93A} mice and evaluated their phenotypic profile, inflammatory responses and phagocytic/autophagic ability when cultured for short or long-term [2 and 16 days *in vitro* (DIV), respectively]. A coculture system was used to understand the influence of microglia-astrocyte communication in ALS neuroinflammatory pathways. The expression profile of microglial phenotypic markers showed that a pro-inflammatory polarization in 2 DIV *SOD1*^{G93A} spinal microglia progresses to a dysfunctional state, while a 16 DIV microglia population retain the proinflammatory phenotype. TLR4/NF-κB signaling pathway and nitric oxide release are activated in short-term cultured *SOD1*^{G93A} spinal microglia, mechanisms that are lost with time in culture. Additionally, impaired beads phagocytosis and MFG-E8 production were observed in both time-points in *SOD1*^{G93A} spinal microglia and LC3-related autophagy was only induced in 16 DIV *SOD1*^{G93A} cells. We also demonstrated that *SOD1*^{G93A} spinal astrocytes produce toxic effects in WT spinal microglia while inducing heterogeneous M1, M2b and M2c subsets in *SOD1*^{G93A} spinal microglia. Interestingly, *SOD1*^{G93A} spinal astrocytes-to-microglia communication promoted *Nlrp3-inflammasome* upregulation and HMGB1 release. Also, in this coculture pair, astrocytes upregulate *S100b* and *Panx1*. Overall, microglia acquire multiple phenotypes *in vitro* and upon astrocytes interaction reflecting the complexity of microglia responses in ALS. We further highlight the importance of designing combined therapies as specific non-cell autonomous neurotoxic mechanisms require microglia-astrocyte cross-talk.

Keywords: Phenotype heterogeneity, inflamma-miRs deregulation, microglia-astrocyte cross-talk

1. Introduction

Amyotrophic lateral sclerosis (ALS) is a late-onset fast progressing motor neuron disease caused by selective denervation and death of upper and lower motor neurons leading to muscular weakness and atrophy. The heterogeneity of symptoms underlies the involvement of different central nervous system (CNS) regions including motor cortex, brainstem and spinal cord (SC). Sporadic and familial ALS (only 10%) share very similar clinical manifestations and patients generally die by respiratory failure 2-5 years after disease onset (Taylor et al. 2016; Van Damme et al. 2017). In this line, transgenic rodents carrying superoxide dismutase 1 (SOD1) mutations (first ALS-causing mutant protein described) are the most studied model as they develop a progressive motor neuron degeneration similar to ALS patients (Turner and Talbot 2008; Van Damme et al. 2017).

Despite a typical motor neuron disease, different studies have shown the intimate association of glial cells activation with motor neuron degeneration in ALS. Transgenic mice selectively expressing mutant SOD1 (mSOD1) in motor neurons did not develop motor neuron disease (Lino et al. 2002; Pramatarova et al. 2001). By producing chimeric mice, Clement and colleagues (2003) showed that mSOD1-nonneuronal cells induce an ALS-like pathology in healthy motor neurons. Additionally, mSOD1 gene targeting in microglia (Boillée et al. 2006b) or astrocytes (Yamanaka et al. 2008b) significantly delayed disease progression, illustrating the importance of glial cells to the overall picture of ALS.

Amongst the multifactorial processes involved in ALS, neuroinflammation has gain increased attention over the last years. Several efforts have been made to develop new therapies targeting inflammation and microglia activation but despite the positive outcome in transgenic mice, they constantly fail when transferred to human clinical trials (Crisafulli et al. 2017). In fact, the underlying mechanisms of inflammation-induced motor neuron degeneration as well as the diversity of microglial phenotypes are not fully understood.

Microglia are highly ramified surveillant cells whose functions go far beyond immune defense mechanisms as they actively contribute to normal CNS development and homeostasis (Wolf et al. 2017). Microglial phenotype designations have been recently debated as the typical M1/M2 phenotypes begin to be unsuccessful in completely explaining microglial responses in normal and diseased CNS (Ransohoff 2016; Song and Suk 2017). Rather, microglia activation is extremely plastic and specific for the confined environment they face and novel studies have started to unravel particular microglia molecular signatures (Butovsky et al. 2014; Chiu et al. 2013). Nevertheless, a set of phenotype markers ranging from the pro-inflammatory M1 to anti-inflammatory M2, typically described for macrophages, can be useful to understand microglia pathogenic involvement in neurodegeneration and have been reviewed elsewhere (Brites and Vaz 2014; Moehle and West 2014).

Controversial data have been published concerning the transition of microglial phenotypes along ALS progression. While *in vitro* studies point to a pro-inflammatory and neurotoxic mSOD1-expressing microglia (Frakes et al. 2014; Xiao et al. 2007), *in vivo* data address a specific microglial signature in late symptomatic ALS-rodents (Chiu et al. 2013; Nikodemova et al. 2014). A transition from M2-neuroprotective at disease onset to a M1-neurotoxic phenotype at the end-stage was also reported (Liao et al. 2012). We recently showed that microglia neuroprotective functions were reduced in presymptomatic $SOD1^{G93A}$ mice progressing to a mixture of phenotypes with prevalent pro-inflammatory properties at the symptomatic stage (Cunha et al. 2017). Interestingly, a series of inflammation-related microRNAs (miRNAs) denominated as inflamma-miRs emerged as new tools to identify microglia phenotypes (Freilich et al. 2013; Ponomarev et al. 2013). Both pro-inflammatory (miR-155 and miR-125b) and anti-inflammatory (miR-21 and miR-146a) miRNAs were upregulated in symptomatic ALS mice (Butovsky et al. 2015; Butovsky et al. 2012; Cunha et al. 2017), corroborating the acquisition of multiple microglial subsets in ALS late stages. Of notice, the role of microglia phagocytosis in ALS has been neglected. Some reports indicate impairment of mSOD1 microglia phagocytic capacity (Butovsky et al. 2015; Sargsyan et al. 2011) and we described that downregulation of milk fat globule EGF factor 8 (MFG-E8), an adaptor molecule involved in facilitating microglia phagocytosis upon recognition of phosphatidylserine (PS), was sustained throughout disease course in $SOD1^{G93A}$ mice (Cunha et al. 2017).

Here we explored the phenotype of SC-derived microglia cultured for a short and a longer period of time to mimic reactive *vs.* senescent-like behavior, as we previously showed (Caldeira et al. 2014), in order to establish a model that could represent microglia in early and late stages of ALS. Moreover, we also explore the effect produced by astrocytes secretome in microglia polarization since very little is known about the cross-talk between them in this disease. Our data indicate that microglia may acquire distinct phenotypes in ALS and the communication between microglia and astrocytes drives the upregulation of specific neurotoxic mechanisms. Our data not only propose a useful model to further explore strategies to modulate microglial function in ALS but also highlights the importance of designing target-driven solutions taking into account the properties of microglia in a specific disease stage.

2. Materials and Methods

2.1. Transgenic *SOD1^{G93A}* mouse model

Transgenic B6SJL-TgN (SOD1G93A)1Gur/J males (Jackson Laboratory, No. 002726) overexpressing the human *SOD1* (h*SOD1*) gene carrying a glycine to alanine point mutation at residue 93 (G93A) (*SOD1^{G93A}*) (Gurney et al. 1994) and B6SJLF1/J non transgenic, wild type (WT) females were purchased from The Jackson Laboratory (Bar Harbor, ME, USA). Maintenance and handling took place at Instituto de Medicina Molecular animal house facilities, where a colony was established. Mice were maintained on a background B6SJL by breeding *SOD1^{G93A}* transgenic males with WT females. In this study we used 7 day-old pups. A section of the tail was used in the genotyping protocol through polymerase chain reaction (PCR) (Rosen 1993) to identify *SOD1^{G93A}* and WT mice.

The present study was performed in accordance with the European Community guidelines (Directives 86/609/EU and 2010/63/EU, Recommendation 2007/526/CE, European Convention for the Protection of Vertebrate Animals used for Experimental or Other Scientific Purposes ETS 123/Appendix A) and Portuguese Laws on Animal Care (Decreto-Lei 129/92, Portaria 1005/92, Portaria466/95, Decreto-Lei 197/96, Portaria 1131/97). All the protocols used in this study were approved by the Portuguese National Authority (General Direction of Veterinary) and the Ethics Committee of the Instituto de Medicina Molecular of the Faculty of Medicine, Universidade de Lisboa, Lisbon, Portugal. All animal procedures were approved by the Institutional Animal Care and Use Committee and studies were conducted in accordance with the United States Public Health Service's Policy on Humane Care and Use of Laboratory Animals. Every effort was made to minimize the number of animals used and their suffering.

2.2. Primary microglia cultures from the spinal cord

In this work we used the method of Saura et al. (2003) described to isolate microglia from cerebral cortices, instead of the shaking method (Giulian and Baker 1986) or the Percoll gradient (Cardona et al. 2006a), due to its simplicity, reproducibility and high-yield advantages. The method revealed to produce microglia with low contamination by astrocytes (Gordo et al. 2006) and to be adequate to isolate such cells from the spinal cord of transgenic mice, as well as for protein/mRNA assessment (Saura et al. 2003). Indeed, other methods used to extract microglia from the spinal cord result in preparations with 30% astrocyte contamination, at least for adult microglia (Bronstein et al. 2013). Our primary mixed glial cultures were prepared from the SC of 7 day-old WT and *SOD1^{G93A}* mice. At this age, microglia dramatically increase in number (Harry and Kraft 2012), and although the microglia amoeboid morphology is still abundant, transition into a ramified shape is already

visible (Cardoso et al. 2015). To note that microglia morphological features and their colonization of the mouse brain were shown to be similar to humans (Torres-Platas et al. 2014). After dissecting the whole SC (C1-L5 segments), meninges as well as the attached dorsal and ventral roots were peeled away under a dissection microscope. The SC tissue was divided into small pieces using the forceps and then quickly triturated with 1 ml pipette. The lysate was then filtered consecutively in a 230- and 104-µm filter to remove large debris and dissociate cell clusters. After spin down the cell suspension at 700 g for 10 min, cells isolated from one SC were resuspended in culture medium [DMEM-Ham's F-12 with 2 mM L-glutamine, 1 mM sodium pyruvate, non-essential amino acids 1x, 10% fetal bovine serum (FBS), and 1% antibiotic-antimycotic solution] and seeded on 6 wells of an uncoated 12-well tissue culture plate ($7x10^3$ cells/cm^2). Glial cultures were maintained at 37°C in a humidified atmosphere of 5% CO_2 for 21 days *in vitro* (DIV) and medium was changed once a week. This period was shown to produce microglia with maximal yield and purity (Saura et al. 2003), usually more than five times of the shaking method (Giulian and Baker 1986). In contrast with the shaking method such procedure has a lower level of isolation procedure stress leading only to a mild state of microglia activation, with cells showing amoeboid, bipolar and unipolar morphologies. The confluent mixed glial cultures were then subjected to mild trypsinization using a trypsin-EDTA solution diluted 1:3 in DMEM-Ham's F12 (DMEM-F12) to detach an intact upper layer of astrocytes, which were collected and used in cocultures of microglia-astrocytes. The reaction was stopped after 45 min by adding DMEM-F12 supplemented with 10% FBS. Microglia that remained firmly attached to the bottom were used after short-term (2 DIV) and long-term cultures (16 DIV), as described for cortical microglia (Caldeira et al. 2014). With this *in vitro* aging (Lesuisse and Martin 2002; Phipps et al. 2007) we intend to assess changes in microglia phenotypes that mimic ALS progression. The number of contaminating astrocytes in the microglial seeded plate was between 2 and 4% in all experiments.

2.3. Microglia-astrocyte cocultures

Cocultures were used to study the effect of astrocytes on microglia phenotype, as well as the pathways involved in astrocytes-microglia interplay in ALS. Our primary mixed glial cultures were prepared, as aforementioned from the SC of 7 day-old WT and *SOD1*^{G93A} mice. To the best of our knowledge, we are the first establishing this procedure. The mixed culturing and the separation of microglia and astrocytes from the same culture has several advantages, as follows: more accurately mimic the developing brain and the CNS environment; allow the isolation of the two types of glial cells whose development and differentiation took place in parallel; show low contamination of microglia in the astrocyte

layer in contrast with usual astroglial-enriched (Saura 2007); and minimize the number of animals used and better coordinate the culturing times of astrocytes and microglia.

After the mild-trypsinization, previously described, the isolated astrocytes were collected, spin down at 900 g for 5 min and re-plated on 6 coverslips (12-well tissue culture plate) with paraffin wax feet (Phatnani et al. 2013) in the same medium composition used in the mixed culture. After 2 DIV, the coverslips containing WT or *SOD1^{G93A}* astrocytes were inverted over a layer of WT or *SOD1^{G93A}* microglia, so that 4 coculture pairs were established: WT microglia-WT astrocytes; WT microglia-*SOD1^{G93A}* astrocytes; *SOD1^{G93A}* microglia-WT astrocytes; and *SOD1^{G93A}* microglia-*SOD1^{G93A}* astrocytes. At the moment of coculture, fresh medium was added to each well. Cells were maintained in coculture for 48h, and then harvested separately.

Recently, novel protocols have been developed to isolate and culture adult astrocytes to a better understanding of astrocytes biology in human adult-onset diseases (Diaz-Amarilla et al. 2011; Tripathi et al. 2017). In rodent brain, astrocytes reach their plateau number between postnatal day 7 and 10, where gene expression profiles are nearly indistinguishable from their adult gene profiles (Foo et al. 2011). Astrocytes obtained with this procedure from the spinal cord of pups expressed common markers of mature astrocytes, such as the filamentous GFAP in their processes, as well as the astrocytic glutamate transporter 1 (GLT-1) and S100B immunostaining, indicated to characterize both adult and postnatal astrocytes (Diaz-Amarilla et al. 2011; Foo et al. 2011; Raponi et al. 2007; Tripathi et al. 2017).

2.4. Immunocytochemistry

Spinal microglial cells were fixed with freshly prepared 4% (w/v) paraformaldehyde in PBS and a standard immunocytochemistry was performed as previously indicated (Fernandes et al. 2006). Briefly, cells were incubated overnight at 4ºC with the primary antibodies: mouse anti-iNOS (1:100, 610328, BD Biosciences, San Jose, CA, USA), goat anti-arginase 1 (1:50, sc-18355, Santa Cruz Biotechnology®, CA, USA), rabbit anti-NF-κB p65 phospho S536 (1:250, Ab131109, Abcam, Cambridge, UK) and rabbit anti-LC3 (1:200, 2775S, Cell Signaling, Danvers, MA, USA). The secondary antibodies incubated for 2 h at room temperature were anti-mouse FITC (1:227, FI-2001, Vector, Burlingame, CA, USA), goat anti-rabbit Alexa Fluor 488 (A11008) and chicken anti-goat 594 (A21468) (1:1000, Invitrogen Corporation™, Carlsbad, CA, USA). Cell nuclei were stained with Hoechst 33258 dye (blue, Sigma, Saint Louis, MO, USA). Fluorescence was visualized using an AxioCam HR camera adapted to an AxioScope A1® microscope (Zeiss, Germany). Merged images of UV and fluorescence of ten random microscopic fields were acquired per sample by using Zen 2012 (blue edition, Zeiss) software.

2.5. Quantitative RT-PCR

Total RNA was extracted from spinal microglia using TRIzol® Reagent (LifeTechnologies, Carlsbad, CA, USA), as usual in our laboratory (Cunha et al. 2017). Total RNA was quantified using Nanodrop ND-100 Spectrophotometer (NanoDrop Technologies, Wilmington, DE, USA) and conversion to cDNA was performed with SensiFAST™ cDNA synthesis (BIO-65054, BIOLINE, London, UK). Quantitative RT-PCR (qRT-PCR) was performed to evaluate mRNA expression of the genes indicated in Supplementary Table V.1, using β-actin as an endogenous control to normalize gene expression levels. qRT-PCR was performed on a Quantstudio 7 Flex Real Time PCR System (LifeTechnologies) using SensiFAST™ SYBR® (Hi-ROX, BIO-92002/S, BIOLINE). qRT-PCR was performed under optimized conditions: 50°C for 2 min and 95°C also for 2 min, followed by 40 cycles at 95°C for 5 sec and 62°C for 30 sec. In order to verify the specificity of the amplification, a melt-curve analysis was performed, immediately after the amplification protocol. Non-specific products of PCR were not found in any case.

Expression of miRNAs was also performed by qRT-PCR. Here, cDNA conversion was performed with the universal cDNA Synthesis Kit (Exiqon, Vedbaek, Denmark), as described by us (Caldeira et al. 2014), using 5 ng of total RNA according to the following protocol: 60 min at 42°C followed by heat-inactivation of the reverse transcriptase for 5 min at 95°C. For miRNA quantification, the miRCURY LNA™ Universal RT microRNA PCR system (Exiqon) was used in combination with the pre-designed primers (Exiqon) for mmu-miR-155-5p (miR-155, 5'-UUAAUGCUAAUUGUGAUAGGGGU-3'), hsa-miR-124-3p (miR-124, 5'-UAAGGCACGCGGUGAAUGCC-3'), hsa-miR-146a-5p (miR-146a 5'-UGAGAACUGAA UUCCAUGGGUU-3'), hsa-miR-21-5p (miR-21, 5'-UAGCUUAUCAGACUGAUGUUGA-3'), hsa-miR-125b-5p (miR-125b, 5'-UCCCUGAGACCCUAACUUGUGA-3') and SNORD110 (reference gene). The reaction conditions consisted of polymerase activation/denaturation and well-factor determination at 95°C for 10 min, followed by 50 amplification cycles at 95°C for 10 sec and 60°C for 1 min (ramp-rate of 1.6°/s).

In both cases, relative mRNA/miRNA concentrations were calculated using the ΔΔCT equation and results were represented as fold change.

2.6. Western blot

Total protein isolation from organic phases of TRizol-chloroforms from spinal microglia was performed by using TRIzol® Reagent (LifeTechnologies) and protein expression was performed by Western blot analysis as usual in our laboratory (Cunha et al. 2017). Protein extracts were separated on sodium dodecyl sulfate-polyacrilamide gel electrophoresis (SDS-PAGE) and transferred to a nitrocellulose membrane. The membranes were blocked with 5%

non-fat milk in TBS-T (0.1% Tween-20) and incubated overnight at 4ºC with specific primary antibodies: rabbit anti-TLR4 (1:100, sc-10741, Santa Cruz Biotechnology®), mouse anti-beclin (1:100, MABC34, Merck, Darmstadt,Germany) and mouse anti-β-actin (1:5000, A5441, Sigma). Blots were washed and incubated with anti-rabbit (1:5000, sc-2004, Santa Cruz Biotechnology®) or anti-mouse (1:5000, sc-2005, Santa Cruz Biotechnology®) secondary antibodies conjugated with horseradish peroxidase for 1 h at RT. Finally, the chemiluminescent detection was performed after membrane incubation with Western Bright™ Sirius (K-12043-D10, Advansta, Menlo Park, CA, USA). The relative intensities of protein bands were analyzed using the Image Lab™ analysis software, after scanning with ChemiDocXRS, both from Bio-Rad Laboratories (Hercules, CA, USA). Results were normalized to β-actin and expressed as fold change.

2.7. Microglial phagocytosis assay

To evaluate the phagocytic ability of spinal microglia, cells were incubated with 0.0025% (*w/w*) fluorescent latex beads (diameter 1 µm, L1039, Sigma) for 75 min at 37ºC and fixed with freshly prepared 4% (*w/v*) paraformaldehyde in PBS, as previously (Cunha et al. 2017). Nuclei were stained with Hoechst 33258 dye (blue). UV and fluorescence images of ten random microscopic fields (original magnification: 400X) were acquired per sample by using Zen 2012 (blue edition, Zeiss) software. The number of ingested beads per cell were counted using ImageJ software.

2.8. Extracellular HMGB1

In order to study the release of high mobility group box 1 (HMGB1) to the extracellular media, we used HMGB1 Detection Kit (catalog#6010, Gentaur Molecular Products, Kampenhout, Belgium). Briefly, the capture antibody was incubated ON at 4ºC in a 96-well plate. In the following day, after the addition of the detection antibody, the collected supernatant or HMGB1 standard was added to each well. The plate was incubated for 1 h at 37ºC, and afterwards for approximately 20 h at 4ºC. In the following day, the plate was incubated with streptavidin peroxidase for 30 min at RT, followed by TMB for 30 min at RT, and finally the stop solution (2N sulfuric acid) was added to each well. Optical density values were read within 30 min in a microplate absorbance spectrophotometer (PR 2100, BioRad Laboratories, Inc.) at 450 nm (sample) and 630 nm (reference filter).

2.9. Quantification of nitrite levels

Nitric oxide (NO) levels were estimated by assessing the concentration of nitrites (NO_2), the stable end-product from NO metabolism, in culture media by the Griess method, as we

published (Silva et al. 2011). Briefly, extracellular media free from cellular debris were mixed with Griess reagent in 96-well tissue culture plates for 10 min in the dark, at RT. The absorbance at 540 nm was determined using a microplate reader. A calibration curve was used for each assay. All samples were measured in duplicate and the mean value was used.

2.10. Determination of cell death

We used phycoerythrin-conjugated annexin V (annexin V-PE) and 7-amino-actinomycin D (7-AAD; Guava Nexin® Reagent, #4500-0450, Millipore) to determine the percentage of viable, early- apoptotic and late-apoptotic/necrotic cells by flow cytometry. After coculturing with astrocytes, adherent WT and *SOD1*^{G93A} spinal microglia were collected by trypsinization and added to the cells present in the harvested coculture media. After centrifugation cells were resuspended in PBS containing 1% bovine serum albumin (BSA), stained with annexin V-PE and 7-AAD, following manufacturer's instructions, and analyzed on a Guava easyCyte 5HT flow cytometer (GuavaNexin® Software module, Millipore), as previously described (Caldeira et al. 2014). Three populations of cells can be distinguished by this assay: viable cells (annexin V-PE and 7-AAD negative), early apoptotic cells (annexin V-PE positive and 7-AAD negative), and late stages of apoptosis or dead cells (annexin V-PE and 7-AAD positive).

2.11. Statistical analysis

Results were expressed as mean + SEM. Differences between 2 DIV and 16 DIV WT spinal microglia (Table V.1) as well as WT and *SOD1*^{G93A} spinal microglia in each time point were determined by unpaired Student's *t*-test. Welch´s correction was applied when variances where different between groups. Two-way ANOVA followed by Bonferroni's multiple comparisons *post hoc* correction was used to analyze microglia phenotypic populations, beads phagocytosis and microglia-astrocyte coculture experiments. Statistical analysis was performed using GraphPad Prism 5 (GraphPad Software; San Diego, CA, USA). Values of $p < 0.05$ were considered statistically significant.

3. Results

3.1. Spinal microglia isolated from WT mice show downregulated M1/M2 markers and reduced autophagy with long-term in cultures

Senescent microglia show reduced neuroprotective properties during aging in the human brain (Streit et al. 2004; Wong 2013) and a dysfunctional microglia phenotype was reported in the spinal cord of *SOD1*^{G93A} rats at the end-stage (Nikodemova et al. 2014). Before

evaluating dissimilarities between WT and *SOD1*^{G93A} spinal microglia considering short- (2 DIV) and long-term (16 DIV) cultures, we assessed whether the WT spinal microglia behaved differently from the cortical microglia used in previous studies (Caldeira et al. 2014). Here, we used 7-day-old pups, and not 1-day-old animals as in the prior study, to isolate microglia. However, both correspond to the period of late gestation in humans and precede the period of microglia proliferation and ramification (Brites and Fernandes 2015). As indicated in Table V.1, the 16 DIV spinal cord microglia showed decreased levels of M1 markers [CD80 and interleukin (IL)-1β genes], but specially M2 ones [arginase 1 (Arg1), transforming growth factor beta (TGF-β), Cd206 and IL-10 genes]. Data are suggestive that a more senescent-like microglia is obtained with the time in culture, as observed for the cortical microglia and corroborate the existence of non-M1 and non-M2 typical phenotypes (Caldeira et al. 2014).

Recent evidences showed that miRNAs play an important role in the regulation of gene expression at cytoplasmic and nuclear levels, and are believed to constitute promising molecular biomarkers (Catalanotto et al. 2016). Therefore, we decided to investigate a set of 5 inflamma-miRNAs, including miR-155, miR-125, miR-146, miR-21 and miR-124, considered to be associated with microglia polarization, neuroinflammation and ageing (Che et al. 2014; Olivieri et al. 2015; Ponomarev et al. 2013). Although not statistically significant, we have observed almost doubled expression levels for miR-155 (pro-inflammatory/aged-associated), miR-125 (pro-inflammatory) and miR-21 (anti-inflammatory/aged-associated), attesting microglia phenotypic diversity with in vitro culturing.

We further assessed spinal microglia dysfunction by ageing in culture, and we observed that the cells were less able to phagocytose latex beads and showed decreased expression of phagocytic-related proteins such as triggering receptor expressed by myeloid cells 2 (TREM2) and MFG-E8 (Table V.1). Finally, in the same way as cortical microglia (Caldeira et al. 2014), we also observed that beclin-1 expression was reduced in “aged”-spinal microglia (Table V.1), suggesting the existence of compromised autophagy.

The establishment of such findings is important to discriminate whether microglia isolated from the spinal cord of *SOD1*^{G93A} mice and cultivated for 2 and 16 DIV, to be explored in next sections, show additional particular susceptibilities in their function/dysfunction relatively to the WT profile. Data may have relevance when designing of novel medicines targeting features and timing of microglia activation is intended.

Table V.1 - Changes of long-term vs. short-term cultures in wild type (WT) microglia phenotype

Gene/Protein	Fold (16 DIV *vs.* 2 DIV) Mean ± SEM	p values
M1 phenotype		
Nos2	1.4 ± 0.7	0.293
Mhc class II	1.0 ± 0.4	0.459
Cd80	0.6 ± 0.3	0.139
Il-1beta	**0.4 ± 0.1**	**0.003**
M2 phenotype		
Arg1	**0.5 ± 0.1**	**0.001**
Socs1	0.7 ± 0.2	0.059
Cd206	**0.1 ± 0.1**	**0.007**
Tgfb1	**0.6 ± 0.1**	**0.001**
Il-10	**0.3 ± 0.1**	**0.002**
Inflamma-miRs		
mmu-miR-155-5p	1.7 ± 0.7	0.159
hsa-miR-125b-5p	1.8 ± 0.9	0.211
hsa-miR-146a-5p	0.7 ± 0.4	0.233
hsa-miR-21-5p	1.9 ± 1.0	0.196
hsa-miR-124-3p	0.8 ± 0.3	0.209
Phagocytosis/Autophagy		
Number of phagocytic cells	0.4 ± 0.2	0.084
Mfge8	0.6 ± 0.4	0.183
Trem2	**0.3 ± 0.1**	**0.004**
$LC3^+$ cells	1.1 ± 0.6	0.437
Beclin	**0.5 ± 0.2**	**0.042**

Data is expressed as fold change and p values were calculated by Student's *t*-test; bold values highlight statistical significance ($p < 0.05$, n=4-6). DIV, days *in vitro*.

3.2. Short-term (2 DIV) cultured *SOD1^{G93A}* spinal microglia show increased M1/M2b polarization but a depressed inflammatory status when cultured for 16 DIV

Contradictory reports on microglia phenotypic heterogeneity along ALS disease course may arise from the reduced spectrum of markers that have been used. Some screening studies identified a degenerative specific phenotype at the mSOD1 mice end-stage (Chiu et al. 2013), and others different stages of reactive microglia (Ohgomori et al. 2016). Therefore, we decided to characterize the expression of several well-known phenotypic markers of M1/M2 microglial polarization (Brites and Vaz 2014; Chhor et al. 2013; Crain et al. 2013), after confirming that the *SOD1^{G93A}* spinal microglia cultured for both 2 and 16 DIV

overexpressed SOD1 (Supplementary Figure V.1). We have observed that *SOD1*^{G93A} spinal microglia cultured for only 2 DIV had increased expression of *Cd80/Nos2* (M1-markers) and *Mhc class II* (M1/M2b-marker), but reduced levels of *Cebpa* (M1/M2b marker), *Arg1* (M2a/M2c marker) and *Il-10* (M2 marker), when compared to correspondent WT microglia (Figure V.1A). Data suggest that microglia in short-term cultures show a prevalent inflammatory phenotype, although not expressing all the markers of the M1 classical activated microglia. In addition, the decrease of *Socs1*, manifested by the 2 DIV mutated microglia, further favor the pro-inflammatory phenotype of the cell, since it will not be able to provide inhibition of inflammatory signaling pathways (Cai et al. 2016; Cianciulli et al. 2017; Whyte et al. 2011). If maintained *in vitro* for 16 DIV, *SOD1*^{G93A} spinal microglia lose or even suppress the M1 and M2b phenotypic markers, while match the M2a/M2c-like phenotypes of the controls, apart from *Tgfb1*.

To better explore differences between WT and *SOD1*^{G93A} spinal cord microglia and the influence of culturing, we assessed distribution patterns of NOS2 and Arg1 using double immunostaining (Figure V.1B). Clearly, striking differences were observed in the increased proportion of Arg1^{low}/NOS2^{high} cells in *SOD1*^{G93A} spinal cord microglia cultured for both 2 and 16 DIV (48 and 36%, respectively). Also interesting was the significant reduction in the number of Arg1^{high}/NOS2^{low} microglia in *SOD1*^{G93A} 2 DIV cultures (from 39% in the WT to 9% in the mutated cells). Altogether, pro-inflammatory/anti-inflammatory microglia subsets coexist and the Arg1^{low}/NOS2^{high} profile is a characteristic feature of *SOD1*^{G93A} spinal microglia, independently of the age in culture. In addition, aging should be envisaged as a potential inducer of microglial Arg1^{low}/NOS2^{low} subclasses in both WT (60% vs. 40%) and mutated (46% *vs.* 28%) cells, supporting sets of senescent cells in long-term cultures.

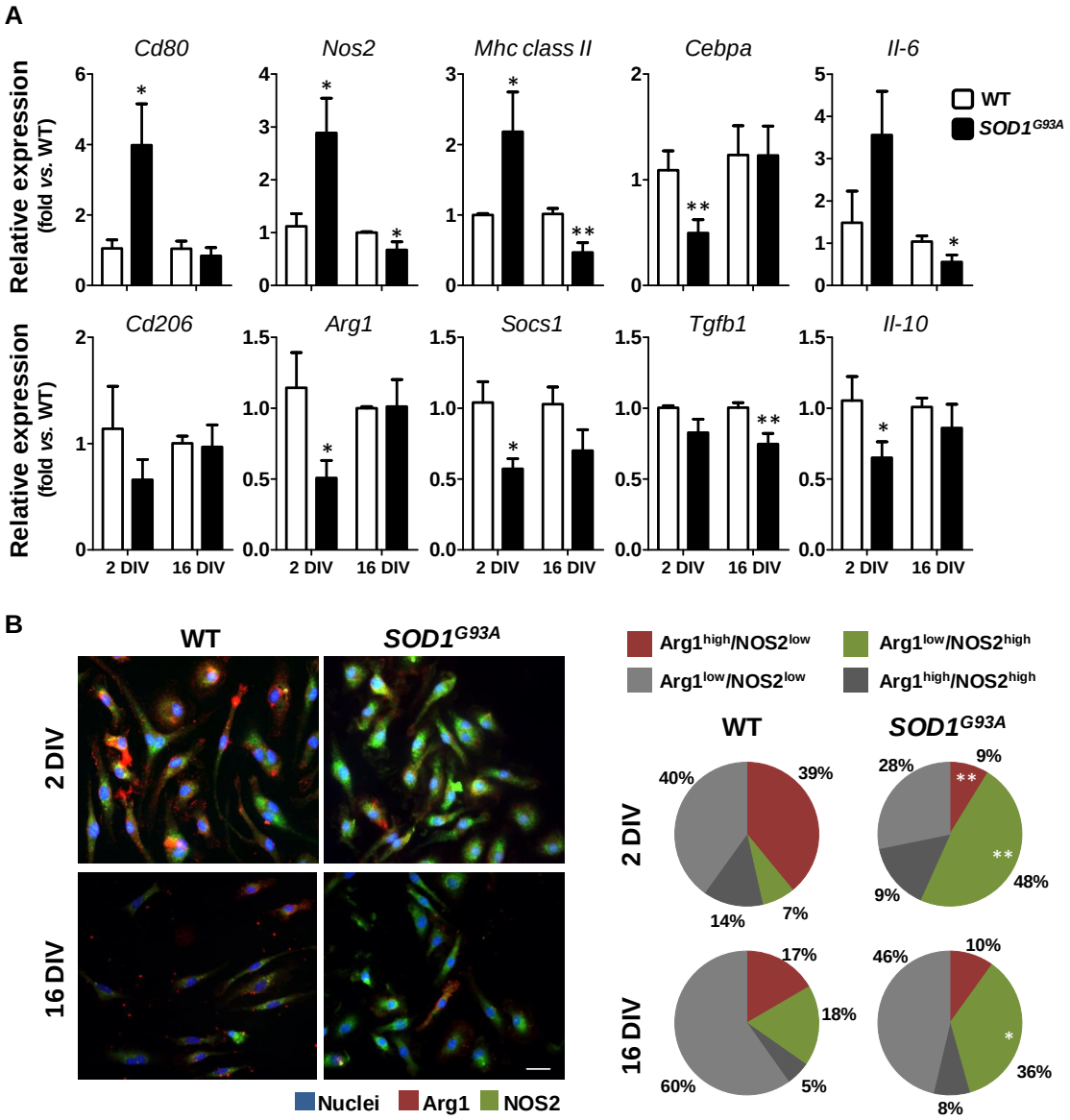

Figure V.1 - 2 DIV *SOD1*^{G93A} spinal microglia acquire a predominant M1/M2b-polarization that switch into a deactivated phenotype at 16 DIV. (A) Markers for M1 (*Cd80*, *Nos2* and *Mhc class II*), M2b (*Mhc class II*, *Cebpa, IL-6*, *Socs1,* and *Il-10*), M2a (*Cd206*, *Arg1*, *Socs1, Tgfb1* and *IL-10*) and M2c (*Arg1*, *Tgfb1, Socs1* and *Il-10*) microglia phenotypes were evaluated by qRT-PCR. (B) Representative images of double immunostaining against NOS2 (green) and Arg1 (red) show the coexistence of different microglia subpopulations. Nuclei were counterstained with Hoechst dye (blue). Scale bar represents 20 µm. Pie charts represent the percentage of each microglia subpopulation as follows: Arg^{high}/NOS2^{low} (red), Arg^{low}/NOS2^{high} (green), Arg^{low}/NOS2I^{ow} (light grey) and Arg^{high}/NOS2^{high} (dark grey). Results are expressed as mean + SEM. (*p < 0.05 and **p < 0.01 vs. respective wild type (WT), n = 4-8, unpaired Student's *t*-test (A) and two-way ANOVA followed by Bonferroni's *post hoc* test (B)).

3.3. *SOD1*^{G93A} spinal microglia show a sustained decreased phagocytic function and enhanced autophagy when aged in culture

The clearance of neuronal debris by microglia enables the restoration of CNS homeostasis after injury, and though deficits in microglia phagocytosis in neurodegenerative diseases have been addressed by different studies (reviewed in (Fu et al. 2014)), little is

known in ALS. It is also becoming increasingly clear that a return to homeostasis after activation of immune signaling cascades critically depends on autophagy (Cadwell 2016). Considering the coexistence of multiple phenotypes, but also their different distribution accordingly to short- or long-term cultures, we next evaluated whether phagocytosis and autophagy were diversely altered in 2 DIV and 16 DIV *SOD1*^{G93A} spinal microglia.

As shown in Figure V.2A, 2 DIV *SOD1*^{G93A} spinal microglia showed a reduced capacity to engulf latex beads, with a marked decrease in the number of cells able to phagocytose more than 11 beads (41% vs. 67% in WT cells), thus consequently increasing the number of cells with only 1-6 beads (25% vs. 7% in WT cells). As in our prior studies, aging of the cells led to a high amount of them not engulfing any bead with a percentage of 61% in WT cells that increased to 79% in 16 DIV *SOD1*^{G93A} spinal microglia. This result thus reinforces the loss of function in senescent-microglia and highlights such failure in the mutated cells. Removal of apoptotic cells by microglia is mediated by MFG-E8 that recognizes PS at the surface of injured neurons and also by TREM2. Our results showed that *Mfge8* (Figure V.2B) was markedly downregulated in 2 DIV *SOD1*^{G93A} spinal microglia and even more after 16 DIV, indicating that *Mfge8*-mediated microglia phagocytosis is deficient in the ALS mice. Corroborating that microglia in the ALS mice may coexpress potentially toxic and neuroprotective factors (Chiu et al. 2013), we did not find alterations in *Trem2* expression that showed equivalent levels in both 2 and 16 DIV *SOD1*^{G93A} spinal microglia.

Now considering microglial autophagy, while no changes were observed for 2 DIV cells considering LC3-positive punctate cells, or the autophagy-related gene beclin-1 (Supplementary Figure 2), punctate LC3 stains increased in 16 DIV *SOD1*^{G93A} spinal microglia. Upregulation of LC3, which is frequently used as a marker of macroautophagy, was indeed shown to increase by aging (Carroll et al. 2013) and found enhanced in spinal cord MNs of SOD1 mutant mice at 3 months-old (Li et al. 2008). Recently, it was shown that autophagy can be induced or repressed by immune mediators (Cadwell 2016) and that miRNA may regulate inflammatory response and autophagy in microglia (Su et al. 2016). Indeed, miR-155, whose expression is usually associated to inflammation (Su et al. 2016), was also identified as an inducer of autophagy in monocytes (Wu et al. 2016a). Therefore, we next assessed a set of miRNAs known to be critical in microglia-immune response (Guedes et al. 2013) and to be deregulated in ALS (Parisi et al. 2013).

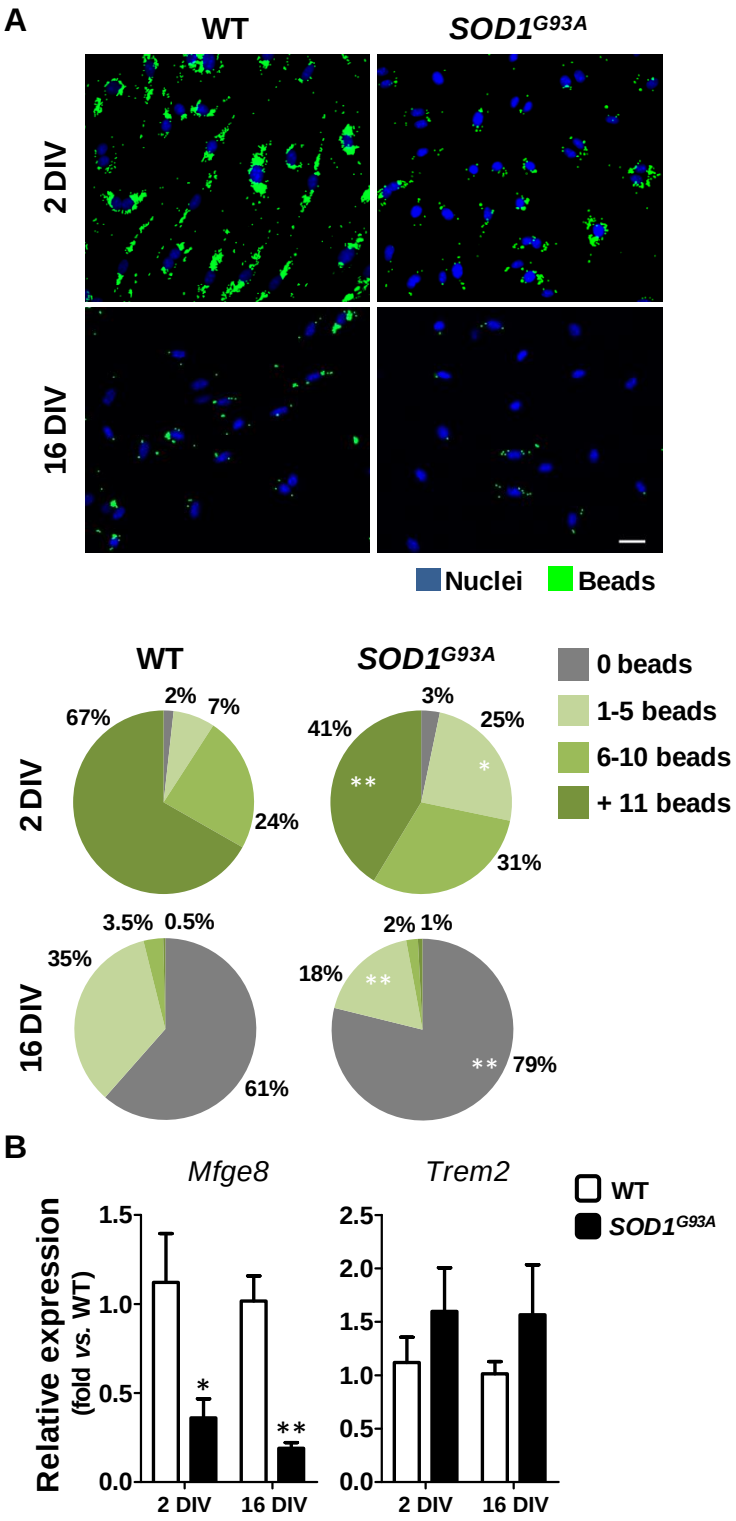

Figure V.2 – Reduced phagocytic capacity of primary microglia with time in culture is increasingly diminished in *SOD1*^{G93A} spinal cells, and further aggravated by lower *Mfge8* levels. (A) Representative images of engulfed latex beads (in green) showing that the high phagocytic capacity of wild type (WT) spinal microglia is lost in long-term cultures, and that *SOD1*^{G93A} spinal microglia have an increased impaired clearance. Nuclei were counterstained with Hoechst dye (blue). Scale bar represents 20 µm. Pie charts represent the percentage of cells that phagocytosed a specific number of beads as follows: 0 beads (grey), 1-5 beads (greyish green), 6-10 beads (light green) and more than 11 beads (green). (B) *Mfg-e8* and *Trem2* expression was evaluated by RT-PCR. Whereas *Mfg-e8* decreased by age and *SOD1*^{G93} mutation, *Trem2* levels did not change. Results are expressed as mean + SEM (*p < 0.05 and **p < 0.01 vs. respective WT, n=4-7, two-way ANOVA followed by Bonferroni's *post hoc* test (A) and unpaired Student's *t*-test (B)).

3.4. 2 DIV *SOD1^{G93A}* spinal microglia showing miR-155^{high}/-124^{low} and activation of inflammatory signaling pathways give way to deactivated 16 DIV *SOD1^{G93A}* cells with upregulated inflamma-miRs

Different inflamma-miRs regulate microglia responses in normal and neurodegenerative conditions, as previously noted. Usually, it is considered that miR-155 and miR-125b augment inflammation, while miR-146a, miR-21 and miR-124 act as negative regulators and promote neuroprotective responses, although there is some controversy. Our data showed that miR-155 was upregulated in *SOD1^{G93A}* spinal microglia cultured for 2 DIV together with miR-124 downregulation (Figure V.3), a profile that is typical of M1-activated microglia (Freilich et al. 2013). Interestingly, after 16 DIV in culture, all of the assessed miRNAs, excluding miR-21 were upregulated. This miR-21 was shown to protect against microglia-mediated neuronal death (Zhang et al. 2012b). The co-induction of miR-155, miR-125b, miR-146a and miR-124 in the 16 DIV *SOD1^{G93A}* spinal microglia may be associated with conditions favoring motor neuron death and the existence of a dual profile composed by M2 and dormant/senescent states (Butovsky et al. 2015; Olivieri et al. 2015; Parisi et al. 2016; Yu et al. 2017).

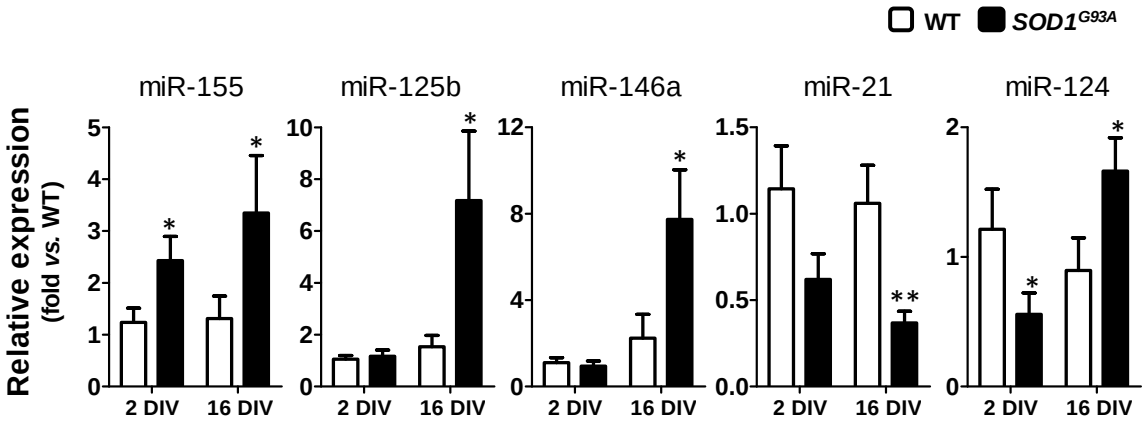

Figure V.3 – Profiling of inflammatory-associated microRNAs (inflamma-miRs) shows that 2 DIV *SOD1^{G93A}* spinal microglia acquire a prominent M1-associated miR-155^{high}/-124^{low} phenotype, while the correspondent 16 DIV cells exhibit a set of upregulated inflamma-miRs that characterize the existence of M1/M2 mixed subtypes. The expression of miR-155, miR-125b, miR-146a, miR-21 and miR-124 were assessed by qRT-PCR. Results are expressed as mean + SEM (*p < 0.05 and **p < 0.01 vs. respective wild type (WT), n = 6-7, unpaired Student's *t*-test).

To deeply understand the pro-/anti-inflammatory properties of the *SOD1^{G93A}* spinal microglia by short-term and long-term culturing, we next assessed the activation of inflammatory signaling cascades. As depicted in Figure V.4, elevation of TLR4, phosphorylated NF-κB, *Il-1beta* and NO release was noticed in 2 DIV mutated cells, attesting their activated state (Yao et al. 2013). In contrast, both TLR4 and *Il-1beta* were downregulated in 16 DIV cells, sustaining that these cells are less able to mount an

inflammatory response. How far this model reproduces the late stages of ALS is to be assessed in future studies. In contrast with other neurodegenerative diseases revealing microglial NOD-like receptor pyrin domain containing 3 (NLRP3)-inflammasome activation and IL-18 (for review see (Wang et al. 2015a)), in our ALS model such findings were not reproduced in either 2 or 16 DIV cultured microglia. Therefore, we may hypothesize that the increased *Nlrp3* in the absence of *Il-18* in the SC of *SOD1*^{G93A} mice at the symptomatic stage (Cunha et al. 2017), may derive from astrocyte influence. Reduced levels of released HMGB1 by the mutated microglia point out that the elevated intracellular HMGB1 we found in the symptomatic *SOD1*^{G93A} mice (Cunha et al. 2017) should have derived from reactive ALS astrogliosis (Li et al. 2014) and/or neuronal demise (Faraco et al. 2007). Nevertheless, the decrease here observed may also derive from an increased HMGB1 degradation by the *SOD1*^{G93A} spinal microglia, as observed in other conditions (Liu et al. 2016a; Yeo et al. 2016), or retention at the nucleus as in the SC of ALS patients (Lo Coco et al. 2007).

3.5. *SOD1*^{G93A} spinal neonatal astrocytes increasingly favor M1/M2b phenotype of *SOD1*^{G93A} spinal microglia

Recently it was demonstrated that classically activated neuroinflammatory microglia induce the formation of neurotoxic reactive astrocytes termed as A1 (Liddelow et al. 2017). On the other hand ALS astrocytes showed an aberrant reactive profile (Diaz-Amarilla et al. 2011) and revealed to strongly promote the death of motor neurons (Haidet-Phillips et al. 2011; Meyer et al. 2014). Such dysfunctional astrocytes isolated from the spinal cord cultures of symptomatic rats have shown proliferative capacity and a characteristic profile represented by GFAP^{low}, connexin-43^{high}, S100B^{high} and (GLT1)^{low} (Diaz-Amarilla et al. 2011), although not definitively characterized as A1 astrocytes. We anticipated that such dysfunctional astrocytes, besides being influenced by activated microglia, could also have a role in promoting microglia activated phenotypes. Actually, not much is known about the influence of astrocytes on microglia polarization and even less on their influence over microglia activation and pro-inflammatory phenotype in ALS.

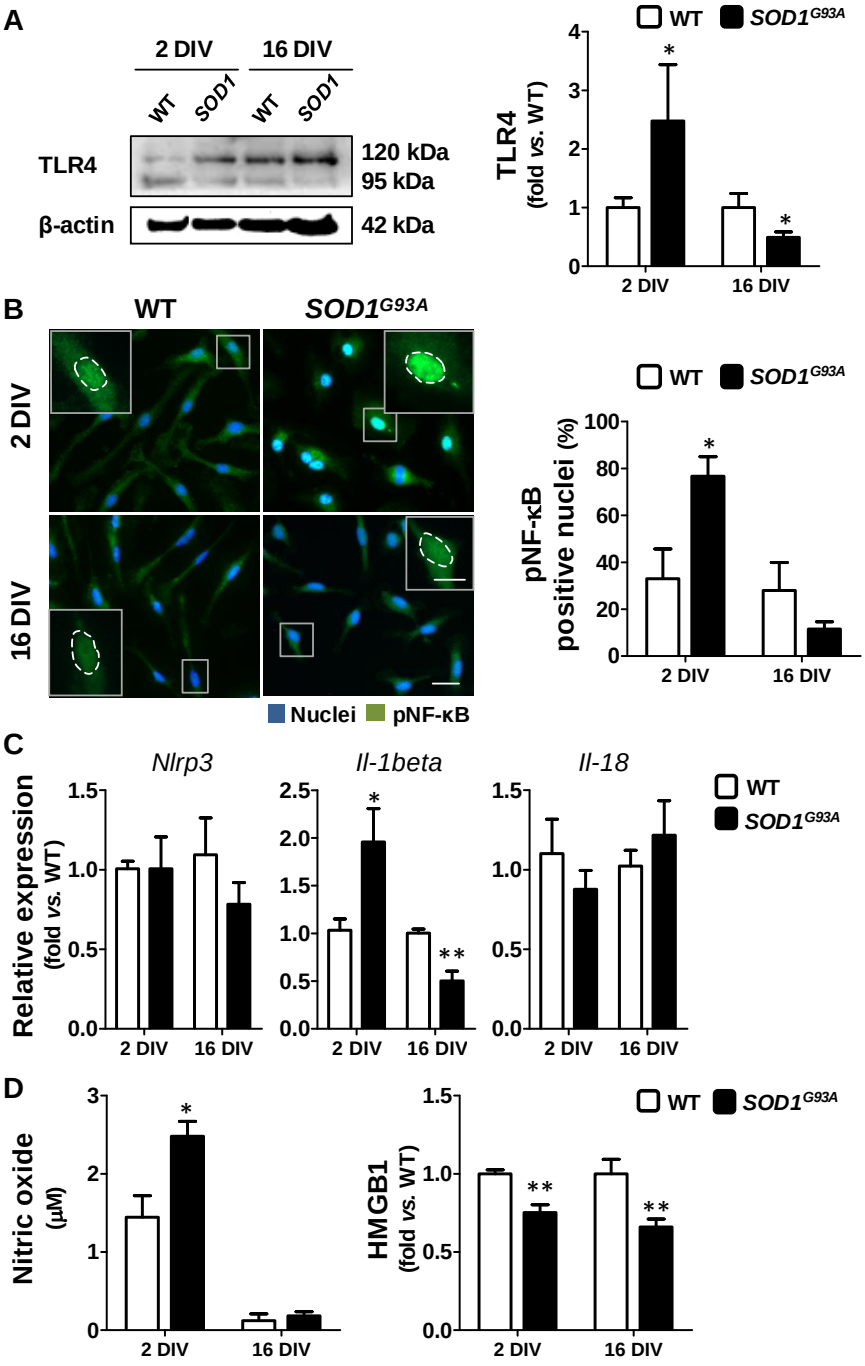

Figure V.4 – Upregulated TLR4/NF-κB/*Il-1beta* signaling in 2 DIV *SOD1*^{G93A} spinal microglia is depressed 16 DIV *SOD1*^{G93A} cells, while downregulated HMGB1 is observed in both. (A) TLR4 expression was assessed by Western Blot and show opposite profiles with the time in culture. Representative images of glycosylated (120 kDa) and non-glycosylated (95 kDa) forms of TLR4. (B) Representative images of NF-κB phospho S356 (pNF-κB) expression assessed by immunocytochemistry (in green). Nuclei were counterstained with Hoechst dye (blue). Scale bar represents 20 μm and 10 μm in close-up insets. Dashed line indicates the nucleus. The percentage of pNF-κB positive nucleus were quantified and indicates that NF-κB pathway is activated in 75% of 2 DIV *SOD1*^{G93A} cells that disappears in 16 DIV cells. (C) The inflammasome components *Nlrp3*, *Il-1beta* and *Il-18* were evaluated by qRT-PCR. Only Il-1beta levels differed in *SOD1*^{G93A} cells with a profile similar to TLR4/pNF-κB. (D) Nitric oxide release was assessed by detection of nitrite levels in the supernatant using Griess Reagent. Increased values at 2 DIV *SOD1*^{G93A} spinal microglia further corroborate their preferential M1 polarization. HMGB1 was measured in the supernatant by ELISA showing that HMGB1 release is decreased in both 2 and 16 DIV *SOD1*^{G93A} spinal microglia. Results are expressed as mean + SEM (*$p < 0.05$ and **$p < 0.01$ vs. respective wild type (WT), n=4-7, unpaired Student's *t*-test).

We then decided to study the effect of the secretome released by 2 DIV-cultured WT and *SOD1*^{G93A} spinal astrocytes in the phenotype of 2 DIV-cultured microglia, either WT or *SOD1*^{G93A}, using cocultures. Based on the previous results we choose to only assess such alterations in cells from short-term cultures due to the prevailing pro-inflammatory state found for *SOD1*^{G93A} microglia in such condition, which was shown to characterize the symptomatic inflammatory stage (Cunha et al. 2017). For that we initially confirmed that the mutated astrocytes exhibited a profile compatible with the reactive astrocyte phenotype, as described (Diaz-Amarilla et al. 2011). We observed that *SOD1*^{G93A} astrocytes isolated from the spinal cord had increased levels of SOD1 concomitantly with a reduction in GFAP (Supplementary Figure V.3). These SOD1^{high}/GFAP^{low} astrocytes also showed increased immunostaining of S100B in the cytoplasm, enhanced Ki-67 in the nucleus and reduced cellular GLT-1, corroborating their reactive, proliferative and aberrant phenotype.

We first noticed that WT astrocytes and *SOD1*^{G93A} astrocytes did not determine any significant alteration on the WT microglia (Figure V.5A). We next observed that WT spinal astrocytes induced protective anti-inflammatory properties on 2 DIV *SOD1*^{G93A} spinal microglia by promoting *Socs1* and *Tgfb1*, which were shown to reduce microglia activation (Cai et al. 2016; Taylor et al. 2017). In opposite, *SOD1*^{G93A} spinal astrocytes promoted the upregulation of *Nos2*, *Mhc class II*, *Il-6* and *Il-10*, as well as downregulation of *Cebpa* in *SOD1*^{G93A} spinal microglia, thus increasing the proportion of pro-inflammatory M1/M2b subclasses in the mutated microglia.

Interestingly, in all coculture pairs, we observed that microglia acquire a less reactive state (Arg1^{low}/NOS2^{low}), especially in the WT coculture (Figure V.5B, C). Moreover, and in accordance with the gene expression data, increased pro-inflammatory Arg1^{low}/NOS2^{high} profile (from 22% to 40%) was observed in the *SOD1*^{G93A} spinal microglia after stimulation by reactive mutant astrocytes. Such astrocytes also induced pro-inflammatory properties in WT spinal microglia, as indicated by the increase in miR-155, miR-125b and miR-21, reinforcing their reactive phenotype (Figure V.6). *SOD1*^{G93A} astrocytes also induced the upregulation of miR-125b, miR-21 and miR-124 expression in the *SOD1*^{G93A} microglia, thus originating the formation of a heterogeneous population of cells. Interestingly, elevation of miR-125b and miR-21 seems to be a specific feature induced by the mutated astrocytes in either WT or *SOD1*^{G93A} microglia, and those miRNAs were already suggested to be associated to neurodegeneration and microglial activation (Harrison et al. 2016; Parisi et al. 2016; Yelamanchili et al. 2015). To finally note that whereas no differences in miR-146a were observed in any case, the increased expression of *SOD1*^{G93A} spinal microglia miR-124, although considered neuroprotective (Huang et al. 2017), was also shown to reduce microglia motility and phagocytic capacity (Svahn et al. 2016).

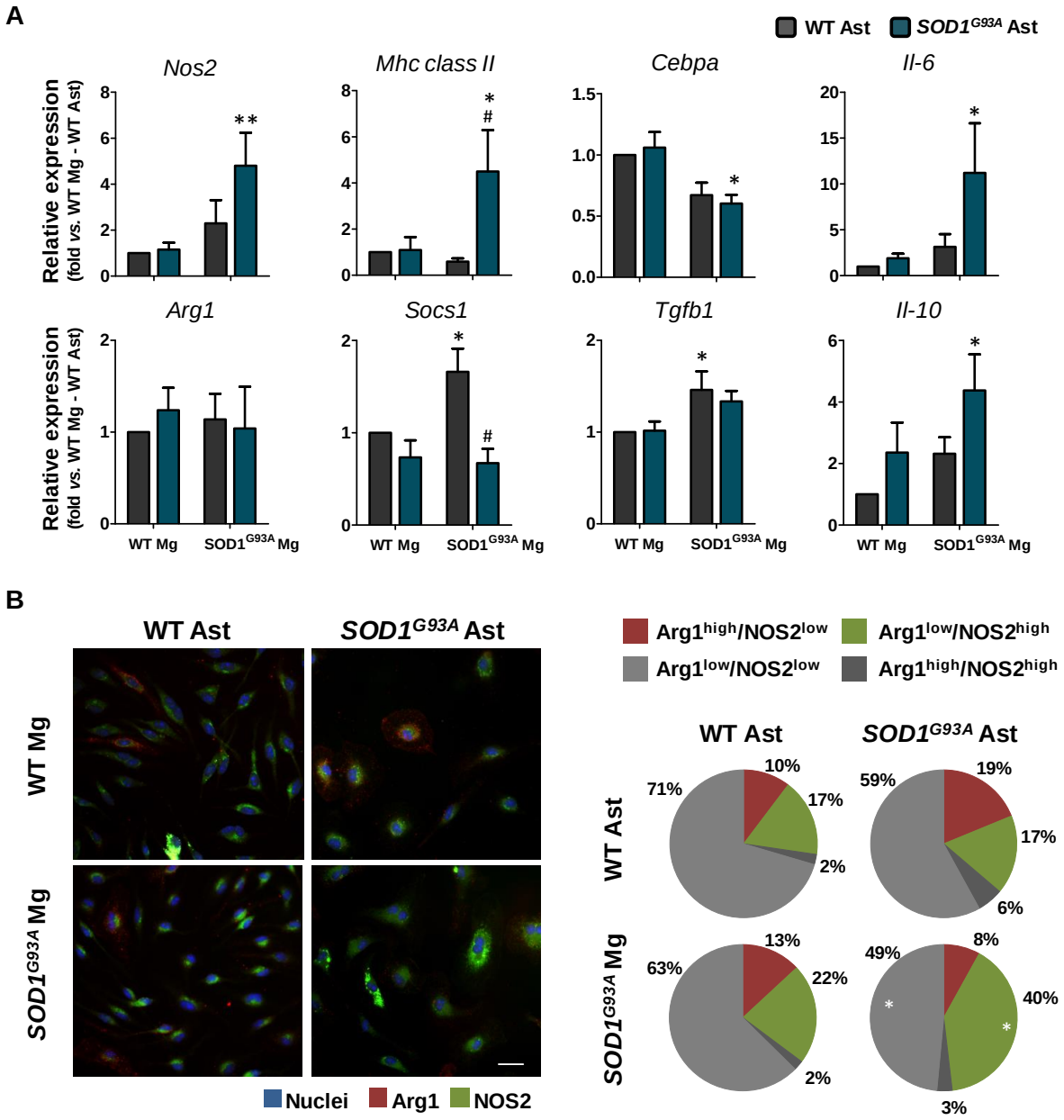

Figure V.5 – Wild type (WT) spinal astrocytes show benefits in increasing the anti-inflammatory status of *SOD1^{G93A}* microglia, whereas *SOD1^{G93A}* astrocytes exacerbate the M1/M2b-polarization of those cells. A) Markers for M1 (*Cd80*, *Nos2* and *Mhc class II*), M2b (*Mhc class II*, *Cebpa, IL-6, Socs1* and *Il-10*), M2a (*Cd206*, *Arg1*, *Socs1, Tgfb1* and *IL-10*) and M2c (*Arg1*, *Tgfb1, Socs1* and *Il-10*) microglia phenotypes were evaluated by qRT-PCR. (B) Representative images of double immunostaining against NOS2 (green) and Arg1 (red). Nuclei were counterstained with Hoechst dye (blue). Scale bar represents 20 µm. Pie charts represent the percentage of each microglia subpopulation as follows: Arg^{high}/NOS2^{low} (red), Arg^{low}/NOS2^{high} (green), Arg^{low}/NOS2l^{ow} (light grey) and Arg^{high}/NOS2^{high} (dark grey). Results are expressed as mean + SEM. (*p < 0.05 and **p < 0.01 vs. WT coculture, $^{\#}$p<0.05 vs. *SOD1^{G93A}* microglia – WT astrocytes coculture, n=8-9, two-way ANOVA followed by Bonferroni's *post hoc* test). Mg, microglia; Ast, astrocyte.

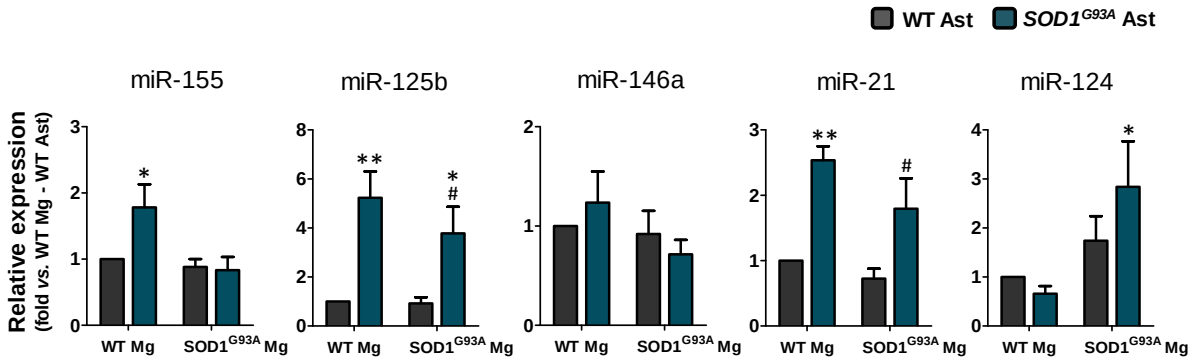

Figure V.6 – Profiling of inflammatory-associated microRNAs (inflamma-miRs) shows that reactive *SOD1^{G93A}* spinal astrocytes induce a set of inflamma-miRs-associated to microglia activation in the wild type (M1) and mutated cells (M1/M2). The expression of the inflamma-miRs miR-155, miR-125b, miR-146a, miR-21 and miR-124 were evaluated by qRT-PCR. Results are expressed as mean +SEM (*p < 0.05 and **p < 0.01 vs. WT coculture, $^{\#}$p<0.05 vs. *SOD1^{G93A}* microglia – WT astrocytes coculture, n = 7-8, two-way ANOVA followed by Bonferroni's *post hoc* test). Mg, microglia; Ast, astrocyte.

3.6. Upregulation of *Nlrp3-inflammasome* and of *Cx43/Panx1* hemichannels, as well as release of HMGB1 requires *SOD1^{G93A}* astrocytes-microglia interplay

Deregulated cell-to-cell signaling mechanisms were shown to play a crucial role in several neurodegenerative diseases, including ALS (Brites and Vaz 2014). M1 activated microglia were shown to induce astrocyte necroptosis by activating TLR4/MyD88 signaling (Fan et al. 2016) and to promote neurotoxic, reactive A1 astrocyte formation mediated by IL-1α and TNF-β (Liddelow et al. 2017). Therefore, we initially investigated the effect of WT and mutated microglia on the expression of S100B and the hemichannels Connexin-43 (Cx43) and Pannexin-1 (Panx1) that are related with astrocyte reactivity and intercellular communication. Our results showed that augmented levels of *S100b* and *Panx1* occur in *SOD1^{G93A}* spinal astrocytes after coculturing with transgenic microglia, but we couldn't notice any effect on the WT astrocytes (Figure V.7). Increased *Panx1* gene expression was previously observed by us in the SC of *SOD1^{G93A}* mice at the symptomatic stage (Cunha et al. 2017). We also noticed that WT astrocytes determine the decrease of *S100b* and increase of *Panx1* gene expression in the *SOD1^{G93A}* spinal microglia. Such type of influence of astrocytes on microglia activation is only scarcely investigated and it is not clarified how astrocyte release of pro-inflammatory signals may activate or damage microglia. Notably, our results indicate that mutated astrocytes are able to determine a loss in the viability of WT spinal microglia, by increasing the percentage of late apoptotic/necrotic cells, thus emphasizing their harmful effects on microglia (Supplementary Figure V.4).

Since *Nlrp3-inflammasome* expression is not induced in *SOD1^{G93A}* spinal microglia, despite their pro-inflammatory status, we questioned whether an astrocyte-dependent second signal would generate its activation (Walsh et al. 2014). In this context, we found that

Nlrp3 expression was upregulated in *SOD1*^{G93A} spinal microglia exposed to *SOD1*^{G93A} spinal astrocytes (Figure V.8A). Cross-talk was also shown to be required for the overexpression of *Il-18* in the mutated astrocytes upon incubation with *SOD1*^{G93A} microglia. In contrast, the upregulation of *Il-18* in mutated microglia only occurred by the influence of WT astrocytes, as observed for *Panx1. SOD1*^{G93A} spinal astrocytes revealed to similarly trigger elevation of *Il-1beta* expression and NO levels in the WT microglia (Figure V.8B, C), supporting the activation of inflamma-miRs previously observed. Probably related with the NLP3-inflammasome activation in the *SOD1*^{G93A} microglia when cocultured with the mutated astrocytes, the release of HMGB1 was only noticed in the supernatants of mutated astrocytes and microglia cocultures, and may relate with microglia pathogenicity. Taken together, our data indicate that microglia-astrocyte cross-talk is essential for the activation of specific pathways identified to be linked to motor neuron degeneration.

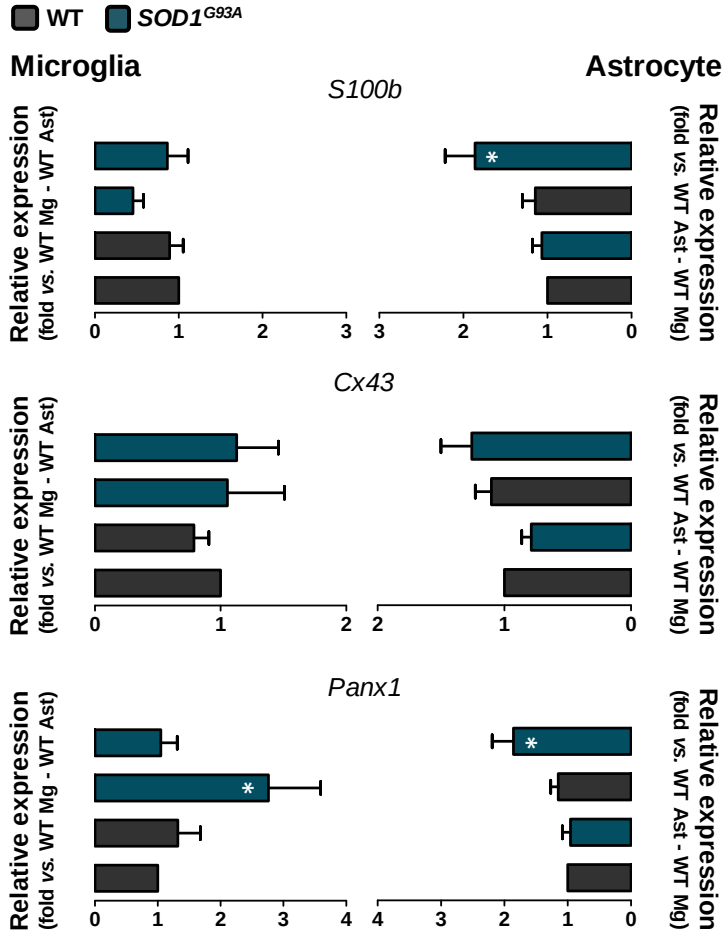

Figure V.7 – *SOD1*^{G93A} spinal microglia determine *S100b* and *Panx1* upregulation in paired mutated astrocytes. *S100b*, *Cx43* and *Panx1* expression was assessed in microglia and astrocytes, after coculturing, by qRT-PCR. *S100b* and *Panx1* are the molecules more influenced by the microglia-astrocyte communication in the mutated cells. Results are expressed as mean+ SEM (*p < 0.05 vs. WT coculture, n=6-9, two-way ANOVA followed by Bonferroni's *post hoc* test). Mg, microglia; Ast, astrocyte.

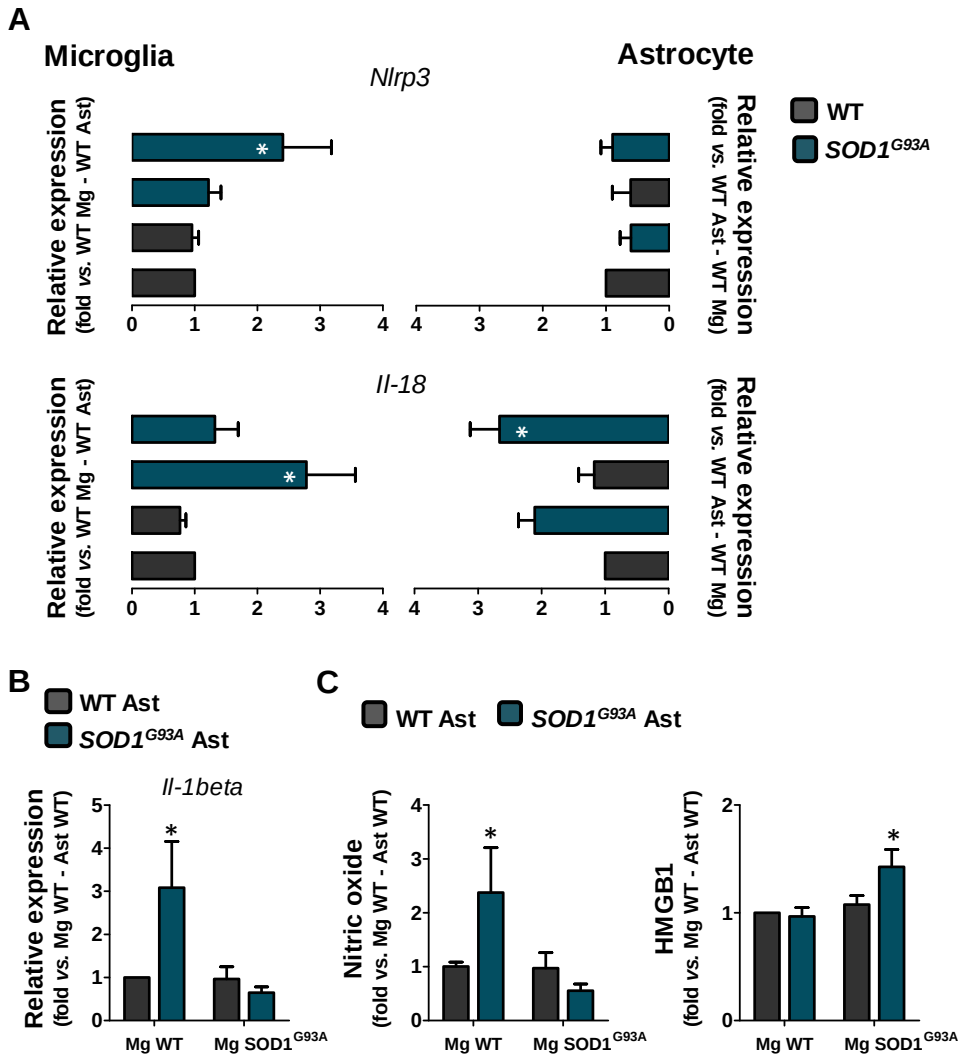

Figure V.8 – *SOD1*^{G93A} spinal astrocytes activate *IL-1beta*/NO signaling pathways in wild type (WT) microglia, while upregulate *NLRP3-inflammasome* expression and HMGB1 release in paired mutated microglia. (A) *Nlrp3-inflammasome* and *Il-18* expression was assessed in both microglia and astrocytes, after coculturing, by qRT-PCR. *Nlrp3-inflammasome* expression is induced in microglia and *Il-18* in astrocytes in paired *SOD1*^{G93A} cocultures. *Il-18* is also upregulated in *SOD1*^{G93A} spinal microglia stimulated by WT astrocytes. (B) *Il-1beta* expression evaluated by qRT-PCR is increased in WT microglia upon incubation with *SOD1*^{G93A} astrocytes. (C) Nitric oxide was assessed by detection of nitrite levels in the supernatant using Griess Reagent, and follows the same profile of *Il1beta*. HMGB1 was measured in the supernatant by ELISA and shows to increase in paired *SOD1*^{G93A} astrocytes-microglia. Results are expressed as mean+ SEM (*p < 0.05 vs. WT coculture, n=6-9, two-way ANOVA followed by Bonferroni's *post hoc* test). Mg, microglia; Ast, astrocyte.

4. Discussion

Ever since targeting mSOD1 in microglia and replacement of resident microglia by WT microglia or WT myeloid cells were shown to slow disease progression in transgenic ALS rodent models (Beers et al. 2006; Boillée et al. 2006b; Lee et al. 2012a), microglia emerged to the core of ALS pathogenesis. Recent studies conducting inhibition of NF-κB or miR-155 have started to disclose some of the mechanisms by which microglia cause motor neuron

death (Butovsky et al. 2015; Frakes et al. 2014). Once modulation in these studies occurred before or at the onset, is still unknown whether they would also be effective later over disease progression, better translating to the window of action in patients, specially the sporadic cases. In fact, an important aspect of ALS pathoprogression relies in the diversity of responses experienced by microglia during disease course (Chiu et al. 2013; Cunha et al. 2017; Liao et al. 2012; Nikodemova et al. 2014). In the present study, we showed that *SOD1*^{G93A} spinal microglia acquire diverse phenotypes over time in culture, transitioning from a pro-inflammatory to a dysfunctional state, and also that communication with astrocytes is essential for the activation of pathways associated with motor neuron degeneration in ALS.

Given that we recently settle an *in vitro* model of cortical microglia aging in culture (Caldeira et al. 2014), that microglia aging dysfunction is region-dependent (Grabert et al. 2016) and that cortical and spinal microglia seem to behave differently in ALS (Nikodemova et al. 2014), we first evaluate if WT spinal microglia also presented senescence-related features with time in culture. Indeed, we observed that 16 DIV WT spinal microglia face downregulation of common M1/M2 activation markers, inflamma-miRs deregulation and compromised autophagy and phagocytic ability. Although conflicting reports indicate that aged microglia became less responsive to stimulation while others endorse an exacerbation of pro-inflammatory responses due to a low-grade inflammatory status, called inflamm-aging, the impairment of phagocytosis and motility are consensual in aged microglia (Koellhoffer et al. 2017; Rawji et al. 2016) as well as the acquisition of dystrophic morphology (Streit et al. 2004). Despite no direct evidence linking microglia aging with autophagy impairment, deficits in autophagy have been associated with aging in the CNS (Plaza-Zabala et al. 2017) and, as recently showed, macrophages present aging-associated features due to lack of autophagy capacity (Stranks et al. 2015). Linked to inflamm-aging, recent data indicate that miR-155, miR-146a and miR-21 are associated with DNA damage response-induced senescence that is observed under neurodegenerative conditions (Olivieri et al. 2015). Whereas miR-155 may inhibit or promote senescence depending on the specific gene expression program (Olivieri et al. 2015), miR-146a is upregulated in aged mice promoting macrophage dysfunction (Jiang et al. 2012) and miR-21 overexpression induced growth arrest and senescence in human endothelial cells (Dellago et al. 2013).

Having established that WT spinal microglia presented a dysfunctional/irresponsive behavior with time in culture, we focused on the phenotype alterations faced by *SOD1*^{G93A} spinal microglia. Microglia activation and proliferation is observed at pre-clinical stages in the spinal cord of mSOD1 rodent models (Graber et al. 2010), suggesting that microglia-mediated motor neuron injury could start early in the degenerative process. However, targeting microglia in ALS mice showed a slow course post-symptoms but no effect in the onset of the disease (Beers et al. 2006; Boillée et al. 2006b). Interestingly, it was recently

reported that before disease onset, microglia upregulate IL-10, encompassing reduced innate immune responses (Gravel et al. 2016), and several genes involved in microglia functionality are downregulated (Cunha et al. 2017), both referred as protective mechanisms attempting to prevent disease initiation. In addition, the M2-markers Ym1 and CD206 were found increased in the SC of *SOD1*^{G93A} mice at the onset and slowly progressing phase with isolated microglia inducing motor neuron protection *in vitro*, whereas at the end-stage the downregulation of these markers and upregulation of NOX2 represents a neurotoxic M1-polarized microglia (Liao et al. 2012). Our recent data additionally demonstrates that *SOD1*^{G93A} spinal microglia acquire pro-inflammatory properties earlier in the symptomatic phase, pointed by NF-κB activation and upregulation of CD80, MHC-II, IL-6, IL-1β and TNF-α, suggesting that the transition of M2-to-M1 phenotype may occur even faster (Cunha et al. 2017). Intriguingly, two recent studies showed that microglia acquire specific signatures along ALS progression. Nikodemova and colleagues (2014) showed that at the onset, neither M1 nor M2 phenotype markers change in microglia. At the end-stage, however, microglia acquire an atypical phenotype characterized by upregulation of VEGF, galectin3 and osteopontin and downregulation of M1/M2 markers that is associated with severe motor neuron degeneration. Interestingly, the authors showed that this phenotype does not respond to lipopolysaccharide (LPS) indicating its irresponsive state. An ALS-specific phenotype was also reported differing form M1 and M2 polarization states and also from LPS-stimulated microglia (Chiu et al. 2013). Taken together, our data could replicate some of the transition phenotypes of microglia as the reactive 2 DIV *SOD1*^{G93A} spinal microglia recapitulate the features of the symptomatic pro-inflammatory microglia whereas 16 DIV microglia can represent the dysfunction at the end-stage. We also demonstrated that different populations coexist (M1/M2b at 2 DIV vs. M1/dysfunctional at 16 DIV), which is in accordance with previous data (Cunha et al. 2017; Nikodemova et al. 2014), highlighting that more detailed characterization of the phenotype and responses of microglia *in vivo* is required. Importantly, because we observe that the senescence-associated features of WT spinal microglia were exacerbated in *SOD1*^{G93A} cells, our data further suggests that during disease progression the sequence of events inducing microglia “aging” and dysfunction occur faster in ALS possibly due to the continuous stimulation of microglia by the surrounding inflammatory milieu (Ehrhart et al. 2015; Yiangou et al. 2006; Yu et al. 2012).

Several studies reported upregulation of miR-155 in rodent ALS models as well as human samples, both from familial and sporadic patients (Butovsky et al. 2012; Koval et al. 2013). Targeting miR-155 specifically in microglia was showed to reverse their abnormal phenotype and to induce increased *SOD1*^{G93A} mice survival (Butovsky et al. 2015). In line with these findings, we found that miR-155 was upregulated in *SOD1*^{G93A} spinal microglia in both time points and only at 16 DIV other inflamma-miRs were additionally elevated. While miR-155 is

shown to influence ALS progression throughout all disease stages, inflamma-miRs deregulation reinforce that pro-inflammatory and senescent microglia coexist in late stages, phenotypes strongly correlated with motor neuron degeneration (Frakes et al. 2014; Nikodemova et al. 2014). In more detail, miR-125b was shown to potentiate NF-κB activation in *SOD1*^{G93A} microglia by targeting A20 (Parisi et al. 2016) and miR-146a has been consistently reported as one key deregulated miRNA in ALS (Campos-Melo et al. 2013; Koval et al. 2013). MiR-146a expression is induced after TLR/NF-κB signaling pathway, however, since it acts as a negative feedback regulator, its continuous expression may mediate a sustained NF-κB inhibition underlying its role in mediating senescence (Caldeira et al. 2014; Jiang et al. 2012). MiR-21 also regulates NF-κB transactivation by negative feedback (He et al. 2014), but in opposite to miR-146a, it inhibits microglia-induced toxicity. In particular, by targeting Fas ligand, miR-21 prevented microglia-mediated neuronal death after hypoxia, highlighting the neurotoxic potential of *SOD1*^{G93A} spinal microglia (Zhang et al. 2012b). Although it has been shown that miR-124 transitions microglia towards neuroprotective profiles (Ponomarev et al. 2011; Veremeyko et al. 2013), its high expression was also associated with reduced microglial motility and phagocytosis (Svahn et al. 2016). Interestingly, miR-124 has emerged as another potential target in ALS due its upregulation in motor neurons expressing *SOD1*^{G93A} (Pinto et al. 2017) and its reported role in decreasing neurotransmitter release at the neuromuscular junction in a model of neuromuscular disease (Zhu et al. 2013). Nevertheless, the impact of miR-124 upregulation in ALS progression remains unknown.

At 2 DIV, the majority of *SOD1*^{G93A} spinal microglia acquire an M1-phenotype associated with TLR4/NF-κB activation and release of NO which is in accordance with the *in vitro* studies reporting motor neuron-degeneration mediated by microglia production of pro-inflammatory mediators (Liao et al. 2012; Xiao et al. 2007). Similarly to a set of inflammatory markers detected in serum, CSF or SC tissue (Ehrhart et al. 2015; Liu et al. 2015a; Yiangou et al. 2006), high levels of HMGB1 were found in SC samples from ALS patients (Casula et al. 2011). Surprisingly, HMGB1 release was decreased in 2 and 16 DIV *SOD1*^{G93A} spinal microglia. Since HMGB1 gene expression did not change (data not shown), we may hypothesize that it is being retained inside the cell or even eliminated. Interestingly, Lo Coco and colleagues (2007) reported the accumulation of HMGB1 in the nucleus of microglia in the SC of *SOD1*^{G93A} mice at the symptomatic stage, which was associated with increased proliferation and hypertrophy.

Accumulating evidences show impairment of microglia phagocytic ability in ALS (Cunha et al. 2017; Radford et al. 2015; Sargsyan et al. 2011), as we also observed. The extraordinary importance of phagocytosis under neurodegenerative conditions, such as in clearance of Aβ plaques or removal of myelin debris in multiple sclerosis (Fu et al. 2014; Krabbe et al. 2013),

highlights this function as a strong candidate to add on the mechanism linking motor neuron degeneration and microglia activation. Our data further suggests that the reported inability to phagocytose *SOD1^{G93A}* apoptotic neurons (Sargsyan et al. 2011) may be attributable to MFG-E8 downregulation, which we observe in both 2 and 16 DIV cells correlating with our previous *in vivo* data (Cunha et al. 2017). Mutations in TREM2 were lately described as a risk factor for the development of ALS (Cady et al. 2014). Hence, our data suggest that the underlying mechanism may rely in loss of function rather than compromised gene expression. Curiously, phagocytosis and autophagy are closely linked functions but we observe that after 16 DIV *SOD1^{G93A}* spinal microglia have an increased number of cells with LC3 punctates, suggestive of autophagosome assembling and autophagy (Plaza-Zabala et al. 2017). Upregulation of lysosomal proteins and cathepsins was observed in *SOD1^{G93A}* microglia (Chiu et al. 2013) where the authors suggested the activation of these pathways as an attempt to degrade mSOD1 aggregates.

Appealing studies have shown that astrocytes directly contribute to motor neuron degeneration in ALS (Diaz-Amarilla et al. 2011; Meyer et al. 2014; Yamanaka et al. 2008b). Whereas microglia-astrocyte interaction is referred as an essential mechanism not only in normal brain function but in pathological circumstances as well, the specific mediators involved are still sparse. It was shown that LPS-stimulated microglia induce reactive A1 astrocytes through release of IL-1α, TNF and C1q (Liddelow et al. 2017). On the other side, reduction of mSOD1 in astrocytes promoted a delay in microglia activation in the SC of *SOD1^{G93A}* mice as well as in disease course (Yamanaka et al. 2008b). Moreover, astrocytes-derived TGF-β inhibits microglia neuroprotective properties promoting accelerated disease progression in the *SOD1^{G93A}* mouse model (Endo et al. 2015). We then decided to study the effect of *SOD1^{G93A}* spinal astrocytes in microglia phenotype. The toxic potential of theses astrocytes was shown after coculturing with WT spinal microglia, which induced microglia activation with increase production of miR-155, miR-125b, *Il-1beta* and NO release, as well as degeneration. Interestingly, they change the pro-inflammatory-polarized *SOD1^{G93A}* spinal microglia towards heterogeneous phenotypes, further supported by upregulation of miR-125b, miR-21 and miR-124. As previously referred, upregulation of miR-125b and miR-21 has been associated with neurodegeneration and microglial activation (Harrison et al. 2016; Parisi et al. 2016; Yelamanchili et al. 2015). More importantly, this finding could be translated to other neurodegenerative conditions as the reactive astrocytes act equally in both WT and *SOD1^{G93A}* microglia. Surprisingly, miR-155 was not upregulated in this condition which may indicate that in this two-edge coculture system, astrocytes became the major miR-155 producing cell. Of notice, interaction with WT astrocytes had a positive outcome in *SOD1^{G93A}* spinal microglia by inducing the expression of protective markers, which highlight that

strategies to modulate astrocytes in ALS would also produce neuroprotective actions in microglia.

We finally explore the expression of NLRP3-inflammasome complex and Cx43/Panx1 hemichannels in our coculture system. NLRP3-inflammasome acts as an intracellular sensor, able to recognize a wide variety of signals and is composed by a multimolecular complex including NALP3 receptor, adaptor apoptosis-associated speck-like protein containing a CARD (ASC), and caspase-1 (Lamkanfi and Dixit 2012; Walsh et al. 2014). Upon activation, all players are assembled promoting the activation of caspase-1 and the consequent cleavage of pro-IL-1β and pro-IL-18 into their active forms. The activation of NLRP3-inflammasome has been demonstrated under neurodegenerative conditions (Walsh et al. 2014), including ALS. Despite the recent report showing that NLRP3 expression is restricted to astrocytes in the SC of mSOD1 mice and ALS patients (Johann et al. 2015), our data show that only *SOD1*^{G93A} spinal microglia upregulate the expression of the *NLRP3-inflammasome* when stimulated by mutant astrocytes. In accordance, Gustin and colleagues (2015) have shown that NLRP3-inflammasome is functional in microglia inducing IL-1β secretion, but this mechanism does not occur in astrocytes. Importantly, our data suggest that the activation of NLRP3-inflammasome is mediating the release of HMGB1 to the extracellular media, as reported by others (Lamkanfi et al. 2010; Willingham et al. 2009). Whereas Cx43 upregulation have been associated with astrocytes-mediated motor neuron injury (Almad et al. 2016; Diaz-Amarilla et al. 2011), the role of Panx1 in ALS is unknown. These hemichannels are part of a group of gap-junctions involved in the transfer of ions, metabolites and second messengers between adjacent cells, regulating different physiological mechanisms (Montero and Orellana 2015). We recently reported that downregulation of *Cx43/Panx1* compromise the homeostatic balance in presymptomatic *SOD1*^{G93A} mice while after symptom onset both channels are upregulated (Cunha et al. 2017). Our results demonstrated that along with Cx43, Panx1 may be involved in motor neuron degeneration and that the communication between microglia and astrocytes are crucial for astrocytic *Panx1* expression. The functional outcome of Panx1 stimulation requires, however, further investigation.

In conclusion, in the present study we present a new model to explore microglia responses in ALS that can be useful to test novel and stage-specific therapeutic strategies. We showed that microglia responses are produced by mixed phenotypes and a main pro-inflammatory status progress to dysfunction and irresponsiveness over time in culture. Among the described activated mechanisms, we suggest TLR4/NF-κB activation and declined MFG-E8-linked phagocytic ability as important effectors in microglia-mediated motor neuron injury. Also, functional microglia-astrocyte interplay is critically important for the

neuroinflammatory milieu of ALS symptomatic stages as demonstrated by upregulation of *NLRP3-inflammasome*, *Panx1* and HMGB1 release. Of notice, C9ORF2 reduction promotes microglia dysfunction (O'Rourke et al. 2016) and TDP-43 induces activation of NF-KB and NLRP3-inflammasome in microglia (Zhao et al. 2015), reflecting the translational potential of our data to other forms of ALS pathology. Taken together, our data emphasize the magnitude of developing combined therapies acting in a given stage of ALS disease progression.

5. Supplementary Material

Supplementary Table V.1 - List of primer sequences used for mRNA analysis

Gene	Sequence (5'-3') / Source
S100b	5'-GAGAGAGGGTGACAAGCACAA-3' (fwr)
	5'-GGCCATAAACTCCTGGAAGTC-3' (rev)
Nos2	5'-ACCCACATCTGGCAGAATGAG-3' (fwr)
	5'-AGCCATGACCTTTCGCATTAG-3' (rev)
Mhc-II	5'-TGGGCACCATCTTCATCATTC-3' (fwr)
	5'-GGTCACCCAGCACACCACTT-3' (rev)
Cebpa	5'-AGCTTACAACAGGCCAGGTTTC-3' (fwr)
	5'-CGGCTGGCGACATACAGTAC-3' (rev)
Arg1	5'-CTTGGCTTGCTTCGGAACTC-3' (fwr)
	5'-GGAGAAGGCGTTTGCTTAGTTC-3' (rev)
Socs1	5'-CACCTTCTTGGTGCGCG-3' (fwr)
	5'-AAGCCATCTTCACGCTGAGC-3' (rev)
Tgfb1	5'-CAGAGCTGCGCTTGCAGAG-3' (fwr)
	5'-GTCAGCAGCCGGTTACCAAG3' (rev)
Nlrp3	5'-TGCTCTTCACTGCTATCAAGCCCT-3' (fwr)
	5'-ACAAGCCTTTGCTCCAGACCCTAT-3' (rev)
Il-18	5'-TGGTTCCATGCTTTCTGGACTCCT-3' (fwr)
	5'-TTCCTGGGCCAAGAGGAAGTG-3' (rev)
Il-1beta	5'-CAGGCTCCGAGATGAACAAC-3' (fwr)
	5'-GGTGGAGAGCTTTCAGCTCATA-3' (rev)
Cx43	5'-ACAGCGGTTGAGTCAGCTTG-3' (fwr)
	5'-GAGAGATGGGGAAGGACTTGT-3' (rev)
Panx1	5'-TGTGGCTGCACAAGTTCTTC-3' (fwr)
	5'-ACAGACTCTGCCCCACATTC-3'(rev)
Cd80	5'-ACTAGTTTCTCTTTTTCAGGTTGTG-3' (fwr)
	5'-GAGCCAATGGAGCTTAGGCA-3' (rev)
Cd206	5'-GTGGAGTGATGGAACCCCAG-3' (fwr)
	5'-CTGTCCGCCCAGTATCCATC-3' (rev)
b-actin	5'-GCTCCGGCATGTGCAA-3' (fwr)
	5'-AGGATCTTCATGAGGTAGT-3' (rev)

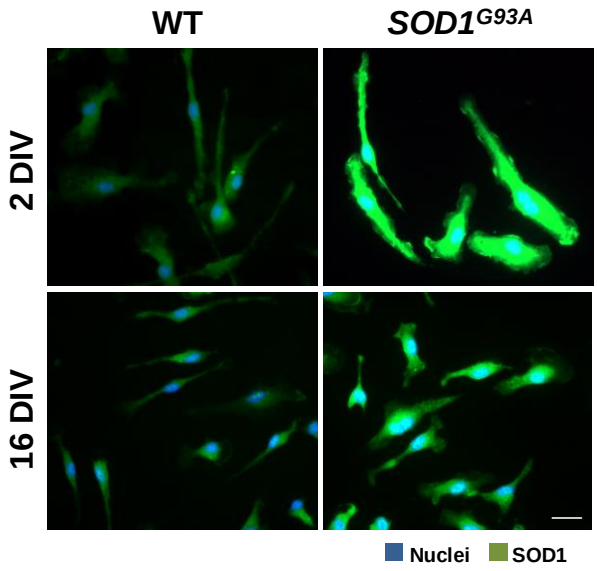

Supplementary Figure V.1 - *SOD1*^{G93A} spinal microglia have increased expression of SOD1. Representative images of immunostaining against SOD1 (green) showing increased staining in *SOD1*^{G93A} spinal microglia both in 2 and 16 DIV. Nuclei were counterstained with Hoechst dye (blue). Scale bar represents 20 µm.

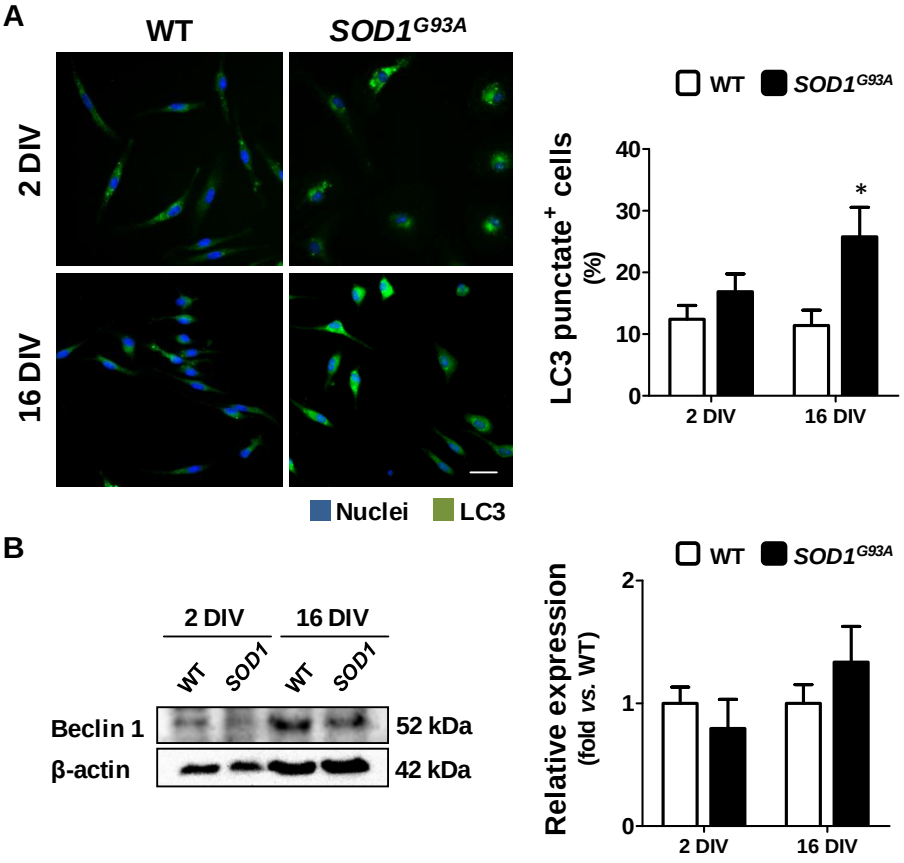

Supplementary Figure V.2 - LC3-associated autophagy is increased in 16 DIV *SOD1*^{G93A} spinal microglia. (A) Representative images of immunocytochemistry staining of LC3 punctates (in green). Nuclei were counterstained with Hoechst dye (blue). Scale bar represents 20 µm. The percentage of LC3 punctate positive cells was quantified. (B) Beclin-1 expression was assessed by Western Blot. Representative images are shown and results expressed as mean + SEM (*p < 0.05 vs. respective WT, n=4-8, unpaired student´s *t*-test).

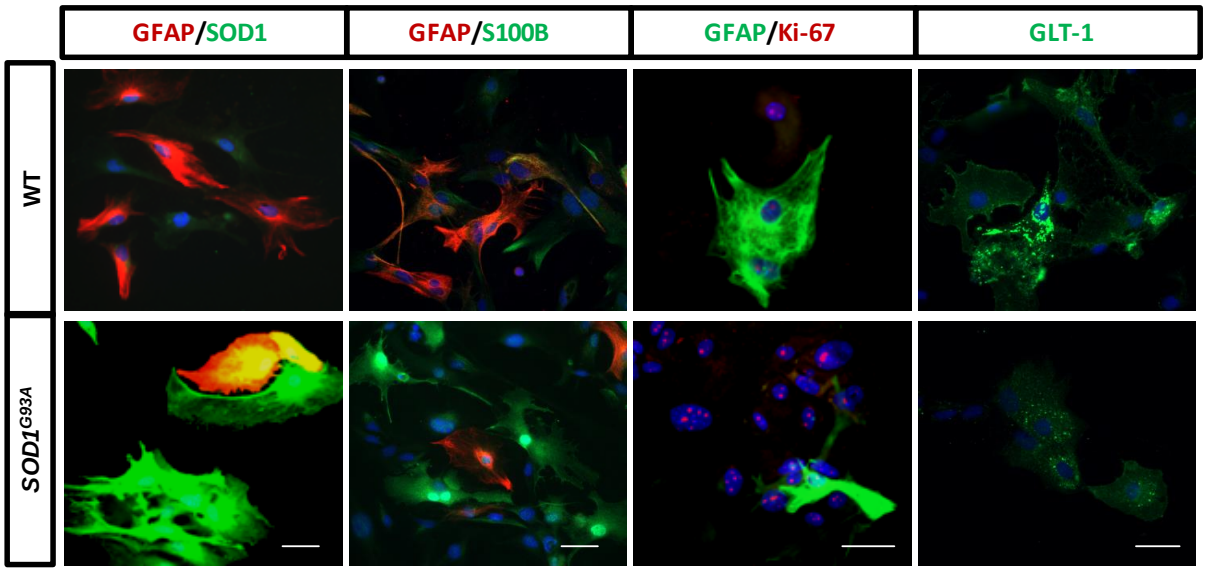

Supplementary Figure V.3 - *SOD1*^{G93A} spinal astrocytes have a reactive and proliferative phenotype. Representative images of double immunostaining against GFAP/SOD1, GFAP/S100B, GFAP/Ki-67 and GLT-1 showing a SOD1^{high}/GFAP^{low}/S100B^{high}/GLT-1^{low} profile. Nuclei were counterstained with Hoechst dye (blue). Scale bar represents 20 µm.

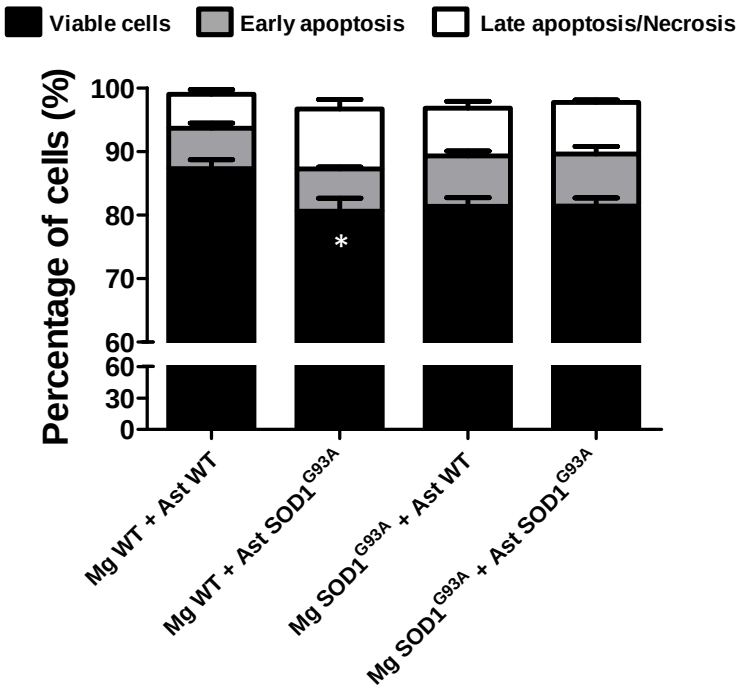

Supplementary Figure V.4 - *SOD1*^{G93A} spinal astrocytes are toxic to WT spinal microglia by decreasing their viability. The percentage of viable, early apoptotic and late apoptotic/necrotic cells was assessed by flow cytometry with the GUAVA Nexin reagent. Results are expressed as mean + SEM (*p < 0.05 vs. WT coculture, n=5, one-way ANOVA followed by Tukey's *post hoc* test).

Chapter VI

CONCLUDING REMARKS

Concluding Remarks

Despite the great effort over the years to improve ALS diagnosis and treatment, ALS patients still have to face almost a year for a definite diagnosis, and to wait for their lethal fate without a promising strategy to improve their lifespan (Kiernan et al. 2011; Vucic et al. 2014). Nonetheless, in the last years, a lot of progress has been made, increasing the hope for great achievements in the near future. Novel therapies that are being developed and launched in the market, as the recent edaravone both in Japan and USA, and the promising use of iPSCs in drug discovery and screening, with potential in personalized medicine (Takahashi et al. 2007), are some examples of the progress achieved. To also note that iPSCs are a new gold standard in regenerative medicine and important to identify risk factors in the sporadic forms of ALS, which constitute approximately 90% of the cases (Ameku et al. 2016; Renton et al. 2014; Singh et al. 2015; Zhang et al. 2016). We are just starting studies with iPSCs from ALS patients thanks to our funded project from Santa Casa da Misericórdia on ALS. However, when this thesis started available methods were the mouse MN-like NSC-34 cell line stably transfected with human $SOD1^{G93A}$ (a gift from Julia Costa from ITQB) and the *$SOD1^{G93A}$* transgenic mouse model produced by Jackson Laboratories, which are still the most widely used models to investigate ALS. Actually, mutant SOD1 transgenic rodents recapitulate many features of the disease, including progressive neuromuscular dysfunction, axonal and mitochondrial dysfunction, motor neuron loss and gliosis, and consequently have been central to explore the pathophysiological mechanisms of ALS (McGoldrick et al. 2013). In what concerns the NCS-34/$hSOD1^{G93A}$ cells they have been considered a suitable model to study several dysfunctional processes in ALS (Gomes et al. 2008; Vaz et al. 2015). Therefore, *in vitro* and *in vivo* experiments were performed based on the expression of a mutant SOD1 (*$SOD1^{G93A}$*). At the molecular level, misfolding and accumulation of SOD1 in MNs characterize such models being transversal to other disease forms where protein inclusions are always observed (Taylor et al. 2016).

Another model used in the present thesis was the microglial cell line N9. These immortalized cells isolated from the cortex of CD1 mouse embryos were shown to respond similarly to primary microglial cells in terms of migration, phagocytosis and inflammation-related features (Falcão et al. 2017). Actually, one of the main aims of this thesis was to bring new insights on microglia phenotypes and inflammatory pathways in different stages of the disease, as well as in the modulatory effect of MNs and astrocyte-derived signals. Together with the increased knowledge on the mechanisms involved in MN degeneration, glial cells activation and neuroinflammation are now considered to also be key elements in ALS pathogenesis. This was firstly demonstrated by targeting SOD1 specifically in MNs and in glial cells (Clement et al. 2003), and further reinforced by directed modulation of microglia

or astrocytes (Boillée et al. 2006b; Yamanaka et al. 2008a). However, the role of microglia activation in ALS is still controversial and accumulating data indicates that at the same time that disease progresses, microglia change their responses, phenotypes and functional outcome (Beers et al. 2011; Liao et al. 2012; Nikodemova et al. 2014). Additionally, the well-known process of anatomical disease progression in patients underlies the importance of intercellular communication, where we believe that exosomes play a crucial role. Importantly, mounting evidences have demonstrated that misfolded SOD1 can be transported in exosomes and collected by other cells, where it accumulates and promotes protein aggregation, thus demonstrating the role of exosomes in the prion-like propagation character of ALS (Basso et al. 2013; Grad et al. 2014), although the misfolded SOD1 was also shown to be transferred in exosome-independent ways (Silverman et al. 2016). Interestingly, such extracellular vesicles, due to their relevant role in intercellular communication, were also lately proposed as a potential therapeutic approach in ALS (Bonafede and Mariotti 2017) and the generation of engineered cells releasing exosomes enriched with specific molecules is one of our main interests in the group.

By improving the knowledge on stage-specific altered mechanisms in ALS, the results here presented identify new pathways, either prior or subsequent to disease onset. In addition, data provide a better comprehension on how the surrounding environment may change microglia behavior, and deepens the key role of astrocytes in the disease process, emphasizing glial cells as central players in ALS pathology. However, not forgetting that ALS is marked by the loss of MNs leading to fatally debilitating weakness, we also demonstrate that exosomes from *SOD1*^{G93A}-expressing MNs, together with the secretome of reactive *SOD1*^{G93A} astrocytes, change microglia phenotype in a signal-dependent manner. Importantly, data indicate that microglia acquire distinct phenotypes along disease progression and that a mixture of microglia subtypes coexist throughout disease course. Additionally, the present work shows that compromised microglial phagocytosis may underlie a crucial neurotoxic mechanism in ALS. In fact, inefficient clearance of cellular debris and/or protein aggregates, such as those of SOD1, may promote the spread of the injury as indicated for other pathologies (Domingues et al. 2016; Neher et al. 2012), and support the prion-like dissemination (Grad et al. 2015). Finally, we identify miR-155 and MFG-E8 as biomarkers for early ALS events and recognize promising targets, whose modulation in the symptomatic disease may hopefully delay or stop ALS progression. Having these findings into account, we propose that multi-target and multifunctional pharmaceuticals, acting at different pathological ALS features may constitute a more effective therapeutic solution considering the complex etiology of the disease.

M1-polarized N9 microglia release MFG-E8, HMGB1 and miR-155 and miR-146a as exosome cargo

In the **Chapter II**, the mechanisms underlying M1-polarization of N9 microglial cells after LPS exposure were determined by exploring the combination of well-known activation markers, as well as novel pathways. Given the functional plasticity of microglia, the collective events leading to microglia activation in a specific context are essential to completely understand their responses. The study showed that LPS-stimulated N9 cells acquire a typical M1-phenotype profile, amoeboid morphology and reduced chemotaxis towards ATP, which was accompanied by activation of the TLRs/NF-κB pathway and the production of inflammatory mediators. Allied with these classical M1-polarization characteristics, LPS-stimulation induced NLRP3-inflammasome activation and shuttling of HMGB1 from the nucleus to the cytoplasm, followed by its release, pathways that are mainly explored in macrophages. Enhanced production and secretion of MFG-E8 associated with increased phagocytic ability, and the release of miR-155 and miR-146a in exosomes derived from M1-polarized N9 microglia, all constitute novel findings. Since exosomes recapitulated the inflamma-miRNAs profile of the cells, our data indicate that horizontal transfer of miRNAs may account for the dissemination of inflammatory responses.

This study not only confirm the potential of N9 cells as a useful model to explore microglia activation in normal or pathological circumstances, in particular in understanding N9 microglia response towards *SOD1*^{G93A} motor neuron-derived exosomes (Chapter III) and SOD1^{G93A} overexpression (ongoing studies), but more importantly identify novel and promising biomarkers of microglia M1-polarization. Since this phenotype is described in close association with neurodegenerative processes (Song and Suk 2017), these findings highlight potential targets that once modulated may shift microglia towards a neuroprotective response.

Motor neurons-to-microglia transfer of miR-124-containing exosomes drive microglia acute M1-polarization followed by M1/M2/senescent subclasses

The role of exosomes derived from NSC-34/SOD1^{G93A} motor neurons in naïve microglia performance *in vitro* was described in **Chapter III**. We evaluated whether exosomes from NSC-34/SOD1^{G93A} motor neurons could change N9 microglia phenotype and inflammatory profile when exposed for short (2 and 4h) or long (24h) periods. This study showed that NSC-34/SOD1^{G93A} motor neurons and their-derived exosomes, with a diameter size of ~130 nm, are enriched in miR-124 and that when incubated in NSC-34 and N9 cells cocultures, exosomes are preferentially internalized by microglial cells. Early M1-polarization followed by

the acquisition of M1/M2/senescent subclasses and increase of receptors TREM2, RAGE and TLR4, characterize microglia reactivity to *SOD1^{G93A}* exosomes over time. In addition, we observed sustained NF-κB activation and decreased phagocytic ability in all the studied time points, highlighting the relevance of these pathways in microglia activation in ALS. Whereas the data presented in this study also suggest that miR-124 is transferred to naïve N9 cells, one may assume that misfolded SOD1^{G93A} in exosomes (Gomes et al. 2007; Grad et al. 2014b) account as triggers of microglia responsiveness. Our data is innovative in showing that exosomes are able to mediate alterations in microglia polarization and behavior, emphasizing their potential for therapeutic targeting of neuroinflammatory pathways.

MFG-E8 (low) and miR-155 (high) may serve as early biomarkers and precede the onset and the symptomatic inflammatory milieu in ALS

In order to understand the specific features of microglia activation prior to disease onset *in vivo*, in the **Chapter IV**, the changes in inflammation-related markers and cellular interplay in the spinal cord of *SOD1^{G93A}* mice at presymptomatic and symptomatic stages were investigated. Whereas activation of glial cells has been tackled in symptomatic mice, especially at end-stage, data are missing regarding what happens prior to disease initiation (Chiu et al. 2013; Nikodemova et al. 2014). Altered mechanisms in motor neuron start before the appearance of symptoms in ALS mice (Ferraiuolo et al. 2011b) and, although microglia and astrocytes were only shown to contribute to exacerbate disease progression (Boillée et al. 2006b; Yamanaka et al. 2008a), one postulate that both glial cells sense stressed motor neurons and change their behavior accordingly. Therefore, the study showed that prior to disease onset, intercellular communication is compromised as the chemokines CX3CL1 and CCL21 and the hemichannels Cx43 and Panx1 are downregulated, which is accompanied by depressed astrocytes and microglia functionality. Although some potential neuroprotective mechanisms turn up (such as increase in autotaxin and IL-10), probably as an attempt to moderate pathogenicity in the symptomatic *SOD1^{G93A}* mice, reactive astrocytes, predominant M1-microglial responses, deregulated inflamma-miRNAs and a prevalent inflammatory milieu characterizes this stage. Existence of an inflammatory micro-environment has been referred by several studies (Beers et al. 2006; Diaz-Amarilla et al. 2011; Frakes et al. 2014; Hensley et al. 2002; Hu et al. 2017). Data additionally suggest upregulation of miR-155 and downregulation of MFG-E8 as crucial mechanisms in ALS pathogenesis. Such biomarkers start very early in the disease process and are maintained along progression mechanisms, highlighting their promising use as ALS biomarkers. As recently demonstrated by Frakes and colleagues (2017), combined therapies may improve disease outcome by targeting multiple pathways. Therefore, accordingly to what we observed in symptomatic *SOD1^{G93A}* mice,

HMGB1, NLRP3-inflammasome, miR-155/miR-125b, shed CX3CL1 and Cx43/Panx1 emerge as targets to slow disease progression while enhancing microglia phagocytic ability and M2 subtypes further accounting for neuroprotection.

Transition from pro-inflammatory *SOD1^{G93A}* microglia to multiple phenotypes ensues from cell culture aging and cross talk with reactive astrocytes

To further explore the intrinsic properties of *SOD1^{G93A}* microglia and the contribution of astrocytes in the acquisition of the observed M1/M2 microglial phenotypes, in the **Chapter V**, spinal microglia was cultured for short-term and long-term periods (in an attempt to mimic the influence of disease progression mechanisms on microglia plasticity), or cocultured with spinal astrocytes to establish cell-to-cell communication. Acutely isolated microglia from the spinal cord of pre- and symptomatic *SOD1^{G93A}* mice were shown to be engaged in M2-protective or M1-cytotoxic profiles, respectively (Beers et al. 2011; Liao et al. 2012). Our group has previously developed an *in vitro* model where postnatal cortical microglia show reactive (2 DIV) *vs.* senescent-like (16 DIV) properties in culture. Based on this model, we have demonstrated that *SOD1^{G93A}* spinal microglia in short-term cultures evidence predominantly the M1-phenotype observed at the symptomatic stage. While distinct phenotypes coexist in all time-points, this M1 polarized phenotype was confirmed by the high expression of M1-markers together with low M2-markers, and with the typical M1-associated profile provided by miR-155^{high}/miR-124^{low}. Activation of TLR4/NF-κB pathway was additionally observed. However, activation of NLRP3-inflammasome was not shown to be involved in *SOD1^{G93A}* spinal microglia reactivity in this condition. In opposite, long-term culture of *SOD1^{G93A}* spinal microglia reduced their reactive capacity by decreasing M1-markers and the TLR/NF-κB pathway. These findings indicate that, with time, microglia shift from a M1-proinflammatory to a set of miscellaneous phenotypes that include dysfunctional cells, which were previously found in the spinal cord of *SOD1^{G93A}* mice at the end-stage of the disease (Nikodemova et al. 2014). Interestingly, *SOD1^{G93A}* spinal microglia also presented low phagocytic ability, MFG-E8 downregulation and miR-155 upregulation in both culture schemes, reinforcing the relevance of these pathways in ALS, and as so their potentiality as targets to driven medicines.

In this study we further demonstrated that WT astrocytes have anti-inflammatory benefits in *SOD1^{G93A}* spinal microglia and that *SOD1^{G93A}* spinal astrocytes damage WT microglia and induce the transition of M1-polarized *SOD1^{G93A}* spinal microglia into heterogeneous phenotypes. *SOD1^{G93A}* spinal astrocyte-microglia communication was here shown to be required to activate some ALS-linked inflammatory pathways, as the upregulation of microglial NLRP3-inflammasome components and HMGB1 release. Taken together, intrinsic

action of *SOD1*^{G93A} in microglia determines certain features of microglia polarization, while interaction with astrocytes potentiates the negative effects of mutated microglia. A great deal of studies showed that microglia activation precedes and mediates astrocyte reactivity under neurodegenerative conditions (Kirkley et al. 2017; Liddelow et al. 2017). We now show that astrocytes are also able to determine microglia performance deficits in ALS and that close interplay between these two glial cells coordinates the responses observed *in vivo*, probably exerting synergistic and cross-talk deregulated mechanisms that culminate with the escalation of motor neuron death in ALS late stages.

Overall, the present thesis provides new insights into the inflammatory pathways governing both pre- and symptomatic ALS stages, as well as into drivers and mechanisms of *SOD1*^{G93A} microglia activation that underlie their contribution to motor neuron degeneration. We evidence that *SOD1*^{G93A} microglia switch from a compromised/declined cell functionality at the preonset clinical stage to mixed subtypes with a prevalent pro-inflammatory phenotype in the symptomatic phase. The observed M1-polarization is recapitulated *in vitro* and is in accordance with the described disease-specific microglia profile in ALS. We show the reactivity of SOD1 mutated astrocytes and their harmful role in inducing heterogeneous responses and ALS-related neurotoxic mechanisms in microglia. NLRP3-inflammasome, HMGB1 release, miR-155/miR-125b and Cx43/Panx1 emerge as very promising targets for developing new therapies, while miR-155 and MFG-E8 offer reliability as disease biomarkers. Finally, our data on the transfer of exosomes, and likely of miR-124 together with misfolded/mutated proteins and other genetic and pro-inflammatory material, from motor neurons to microglia reinforce their relevance in the disease-spreading mechanisms. Then, the activated recipient microglia, by releasing inflamma-miRNAs into their exosomal cargo, ends up intensifying the inflammation spread to neighboring areas. Main findings of this thesis are depicted in Figure VI.1.

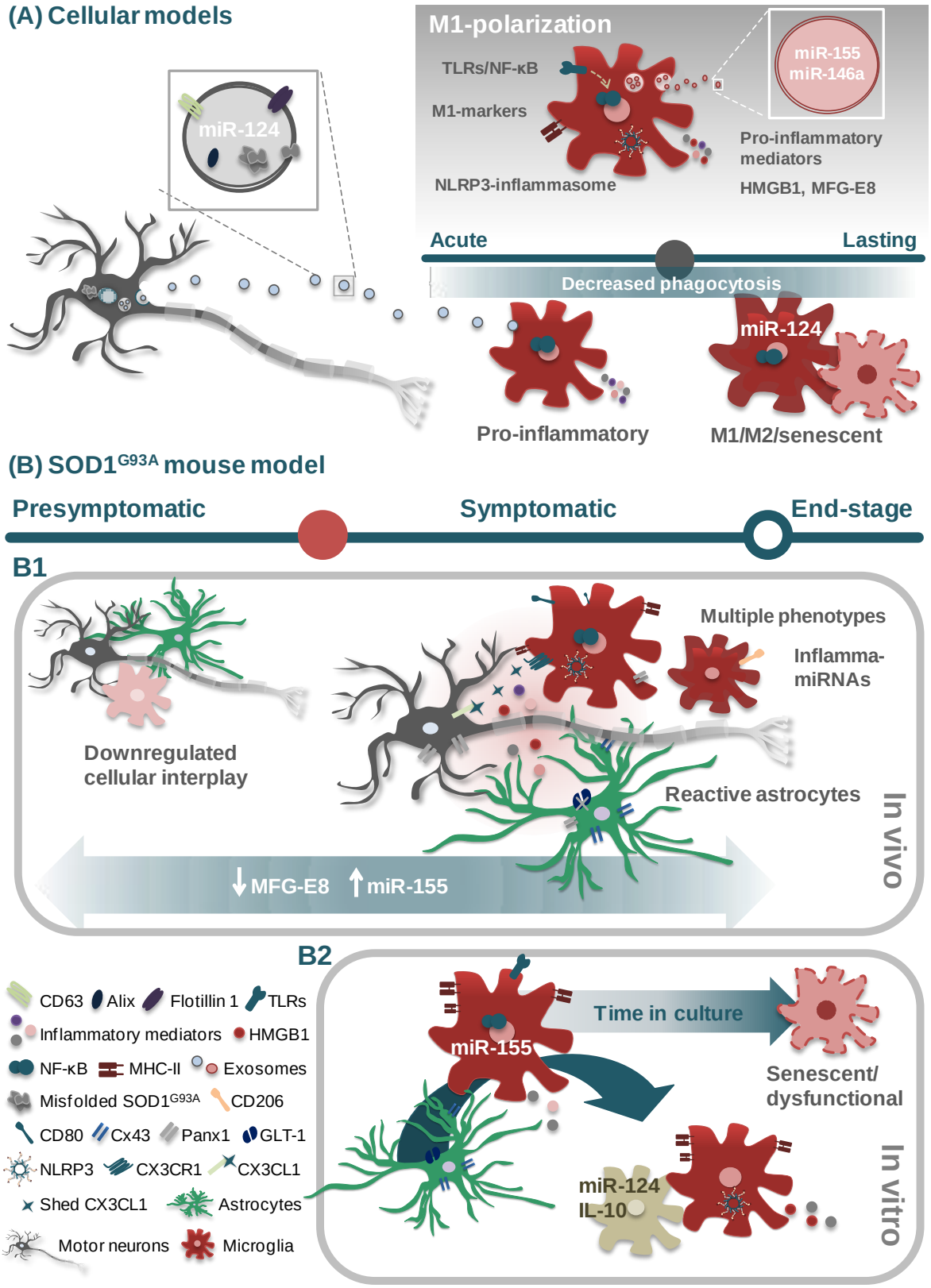
(A) Cellular models
M1-polarization
TLRs/NF-κB
M1-markers
NLRP3-inflammasome
miR-155
miR-146a
Pro-inflammatory mediators
HMGB1, MFG-E8
miR-124
Acute
Lasting
Decreased phagocytosis
miR-124
Pro-inflammatory
M1/M2/senescent
(B) SOD1G93A mouse model
Presymptomatic
Symptomatic
End-stage
B1
Multiple phenotypes
Inflamma-miRNAs
Downregulated cellular interplay
Reactive astrocytes
MFG-E8
miR-155
In vivo
B2
CD63
Alix
Flotillin 1
TLRs
Inflammatory mediators
HMGB1
NF-κB
MHC-II
Exosomes
Misfolded SOD1G93A
CD206
CD80
Cx43
Panx1
GLT-1
NLRP3
CX3CR1
CX3CL1
Shed CX3CL1
Astrocytes
Motor neurons
Microglia
Time in culture
miR-155
Senescent/ dysfunctional
miR-124
IL-10
In vitro

Figure VI.1 – Schematic representation of the main findings of the present work. (A) N9 microglia exposed to LPS acquire a M1-polarization, characterized by activation of TLRs/NF-κB and NLRP3-inflammasome pathways and release of pro-inflammatory mediators, including HMGB1 and MFG-E8. Release of miR-155 and miR-146a in exosomes recapitulate the profile of LPS-stimulated N9 microglia. When exposed to *SOD1*^{G93A} motor neuron-derived exosomes that carry miR-124, N9 microglia develop an early pro-inflammatory response followed by the acquisition of M1, M2 and senescent populations. (B) The studies here presented were also performed in the spinal cord of the transgenic *SOD1*^{G93A} mouse model. (B1) *In vivo* data showed that in the presymptomatic stage intercellular communication and glia functionality are impaired, which progresses after clinical onset towards an inflammatory microenvironment. Multiple phenotypes of microglia coexist, although pro-inflammatory/neurotoxic actions are prominent. Early and sustained upregulation of miR-155 and downregulation of MFG-E8 emerge as potential biomarkers. (B2) In short-term cultures, spinal microglia acquire a pro-inflammatory profile, resembling the symptomatic stage, and become dysfunctional with time in culture. Spinal reactive astrocytes, observed *in vivo*, transform spinal M1-like microglia into mixed phenotypes and induce upregulation of NLRP3-inflammasome and HMGB1 release. NF-kB activation, upregulation of NLRP3-inflammasome and HMGB1, as well as decreased phagocytic capacity, are consistent findings among *in vitro* and *in vivo* models, suggesting their crucial role as players in ALS pathogenesis.

LPS, lipopolysaccharide; TLR/NF-κB, toll-like receptors/nuclear factor kappa B, NLRP3, NOD-like receptor pyrin domain containing 3; HMGB1, high mobility group box 1; MFG-E8, milk-fat globule EGF factor 8; miR, microRNA; *SOD1*^{G93A}, superoxide dismutase 1 with G93A mutation; Cx43, connexin-43; Panx1, Pannexin-1; CD, cluster of differentiation; MHC-II, major histocompatibility complex class II.

Chapter VII

FUTURE PERSPECTIVES

Future Perspectives

The work here presented highlight miR-155 and MFG-E8 as potential early disease biomarkers. Whereas circulating miRNAs have been detected in the CSF and serum of patients with ALS (Benigni et al. 2016; Waller et al. 2017), to the best of our knowledge the levels of MFG-E8 were never explored. As a bridge in the process of PS recognition by microglia, MFG-E8 can be released and, hence, it can be found in such body fluids as well. Additionally, we point out a set of inflammatory-related targets for the development of combined therapeutic strategies, aimed at modulating the behavior of motor neurons (shed CX3CL1, miR-124), as well as of glial cells (miR-155/miR-125b, NF-κB, NLRP3, HMGB1, Cx43/Panx1). Although our studies were performed in the most used and studied ALS model, further investigation in other models would be of great importance to confirm our results and their transversal character in ALS.

Collectively, our data also suggest a critical contribution of phagocytic impairment for ALS development. Because this topic is largely unknown in ALS, studying the underlying mechanisms of such impairment would provide a future direction to develop target-driven therapies. We believe that modulation of this pathway may have a huge impact on motor neuron survival once reestablished.

By showing that microglia phenotype switch between activation states along ALS disease progression, our findings have raised new questions related to the contribution of each specific phenotype to disease initiation and/or progression. In future studies, it would be important to isolate the different populations of microglia in each step of disease development and progression aiming at evaluating their transcriptional profile and motor neuron induced toxicity. In addition, we believe that upcoming work should be focused in microglia differentiated from iPSCs derived from ALS patient fibroblasts, once we and others believe to better recapitulate the disease. In a broad overview, this cutting-edge model will uncover novel insights into the complexity of human microglia dysfunction in ALS. More specifically, it is a great opportunity to explore disease-specific mechanisms by using both familial and sporadic forms of ALS, as well as a tool to develop personalized therapies. In fact, due to the expertise acquired during my training period in the Jari Koistinaho's laboratory, in the University of Eastern Finland, we have been implementing the protocols for differentiating, not only microglia, but also astrocytes, neurons and motor neurons from iPSCs. As pointed out in this thesis, we are particularly interested in modulating the deregulated cellular interplay mechanisms in ALS. Therefore, we intend to establish microglia-motor neurons and astrocyte-motor neurons cocultures, using cells derived from iPSCs generated from the fibroblasts of ALS patients, to determine disease- and patient-specific players involved in cross-talk impairment in ALS.

We additionally showed that N9 cells are a useful model to study the mechanisms involved in microglia activation under different circumstances. As an alternative to primary *SOD1*^{G93A} spinal microglia cultures that produce low-yield and are time-consuming, we further decided to transduce the N9 cell line with *SOD1*^{WT} and *SOD1*^{G93A} lentiviral vectors and study their phenotype and exosomes cargo (ongoing studies). As described in Figure VI.2, *SOD1*^{G93A} N9 microglia have a pro-inflammatory profile related to enhanced expression of the M1-markers *Nos2* and *Mhc-II*, *Il-1beta* and miR-155 together with downregulation of *Arg1*, miR-146a and miR-124. In accordance with our previous data, this inflamma-miRNAs profile was recapitulated in exosomes (unpublished data). Given that internalization of motor neuron-derived exosomes drive microglia activation, that *SOD1*^{G93A} N9 microglia release miR-155 in exosomes, and that microglia are the cell preferentially collecting exosomes, we propose that the horizontal transfer of exosomal miR-155 between microglial cells may account for the propagation of inflammatory responses in a paracrine manner. Despite our belief that prevention of either miR-155 production, or its release in exosomes, may reduce the dissemination of neuroinflammation that occurs along ALS, this issue requires further investigation.

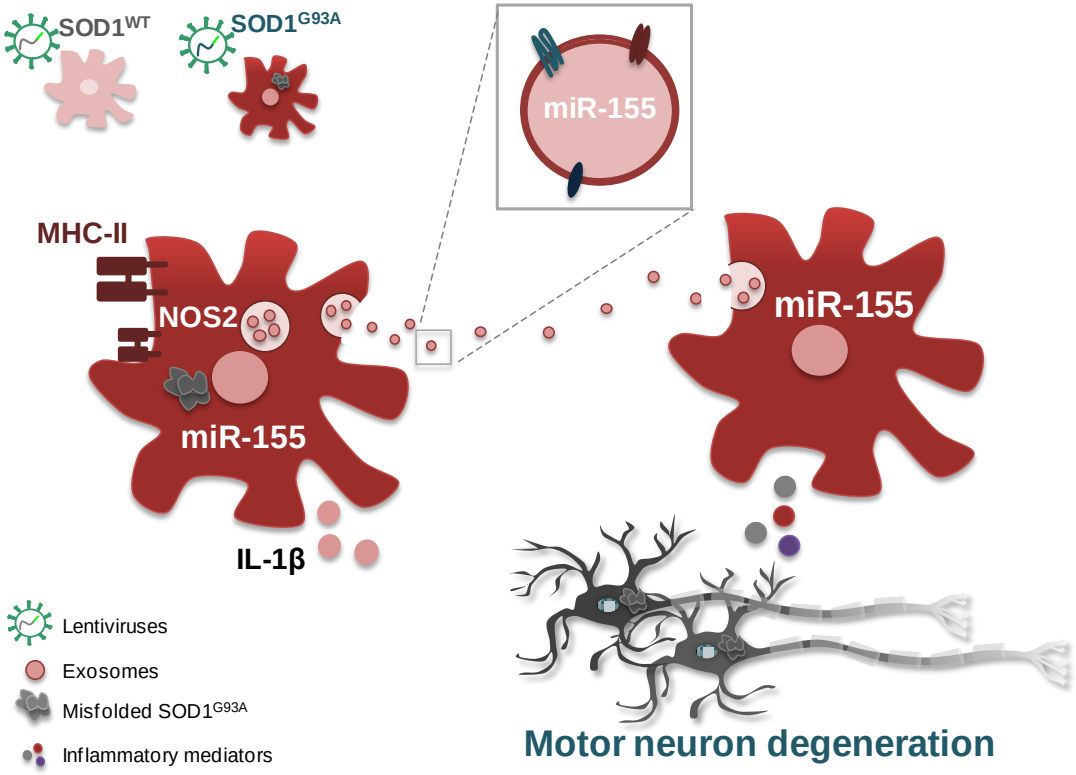

Figure VII.1 - N9 microglia expressing *SOD1*^{G93A} acquire pro-inflammatory properties and may spread inflammatory mediators by paracrine transfer of miR-155 in exosomes. Upregulation of MHC-II, NOS2, IL-1β and miR-155 underline the pro-inflammatory state of N9 microglia after transduction with superoxide dismutase 1 with G93A mutation (*SOD1*^{G93A}). The transfer of miR-155 from an activated to a naïve microglial cell may induce a pro-inflammatory profile by regulating their gene expression, further spreading inflammation-induce motor neuron degeneration to neighboring areas.
MHC-II, major histocompatibility complex class II; NOS2, nitric oxide synthase 2; IL-1β, interleukin-1 beta; miR, microRNA.

Importantly, once miR-155 upregulation was found in the spinal cord of fALS and sALS patients (Butovsky et al. 2015; Koval et al. 2013), and miR-155-based therapies are being developed (MRG-107, miRagen), studying its expression in iPSCs-differentiated into astrocytes and microglia will add on the relevance of miR-155 in a patient-specific basis, while driven patient-personalized therapeutic interventions. Together with miR-155, we are confident on the horizontal transfer of other miRNAs in exosomes as participating in the dysregulation of neural cells at distance. Therefore, we are much interested in the modulation of inflamma-miRNA expression, in both astrocytes (ELA Project, Santa Casa da Misericórdia de Lisboa) and microglia, in order to neutralize the reactive profile of both glial cells, as well as to prevent their sorting into exosomes. Furthermore, differentiation of neural cells from ALS-iPSCs, besides their application for disease modeling, will allow effective drug screening and potential use in regenerative medicine, including precision medicine.

References

Abels ER, Breakefield XO. 2016. Introduction to Extracellular Vesicles: Biogenesis, RNA Cargo Selection, Content, Release, and Uptake. Cell Mol Neurobiol 36(3):301-12.

Abiega O, Beccari S, Diaz-Aparicio I, Nadjar A, Laye S, Leyrolle Q, Gomez-Nicola D, Domercq M, Perez-Samartin A, Sanchez-Zafra V and others. 2016. Neuronal Hyperactivity Disturbs ATP Microgradients, Impairs Microglial Motility, and Reduces Phagocytic Receptor Expression Triggering Apoptosis/Microglial Phagocytosis Uncoupling. PLoS Biol 14(5):e1002466.

Abud EM, Ramirez RN, Martinez ES, Healy LM, Nguyen CHH, Newman SA, Yeromin AV, Scarfone VM, Marsh SE, Fimbres C and others. 2017. iPSC-Derived Human Microglia-like Cells to Study Neurological Diseases. Neuron 94(2):278-293 e9.

Al-Chalabi A, Hardiman O. 2013. The epidemiology of ALS: a conspiracy of genes, environment and time. Nat Rev Neurol 9(11):617-28.

Alexander M, Hu R, Runtsch MC, Kagele DA, Mosbruger TL, Tolmachova T, Seabra MC, Round JL, Ward DM, O'Connell RM. 2015. Exosome-delivered microRNAs modulate the inflammatory response to endotoxin. Nat Commun 6:7321.

Alliot F, Godin I, Pessac B. 1999. Microglia derive from progenitors, originating from the yolk sac, and which proliferate in the brain. Brain Res Dev Brain Res 117(2):145-52.

Almad AA, Doreswamy A, Gross SK, Richard JP, Huo Y, Haughey N, Maragakis NJ. 2016. Connexin 43 in astrocytes contributes to motor neuron toxicity in amyotrophic lateral sclerosis. Glia 64(7):1154-69.

ALSA. 2017. miRagen therapeutics receives ALS Association grant to advance the development of MRG-107. http://wwwalsaorg/news/media/press-releases/miragen-therapeutics-060216html

Ameku T, Taura D, Sone M, Numata T, Nakamura M, Shiota F, Toyoda T, Matsui S, Araoka T, Yasuno T and others. 2016. Identification of MMP1 as a novel risk factor for intracranial aneurysms in ADPKD using iPSC models. Sci Rep 6:30013.

Andersson U, Tracey KJ. 2011. HMGB1 is a therapeutic target for sterile inflammation and infection. Annu Rev Immunol 29:139-62.

Antonucci F, Turola E, Riganti L, Caleo M, Gabrielli M, Perrotta C, Novellino L, Clementi E, Giussani P, Viani P and others. 2012. Microvesicles released from microglia stimulate synaptic activity via enhanced sphingolipid metabolism. EMBO J 31(5):1231-40.

Apolloni S, Fabbrizio P, Amadio S, Volonte C. 2016. Actions of the antihistaminergic clemastine on presymptomatic SOD1-G93A mice ameliorate ALS disease progression. J Neuroinflammation 13(1):191.

Arcuri C, Mecca C, Bianchi R, Giambanco I, Donato R. 2017. The Pathophysiological Role of Microglia in Dynamic Surveillance, Phagocytosis and Structural Remodeling of the Developing CNS. Front Mol Neurosci 10:191.

Aryani A, Denecke B. 2016. Exosomes as a Nanodelivery System: a Key to the Future of Neuromedicine? Mol Neurobiol 53(2):818-34.

Atassi N, Beghi E, Blanquer M, Boulis NM, Cantello R, Caponnetto C, Chio A, Dunnett SB, Feldman EL, Vescovi A and others. 2016. Intraspinal stem cell transplantation for amyotrophic lateral sclerosis: Ready for efficacy clinical trials? Cytotherapy 18(12):1471-1475.

Atkin JD, Farg MA, Walker AK, McLean C, Tomas D, Horne MK. 2008. Endoplasmic reticulum stress and induction of the unfolded protein response in human sporadic amyotrophic lateral sclerosis. Neurobiol Dis 30(3):400-7.

Au NPB, Ma CHE. 2017. Recent Advances in the Study of Bipolar/Rod-Shaped Microglia and their Roles in Neurodegeneration. Front Aging Neurosci 9:128.

Awada R, Rondeau P, Gres S, Saulnier-Blache JS, Lefebvre d'Hellencourt C, Bourdon E. 2012. Autotaxin protects microglial cells against oxidative stress. Free Radic Biol Med 52(2):516-26.

Ayers JI, Fromholt SE, O'Neal VM, Diamond JH, Borchelt DR. 2016. Prion-like propagation of mutant SOD1 misfolding and motor neuron disease spread along neuroanatomical pathways. Acta Neuropathol 131(1):103-14.

Baalman K, Marin MA, Ho TS, Godoy M, Cherian L, Robertson C, Rasband MN. 2015. Axon initial segment-associated microglia. J Neurosci 35(5):2283-92.

Babcock AA, Kuziel WA, Rivest S, Owens T. 2003. Chemokine expression by glial cells directs leukocytes to sites of axonal injury in the CNS. J Neurosci 23(21):7922-30.

Bai Y, Zhu Z, Gao Z, Kong Y. 2014. TLR2 signaling directs NO-dependent MMP-9 induction in mouse microglia. Neurosci Lett 571:5-10.

Baixauli F, Lopez-Otin C, Mittelbrunn M. 2014. Exosomes and autophagy: coordinated mechanisms for the maintenance of cellular fitness. Front Immunol 5:403.

Banjara M, Ghosh C. 2017. Sterile Neuroinflammation and Strategies for Therapeutic Intervention. Int J Inflam 2017:8385961.

Barateiro A, Afonso V, Santos G, Cerqueira JJ, Brites D, van Horssen J, Fernandes A. 2015. S100B as a Potential Biomarker and Therapeutic Target in Multiple Sclerosis. Mol Neurobiol 53(6):3976-3991.

Barateiro A, Miron VE, Santos SD, Relvas JB, Fernandes A, Ffrench-Constant C, Brites D. 2013. Unconjugated bilirubin restricts oligodendrocyte differentiation and axonal myelination. Mol Neurobiol 47(2):632-44.

Barateiro A, Vaz AR, Silva SL, Fernandes A, Brites D. 2012. ER Stress, Mitochondrial Dysfunction and Calpain/JNK Activation are Involved in Oligodendrocyte Precursor Cell Death by Unconjugated Bilirubin. Neuromolecular Med.

Baroja-Mazo A, Martin-Sanchez F, Gomez AI, Martinez CM, Amores-Iniesta J, Compan V, Barbera-Cremades M, Yague J, Ruiz-Ortiz E, Anton J and others. 2014. The NLRP3 inflammasome is released as a particulate danger signal that amplifies the inflammatory response. Nat Immunol 15(8):738-48.

Bartanusz V, Jezova D, Alajajian B, Digicaylioglu M. 2011. The blood-spinal cord barrier: morphology and clinical implications. Ann Neurol 70(2):194-206.

Basso M, Bonetto V. 2016. Extracellular Vesicles and a Novel Form of Communication in the Brain. Front Neurosci 10:127.

Basso M, Pozzi S, Tortarolo M, Fiordaliso F, Bisighini C, Pasetto L, Spaltro G, Lidonnici D, Gensano F, Battaglia E and others. 2013. Mutant copper-zinc superoxide dismutase (SOD1) induces protein secretion pathway alterations and exosome release in astrocytes: implications for disease spreading and motor neuron pathology in amyotrophic lateral sclerosis. J Biol Chem 288(22):15699-711.

Bauernfeind FG, Horvath G, Stutz A, Alnemri ES, MacDonald K, Speert D, Fernandes-Alnemri T, Wu J, Monks BG, Fitzgerald KA and others. 2009. Cutting edge: NF-kappaB activating pattern recognition and cytokine receptors license NLRP3 inflammasome activation by regulating NLRP3 expression. J Immunol 183(2):787-91.

Beers DR, Henkel JS, Xiao Q, Zhao W, Wang J, Yen AA, Siklos L, McKercher SR, Appel SH. 2006. Wild-type microglia extend survival in PU.1 knockout mice with familial amyotrophic lateral sclerosis. Proc Natl Acad Sci U S A 103(43):16021-6.

Beers DR, Henkel JS, Zhao W, Wang J, Appel SH. 2008. CD4+ T cells support glial neuroprotection, slow disease progression, and modify glial morphology in an animal model of inherited ALS. Proc Natl Acad Sci U S A 105(40):15558-63.

Beers DR, Henkel JS, Zhao W, Wang J, Huang A, Wen S, Liao B, Appel SH. 2011. Endogenous regulatory T lymphocytes ameliorate amyotrophic lateral sclerosis in mice and correlate with disease progression in patients with amyotrophic lateral sclerosis. Brain 134(Pt 5):1293-314.

Beers DR, Zhao W, Wang J, Zhang X, Wen S, Neal D, Thonhoff JR, Alsuliman AS, Shpall EJ, Rezvani K and others. 2017. ALS patients' regulatory T lymphocytes are dysfunctional, and correlate with disease progression rate and severity. JCI Insight 2(5):e89530.

Bell-Temin H, Culver-Cochran AE, Chaput D, Carlson CM, Kuehl M, Burkhardt BR, Bickford PC, Liu B, Stevens SM, Jr. 2015. Novel Molecular Insights into Classical and Alternative Activation States of Microglia as Revealed by Stable Isotope Labeling by Amino Acids in Cell Culture (SILAC)-based Proteomics. Mol Cell Proteomics 14(12):3173-84.

Benatar M, Stanislaw C, Reyes E, Hussain S, Cooley A, Fernandez MC, Dauphin DD, Michon SC, Andersen PM, Wuu J. 2016. Presymptomatic ALS genetic counseling and testing: Experience and recommendations. Neurology 86(24):2295-302.

Benatar M, Wuu J. 2012. Presymptomatic studies in ALS: rationale, challenges, and approach. Neurology 79(16):1732-9.

Benigni M, Ricci C, Jones AR, Giannini F, Al-Chalabi A, Battistini S. 2016. Identification of miRNAs as Potential Biomarkers in Cerebrospinal Fluid from Amyotrophic Lateral Sclerosis Patients. Neuromolecular Med 18(4):551-560.

Bertheloot D, Naumovski AL, Langhoff P, Horvath GL, Jin T, Xiao TS, Garbi N, Agrawal S, Kolbeck R, Latz E. 2016. RAGE Enhances TLR Responses through Binding and Internalization of RNA. J Immunol 197(10):4118-4126.

Bezbradica JS, Coll RC, Schroder K. 2017. Sterile signals generate weaker and delayed macrophage NLRP3 inflammasome responses relative to microbial signals. Cell Mol Immunol 14(1):118-126.

Bianco F, Perrotta C, Novellino L, Francolini M, Riganti L, Menna E, Saglietti L, Schuchman EH, Furlan R, Clementi E and others. 2009. Acid sphingomyelinase activity triggers microparticle release from glial cells. EMBO J 28(8):1043-54.

Blasi E, Barluzzi R, Bocchini V, Mazzolla R, Bistoni F. 1990. Immortalization of murine microglial cells by a v-raf/v-myc carrying retrovirus. J Neuroimmunol 27(2-3):229-37.

Block ML, Zecca L, Hong JS. 2007. Microglia-mediated neurotoxicity: uncovering the molecular mechanisms. Nat Rev Neurosci 8(1):57-69.

Boddeke EW, Meigel I, Frentzel S, Biber K, Renn LQ, Gebicke-Harter P. 1999. Functional expression of the fractalkine (CX3C) receptor and its regulation by lipopolysaccharide in rat microglia. Eur J Pharmacol 374(2):309-13.

Boehme SA, Lio FM, Maciejewski-Lenoir D, Bacon KB, Conlon PJ. 2000. The chemokine fractalkine inhibits Fas-mediated cell death of brain microglia. J Immunol 165(1):397-403.

Bohlen CJ, Bennett FC, Tucker AF, Collins HY, Mulinyawe SB, Barres BA. 2017. Diverse Requirements for Microglial Survival, Specification, and Function Revealed by Defined-Medium Cultures. Neuron 94(4):759-773 e8.

Boillée S, Vande Velde C, Cleveland DW. 2006a. ALS: a disease of motor neurons and their nonneuronal neighbors. Neuron 52(1):39-59.

Boillée S, Yamanaka K, Lobsiger CS, Copeland NG, Jenkins NA, Kassiotis G, Kollias G, Cleveland DW. 2006b. Onset and progression in inherited ALS determined by motor neurons and microglia. Science 312(5778):1389-92.

Bonafede R, Mariotti R. 2017. ALS Pathogenesis and Therapeutic Approaches: The Role of Mesenchymal Stem Cells and Extracellular Vesicles. Front Cell Neurosci 11:80.

Bonnay F, Nguyen XH, Cohen-Berros E, Troxler L, Batsche E, Camonis J, Takeuchi O, Reichhart JM, Matt N. 2014. Akirin specifies NF-kappaB selectivity of Drosophila innate immune response via chromatin remodeling. EMBO J 33(20):2349-62.

Bosco DA, Morfini G, Karabacak NM, Song Y, Gros-Louis F, Pasinelli P, Goolsby H, Fontaine BA, Lemay N, McKenna-Yasek D and others. 2010. Wild-type and mutant SOD1 share an aberrant conformation and a common pathogenic pathway in ALS. Nat Neurosci 13(11):1396-403.

Bose S, Kim S, Oh Y, Moniruzzaman M, Lee G, Cho J. 2016. Effect of CCL2 on BV2 microglial cell migration: Involvement of probable signaling pathways. Cytokine 81:39-49.

Boylan KB, Glass JD, Crook JE, Yang C, Thomas CS, Desaro P, Johnston A, Overstreet K, Kelly C, Polak M and others. 2013. Phosphorylated neurofilament heavy subunit (pNF-H) in peripheral blood and CSF as a potential prognostic biomarker in amyotrophic lateral sclerosis. J Neurol Neurosurg Psychiatry 84(4):467-72.

Bretz NP, Ridinger J, Rupp AK, Rimbach K, Keller S, Rupp C, Marme F, Umansky L, Umansky V, Eigenbrod T and others. 2013. Body fluid exosomes promote secretion of inflammatory cytokines in monocytic cells via Toll-like receptor signaling. J Biol Chem 288(51):36691-702.

Brites D. 2015. Cell ageing: a flourishing field for neurodegenerative diseases. AIMS Molecular Science 2(3):225-258.

Brites D, Fernandes A. 2015. Bilirubin-induced neural impairment: A special focus on myelination, age-related windows of susceptibility and associated co-morbidities. Semin Fetal Neonatal Med 20(1):14-19.

Brites D, Fernandes A. 2016. Neuroinflammation and Depression: Microglia Activation, Extracellular Microvesicles and microRNA Dysregulation. Front Cell Neurosci 9:476.

Brites D, Gomes C, Pinheiro R, Falcão AS. 2015. New Insights in the Pro- and Anti-Neurogenic Interventions of Microglia and Their Association to Gliomas. in Microglia. New York: NY: Nova Science Publishers.

Brites D, Vaz AR. 2014. Microglia centered pathogenesis in ALS: insights in cell interconnectivity. Front Cell Neurosci 8:117.

Bronstein R, Torres L, Nissen JC, Tsirka SE. 2013. Culturing microglia from the neonatal and adult central nervous system. J Vis Exp(78):50647.

Brown GC, Neher JJ. 2014. Microglial phagocytosis of live neurons. Nat Rev Neurosci 15(4):209-16.

Bruce-Keller AJ, Keeling JL, Keller JN, Huang FF, Camondola S, Mattson MP. 2000. Antiinflammatory effects of estrogen on microglial activation. Endocrinology 141(10):3646-56.

Bruijn LI, Houseweart MK, Kato S, Anderson KL, Anderson SD, Ohama E, Reaume AG, Scott RW, Cleveland DW. 1998. Aggregation and motor neuron toxicity of an ALS-linked SOD1 mutant independent from wild-type SOD1. Science 281(5384):1851-4.

Budini M, Buratti E, Morselli E, Criollo A. 2017. Autophagy and Its Impact on Neurodegenerative Diseases: New Roles for TDP-43 and C9orf72. Front Mol Neurosci 10:170.

Budnik V, Ruiz-Canada C, Wendler F. 2016. Extracellular vesicles round off communication in the nervous system. Nat Rev Neurosci 17(3):160-72.

Burm SM, Zuiderwijk-Sick EA, t Jong AE, van der Putten C, Veth J, Kondova I, Bajramovic JJ. 2015. Inflammasome-induced IL-1beta secretion in microglia is characterized by delayed kinetics and is only partially dependent on inflammatory caspases. J Neurosci 35(2):678-87.

Bussi C, Ramos JM, Arroyo DS, Gaviglio EA, Gallea JI, Wang JM, Celej MS, Iribarren P. 2017. Autophagy down regulates pro-inflammatory mediators in BV2 microglial cells and rescues both LPS and alpha-synuclein induced neuronal cell death. Sci Rep 7:43153.

Butovsky O, Jedrychowski MP, Cialic R, Krasemann S, Murugaiyan G, Fanek Z, Greco DJ, Wu PM, Doykan CE, Kiner O and others. 2015. Targeting miR-155 restores abnormal microglia and attenuates disease in SOD1 mice. Ann Neurol 77(1):75-99.

Butovsky O, Jedrychowski MP, Moore CS, Cialic R, Lanser AJ, Gabriely G, Koeglsperger T, Dake B, Wu PM, Doykan CE and others. 2014. Identification of a unique TGF-beta-dependent molecular and functional signature in microglia. Nat Neurosci 17(1):131-43.

Butovsky O, Siddiqui S, Gabriely G, Lanser AJ, Dake B, Murugaiyan G, Doykan CE, Wu PM, Gali RR, Iyer LK and others. 2012. Modulating inflammatory monocytes with a unique microRNA gene signature ameliorates murine ALS. J Clin Invest 122(9):3063-87.

Cadwell K. 2016. Crosstalk between autophagy and inflammatory signalling pathways: balancing defence and homeostasis. Nat Rev Immunol 16(11):661-675.

Cady J, Koval ED, Benitez BA, Zaidman C, Jockel-Balsarotti J, Allred P, Baloh RH, Ravits J, Simpson E, Appel SH and others. 2014. TREM2 variant p.R47H as a risk factor for sporadic amyotrophic lateral sclerosis. JAMA Neurol 71(4):449-53.

Cai H, Liang Q, Ge G. 2016. Gypenoside Attenuates beta Amyloid-Induced Inflammation in N9 Microglial Cells via SOCS1 Signaling. Neural Plast 2016:6362707.

Caldeira C, Oliveira AF, Cunha C, Vaz AR, Falcao AS, Fernandes A, Brites D. 2014. Microglia change from a reactive to an age-like phenotype with the time in culture. Front Cell Neurosci 8:152.

Calvo M, Bennett DL. 2011. The mechanisms of microgliosis and pain following peripheral nerve injury. Exp Neurol 234(2):271-82.

Campos-Melo D, Droppelmann CA, He Z, Volkening K, Strong MJ. 2013. Altered microRNA expression profile in Amyotrophic Lateral Sclerosis: a role in the regulation of NFL mRNA levels. Mol Brain 6:26.

Cardona AE, Huang D, Sasse ME, Ransohoff RM. 2006a. Isolation of murine microglial cells for RNA analysis or flow cytometry. Nat Protoc 1(4):1947-51.

Cardona AE, Pioro EP, Sasse ME, Kostenko V, Cardona SM, Dijkstra IM, Huang D, Kidd G, Dombrowski S, Dutta R and others. 2006b. Control of microglial neurotoxicity by the fractalkine receptor. Nat Neurosci 9(7):917-24.

Cardoso AL, Guedes JR, de Lima MC. 2016. Role of microRNAs in the regulation of innate immune cells under neuroinflammatory conditions. Curr Opin Pharmacol 26:1-9.

Cardoso AL, Guedes JR, Pereira de Almeida L, Pedroso de Lima MC. 2012. miR-155 modulates microglia-mediated immune response by down-regulating SOCS-1 and promoting cytokine and nitric oxide production. Immunology 135(1):73-88.

Cardoso FL, Herz J, Fernandes A, Rocha J, Sepodes B, Brito MA, McGavern DB, Brites D. 2015. Systemic inflammation in early neonatal mice induces transient and lasting neurodegenerative effects. J Neuroinflammation 12:82.

Carlesi C, Pasquali L, Piazza S, Lo Gerfo A, Caldarazzo Ienco E, Alessi R, Fornai F, Siciliano G. 2011. Strategies for clinical approach to neurodegeneration in Amyotrophic lateral sclerosis. Arch Ital Biol 149(1):151-67.

Carroll B, Hewitt G, Korolchuk VI. 2013. Autophagy and ageing: implications for age-related neurodegenerative diseases. Essays Biochem 55:119-31.

Cashman NR, Durham HD, Blusztajn JK, Oda K, Tabira T, Shaw IT, Dahrouge S, Antel JP. 1992. Neuroblastoma x spinal cord (NSC) hybrid cell lines resemble developing motor neurons. Dev Dyn 194(3):209-21.

Casula M, Iyer AM, Spliet WG, Anink JJ, Steentjes K, Sta M, Troost D, Aronica E. 2011. Toll-like receptor signaling in amyotrophic lateral sclerosis spinal cord tissue. Neuroscience 179:233-43.

Catalanotto C, Cogoni C, Zardo G. 2016. MicroRNA in Control of Gene Expression: An Overview of Nuclear Functions. Int J Mol Sci 17(10).

Cãtaña CS, Calin GA, Berindan-Neagoe I. 2015. Inflamma-miRs in Aging and Breast Cancer: Are They Reliable Players? Front Med (Lausanne) 2:85.

Chapman GA, Moores K, Harrison D, Campbell CA, Stewart BR, Strijbos PJ. 2000. Fractalkine cleavage from neuronal membranes represents an acute event in the inflammatory response to excitotoxic brain damage. J Neurosci 20(15):RC87.

Che P, Liu J, Shan Z, Wu R, Yao C, Cui J, Zhu X, Wang J, Burnett MS, Wang S. 2014. miR-125a-5p impairs endothelial cell angiogenesis in aging mice via RTEF-1 downregulation. Aging Cell 13(5):926-34.

Chen SC, Leach MW, Chen Y, Cai XY, Sullivan L, Wiekowski M, Dovey-Hartman BJ, Zlotnik A, Lira SA. 2002. Central nervous system inflammation and neurological disease in transgenic mice expressing the CC chemokine CCL21 in oligodendrocytes. J Immunol 168(3):1009-17.

Chen SM, Chou WC, Hu LY, Hsiung CN, Chu HW, Huang YL, Hsu HM, Yu JC, Shen CY. 2015. The Effect of MicroRNA-124 Overexpression on Anti-Tumor Drug Sensitivity. PLoS One 10(6):e0128472.

Chen WX, Liu XM, Lv MM, Chen L, Zhao JH, Zhong SL, Ji MH, Hu Q, Luo Z, Wu JZ and others. 2014. Exosomes from drug-resistant breast cancer cells transmit chemoresistance by a horizontal transfer of microRNAs. PLoS One 9(4):e95240.

Chen X, Chen Y, Wei Q, Ou R, Cao B, Zhao B, Shang HF. 2016. Assessment of a multiple biomarker panel for diagnosis of amyotrophic lateral sclerosis. BMC Neurol 16:173.

Chen X, Shang HF. 2015. New developments and future opportunities in biomarkers for amyotrophic lateral sclerosis. Transl Neurodegener 4:17.

Chen Z, Jalabi W, Shpargel KB, Farabaugh KT, Dutta R, Yin X, Kidd GJ, Bergmann CC, Stohlman SA, Trapp BD. 2012. Lipopolysaccharide-induced microglial activation and neuroprotection against experimental brain injury is independent of hematogenous TLR4. J Neurosci 32(34):11706-15.

Cheng Y, Schorey JS. 2016. Targeting soluble proteins to exosomes using a ubiquitin tag. Biotechnol Bioeng 113(6):1315-24.

Cherry JD, Olschowka JA, O'Banion MK. 2014. Neuroinflammation and M2 microglia: the good, the bad, and the inflamed. J Neuroinflammation 11:98.

Chhor V, Le Charpentier T, Lebon S, Ore MV, Celador IL, Josserand J, Degos V, Jacotot E, Hagberg H, Savman K and others. 2013. Characterization of phenotype markers and neuronotoxic potential of polarised primary microglia in vitro. Brain Behav Immun 32:70-85.

Chiò A, Logroscino G, Traynor BJ, Collins J, Simeone JC, Goldstein LA, White LA. 2013. Global epidemiology of amyotrophic lateral sclerosis: a systematic review of the published literature. Neuroepidemiology 41(2):118-30.

Chio A, Mora G, Leone M, Mazzini L, Cocito D, Giordana MT, Bottacchi E, Mutani R. 2002. Early symptom progression rate is related to ALS outcome: a prospective population-based study. Neurology 59(1):99-103.

Chiu IM, Chen A, Zheng Y, Kosaras B, Tsiftsoglou SA, Vartanian TK, Brown RH, Jr., Carroll MC. 2008. T lymphocytes potentiate endogenous neuroprotective inflammation in a mouse model of ALS. Proc Natl Acad Sci U S A 105(46):17913-8.

Chiu IM, Morimoto ET, Goodarzi H, Liao JT, O'Keeffe S, Phatnani HP, Muratet M, Carroll MC, Levy S, Tavazoie S and others. 2013. A neurodegeneration-specific gene-expression signature of acutely isolated microglia from an amyotrophic lateral sclerosis mouse model. Cell Rep 4(2):385-401.

Cho GW, Kim GY, Baek S, Kim H, Kim T, Kim HJ, Kim SH. 2011. Recombinant human erythropoietin reduces aggregation of mutant Cu/Zn-binding superoxide dismutase (SOD1) in NSC-34 cells. Neurosci Lett 504(2):107-11.

Cho KO, La HO, Cho YJ, Sung KW, Kim SY. 2006. Minocycline attenuates white matter damage in a rat model of chronic cerebral hypoperfusion. J Neurosci Res 83(2):285-91.

Cianciulli A, Calvello R, Porro C, Trotta T, Panaro MA. 2017. Understanding the role of SOCS signaling in neurodegenerative diseases: Current and emerging concepts. Cytokine Growth Factor Rev.

Cirulli ET, Lasseigne BN, Petrovski S, Sapp PC, Dion PA, Leblond CS, Couthouis J, Lu YF, Wang Q, Krueger BJ and others. 2015. Exome sequencing in amyotrophic lateral sclerosis identifies risk genes and pathways. Science 347(6229):1436-41.

Ciryam P, Kundra R, Freer R, Morimoto RI, Dobson CM, Vendruscolo M. 2016. A transcriptional signature of Alzheimer's disease is associated with a metastable subproteome at risk for aggregation. Proc Natl Acad Sci U S A 113(17):4753-8.

Clark AK, Gentry C, Bradbury EJ, McMahon SB, Malcangio M. 2007. Role of spinal microglia in rat models of peripheral nerve injury and inflammation. Eur J Pain 11(2):223-30.

Clement AM, Nguyen MD, Roberts EA, Garcia ML, Boillee S, Rule M, McMahon AP, Doucette W, Siwek D, Ferrante RJ and others. 2003. Wild-type nonneuronal cells extend survival of SOD1 mutant motor neurons in ALS mice. Science 302(5642):113-7.

Cobos Jimenez V, Bradley EJ, Willemsen AM, van Kampen AH, Baas F, Kootstra NA. 2014. Next-generation sequencing of microRNAs uncovers expression signatures in polarized macrophages. Physiol Genomics 46(3):91-103.

Colton CA. 2009. Heterogeneity of microglial activation in the innate immune response in the brain. J Neuroimmune Pharmacol 4(4):399-418.

Corcia P, Tauber C, Vercoullie J, Arlicot N, Prunier C, Praline J, Nicolas G, Venel Y, Hommet C, Baulieu JL and others. 2013. Molecular imaging of microglial activation in amyotrophic lateral sclerosis. PLoS One 7(12):e52941.

Costa J, Swash M, de Carvalho M. 2012. Awaji criteria for the diagnosis of amyotrophic lateral sclerosis:a systematic review. Arch Neurol 69(11):1410-6.

Crain JM, Nikodemova M, Watters JJ. 2013. Microglia express distinct M1 and M2 phenotypic markers in the postnatal and adult central nervous system in male and female mice. J Neurosci Res 91(9):1143-51.

Crain JM, Watters JJ. 2016. Microglial P2 Purinergic Receptor and Immunomodulatory Gene Transcripts Vary By Region, Sex, and Age in the Healthy Mouse CNS. Transcr Open Access 3(2).

Crisafulli SG, Brajkovic S, Cipolat Mis MS, Parente V, Corti S. 2017. Therapeutic Strategies Under Development Targeting Inflammatory Mechanisms in Amyotrophic Lateral Sclerosis. Mol Neurobiol.

Cui YH, Le Y, Gong W, Proost P, Van Damme J, Murphy WJ, Wang JM. 2002. Bacterial lipopolysaccharide selectively up-regulates the function of the chemotactic peptide receptor formyl peptide receptor 2 in murine microglial cells. J Immunol 168(1):434-42.

Cunha C, Gomes C, Vaz AR, Brites D. 2016. Exploring New Inflammatory Biomarkers and Pathways during LPS-Induced M1 Polarization. Mediators Inflamm 2016:6986175.

Cunha C, Santos C, Gomes C, Fernandes A, Correia AM, Sebastiao AM, Vaz AR, Brites D. 2017. Downregulated Glia Interplay and Increased miRNA-155 as Promising Markers to Track ALS at an Early Stage. Mol Neurobiol.

Cunningham CL, Martinez-Cerdeno V, Noctor SC. 2013. Microglia regulate the number of neural precursor cells in the developing cerebral cortex. J Neurosci 33(10):4216-33.

Czochor JR, Sulkowski P, Glazer PM. 2016. miR-155 Overexpression Promotes Genomic Instability by Reducing High-fidelity Polymerase Delta Expression and Activating Error-Prone DSB Repair. Mol Cancer Res 14(4):363-73.

Das A, Ghatak S, Sinha M, Chaffee S, Ahmed NS, Parinandi NL, Wohleb ES, Sheridan JF, Sen CK, Roy S. 2016. Correction of MFG-E8 Resolves Inflammation and Promotes Cutaneous Wound Healing in Diabetes. J Immunol 196(12):5089-100.

Davalos D, Grutzendler J, Yang G, Kim JV, Zuo Y, Jung S, Littman DR, Dustin ML, Gan WB. 2005. ATP mediates rapid microglial response to local brain injury in vivo. Nat Neurosci 8(6):752-8.

Davalos D, Ryu JK, Merlini M, Baeten KM, Le Moan N, Petersen MA, Deerinck TJ, Smirnoff DS, Bedard C, Hakozaki H and others. 2012. Fibrinogen-induced perivascular microglial clustering is required for the development of axonal damage in neuroinflammation. Nat Commun 3:1227.

David S, Kroner A. 2011. Repertoire of microglial and macrophage responses after spinal cord injury. Nat Rev Neurosci 12(7):388-99.

De Biase LM, Schuebel KE, Fusfeld ZH, Jair K, Hawes IA, Cimbro R, Zhang HY, Liu QR, Shen H, Xi ZX and others. 2017. Local Cues Establish and Maintain Region-Specific Phenotypes of Basal Ganglia Microglia. Neuron 95(2):341-356 e6.

De Carvalho M, Dengler R, Eisen A, England JD, Kaji R, Kimura J, Mills K, Mitsumoto H, Nodera H, Shefner J and others. 2008. Electrodiagnostic criteria for diagnosis of ALS. Clin Neurophysiol 119(3):497-503.

De Carvalho M, Ryczkowski A, Andersen P, Gromicho M, Grosskreutz J, Kuzma-Kozakiewicz M, Petri S, Piotrkiewicz M, Miltenberger Miltenyi G. 2017. International Survey of ALS Experts about Critical Questions for Assessing Patients with ALS. Amyotroph Lateral Scler Frontotemporal Degener:1-6.

de Haas AH, Boddeke HW, Biber K. 2008. Region-specific expression of immunoregulatory proteins on microglia in the healthy CNS. Glia 56(8):888-94.

de Jong EK, Dijkstra IM, Hensens M, Brouwer N, van Amerongen M, Liem RS, Boddeke HW, Biber K. 2005. Vesicle-mediated transport and release of CCL21 in endangered neurons: a possible explanation for microglia activation remote from a primary lesion. J Neurosci 25(33):7548-57.

De Lucia C, Rinchon A, Olmos-Alonso A, Riecken K, Fehse B, Boche D, Perry VH, Gomez-Nicola D. 2016. Microglia regulate hippocampal neurogenesis during chronic neurodegeneration. Brain Behav Immun 55:179-190.

De Vos KJ, Chapman AL, Tennant ME, Manser C, Tudor EL, Lau KF, Brownlees J, Ackerley S, Shaw PJ, McLoughlin DM and others. 2007. Familial amyotrophic lateral sclerosis-linked SOD1 mutants perturb fast axonal transport to reduce axonal mitochondria content. Hum Mol Genet 16(22):2720-2728.

Debacq-Chainiaux F, Erusalimsky JD, Campisi J, Toussaint O. 2009. Protocols to detect senescence-associated beta-galactosidase (SA-betagal) activity, a biomarker of senescent cells in culture and in vivo. Nat Protoc 4(12):1798-806.

Deguise MO, Kothary R. 2017. New insights into SMA pathogenesis: immune dysfunction and neuroinflammation. Ann Clin Transl Neurol 4(7):522-530.

DeJesus-Hernandez M, Mackenzie IR, Boeve BF, Boxer AL, Baker M, Rutherford NJ, Nicholson AM, Finch NA, Flynn H, Adamson J and others. 2011. Expanded GGGGCC hexanucleotide repeat in noncoding region of C9ORF72 causes chromosome 9p-linked FTD and ALS. Neuron 72(2):245-56.

Deleidi M, Jaggle M, Rubino G. 2015. Immune aging, dysmetabolism, and inflammation in neurological diseases. Front Neurosci 9:172.

Dellago H, Preschitz-Kammerhofer B, Terlecki-Zaniewicz L, Schreiner C, Fortschegger K, Chang MW, Hackl M, Monteforte R, Kuhnel H, Schosserer M and others. 2013. High levels of oncomiR-21 contribute to the senescence-induced growth arrest in normal human cells and its knock-down increases the replicative lifespan. Aging Cell 12(3):446-58.

Deng HX, Chen W, Hong ST, Boycott KM, Gorrie GH, Siddique N, Yang Y, Fecto F, Shi Y, Zhai H and others. 2011. Mutations in UBQLN2 cause dominant X-linked juvenile and adult-onset ALS and ALS/dementia. Nature 477(7363):211-5.

Deng T, Feng X, Liu P, Yan K, Chen Y, Han D. 2013. Toll-like receptor 3 activation differentially regulates phagocytosis of bacteria and apoptotic neutrophils by mouse peritoneal macrophages. Immunol Cell Biol 91(1):52-9.

Denieffe S, Kelly RJ, McDonald C, Lyons A, Lynch MA. 2013. Classical activation of microglia in CD200-deficient mice is a consequence of blood brain barrier permeability and infiltration of peripheral cells. Brain Behav Immun 34:86-97.

Dharmadasa T, Henderson RD, Talman PS, Macdonell RA, Mathers S, Schultz DW, Needham M, Zoing M, Vucic S, Kiernan MC. 2017. Motor neurone disease: progress and challenges. Med J Aust 206(8):357-362.

Diaz-Amarilla P, Olivera-Bravo S, Trias E, Cragnolini A, Martinez-Palma L, Cassina P, Beckman J, Barbeito L. 2011. Phenotypically aberrant astrocytes that promote motoneuron damage in a model of inherited amyotrophic lateral sclerosis. Proc Natl Acad Sci U S A 108(44):18126-31.

Dibaj P, Nadrigny F, Steffens H, Scheller A, Hirrlinger J, Schomburg ED, Neusch C, Kirchhoff F. 2010. NO mediates microglial response to acute spinal cord injury under ATP control in vivo. Glia 58(9):1133-44.

Doens D, Fernandez PL. 2014. Microglia receptors and their implications in the response to amyloid beta for Alzheimer's disease pathogenesis. J Neuroinflammation 11:48.

Domingues HS, Portugal CC, Socodato R, Relvas JB. 2016. Oligodendrocyte, Astrocyte, and Microglia Crosstalk in Myelin Development, Damage, and Repair. Front Cell Dev Biol 4:71.

Doorn KJ, Goudriaan A, Blits-Huizinga C, Bol JG, Rozemuller AJ, Hoogland PV, Lucassen PJ, Drukarch B, van de Berg WD, van Dam AM. 2013. Increased amoeboid microglial density in the olfactory bulb of Parkinson's and Alzheimer's patients. Brain Pathol 24(2):152-65.

Dozio V, Sanchez JC. 2017. Characterisation of extracellular vesicle-subsets derived from brain endothelial cells and analysis of their protein cargo modulation after TNF exposure. J Extracell Vesicles 6(1):1302705.

Drechsel DA, Estevez AG, Barbeito L, Beckman JS. 2012. Nitric oxide-mediated oxidative damage and the progressive demise of motor neurons in ALS. Neurotox Res 22(4):251-64.

Dudvarski Stankovic N, Teodorczyk M, Ploen R, Zipp F, Schmidt MH. 2016. Microglia-blood vessel interactions: a double-edged sword in brain pathologies. Acta Neuropathol 131(3):347-63.

Durafourt BA, Moore CS, Zammit DA, Johnson TA, Zaguia F, Guiot MC, Bar-Or A, Antel JP. 2012. Comparison of polarization properties of human adult microglia and blood-derived macrophages. Glia 60(5):717-27.

Dutta S, Warshall C, Bandyopadhyay C, Dutta D, Chandran B. 2014. Interactions between exosomes from breast cancer cells and primary mammary epithelial cells leads to generation of reactive oxygen species which induce DNA damage response, stabilization of p53 and autophagy in epithelial cells. PLoS One 9(5):e97580.

Ehrhart J, Smith AJ, Kuzmin-Nichols N, Zesiewicz TA, Jahan I, Shytle RD, Kim SH, Sanberg CD, Vu TH, Gooch CL and others. 2015. Humoral factors in ALS patients during disease progression. J Neuroinflammation 12:127.

Eisen A, Mezei MM, Stewart HG, Fabros M, Gibson G, Andersen PM. 2008. SOD1 gene mutations in ALS patients from British Columbia, Canada: clinical features, neurophysiology and ethical issues in management. Amyotroph Lateral Scler 9(2):108-19.

Elliott JL. 2001. Cytokine upregulation in a murine model of familial amyotrophic lateral sclerosis. Brain Res Mol Brain Res 95(1-2):172-8.

Endo F, Komine O, Fujimori-Tonou N, Katsuno M, Jin S, Watanabe S, Sobue G, Dezawa M, Wyss-Coray T, Yamanaka K. 2015. Astrocyte-derived TGF-beta1 accelerates disease progression in ALS mice by interfering with the neuroprotective functions of microglia and T cells. Cell Rep 11(4):592-604.

Eun SY, Seo J, Park SW, Lee JH, Chang KC, Kim HJ. 2013. LPS potentiates nucleotide-induced inflammatory gene expression in macrophages via the upregulation of P2Y2 receptor. Int Immunopharmacol 18(2):270-6.

Ezzi SA, Lariviere R, Urushitani M, Julien JP. 2010. Neuronal over-expression of chromogranin A accelerates disease onset in a mouse model of ALS. J Neurochem 115(5):1102-11.

Falcão AS, Carvalho LA, Lidonio G, Vaz AR, Lucas SD, Moreira R, Brites D. 2017. Dipeptidyl Vinyl Sulfone as a Novel Chemical Tool to Inhibit HMGB1/NLRP3-Inflammasome and Inflamma-miRs in Abeta-Mediated Microglial Inflammation. ACS Chem Neurosci 8(1):89-99.

Fan H, Zhang K, Shan L, Kuang F, Chen K, Zhu K, Ma H, Ju G, Wang YZ. 2016. Reactive astrocytes undergo M1 microglia/macrohpages-induced necroptosis in spinal cord injury. Mol Neurodegener 11:14.

Fan Y, Xie L, Chung CY. 2017. Signaling Pathways Controlling Microglia Chemotaxis. Mol Cells 40(3):163-168.

Fang L, Huber-Abel F, Teuchert M, Hendrich C, Dorst J, Schattauer D, Zettlmeissel H, Wlaschek M, Scharffetter-Kochanek K, Tumani H and others. 2009. Linking neuron and skin: matrix metalloproteinases in amyotrophic lateral sclerosis (ALS). J Neurol Sci 285(1-2):62-6.

Fanjul-Fernández M, Folgueras AR, Cabrera S, Lopez-Otin C. 2010. Matrix metalloproteinases: evolution, gene regulation and functional analysis in mouse models. Biochim Biophys Acta 1803(1):3-19.

Faraco G, Fossati S, Bianchi ME, Patrone M, Pedrazzi M, Sparatore B, Moroni F, Chiarugi A. 2007. High mobility group box 1 protein is released by neural cells upon different stresses and worsens ischemic neurodegeneration in vitro and in vivo. J Neurochem 103(2):590-603.

Färber K, Pannasch U, Kettenmann H. 2005. Dopamine and noradrenaline control distinct functions in rodent microglial cells. Mol Cell Neurosci 29(1):128-38.

Fecto F, Yan J, Vemula SP, Liu E, Yang Y, Chen W, Zheng JG, Shi Y, Siddique N, Arrat H and others. 2011. SQSTM1 mutations in familial and sporadic amyotrophic lateral sclerosis. Arch Neurol 68(11):1440-6.

Feldman EL, Boulis NM, Hur J, Johe K, Rutkove SB, Federici T, Polak M, Bordeau J, Sakowski SA, Glass JD. 2014. Intraspinal neural stem cell transplantation in amyotrophic lateral sclerosis: phase 1 trial outcomes. Ann Neurol 75(3):363-73.

Feng X, Deng T, Zhang Y, Su S, Wei C, Han D. 2011. Lipopolysaccharide inhibits macrophage phagocytosis of apoptotic neutrophils by regulating the production of tumour necrosis factor alpha and growth arrest-specific gene 6. Immunology 132(2):287-95.

Fernandes A, Falcão AS, Silva RF, Brito MA, Brites D. 2007. MAPKs are key players in mediating cytokine release and cell death induced by unconjugated bilirubin in cultured rat cortical astrocytes. Eur J Neurosci 25(4):1058-68.

Fernandes A, Falcão AS, Silva RF, Gordo AC, Gama MJ, Brito MA, Brites D. 2006. Inflammatory signalling pathways involved in astroglial activation by unconjugated bilirubin. J Neurochem 96(6):1667-79.

Fernandes A, Miller-Fleming L, Pais TF. 2014. Microglia and inflammation: conspiracy, controversy or control? Cell Mol Life Sci 71(20):3969-85.

Ferraiuolo L, Higginbottom A, Heath PR, Barber S, Greenald D, Kirby J, Shaw PJ. 2011a. Dysregulation of astrocyte-motoneuron cross-talk in mutant superoxide dismutase 1-related amyotrophic lateral sclerosis. Brain 134(Pt 9):2627-41.

Ferraiuolo L, Kirby J, Grierson AJ, Sendtner M, Shaw PJ. 2011b. Molecular pathways of motor neuron injury in amyotrophic lateral sclerosis. Nat Rev Neurol 7(11):616-30.

Ferraiuolo L, Meyer K, Sherwood TW, Vick J, Likhite S, Frakes A, Miranda CJ, Braun L, Heath PR, Pineda R and others. 2016. Oligodendrocytes contribute to motor neuron death in ALS via SOD1-dependent mechanism. Proc Natl Acad Sci U S A 113(42):E6496-E6505.

Fischer LR, Culver DG, Tennant P, Davis AA, Wang M, Castellano-Sanchez A, Khan J, Polak MA, Glass JD. 2004. Amyotrophic lateral sclerosis is a distal axonopathy: evidence in mice and man. Exp Neurol 185(2):232-40.

Fitzner D, Schnaars M, van Rossum D, Krishnamoorthy G, Dibaj P, Bakhti M, Regen T, Hanisch UK, Simons M. 2011. Selective transfer of exosomes from oligodendrocytes to microglia by macropinocytosis. J Cell Sci 124(Pt 3):447-58.

Fleisher-Berkovich S, Filipovich-Rimon T, Ben-Shmuel S, Hulsmann C, Kummer MP, Heneka MT. 2010. Distinct modulation of microglial amyloid beta phagocytosis and migration by neuropeptides (i). J Neuroinflammation 7:61.

Foo LC, Allen NJ, Bushong EA, Ventura PB, Chung WS, Zhou L, Cahoy JD, Daneman R, Zong H, Ellisman MH and others. 2011. Development of a method for the purification and culture of rodent astrocytes. Neuron 71(5):799-811.

Foust KD, Nurre E, Montgomery CL, Hernandez A, Chan CM, Kaspar BK. 2009. Intravascular AAV9 preferentially targets neonatal neurons and adult astrocytes. Nat Biotechnol 27(1):59-65.

Foust KD, Salazar DL, Likhite S, Ferraiuolo L, Ditsworth D, Ilieva H, Meyer K, Schmelzer L, Braun L, Cleveland DW and others. 2013. Therapeutic AAV9-mediated suppression of mutant SOD1 slows disease progression and extends survival in models of inherited ALS. Mol Ther 21(12):2148-59.

Frakes AE, Braun L, Ferraiuolo L, Guttridge DC, Kaspar BK. 2017. Additive amelioration of ALS by co-targeting independent pathogenic mechanisms. Ann Clin Transl Neurol 4(2):76-86.

Frakes AE, Ferraiuolo L, Haidet-Phillips AM, Schmelzer L, Braun L, Miranda CJ, Ladner KJ, Bevan AK, Foust KD, Godbout JP and others. 2014. Microglia induce motor neuron death via the classical NF-kappaB pathway in amyotrophic lateral sclerosis. Neuron 81(5):1009-23.

Frank MG, Barrientos RM, Biedenkapp JC, Rudy JW, Watkins LR, Maier SF. 2006. mRNA up-regulation of MHC II and pivotal pro-inflammatory genes in normal brain aging. Neurobiol Aging 27(5):717-22.

Freilich RW, Woodbury ME, Ikezu T. 2013. Integrated expression profiles of mRNA and miRNA in polarized primary murine microglia. PLoS One 8(11):e79416.

Freischmidt A, Wieland T, Richter B, Ruf W, Schaeffer V, Muller K, Marroquin N, Nordin F, Hubers A, Weydt P and others. 2015. Haploinsufficiency of TBK1 causes familial ALS and fronto-temporal dementia. Nat Neurosci 18(5):631-6.

Fricker M, Neher JJ, Zhao JW, Thery C, Tolkovsky AM, Brown GC. 2012. MFG-E8 mediates primary phagocytosis of viable neurons during neuroinflammation. J Neurosci 32(8):2657-66.

Fritz E, Izaurieta P, Weiss A, Mir FR, Rojas P, Gonzalez D, Rojas F, Brown RH, Jr., Madrid R, van Zundert B. 2013. Mutant SOD1-expressing astrocytes release toxic factors that trigger motoneuron death by inducing hyperexcitability. J Neurophysiol 109(11):2803-14.

Frühbeis C, Frohlich D, Kuo WP, Kramer-Albers EM. 2013. Extracellular vesicles as mediators of neuron-glia communication. Front Cell Neurosci 7:182.

Fu R, Shen Q, Xu P, Luo JJ, Tang Y. 2014. Phagocytosis of microglia in the central nervous system diseases. Mol Neurobiol 49(3):1422-34.

Fujita K, Motoki K, Tagawa K, Chen X, Hama H, Nakajima K, Homma H, Tamura T, Watanabe H, Katsuno M and others. 2016. HMGB1, a pathogenic molecule that induces neurite degeneration via TLR4-MARCKS, is a potential therapeutic target for Alzheimer's disease. Sci Rep 6:31895.

Gaiottino J, Norgren N, Dobson R, Topping J, Nissim A, Malaspina A, Bestwick JP, Monsch AU, Regeniter A, Lindberg RL and others. 2013. Increased neurofilament light chain blood levels in neurodegenerative neurological diseases. PLoS One 8(9):e75091.

Gajardo-Gomez R, Labra VC, Orellana JA. 2016. Connexins and Pannexins: New Insights into Microglial Functions and Dysfunctions. Front Mol Neurosci 9:86.

Gal J, Strom AL, Kilty R, Zhang F, Zhu H. 2007. p62 accumulates and enhances aggregate formation in model systems of familial amyotrophic lateral sclerosis. J Biol Chem 282(15):11068-77.

Galatro TF, Holtman IR, Lerario AM, Vainchtein ID, Brouwer N, Sola PR, Veras MM, Pereira TF, Leite REP, Moller T and others. 2017. Transcriptomic analysis of purified human cortical microglia reveals age-associated changes. Nat Neurosci 20(8):1162-1171.

Gamez J, Corbera-Bellalta M, Nogales G, Raguer N, Garcia-Arumi E, Badia-Canto M, Llado-Carbo E, Alvarez-Sabin J. 2006. Mutational analysis of the Cu/Zn superoxide dismutase gene in a Catalan ALS population: should all sporadic ALS cases also be screened for SOD1? J Neurol Sci 247(1):21-8.

Gao HM, Zhou H, Zhang F, Wilson BC, Kam W, Hong JS. 2011. HMGB1 acts on microglia Mac1 to mediate chronic neuroinflammation that drives progressive neurodegeneration. J Neurosci 31(3):1081-92.

Garbuzova-Davis S, Haller E, Saporta S, Kolomey I, Nicosia SV, Sanberg PR. 2007a. Ultrastructure of blood-brain barrier and blood-spinal cord barrier in SOD1 mice modeling ALS. Brain Res 1157:126-37.

Garbuzova-Davis S, Hernandez-Ontiveros DG, Rodrigues MC, Haller E, Frisina-Deyo A, Mirtyl S, Sallot S, Saporta S, Borlongan CV, Sanberg PR. 2012. Impaired blood-brain/spinal cord barrier in ALS patients. Brain Res 1469:114-28.

Garbuzova-Davis S, Saporta S, Haller E, Kolomey I, Bennett SP, Potter H, Sanberg PR. 2007b. Evidence of compromised blood-spinal cord barrier in early and late symptomatic SOD1 mice modeling ALS. PLoS One 2(11):e1205.

Geevasinga N, Menon P, Ozdinler PH, Kiernan MC, Vucic S. 2016. Pathophysiological and diagnostic implications of cortical dysfunction in ALS. Nat Rev Neurol 12(11):651-661.

Gerber YN, Sabourin JC, Rabano M, Vivanco M, Perrin FE. 2012. Early functional deficit and microglial disturbances in a mouse model of amyotrophic lateral sclerosis. PLoS One 7(4):e36000.

Ghosh S, May MJ, Kopp EB. 1998. NF-kappa B and Rel proteins: evolutionarily conserved mediators of immune responses. Annu Rev Immunol 16:225-60.

Ginhoux F, Greter M, Leboeuf M, Nandi S, See P, Gokhan S, Mehler MF, Conway SJ, Ng LG, Stanley ER and others. 2010. Fate mapping analysis reveals that adult microglia derive from primitive macrophages. Science 330(6005):841-5.

Ginhoux F, Lim S, Hoeffel G, Low D, Huber T. 2013. Origin and differentiation of microglia. Front Cell Neurosci 7:45.

Ginhoux F, Prinz M. 2015. Origin of microglia: current concepts and past controversies. Cold Spring Harb Perspect Biol 7(8):a020537.

Giulian D, Baker TJ. 1986. Characterization of ameboid microglia isolated from developing mammalian brain. J Neurosci 6(8):2163-78.

Glass JD, Hertzberg VS, Boulis NM, Riley J, Federici T, Polak M, Bordeau J, Fournier C, Johe K, Hazel T and others. 2016. Transplantation of spinal cord-derived neural stem cells for ALS: Analysis of phase 1 and 2 trials. Neurology 87(4):392-400.

Godbout JP, Chen J, Abraham J, Richwine AF, Berg BM, Kelley KW, Johnson RW. 2005. Exaggerated neuroinflammation and sickness behavior in aged mice following activation of the peripheral innate immune system. FASEB J 19(10):1329-31.

Goldmann T, Prinz M. 2013. Role of microglia in CNS autoimmunity. Clin Dev Immunol 2013:208093.

Gomes C, Keller S, Altevogt P, Costa J. 2007. Evidence for secretion of Cu,Zn superoxide dismutase via exosomes from a cell model of amyotrophic lateral sclerosis. Neurosci Lett 428(1):43-6.

Gomes C, Palma AS, Almeida R, Regalla M, McCluskey LF, Trojanowski JQ, Costa J. 2008. Establishment of a cell model of ALS disease: Golgi apparatus disruption occurs independently from apoptosis. Biotechnol Lett 30(4):603-10.

Gordo AC, Falcão AS, Fernandes A, Brito MA, Silva RF, Brites D. 2006. Unconjugated bilirubin activates and damages microglia. J Neurosci Res 84(1):194-201.

Gowing G, Philips T, Van Wijmeersch B, Audet JN, Dewil M, Van Den Bosch L, Billiau AD, Robberecht W, Julien JP. 2008. Ablation of proliferating microglia does not affect motor neuron degeneration in amyotrophic lateral sclerosis caused by mutant superoxide dismutase. J Neurosci 28(41):10234-44.

Graber DJ, Hickey WF, Harris BT. 2010. Progressive changes in microglia and macrophages in spinal cord and peripheral nerve in the transgenic rat model of amyotrophic lateral sclerosis. J Neuroinflammation 7:8.

Grabert K, Michoel T, Karavolos MH, Clohisey S, Baillie JK, Stevens MP, Freeman TC, Summers KM, McColl BW. 2016. Microglial brain region-dependent diversity and selective regional sensitivities to aging. Nat Neurosci 19(3):504-16.

Grad LI, Fernando SM, Cashman NR. 2015. From molecule to molecule and cell to cell: prion-like mechanisms in amyotrophic lateral sclerosis. Neurobiol Dis 77:257-65.

Grad LI, Pokrishevsky E, Silverman JM, Cashman NR. 2014a. Exosome-dependent and independent mechanisms are involved in prion-like transmission of propagated Cu/Zn superoxide dismutase misfolding. Prion 8(5):331-5.

Grad LI, Rouleau GA, Ravits J, Cashman NR. 2017. Clinical Spectrum of Amyotrophic Lateral Sclerosis (ALS). Cold Spring Harb Perspect Med 7(8).

Grad LI, Yerbury JJ, Turner BJ, Guest WC, Pokrishevsky E, O'Neill MA, Yanai A, Silverman JM, Zeineddine R, Corcoran L and others. 2014b. Intercellular propagated misfolding of wild-type Cu/Zn superoxide dismutase occurs via exosome-dependent and -independent mechanisms. Proc Natl Acad Sci U S A 111(9):3620-5.

Graeber MB, Streit WJ. 2010. Microglia: biology and pathology. Acta Neuropathol 119(1):89-105.

Gravel M, Beland LC, Soucy G, Abdelhamid E, Rahimian R, Gravel C, Kriz J. 2016. IL-10 Controls Early Microglial Phenotypes and Disease Onset in ALS Caused by Misfolded Superoxide Dismutase 1. J Neurosci 36(3):1031-48.

Graves MC, Fiala M, Dinglasan LA, Liu NQ, Sayre J, Chiappelli F, van Kooten C, Vinters HV. 2004. Inflammation in amyotrophic lateral sclerosis spinal cord and brain is mediated by activated macrophages, mast cells and T cells. Amyotroph Lateral Scler Other Motor Neuron Disord 5(4):213-9.

Greenhalgh AD, David S. 2014. Differences in the phagocytic response of microglia and peripheral macrophages after spinal cord injury and its effects on cell death. J Neurosci 34(18):6316-22.

Greenway MJ, Andersen PM, Russ C, Ennis S, Cashman S, Donaghy C, Patterson V, Swingler R, Kieran D, Prehn J and others. 2006. ANG mutations segregate with familial and 'sporadic' amyotrophic lateral sclerosis. Nat Genet 38(4):411-3.

Gu N, Peng J, Murugan M, Wang X, Eyo UB, Sun D, Ren Y, DiCicco-Bloom E, Young W, Dong H and others. 2016. Spinal Microgliosis Due to Resident Microglial Proliferation Is Required for Pain Hypersensitivity after Peripheral Nerve Injury. Cell Rep 16(3):605-14.

Guedes J, Cardoso AL, Pedroso de Lima MC. 2013. Involvement of microRNA in microglia-mediated immune response. Clin Dev Immunol 2013:186872.

Guedes JR, Custodia CM, Silva RJ, de Almeida LP, Pedroso de Lima MC, Cardoso AL. 2014. Early miR-155 upregulation contributes to neuroinflammation in Alzheimer's disease triple transgenic mouse model. Hum Mol Genet 23(23):6286-301.

Guegan C, Vila M, Rosoklija G, Hays AP, Przedborski S. 2001. Recruitment of the mitochondrial-dependent apoptotic pathway in amyotrophic lateral sclerosis. J Neurosci 21(17):6569-76.

Gupta A, Pulliam L. 2014. Exosomes as mediators of neuroinflammation. J Neuroinflammation 11:68.

Gurney ME. 1994. Transgenic-mouse model of amyotrophic lateral sclerosis. N Engl J Med 331(25):1721-2.

Gurney ME, Pu H, Chiu AY, Dal Canto MC, Polchow CY, Alexander DD, Caliendo J, Hentati A, Kwon YW, Deng HX and others. 1994. Motor neuron degeneration in mice that express a human Cu,Zn superoxide dismutase mutation. Science 264(5166):1772-5.

Guruswamy R, ElAli A. 2017. Complex Roles of Microglial Cells in Ischemic Stroke Pathobiology: New Insights and Future Directions. Int J Mol Sci 18(3).

Gustin A, Kirchmeyer M, Koncina E, Felten P, Losciuto S, Heurtaux T, Tardivel A, Heuschling P, Dostert C. 2015. NLRP3 Inflammasome Is Expressed and Functional in Mouse Brain Microglia but Not in Astrocytes. PLoS One 10(6):e0130624.

Hagemeyer N, Hanft KM, Akriditou MA, Unger N, Park ES, Stanley ER, Staszewski O, Dimou L, Prinz M. 2017. Microglia contribute to normal myelinogenesis and to oligodendrocyte progenitor maintenance during adulthood. Acta Neuropathol.

Haidet-Phillips AM, Hester ME, Miranda CJ, Meyer K, Braun L, Frakes A, Song S, Likhite S, Murtha MJ, Foust KD and others. 2011. Astrocytes from familial and sporadic ALS patients are toxic to motor neurons. Nat Biotechnol 29(9):824-8.

Halle A, Hornung V, Petzold GC, Stewart CR, Monks BG, Reinheckel T, Fitzgerald KA, Latz E, Moore KJ, Golenbock DT. 2008. The NALP3 inflammasome is involved in the innate immune response to amyloid-beta. Nat Immunol 9(8):857-65.

Hanamsagar R, Torres V, Kielian T. 2011. Inflammasome activation and IL-1beta/IL-18 processing are influenced by distinct pathways in microglia. J Neurochem 119(4):736-48.

Hanayama R, Tanaka M, Miwa K, Shinohara A, Iwamatsu A, Nagata S. 2002. Identification of a factor that links apoptotic cells to phagocytes. Nature 417(6885):182-7.

Hanisch UK, Kettenmann H. 2007. Microglia: active sensor and versatile effector cells in the normal and pathologic brain. Nat Neurosci 10(11):1387-94.

Harrison EB, Hochfelder CG, Lamberty BG, Meays BM, Morsey BM, Kelso ML, Fox HS, Yelamanchili SV. 2016. Traumatic brain injury increases levels of miR-21 in extracellular vesicles: implications for neuroinflammation. FEBS Open Bio 6(8):835-46.

Harry GJ, Kraft AD. 2012. Microglia in the developing brain: A potential target with lifetime effects. Neurotoxicology 33(2):191-206.

Hayashi K, Mochizuki Y, Takeuchi R, Shimizu T, Nagao M, Watabe K, Arai N, Oyanagi K, Onodera O, Hayashi M and others. 2016. Clinicopathological characteristics of patients with amyotrophic lateral sclerosis resulting in a totally locked-in state (communication Stage V). Acta Neuropathol Commun 4(1):107.

Haynes SE, Hollopeter G, Yang G, Kurpius D, Dailey ME, Gan WB, Julius D. 2006. The P2Y12 receptor regulates microglial activation by extracellular nucleotides. Nat Neurosci 9(12):1512-9.

He M, Dong H, Huang Y, Lu S, Zhang S, Qian Y, Jin W. 2016a. Astrocyte-Derived CCL2 is Associated with M1 Activation and Recruitment of Cultured Microglial Cells. Cell Physiol Biochem 38(3):859-70.

He X, Jing Z, Cheng G. 2014. MicroRNAs: new regulators of Toll-like receptor signalling pathways. Biomed Res Int 2014:945169.

He Y, Hara H, Nunez G. 2016b. Mechanism and Regulation of NLRP3 Inflammasome Activation. Trends Biochem Sci 41(12):1012-1021.

Henkel JS, Beers DR, Siklos L, Appel SH. 2006. The chemokine MCP-1 and the dendritic and myeloid cells it attracts are increased in the mSOD1 mouse model of ALS. Mol Cell Neurosci 31(3):427-37.

Hensley K, Fedynyshyn J, Ferrell S, Floyd RA, Gordon B, Grammas P, Hamdheydari L, Mhatre M, Mou S, Pye QN and others. 2003. Message and protein-level elevation of tumor necrosis factor alpha (TNF alpha) and TNF alpha-modulating cytokines in spinal cords of the G93A-SOD1 mouse model for amyotrophic lateral sclerosis. Neurobiol Dis 14(1):74-80.

Hensley K, Floyd RA, Gordon B, Mou S, Pye QN, Stewart C, West M, Williamson K. 2002. Temporal patterns of cytokine and apoptosis-related gene expression in spinal cords of the G93A-SOD1 mouse model of amyotrophic lateral sclerosis. J Neurochem 82(2):365-74.

Hessvik NP, Llorente A. 2017. Current knowledge on exosome biogenesis and release. Cell Mol Life Sci.

Hickman SE, Allison EK, El Khoury J. 2008. Microglial dysfunction and defective beta-amyloid clearance pathways in aging Alzheimer's disease mice. J Neurosci 28(33):8354-60.

Hickman SE, Kingery ND, Ohsumi TK, Borowsky ML, Wang LC, Means TK, El Khoury J. 2013. The microglial sensome revealed by direct RNA sequencing. Nat Neurosci 16(12):1896-905.

Hirbec HE, Noristani HN, Perrin FE. 2017. Microglia Responses in Acute and Chronic Neurological Diseases: What Microglia-Specific Transcriptomic Studies Taught (and did Not Teach) Us. Front Aging Neurosci 9:227.

Hoek RM, Ruuls SR, Murphy CA, Wright GJ, Goddard R, Zurawski SM, Blom B, Homola ME, Streit WJ, Brown MH and others. 2000. Down-regulation of the macrophage lineage through interaction with OX2 (CD200). Science 290(5497):1768-71.

Holtman IR, Noback M, Bijlsma M, Duong KN, van der Geest MA, Ketelaars PT, Brouwer N, Vainchtein ID, Eggen BJ, Boddeke HW. 2015. Glia Open Access Database (GOAD): A comprehensive gene expression encyclopedia of glia cells in health and disease. Glia 63(9):1495-506.

Honda S, Sasaki Y, Ohsawa K, Imai Y, Nakamura Y, Inoue K, Kohsaka S. 2001. Extracellular ATP or ADP induce chemotaxis of cultured microglia through Gi/o-coupled P2Y receptors. J Neurosci 21(6):1975-82.

Hooten KG, Beers DR, Zhao W, Appel SH. 2015. Protective and Toxic Neuroinflammation in Amyotrophic Lateral Sclerosis. Neurotherapeutics 12(2):364-75.

Howland DS, Liu J, She Y, Goad B, Maragakis NJ, Kim B, Erickson J, Kulik J, DeVito L, Psaltis G and others. 2002. Focal loss of the glutamate transporter EAAT2 in a

transgenic rat model of SOD1 mutant-mediated amyotrophic lateral sclerosis (ALS). Proc Natl Acad Sci U S A 99(3):1604-9.

Hu Y, Cao C, Qin XY, Yu Y, Yuan J, Zhao Y, Cheng Y. 2017. Increased peripheral blood inflammatory cytokine levels in amyotrophic lateral sclerosis: a meta-analysis study. Sci Rep 7(1):9094.

Huang S, Ge X, Yu J, Han Z, Yin Z, Li Y, Chen F, Wang H, Zhang J, Lei P. 2017. Increased miR-124-3p in microglial exosomes following traumatic brain injury inhibits neuronal inflammation and contributes to neurite outgrowth via their transfer into neurons. FASEB J.

Hutchins KD, Dickson DW, Rashbaum WK, Lyman WD. 1990. Localization of morphologically distinct microglial populations in the developing human fetal brain: implications for ontogeny. Brain Res Dev Brain Res 55(1):95-102.

Igoudjil A, Magrane J, Fischer LR, Kim HJ, Hervias I, Dumont M, Cortez C, Glass JD, Starkov AA, Manfredi G. 2011. In vivo pathogenic role of mutant SOD1 localized in the mitochondrial intermembrane space. J Neurosci 31(44):15826-37.

Iguchi Y, Eid L, Parent M, Soucy G, Bareil C, Riku Y, Kawai K, Takagi S, Yoshida M, Katsuno M and others. 2016. Exosome secretion is a key pathway for clearance of pathological TDP-43. Brain 139(Pt 12):3187-3201.

Ilzecka J. 2011. Serum caspase-9 levels are increased in patients with amyotrophic lateral sclerosis. Neurol Sci 33(4):825-9.

Im HI, Kenny PJ. 2012. MicroRNAs in neuronal function and dysfunction. Trends Neurosci 35(5):325-34.

Inoue K. 2002. Microglial activation by purines and pyrimidines. Glia 40(2):156-63.

Ito Y, Ofengeim D, Najafov A, Das S, Saberi S, Li Y, Hitomi J, Zhu H, Chen H, Mayo L and others. 2016. RIPK1 mediates axonal degeneration by promoting inflammation and necroptosis in ALS. Science 353(6299):603-8.

Jaiswal MK. 2017. Therapeutic opportunities and challenges of induced pluripotent stem cells-derived motor neurons for treatment of amyotrophic lateral sclerosis and motor neuron disease. Neural Regen Res 12(5):723-736.

Ji Q, Ji Y, Peng J, Zhou X, Chen X, Zhao H, Xu T, Chen L, Xu Y. 2016. Increased Brain-Specific MiR-9 and MiR-124 in the Serum Exosomes of Acute Ischemic Stroke Patients. PLoS One 11(9):e0163645.

Jiang M, Xiang Y, Wang D, Gao J, Liu D, Liu Y, Liu S, Zheng D. 2012. Dysregulated expression of miR-146a contributes to age-related dysfunction of macrophages. Aging Cell 11(1):29-40.

Jiang T, Tan L, Zhu XC, Zhang QQ, Cao L, Tan MS, Gu LZ, Wang HF, Ding ZZ, Zhang YD and others. 2014. Upregulation of TREM2 ameliorates neuropathology and rescues spatial cognitive impairment in a transgenic mouse model of Alzheimer's disease. Neuropsychopharmacology 39(13):2949-62.

Jiang T, Zhang YD, Chen Q, Gao Q, Zhu XC, Zhou JS, Shi JQ, Lu H, Tan L, Yu JT. 2016. TREM2 modifies microglial phenotype and provides neuroprotection in P301S tau transgenic mice. Neuropharmacology 105:196-206.

Jin Y, Wang R, Yang S, Zhang X, Dai J. 2017. Role of Microglia Autophagy in Microglia Activation After Traumatic Brain Injury. World Neurosurg 100:351-360.

Johann S, Heitzer M, Kanagaratnam M, Goswami A, Rizo T, Weis J, Troost D, Beyer C. 2015. NLRP3 inflammasome is expressed by astrocytes in the SOD1 mouse model of ALS and in human sporadic ALS patients. Glia 63(12):2260-73.

Jose S, Tan SW, Ooi YY, Ramasamy R, Vidyadaran S. 2014. Mesenchymal stem cells exert anti-proliferative effect on lipopolysaccharide-stimulated BV2 microglia by reducing tumour necrosis factor-alpha levels. J Neuroinflammation 11:149.

Juranek JK, Daffu GK, Geddis MS, Li H, Rosario R, Kaplan BJ, Kelly L, Schmidt AM. 2016. Soluble RAGE Treatment Delays Progression of Amyotrophic Lateral Sclerosis in SOD1 Mice. Front Cell Neurosci 10:117.

Juranek JK, Daffu GK, Wojtkiewicz J, Lacomis D, Kofler J, Schmidt AM. 2015. Receptor for Advanced Glycation End Products and its Inflammatory Ligands are Upregulated in Amyotrophic Lateral Sclerosis. Front Cell Neurosci 9:485.

Kabashi E, Agar JN, Taylor DM, Minotti S, Durham HD. 2004. Focal dysfunction of the proteasome: a pathogenic factor in a mouse model of amyotrophic lateral sclerosis. J Neurochem 89(6):1325-35.

Kabba JA, Xu Y, Christian H, Ruan W, Chenai K, Xiang Y, Zhang L, Saavedra JM, Pang T. 2017. Microglia: Housekeeper of the Central Nervous System. Cell Mol Neurobiol.

Kalra H, Drummen GP, Mathivanan S. 2017. Focus on Extracellular Vesicles: Introducing the Next Small Big Thing. Int J Mol Sci 17(2):170.

Kang R, Chen R, Zhang Q, Hou W, Wu S, Cao L, Huang J, Yu Y, Fan XG, Yan Z and others. 2014. HMGB1 in health and disease. Mol Aspects Med 40:1-116.

Kang SH, Li Y, Fukaya M, Lorenzini I, Cleveland DW, Ostrow LW, Rothstein JD, Bergles DE. 2013. Degeneration and impaired regeneration of gray matter oligodendrocytes in amyotrophic lateral sclerosis. Nat Neurosci 16(5):571-9.

Kaplan A, Spiller KJ, Towne C, Kanning KC, Choe GT, Geber A, Akay T, Aebischer P, Henderson CE. 2014. Neuronal matrix metalloproteinase-9 is a determinant of selective neurodegeneration. Neuron 81(2):333-48.

Kaspar BK, Llado J, Sherkat N, Rothstein JD, Gage FH. 2003. Retrograde viral delivery of IGF-1 prolongs survival in a mouse ALS model. Science 301(5634):839-42.

Kato S, Takikawa M, Nakashima K, Hirano A, Cleveland DW, Kusaka H, Shibata N, Kato M, Nakano I, Ohama E. 2000. New consensus research on neuropathological aspects of familial amyotrophic lateral sclerosis with superoxide dismutase 1 (SOD1) gene mutations: inclusions containing SOD1 in neurons and astrocytes. Amyotroph Lateral Scler Other Motor Neuron Disord 1(3):163-84.

Kawabe K, Takano K, Moriyama M, Nakamura Y. 2017. Microglia Endocytose Amyloid beta Through the Binding of Transglutaminase 2 and Milk Fat Globule EGF Factor 8 Protein. Neurochem Res.

Kawabori M, Kacimi R, Kauppinen T, Calosing C, Kim JY, Hsieh CL, Nakamura MC, Yenari MA. 2015. Triggering receptor expressed on myeloid cells 2 (TREM2) deficiency attenuates phagocytic activities of microglia and exacerbates ischemic damage in experimental stroke. J Neurosci 35(8):3384-96.

Kawamata T, Akiyama H, Yamada T, McGeer PL. 1992. Immunologic reactions in amyotrophic lateral sclerosis brain and spinal cord tissue. Am J Pathol 140(3):691-707.

Keaney J, Campbell M. 2015. The dynamic blood-brain barrier. FEBS J 282(21):4067-79.

Kettenmann H, Hanisch UK, Noda M, Verkhratsky A. 2011. Physiology of microglia. Physiol Rev 91(2):461-553.

Kiaei M, Kipiani K, Calingasan NY, Wille E, Chen J, Heissig B, Rafii S, Lorenzl S, Beal MF. 2007. Matrix metalloproteinase-9 regulates TNF-alpha and FasL expression in neuronal, glial cells and its absence extends life in a transgenic mouse model of amyotrophic lateral sclerosis. Exp Neurol 205(1):74-81.

Kierdorf K, Erny D, Goldmann T, Sander V, Schulz C, Perdiguero EG, Wieghofer P, Heinrich A, Riemke P, Holscher C and others. 2013. Microglia emerge from erythromyeloid precursors via Pu.1- and Irf8-dependent pathways. Nat Neurosci 16(3):273-80.

Kiernan MC, Vucic S, Cheah BC, Turner MR, Eisen A, Hardiman O, Burrell JR, Zoing MC. 2011. Amyotrophic lateral sclerosis. Lancet 377(9769):942-55.

Kim HJ, Kim NC, Wang YD, Scarborough EA, Moore J, Diaz Z, MacLea KS, Freibaum B, Li S, Molliex A and others. 2013. Mutations in prion-like domains in hnRNPA2B1 and hnRNPA1 cause multisystem proteinopathy and ALS. Nature 495(7442):467-73.

Kim JB, Lim CM, Yu YM, Lee JK. 2008. Induction and subcellular localization of high-mobility group box-1 (HMGB1) in the postischemic rat brain. J Neurosci Res 86(5):1125-31.

Kim JB, Sig Choi J, Yu YM, Nam K, Piao CS, Kim SW, Lee MH, Han PL, Park JS, Lee JK. 2006. HMGB1, a novel cytokine-like mediator linking acute neuronal death and delayed neuroinflammation in the postischemic brain. J Neurosci 26(24):6413-21.

Kim SU, de Vellis J. 2005. Microglia in health and disease. J Neurosci Res 81(3):302-13.

Kim WG, Mohney RP, Wilson B, Jeohn GH, Liu B, Hong JS. 2000. Regional difference in susceptibility to lipopolysaccharide-induced neurotoxicity in the rat brain: role of microglia. J Neurosci 20(16):6309-16.

Kirkley KS, Popichak KA, Afzali MF, Legare ME, Tjalkens RB. 2017. Microglia amplify inflammatory activation of astrocytes in manganese neurotoxicity. J Neuroinflammation 14(1):99.

Kloss CU, Bohatschek M, Kreutzberg GW, Raivich G. 2001. Effect of lipopolysaccharide on the morphology and integrin immunoreactivity of ramified microglia in the mouse brain and in cell culture. Exp Neurol 168(1):32-46.

Koellhoffer EC, McCullough LD, Ritzel RM. 2017. Old Maids: Aging and Its Impact on Microglia Function. Int J Mol Sci 18(4).

Koizumi S, Shigemoto-Mogami Y, Nasu-Tada K, Shinozaki Y, Ohsawa K, Tsuda M, Joshi BV, Jacobson KA, Kohsaka S, Inoue K. 2007. UDP acting at P2Y6 receptors is a mediator of microglial phagocytosis. Nature 446(7139):1091-5.

Komura H, Miksa M, Wu R, Goyert SM, Wang P. 2009. Milk fat globule epidermal growth factor-factor VIII is down-regulated in sepsis via the lipopolysaccharide-CD14 pathway. J Immunol 182(1):581-7.

Koning N, Swaab DF, Hoek RM, Huitinga I. 2009. Distribution of the immune inhibitory molecules CD200 and CD200R in the normal central nervous system and multiple sclerosis lesions suggests neuron-glia and glia-glia interactions. J Neuropathol Exp Neurol 68(2):159-67.

Könnecke H, Bechmann I. 2013. The role of microglia and matrix metalloproteinases involvement in neuroinflammation and gliomas. Clin Dev Immunol 2013:914104.

Korkut C, Li Y, Koles K, Brewer C, Ashley J, Yoshihara M, Budnik V. 2013. Regulation of postsynaptic retrograde signaling by presynaptic exosome release. Neuron 77(6):1039-46.

Koval ED, Shaner C, Zhang P, du Maine X, Fischer K, Tay J, Chau BN, Wu GF, Miller TM. 2013. Method for widespread microRNA-155 inhibition prolongs survival in ALS-model mice. Hum Mol Genet 22(20):4127-35.

Krabbe G, Halle A, Matyash V, Rinnenthal JL, Eom GD, Bernhardt U, Miller KR, Prokop S, Kettenmann H, Heppner FL. 2013. Functional impairment of microglia coincides with Beta-amyloid deposition in mice with Alzheimer-like pathology. PLoS One 8(4):e60921.

Kraft AD, Harry GJ. 2011. Features of microglia and neuroinflammation relevant to environmental exposure and neurotoxicity. Int J Environ Res Public Health 8(7):2980-3018.

Kramer-Albers EM, Bretz N, Tenzer S, Winterstein C, Mobius W, Berger H, Nave KA, Schild H, Trotter J. 2007. Oligodendrocytes secrete exosomes containing major myelin and stress-protective proteins: Trophic support for axons? Proteomics Clin Appl 1(11):1446-61.

Kreutzberg GW. 1996. Microglia: a sensor for pathological events in the CNS. Trends Neurosci 19(8):312-8.

Krichevsky AM, Sonntag KC, Isacson O, Kosik KS. 2006. Specific microRNAs modulate embryonic stem cell-derived neurogenesis. Stem Cells 24(4):857-64.

Krol J, Loedige I, Filipowicz W. 2010. The widespread regulation of microRNA biogenesis, function and decay. Nat Rev Genet 11(9):597-610.

Krüger S, Battke F, Sprecher A, Munz M, Synofzik M, Schols L, Gasser T, Grehl T, Prudlo J, Biskup S. 2016. Rare Variants in Neurodegeneration Associated Genes Revealed by Targeted Panel Sequencing in a German ALS Cohort. Front Mol Neurosci 9:92.

Kruse K, Janko C, Urbonaviciute V, Mierke CT, Winkler TH, Voll RE, Schett G, Munoz LE, Herrmann M. 2010. Inefficient clearance of dying cells in patients with SLE: anti-dsDNA autoantibodies, MFG-E8, HMGB-1 and other players. Apoptosis 15(9):1098-113.

Ksiazek-Winiarek DJ, Kacperska MJ, Glabinski A. 2013. MicroRNAs as novel regulators of neuroinflammation. Mediators Inflamm 2013:172351.

Kumar A, Alvarez-Croda DM, Stoica BA, Faden AI, Loane DJ. 2016. Microglial/Macrophage Polarization Dynamics following Traumatic Brain Injury. J Neurotrauma 33(19):1732-1750.

Kuo JJ, Schonewille M, Siddique T, Schults AN, Fu R, Bar PR, Anelli R, Heckman CJ, Kroese AB. 2004. Hyperexcitability of cultured spinal motoneurons from presymptomatic ALS mice. J Neurophysiol 91(1):571-5.

Kurpius D, Wilson N, Fuller L, Hoffman A, Dailey ME. 2006. Early activation, motility, and homing of neonatal microglia to injured neurons does not require protein synthesis. Glia 54(1):58-70.

Kushner PD, Stephenson DT, Wright S. 1991. Reactive astrogliosis is widespread in the subcortical white matter of amyotrophic lateral sclerosis brain. J Neuropathol Exp Neurol 50(3):263-77.

Kye MJ, Goncalves Ido C. 2014. The role of miRNA in motor neuron disease. Front Cell Neurosci 8:15.

Lai AY, Dhami KS, Dibal CD, Todd KG. 2011. Neonatal rat microglia derived from different brain regions have distinct activation responses. Neuron Glia Biol 7(1):5-16.

Lamkanfi M, Dixit VM. 2012. Inflammasomes and their roles in health and disease. Annu Rev Cell Dev Biol 28:137-61.

Lamkanfi M, Sarkar A, Vande Walle L, Vitari AC, Amer AO, Wewers MD, Tracey KJ, Kanneganti TD, Dixit VM. 2010. Inflammasome-dependent release of the alarmin HMGB1 in endotoxemia. J Immunol 185(7):4385-92.

Lan X, Han X, Li Q, Yang QW, Wang J. 2017. Modulators of microglial activation and polarization after intracerebral haemorrhage. Nat Rev Neurol 13(7):420-433.

Larssen P, Wik L, Czarnewski P, Eldh M, Lof L, Ronquist KG, Dubois L, Freyhult E, Gallant CJ, Oelrich J and others. 2017. Tracing Cellular Origin of Human Exosomes Using Multiplex Proximity Extension Assays. Mol Cell Proteomics 16(8):1547.

Lattante S, Conte A, Zollino M, Luigetti M, Del Grande A, Marangi G, Romano A, Marcaccio A, Meleo E, Bisogni G and others. 2012. Contribution of major amyotrophic lateral sclerosis genes to the etiology of sporadic disease. Neurology 79(1):66-72.

Lawson LJ, Perry VH, Dri P, Gordon S. 1990. Heterogeneity in the distribution and morphology of microglia in the normal adult mouse brain. Neuroscience 39(1):151-70.

Lee EJ, Kim HS. 2011. Inhibitory mechanism of MMP-9 gene expression by ethyl pyruvate in lipopolysaccharide-stimulated BV2 microglial cells. Neurosci Lett 493(1-2):38-43.

Lee HM, Kang J, Lee SJ, Jo EK. 2013. Microglial activation of the NLRP3 inflammasome by the priming signals derived from macrophages infected with mycobacteria. Glia 61(3):441-52.

Lee J, Hyeon SJ, Im H, Ryu H, Kim Y. 2016. Astrocytes and Microglia as Non-cell Autonomous Players in the Pathogenesis of ALS. Exp Neurobiol 25(5):233-240.

Lee JC, Seong J, Kim SH, Lee SJ, Cho YJ, An J, Nam DH, Joo KM, Cha CI. 2012a. Replacement of microglial cells using Clodronate liposome and bone marrow transplantation in the central nervous system of SOD1(G93A) transgenic mice as an in vivo model of amyotrophic lateral sclerosis. Biochem Biophys Res Commun 418(2):359-65.

Lee JY, Choi HY, Yune TY. 2015a. MMP-3 secreted from endothelial cells of blood vessels after spinal cord injury activates microglia, leading to oligodendrocyte cell death. Neurobiol Dis 82:141-151.

Lee JY, Lee JD, Phipps S, Noakes PG, Woodruff TM. 2015b. Absence of toll-like receptor 4 (TLR4) extends survival in the hSOD1 G93A mouse model of amyotrophic lateral sclerosis. J Neuroinflammation 12:90.

Lee Y, Morrison BM, Li Y, Lengacher S, Farah MH, Hoffman PN, Liu Y, Tsingalia A, Jin L, Zhang PW and others. 2012b. Oligodendroglia metabolically support axons and contribute to neurodegeneration. Nature 487(7408):443-8.

Lehnardt S. 2010. Innate immunity and neuroinflammation in the CNS: the role of microglia in Toll-like receptor-mediated neuronal injury. Glia 58(3):253-63.

Lepore AC, Dejea C, Carmen J, Rauck B, Kerr DA, Sofroniew MV, Maragakis NJ. 2008a. Selective ablation of proliferating astrocytes does not affect disease outcome in either acute or chronic models of motor neuron degeneration. Exp Neurol 211(2):423-32.

Lepore AC, Rauck B, Dejea C, Pardo AC, Rao MS, Rothstein JD, Maragakis NJ. 2008b. Focal transplantation-based astrocyte replacement is neuroprotective in a model of motor neuron disease. Nat Neurosci 11(11):1294-301.

Lesuisse C, Martin LJ. 2002. Long-term culture of mouse cortical neurons as a model for neuronal development, aging, and death. J Neurobiol 51(1):9-23.

Letiembre M, Hao W, Liu Y, Walter S, Mihaljevic I, Rivest S, Hartmann T, Fassbender K. 2007. Innate immune receptor expression in normal brain aging. Neuroscience 146(1):248-54.

Levy E. 2017. Exosomes in the Diseased Brain: First Insights from In vivo Studies. Front Neurosci 11:142.

Lewis KE, Rasmussen AL, Bennett W, King A, West AK, Chung RS, Chuah MI. 2014. Microglia and motor neurons during disease progression in the SOD1G93A mouse model of amyotrophic lateral sclerosis: changes in arginase1 and inducible nitric oxide synthase. J Neuroinflammation 11:55.

Li L, Zhang X, Le W. 2008. Altered macroautophagy in the spinal cord of SOD1 mutant mice. Autophagy 4(3):290-3.

Li M, Sun L, Luo Y, Xie C, Pang Y, Li Y. 2014. High-mobility group box 1 released from astrocytes promotes the proliferation of cultured neural stem/progenitor cells. Int J Mol Med 34(3):705-14.

Li T, Pang S, Yu Y, Wu X, Guo J, Zhang S. 2013. Proliferation of parenchymal microglia is the main source of microgliosis after ischaemic stroke. Brain 136(Pt 12):3578-88.

Li X, Kong D, Chen H, Liu S, Hu H, Wu T, Wang J, Chen W, Ning Y, Li Y and others. 2016a. miR-155 acts as an anti-inflammatory factor in atherosclerosis-associated foam cell formation by repressing calcium-regulated heat stable protein 1. Sci Rep 6:21789.

Li Z, Qin T, Wang K, Hackenberg M, Yan J, Gao Y, Yu LR, Shi L, Su Z, Chen T. 2015. Integrated microRNA, mRNA, and protein expression profiling reveals microRNA regulatory networks in rat kidney treated with a carcinogenic dose of aristolochic acid. BMC Genomics 16:365.

Li Z, Wei H, Piirainen S, Chen Z, Kalso E, Pertovaara A, Tian L. 2016b. Spinal versus brain microglial and macrophage activation traits determine the differential neuroinflammatory responses and analgesic effect of minocycline in chronic neuropathic pain. Brain Behav Immun 58:107-117.

Lian H, Litvinchuk A, Chiang AC, Aithmitti N, Jankowsky JL, Zheng H. 2016. Astrocyte-Microglia Cross Talk through Complement Activation Modulates Amyloid Pathology in Mouse Models of Alzheimer's Disease. J Neurosci 36(2):577-89.

Liang KJ, Lee JE, Wang YD, Ma W, Fontainhas AM, Fariss RN, Wong WT. 2009. Regulation of dynamic behavior of retinal microglia by CX3CR1 signaling. Invest Ophthalmol Vis Sci 50(9):4444-51.

Liao B, Zhao W, Beers DR, Henkel JS, Appel SH. 2012. Transformation from a neuroprotective to a neurotoxic microglial phenotype in a mouse model of ALS. Exp Neurol 237(1):147-52.

Liddelow SA, Guttenplan KA, Clarke LE, Bennett FC, Bohlen CJ, Schirmer L, Bennett ML, Munch AE, Chung WS, Peterson TC and others. 2017. Neurotoxic reactive astrocytes are induced by activated microglia. Nature 541(7638):481-487.

Lim GP, Backstrom JR, Cullen MJ, Miller CA, Atkinson RD, Tokes ZA. 1996. Matrix metalloproteinases in the neocortex and spinal cord of amyotrophic lateral sclerosis patients. J Neurochem 67(1):251-9.

Lim HM, Woon H, Han JW, Baba Y, Kurosaki T, Lee MG, Kim JY. 2017. UDP-Induced Phagocytosis and ATP-Stimulated Chemotactic Migration Are Impaired in STIM1-/- Microglia In Vitro and In Vivo. Mediators Inflamm 2017:8158514.

Limatola C, Ransohoff RM. 2014. Modulating neurotoxicity through CX3CL1/CX3CR1 signaling. Front Cell Neurosci 8:229.

Ling SC, Polymenidou M, Cleveland DW. 2013. Converging mechanisms in ALS and FTD: disrupted RNA and protein homeostasis. Neuron 79(3):416-38.

Lino MM, Schneider C, Caroni P. 2002. Accumulation of SOD1 mutants in postnatal motoneurons does not cause motoneuron pathology or motoneuron disease. J Neurosci 22(12):4825-32.

Liu G, Abraham E. 2013. MicroRNAs in immune response and macrophage polarization. Arterioscler Thromb Vasc Biol 33(2):170-7.

Liu HC, Zheng MH, Du YL, Wang L, Kuang F, Qin HY, Zhang BF, Han H. 2012. N9 microglial cells polarized by LPS and IL4 show differential responses to secondary environmental stimuli. Cell Immunol 278(1-2):84-90.

Liu J, Gao L, Zang D. 2015a. Elevated Levels of IFN-gamma in CSF and Serum of Patients with Amyotrophic Lateral Sclerosis. PLoS One 10(9):e0136937.

Liu J, Hjorth E, Zhu M, Calzarossa C, Samuelsson EB, Schultzberg M, Akesson E. 2013a. Interplay between human microglia and neural stem/progenitor cells in an allogeneic co-culture model. J Cell Mol Med 17(11):1434-43.

Liu RT, Wang A, To E, Gao J, Cao S, Cui JZ, Matsubara JA. 2014. Vinpocetine inhibits amyloid-beta induced activation of NF-kappaB, NLRP3 inflammasome and cytokine production in retinal pigment epithelial cells. Exp Eye Res 127:49-58.

Liu W, Tang Y, Feng J. 2011. Cross talk between activation of microglia and astrocytes in pathological conditions in the central nervous system. Life Sci 89(5-6):141-6.

Liu XX, Wang C, Huang SF, Chen Q, Hu YF, Zhou L, Gu Y. 2016a. Regnase-1 in microglia negatively regulates high mobility group box 1-mediated inflammation and neuronal injury. Sci Rep 6:24073.

Liu Y, Hao W, Dawson A, Liu S, Fassbender K. 2009. Expression of amyotrophic lateral sclerosis-linked SOD1 mutant increases the neurotoxic potential of microglia via TLR2. J Biol Chem 284(6):3691-9.

Liu Y, Pattamatta A, Zu T, Reid T, Bardhi O, Borchelt DR, Yachnis AT, Ranum LP. 2016b. C9orf72 BAC Mouse Model with Motor Deficits and Neurodegenerative Features of ALS/FTD. Neuron 90(3):521-34.

Liu Y, Wu XM, Luo QQ, Huang S, Yang QW, Wang FX, Ke Y, Qian ZM. 2015b. CX3CL1/CX3CR1-mediated microglia activation plays a detrimental role in ischemic mice brain via p38MAPK/PKC pathway. J Cereb Blood Flow Metab 35(10):1623-31.

Liu Y, Yang X, Guo C, Nie P, Ma J. 2013b. Essential role of MFG-E8 for phagocytic properties of microglial cells. PLoS One 8(2):e55754.

Lively S, Schlichter LC. 2013. The microglial activation state regulates migration and roles of matrix-dissolving enzymes for invasion. J Neuroinflammation 10:75.

Lo Coco D, Veglianese P, Allievi E, Bendotti C. 2007. Distribution and cellular localization of high mobility group box protein 1 (HMGB1) in the spinal cord of a transgenic mouse model of ALS. Neurosci Lett 412(1):73-7.

Loane DJ, Kumar A. 2016. Microglia in the TBI brain: The good, the bad, and the dysregulated. Exp Neurol 275 Pt 3:316-27.

Lopez-Lopez A, Gamez J, Syriani E, Morales M, Salvado M, Rodriguez MJ, Mahy N, Vidal-Taboada JM. 2014. CX3CR1 is a modifying gene of survival and progression in amyotrophic lateral sclerosis. PLoS One 9(5):e96528.

Lorenzl S, Narr S, Angele B, Krell HW, Gregorio J, Kiaei M, Pfister HW, Beal MF. 2006. The matrix metalloproteinases inhibitor Ro 28-2653 [correction of Ro 26-2853] extends survival in transgenic ALS mice. Exp Neurol 200(1):166-71.

Lourbopoulos A, Erturk A, Hellal F. 2015. Microglia in action: how aging and injury can change the brain's guardians. Front Cell Neurosci 9:54.

Lu B, Wang H, Andersson U, Tracey KJ. 2013. Regulation of HMGB1 release by inflammasomes. Protein Cell 4(3):163-7.

Lu CH, Macdonald-Wallis C, Gray E, Pearce N, Petzold A, Norgren N, Giovannoni G, Fratta P, Sidle K, Fish M and others. 2015. Neurofilament light chain: A prognostic biomarker in amyotrophic lateral sclerosis. Neurology 84(22):2247-57.

Lu X, Ma L, Ruan L, Kong Y, Mou H, Zhang Z, Wang Z, Wang JM, Le Y. 2010. Resveratrol differentially modulates inflammatory responses of microglia and astrocytes. J Neuroinflammation 7:46.

Lue LF, Schmitz CT, Serrano G, Sue LI, Beach TG, Walker DG. 2015. TREM2 Protein Expression Changes Correlate with Alzheimer's Disease Neurodegenerative Pathologies in Post-Mortem Temporal Cortices. Brain Pathol 25(4):469-80.

Luo C, Jian C, Liao Y, Huang Q, Wu Y, Liu X, Zou D. 2017. The role of microglia in multiple sclerosis. Neuropsychiatr Dis Treat 13:1661-1667.

Madison RD, McGee C, Rawson R, Robinson GA. 2014. Extracellular vesicles from a muscle cell line (C2C12) enhance cell survival and neurite outgrowth of a motor neuron cell line (NSC-34). J Extracell Vesicles 3.

Madry C, Attwell D. 2015. Receptors, ion channels, and signaling mechanisms underlying microglial dynamics. J Biol Chem 290(20):12443-50.

Magna M, Pisetsky DS. 2014. The role of HMGB1 in the pathogenesis of inflammatory and autoimmune diseases. Mol Med 20:138-46.

Majerova P, Zilkova M, Kazmerova Z, Kovac A, Paholikova K, Kovacech B, Zilka N, Novak M. 2014. Microglia display modest phagocytic capacity for extracellular tau oligomers. J Neuroinflammation 11(1):161.

Majounie E, Renton AE, Mok K, Dopper EG, Waite A, Rollinson S, Chio A, Restagno G, Nicolaou N, Simon-Sanchez J and others. 2012. Frequency of the C9orf72 hexanucleotide repeat expansion in patients with amyotrophic lateral sclerosis and frontotemporal dementia: a cross-sectional study. Lancet Neurol 11(4):323-30.

Makeyev EV, Zhang J, Carrasco MA, Maniatis T. 2007. The MicroRNA miR-124 promotes neuronal differentiation by triggering brain-specific alternative pre-mRNA splicing. Mol Cell 27(3):435-48.

Maniecka Z, Polymenidou M. 2015. From nucleation to widespread propagation: A prion-like concept for ALS. Virus Res 207:94-105.

Mariathasan S, Weiss DS, Newton K, McBride J, O'Rourke K, Roose-Girma M, Lee WP, Weinrauch Y, Monack DM, Dixit VM. 2006. Cryopyrin activates the inflammasome in response to toxins and ATP. Nature 440(7081):228-32.

Martinon F, Petrilli V, Mayor A, Tardivel A, Tschopp J. 2006. Gout-associated uric acid crystals activate the NALP3 inflammasome. Nature 440(7081):237-41.

Maruyama H, Morino H, Ito H, Izumi Y, Kato H, Watanabe Y, Kinoshita Y, Kamada M, Nodera H, Suzuki H and others. 2010. Mutations of optineurin in amyotrophic lateral sclerosis. Nature 465(7295):223-6.

Mashimo H, Ohguro N, Nomura S, Hashida N, Nakai K, Tano Y. 2008. Neutrophil chemotaxis and local expression of interleukin-10 in the tolerance of endotoxin-induced uveitis. Invest Ophthalmol Vis Sci 49(12):5450-7.

Matcovitch-Natan O, Winter DR, Giladi A, Vargas Aguilar S, Spinrad A, Sarrazin S, Ben-Yehuda H, David E, Zelada Gonzalez F, Perrin P and others. 2016. Microglia development follows a stepwise program to regulate brain homeostasis. Science 353(6301):aad8670.

Matsumoto K, Morisaki T, Kuroki H, Kubo M, Onishi H, Nakamura K, Nakahara C, Kuga H, Baba E, Nakamura M and others. 2005. Exosomes secreted from monocyte-derived dendritic cells support in vitro naive CD4+ T cell survival through NF-(kappa)B activation. Cell Immunol 231(1-2):20-9.

Mazaheri F, Snaidero N, Kleinberger G, Madore C, Daria A, Werner G, Krasemann S, Capell A, Trumbach D, Wurst W and others. 2017. TREM2 deficiency impairs chemotaxis and microglial responses to neuronal injury. EMBO Rep 18(7):1186-1198.

McGoldrick P, Joyce PI, Fisher EM, Greensmith L. 2013. Rodent models of amyotrophic lateral sclerosis. Biochim Biophys Acta 1832(9):1421-36.

McKimmie CS, Roy D, Forster T, Fazakerley JK. 2006. Innate immune response gene expression profiles of N9 microglia are pathogen-type specific. J Neuroimmunol 175(1-2):128-41.

Menzies FM, Fleming A, Caricasole A, Bento CF, Andrews SP, Ashkenazi A, Fullgrabe J, Jackson A, Jimenez Sanchez M, Karabiyik C and others. 2017. Autophagy and Neurodegeneration: Pathogenic Mechanisms and Therapeutic Opportunities. Neuron 93(5):1015-1034.

Meyer K, Ferraiuolo L, Miranda CJ, Likhite S, McElroy S, Renusch S, Ditsworth D, Lagier-Tourenne C, Smith RA, Ravits J and others. 2014. Direct conversion of patient fibroblasts demonstrates non-cell autonomous toxicity of astrocytes to motor neurons in familial and sporadic ALS. Proc Natl Acad Sci U S A 111(2):829-32.

Michell-Robinson MA, Touil H, Healy LM, Owen DR, Durafourt BA, Bar-Or A, Antel JP, Moore CS. 2015. Roles of microglia in brain development, tissue maintenance and repair. Brain 138(Pt 5):1138-59.

Millecamps S, Boillee S, Le Ber I, Seilhean D, Teyssou E, Giraudeau M, Moigneu C, Vandenberghe N, Danel-Brunaud V, Corcia P and others. 2012. Phenotype difference between ALS patients with expanded repeats in C9ORF72 and patients with mutations in other ALS-related genes. J Med Genet 49(4):258-63.

Millecamps S, Salachas F, Cazeneuve C, Gordon P, Bricka B, Camuzat A, Guillot-Noel L, Russaouen O, Bruneteau G, Pradat PF and others. 2010. SOD1, ANG, VAPB, TARDBP, and FUS mutations in familial amyotrophic lateral sclerosis: genotype-phenotype correlations. J Med Genet 47(8):554-60.

Miron VE, Boyd A, Zhao JW, Yuen TJ, Ruckh JM, Shadrach JL, van Wijngaarden P, Wagers AJ, Williams A, Franklin RJM and others. 2013. M2 microglia and macrophages drive oligodendrocyte differentiation during CNS remyelination. Nat Neurosci 16(9):1211-1218.

Mitchell JC, Constable R, So E, Vance C, Scotter E, Glover L, Hortobagyi T, Arnold ES, Ling SC, McAlonis M and others. 2015. Wild type human TDP-43 potentiates ALS-linked mutant TDP-43 driven progressive motor and cortical neuron degeneration with pathological features of ALS. Acta Neuropathol Commun 3:36.

Mitchell JC, McGoldrick P, Vance C, Hortobagyi T, Sreedharan J, Rogelj B, Tudor EL, Smith BN, Klasen C, Miller CC and others. 2012. Overexpression of human wild-type FUS causes progressive motor neuron degeneration in an age- and dose-dependent fashion. Acta Neuropathol 125(2):273-88.

Mitchell RM, Freeman WM, Randazzo WT, Stephens HE, Beard JL, Simmons Z, Connor JR. 2009. A CSF biomarker panel for identification of patients with amyotrophic lateral sclerosis. Neurology 72(1):14-9.

Mitsumoto H, Santella RM, Liu X, Bogdanov M, Zipprich J, Wu HC, Mahata J, Kilty M, Bednarz K, Bell D and others. 2008. Oxidative stress biomarkers in sporadic ALS. Amyotroph Lateral Scler 9(3):177-83.

Mittelbronn M, Dietz K, Schluesener HJ, Meyermann R. 2001. Local distribution of microglia in the normal adult human central nervous system differs by up to one order of magnitude. Acta Neuropathol 101(3):249-55.

Miyanishi M, Tada K, Koike M, Uchiyama Y, Kitamura T, Nagata S. 2007. Identification of Tim4 as a phosphatidylserine receptor. Nature 450(7168):435-9.

Mizee MR, Miedema SS, van der Poel M, Adelia, Schuurman KG, van Strien ME, Melief J, Smolders J, Hendrickx DA, Heutinck KM and others. 2017. Isolation of primary microglia from the human post-mortem brain: effects of ante- and post-mortem variables. Acta Neuropathol Commun 5(1):16.

Moehle MS, West AB. 2014. M1 and M2 immune activation in Parkinson's Disease: Foe and ally? Neuroscience 302:59-73.

Monier A, Adle-Biassette H, Delezoide AL, Evrard P, Gressens P, Verney C. 2007. Entry and distribution of microglial cells in human embryonic and fetal cerebral cortex. J Neuropathol Exp Neurol 66(5):372-82.

Montero TD, Orellana JA. 2015. Hemichannels: new pathways for gliotransmitter release. Neuroscience 286:45-59.

Moore CS, Rao VT, Durafourt BA, Bedell BJ, Ludwin SK, Bar-Or A, Antel JP. 2013. miR-155 as a multiple sclerosis-relevant regulator of myeloid cell polarization. Ann Neurol 74(5):709-20.

Morel L, Regan M, Higashimori H, Ng SK, Esau C, Vidensky S, Rothstein J, Yang Y. 2013. Neuronal exosomal miRNA-dependent translational regulation of astroglial glutamate transporter GLT1. J Biol Chem 288(10):7105-16.

Morrison HW, Filosa JA. 2013. A quantitative spatiotemporal analysis of microglia morphology during ischemic stroke and reperfusion. J Neuroinflammation 10:4.

Mosher KI, Wyss-Coray T. 2014. Microglial dysfunction in brain aging and Alzheimer's disease. Biochem Pharmacol 88(4):594-604.

Mosser CA, Baptista S, Arnoux I, Audinat E. 2017. Microglia in CNS development: Shaping the brain for the future. Prog Neurobiol 149-150:1-20.

Mulcahy LA, Pink RC, Carter DR. 2014. Routes and mechanisms of extracellular vesicle uptake. J Extracell Vesicles 3.

Nagy D, Kato T, Kushner PD. 1994. Reactive astrocytes are widespread in the cortical gray matter of amyotrophic lateral sclerosis. J Neurosci Res 38(3):336-47.

Nahid MA, Pauley KM, Satoh M, Chan EK. 2009. miR-146a is critical for endotoxin-induced tolerance: IMPLICATION IN INNATE IMMUNITY. J Biol Chem 284(50):34590-9.

Nakamura Y, Si QS, Kataoka K. 1999. Lipopolysaccharide-induced microglial activation in culture: temporal profiles of morphological change and release of cytokines and nitric oxide. Neurosci Res 35(2):95-100.

Napoli I, Neumann H. 2009. Microglial clearance function in health and disease. Neuroscience 158(3):1030-8.

Narita M, Yoshida T, Nakajima M, Miyatake M, Takagi T, Yajima Y, Suzuki T. 2006. Direct evidence for spinal cord microglia in the development of a neuropathic pain-like state in mice. J Neurochem 97(5):1337-48.

Nascimento F, Pousinha PA, Correia AM, Gomes R, Sebastiao AM, Ribeiro JA. 2014. Adenosine A2A receptors activation facilitates neuromuscular transmission in the pre-symptomatic phase of the SOD1(G93A) ALS mice, but not in the symptomatic phase. PLoS One 9(8):e104081.

Nascimento F, Sebastiao AM, Ribeiro JA. 2015. Presymptomatic and symptomatic ALS SOD1(G93A) mice differ in adenosine A1 and A2A receptor-mediated tonic modulation of neuromuscular transmission. Purinergic Signal 11(4):471-80.

Nayak D, Roth TL, McGavern DB. 2014. Microglia development and function. Annu Rev Immunol 32:367-402.

Neher JJ, Emmrich JV, Fricker M, Mander PK, Thery C, Brown GC. 2013. Phagocytosis executes delayed neuronal death after focal brain ischemia. Proc Natl Acad Sci U S A 110(43):E4098-107.

Neher JJ, Neniskyte U, Brown GC. 2012. Primary phagocytosis of neurons by inflamed microglia: potential roles in neurodegeneration. Front Pharmacol 3:27.

Neniskyte U, Neher JJ, Brown GC. 2011. Neuronal death induced by nanomolar amyloid beta is mediated by primary phagocytosis of neurons by microglia. J Biol Chem 286(46):39904-13.

Neo WH, Yap K, Lee SH, Looi LS, Khandelia P, Neo SX, Makeyev EV, Su IH. 2014. MicroRNA miR-124 controls the choice between neuronal and astrocyte differentiation by fine-tuning Ezh2 expression. J Biol Chem 289(30):20788-801.

Neumann H, Daly MJ. 2013. Variant TREM2 as risk factor for Alzheimer's disease. N Engl J Med 368(2):182-4.

Neumann H, Kotter MR, Franklin RJ. 2009. Debris clearance by microglia: an essential link between degeneration and regeneration. Brain 132(Pt 2):288-95.

Neumann M, Sampathu DM, Kwong LK, Truax AC, Micsenyi MC, Chou TT, Bruce J, Schuck T, Grossman M, Clark CM and others. 2006. Ubiquitinated TDP-43 in frontotemporal lobar degeneration and amyotrophic lateral sclerosis. Science 314(5796):130-3.

Ngolab J, Trinh I, Rockenstein E, Mante M, Florio J, Trejo M, Masliah D, Adame A, Masliah E, Rissman RA. 2017. Brain-derived exosomes from dementia with Lewy bodies propagate alpha-synuclein pathology. Acta Neuropathol Commun 5(1):46.

Nicaise C, Mitrecic D, Falnikar A, Lepore AC. 2015. Transplantation of stem cell-derived astrocytes for the treatment of amyotrophic lateral sclerosis and spinal cord injury. World J Stem Cells 7(2):380-98.

Niebroj-Dobosz I, Rafalowska J, Fidzianska A, Gadamski R, Grieb P. 2007. Myelin composition of spinal cord in a model of amyotrophic lateral sclerosis (ALS) in SOD1G93A transgenic rats. Folia Neuropathol 45(4):236-41.

Nijssen J, Comley LH, Hedlund E. 2017. Motor neuron vulnerability and resistance in amyotrophic lateral sclerosis. Acta Neuropathol 133(6):863-885.

Nikodemova M, Small AL, Smith SM, Mitchell GS, Watters JJ. 2014. Spinal but not cortical microglia acquire an atypical phenotype with high VEGF, galectin-3 and osteopontin, and blunted inflammatory responses in ALS rats. Neurobiol Dis 69:43-53.

Nikodemova M, Watters JJ. 2011. Outbred ICR/CD1 mice display more severe neuroinflammation mediated by microglial TLR4/CD14 activation than inbred C57Bl/6 mice. Neuroscience 190:67-74.

Nimmerjahn A, Kirchhoff F, Helmchen F. 2005. Resting microglial cells are highly dynamic surveillants of brain parenchyma in vivo. Science 308(5726):1314-8.

Niraula A, Sheridan JF, Godbout JP. 2016. Microglia Priming with Aging and Stress. Neuropsychopharmacology 42(1):318-333.

Nissen JC. 2017. Microglial Function across the Spectrum of Age and Gender. Int J Mol Sci 18(3).

Noristani HN, Gerber YN, Sabourin JC, Le Corre M, Lonjon N, Mestre-Frances N, Hirbec HE, Perrin FE. 2017. RNA-Seq Analysis of Microglia Reveals Time-Dependent Activation of Specific Genetic Programs following Spinal Cord Injury. Front Mol Neurosci 10:90.

Nzwalo H, de Abreu D, Swash M, Pinto S, de Carvalho M. 2014. Delayed diagnosis in ALS: the problem continues. J Neurol Sci 343(1-2):173-5.

O'Connell RM, Rao DS, Chaudhuri AA, Baltimore D. 2010. Physiological and pathological roles for microRNAs in the immune system. Nat Rev Immunol 10(2):111-22.

O'Rourke JG, Bogdanik L, Yanez A, Lall D, Wolf AJ, Muhammad AK, Ho R, Carmona S, Vit JP, Zarrow J and others. 2016. C9orf72 is required for proper macrophage and microglial function in mice. Science 351(6279):1324-9.

Oak S, Mandrekar P, Catalano D, Kodys K, Szabo G. 2006. TLR2- and TLR4-mediated signals determine attenuation or augmentation of inflammation by acute alcohol in monocytes. J Immunol 176(12):7628-35.

Obora K, Onodera Y, Takehara T, Frampton J, Hasei J, Ozaki T, Teramura T, Fukuda K. 2017. Inflammation-induced miRNA-155 inhibits self-renewal of neural stem cells via

suppression of CCAAT/enhancer binding protein beta (C/EBPbeta) expression. Sci Rep 7:43604.

Obst J, Simon E, Mancuso R, Gomez-Nicola D. 2017. The Role of Microglia in Prion Diseases: A Paradigm of Functional Diversity. Front Aging Neurosci 9:207.

Ohgomori T, Yamada J, Takeuchi H, Kadomatsu K, Jinno S. 2016. Comparative morphometric analysis of microglia in the spinal cord of SOD1(G93A) transgenic mouse model of amyotrophic lateral sclerosis. Eur J Neurosci 43(10):1340-51.

Ohsawa K, Irino Y, Nakamura Y, Akazawa C, Inoue K, Kohsaka S. 2007. Involvement of P2X4 and P2Y12 receptors in ATP-induced microglial chemotaxis. Glia 55(6):604-16.

Ohsawa K, Irino Y, Sanagi T, Nakamura Y, Suzuki E, Inoue K, Kohsaka S. 2010. P2Y12 receptor-mediated integrin-beta1 activation regulates microglial process extension induced by ATP. Glia 58(7):790-801.

Ohsawa K, Kohsaka S. 2011. Dynamic motility of microglia: purinergic modulation of microglial movement in the normal and pathological brain. Glia 59(12):1793-9.

Olah M, Biber K, Vinet J, Boddeke HW. 2011. Microglia phenotype diversity. CNS Neurol Disord Drug Targets 10(1):108-18.

Olivieri F, Albertini MC, Orciani M, Ceka A, Cricca M, Procopio AD, Bonafe M. 2015. DNA damage response (DDR) and senescence: shuttled inflamma-miRNAs on the stage of inflamm-aging. Oncotarget 6(34):35509-21.

Olivieri F, Lazzarini R, Recchioni R, Marcheselli F, Rippo MR, Di Nuzzo S, Albertini MC, Graciotti L, Babini L, Mariotti S and others. 2013. MiR-146a as marker of senescence-associated pro-inflammatory status in cells involved in vascular remodelling. Age (Dordr) 35(4):1157-72.

Ono S, Hu J, Shimizu N, Imai T, Nakagawa H. 2001. Increased interleukin-6 of skin and serum in amyotrophic lateral sclerosis. J Neurol Sci 187(1-2):27-34.

Onyeagucha BC, Mercado-Pimentel ME, Hutchison J, Flemington EK, Nelson MA. 2013. S100P/RAGE signaling regulates microRNA-155 expression via AP-1 activation in colon cancer. Exp Cell Res 319(13):2081-90.

Orellana JA, Froger N, Ezan P, Jiang JX, Bennett MV, Naus CC, Giaume C, Saez JC. 2011. ATP and glutamate released via astroglial connexin 43 hemichannels mediate neuronal death through activation of pannexin 1 hemichannels. J Neurochem 118(5):826-40.

Orr AG, Orr AL, Li XJ, Gross RE, Traynelis SF. 2009. Adenosine A(2A) receptor mediates microglial process retraction. Nat Neurosci 12(7):872-8.

Pabreja K, Dua K, Sharma S, Padi SS, Kulkarni SK. 2011. Minocycline attenuates the development of diabetic neuropathic pain: possible anti-inflammatory and anti-oxidant mechanisms. Eur J Pharmacol 661(1-3):15-21.

Pachot A, Cazalis MA, Venet F, Turrel F, Faudot C, Voirin N, Diasparra J, Bourgoin N, Poitevin F, Mougin B and others. 2008. Decreased expression of the fractalkine receptor CX3CR1 on circulating monocytes as new feature of sepsis-induced immunosuppression. J Immunol 180(9):6421-9.

Paez-Colasante X, Figueroa-Romero C, Sakowski SA, Goutman SA, Feldman EL. 2015. Amyotrophic lateral sclerosis: mechanisms and therapeutics in the epigenomic era. Nat Rev Neurol 11(5):266-79.

Painter MM, Atagi Y, Liu CC, Rademakers R, Xu H, Fryer JD, Bu G. 2015. TREM2 in CNS homeostasis and neurodegenerative disease. Mol Neurodegener 10:43.

Pandya H, Shen MJ, Ichikawa DM, Sedlock AB, Choi Y, Johnson KR, Kim G, Brown MA, Elkahloun AG, Maric D and others. 2017. Differentiation of human and murine induced pluripotent stem cells to microglia-like cells. Nat Neurosci 20(5):753-759.

Paolicelli RC, Bisht K, Tremblay ME. 2014. Fractalkine regulation of microglial physiology and consequences on the brain and behavior. Front Cell Neurosci 8:129.

Paolicelli RC, Bolasco G, Pagani F, Maggi L, Scianni M, Panzanelli P, Giustetto M, Ferreira TA, Guiducci E, Dumas L and others. 2011. Synaptic pruning by microglia is necessary for normal brain development. Science 333(6048):1456-8.

Papageorgiou IE, Lewen A, Galow LV, Cesetti T, Scheffel J, Regen T, Hanisch UK, Kann O. 2016. TLR4-activated microglia require IFN-gamma to induce severe neuronal dysfunction and death in situ. Proc Natl Acad Sci U S A 113(1):212-7.

Parisi C, Arisi I, D'Ambrosi N, Storti AE, Brandi R, D'Onofrio M, Volonte C. 2013. Dysregulated microRNAs in amyotrophic lateral sclerosis microglia modulate genes linked to neuroinflammation. Cell Death Dis 4:e959.

Parisi C, Napoli G, Amadio S, Spalloni A, Apolloni S, Longone P, Volonte C. 2016. MicroRNA-125b regulates microglia activation and motor neuron death in ALS. Cell Death Differ 23(3):531-41.

Park JS, Svetkauskaite D, He Q, Kim JY, Strassheim D, Ishizaka A, Abraham E. 2004. Involvement of toll-like receptors 2 and 4 in cellular activation by high mobility group box 1 protein. J Biol Chem 279(9):7370-7.

Park S, Kim HT, Yun S, Kim IS, Lee J, Lee IS, Park KI. 2009. Growth factor-expressing human neural progenitor cell grafts protect motor neurons but do not ameliorate motor performance and survival in ALS mice. Exp Mol Med 41(7):487-500.

Paschon V, Takada SH, Ikebara JM, Sousa E, Raeisossadati R, Ulrich H, Kihara AH. 2015. Interplay Between Exosomes, microRNAs and Toll-Like Receptors in Brain Disorders. Mol Neurobiol 53(3):2016-2028.

Pasinelli P, Belford ME, Lennon N, Bacskai BJ, Hyman BT, Trotti D, Brown RH, Jr. 2004. Amyotrophic lateral sclerosis-associated SOD1 mutant proteins bind and aggregate with Bcl-2 in spinal cord mitochondria. Neuron 43(1):19-30.

Pasinelli P, Brown RH. 2006. Molecular biology of amyotrophic lateral sclerosis: insights from genetics. Nat Rev Neurosci 7(9):710-23.

Patel AR, Ritzel R, McCullough LD, Liu F. 2013. Microglia and ischemic stroke: a double-edged sword. Int J Physiol Pathophysiol Pharmacol 5(2):73-90.

Pathak S, Grillo AR, Scarpa M, Brun P, D'Inca R, Nai L, Banerjee A, Cavallo D, Barzon L, Palu G and others. 2015. MiR-155 modulates the inflammatory phenotype of intestinal myofibroblasts by targeting SOCS1 in ulcerative colitis. Exp Mol Med 47:e164.

Peferoen L, Kipp M, van der Valk P, van Noort JM, Amor S. 2014a. Oligodendrocyte-microglia cross-talk in the central nervous system. Immunology 141(3):302-13.

Peferoen LA, Vogel DY, Ummenthum K, Breur M, Heijnen PD, Gerritsen WH, Peferoen-Baert RM, van der Valk P, Dijkstra CD, Amor S. 2014b. Activation status of human microglia is dependent on lesion formation stage and remyelination in multiple sclerosis. J Neuropathol Exp Neurol 74(1):48-63.

Perdiguero EG, Klapproth K, Schulz C, Busch K, de Bruijn M, Rodewald HR, Geissmann F. 2015. The Origin of Tissue-Resident Macrophages: When an Erythro-myeloid Progenitor Is an Erythro-myeloid Progenitor. Immunity 43(6):1023-4.

Perry VH, O'Connor V. 2010. The role of microglia in synaptic stripping and synaptic degeneration: a revised perspective. ASN Neuro 2(5):e00047.

Phatnani HP, Guarnieri P, Friedman BA, Carrasco MA, Muratet M, O'Keeffe S, Nwakeze C, Pauli-Behn F, Newberry KM, Meadows SK and others. 2013. Intricate interplay between astrocytes and motor neurons in ALS. Proc Natl Acad Sci U S A 110(8):E756-65.

Philips T, Bento-Abreu A, Nonneman A, Haeck W, Staats K, Geelen V, Hersmus N, Kusters B, Van Den Bosch L, Van Damme P and others. 2013. Oligodendrocyte dysfunction in the pathogenesis of amyotrophic lateral sclerosis. Brain 136(Pt 2):471-82.

Phipps SM, Berletch JB, Andrews LG, Tollefsbol TO. 2007. Aging cell culture: methods and observations. Methods Mol Biol 371:9-19.

Picher-Martel V, Valdmanis PN, Gould PV, Julien JP, Dupre N. 2016. From animal models to human disease: a genetic approach for personalized medicine in ALS. Acta Neuropathol Commun 4(1):70.

Pinto S, Cunha C, Barbosa M, Vaz AR, Brites D. 2017. Exosomes from NSC-34 Cells Transfected with hSOD1-G93A Are Enriched in miR-124 and Drive Alterations in Microglia Phenotype. Front Neurosci 11:273.

Pisetsky DS. 2013. The translocation of nuclear molecules during inflammation and cell death. Antioxid Redox Signal 20(7):1117-25.

Plaza-Zabala A, Sierra-Torre V, Sierra A. 2017. Autophagy and Microglia: Novel Partners in Neurodegeneration and Aging. Int J Mol Sci 18(3).

Pocock JM, Kettenmann H. 2007. Neurotransmitter receptors on microglia. Trends Neurosci 30(10):527-35.

Poliani PL, Wang Y, Fontana E, Robinette ML, Yamanishi Y, Gilfillan S, Colonna M. 2015. TREM2 sustains microglial expansion during aging and response to demyelination. J Clin Invest 125(5):2161-70.

Ponomarev ED, Veremeyko T, Barteneva N, Krichevsky AM, Weiner HL. 2011. MicroRNA-124 promotes microglia quiescence and suppresses EAE by deactivating macrophages via the C/EBP-alpha-PU.1 pathway. Nat Med 17(1):64-70.

Ponomarev ED, Veremeyko T, Weiner HL. 2013. MicroRNAs are universal regulators of differentiation, activation, and polarization of microglia and macrophages in normal and diseased CNS. Glia 61(1):91-103.

Pramatarova A, Laganiere J, Roussel J, Brisebois K, Rouleau GA. 2001. Neuron-specific expression of mutant superoxide dismutase 1 in transgenic mice does not lead to motor impairment. J Neurosci 21(10):3369-74.

Primiani CT, Ryan VH, Rao JS, Cam MC, Ahn K, Modi HR, Rapoport SI. 2014. Coordinated gene expression of neuroinflammatory and cell signaling markers in dorsolateral prefrontal cortex during human brain development and aging. PLoS One 9(10):e110972.

Proctor EA, Fee L, Tao Y, Redler RL, Fay JM, Zhang Y, Lv Z, Mercer IP, Deshmukh M, Lyubchenko YL and others. 2016. Nonnative SOD1 trimer is toxic to motor neurons in a model of amyotrophic lateral sclerosis. Proc Natl Acad Sci U S A 113(3):614-9.

Püntener U, Booth SG, Perry VH, Teeling JL. 2012. Long-term impact of systemic bacterial infection on the cerebral vasculature and microglia. J Neuroinflammation 9:146.

Qian K, Huang H, Peterson A, Hu B, Maragakis NJ, Ming GL, Chen H, Zhang SC. 2017. Sporadic ALS Astrocytes Induce Neuronal Degeneration In Vivo. Stem Cell Reports 8(4):843-855.

Qiu S, Feng Y, LeSage G, Zhang Y, Stuart C, He L, Li Y, Caudle Y, Peng Y, Yin D. 2015. Chronic morphine-induced microRNA-124 promotes microglial immunosuppression by modulating P65 and TRAF6. J Immunol 194(3):1021-30.

Quinn SR, O'Neill LA. 2011. A trio of microRNAs that control Toll-like receptor signalling. Int Immunol 23(7):421-5.

Radford RA, Morsch M, Rayner SL, Cole NJ, Pountney DL, Chung RS. 2015. The established and emerging roles of astrocytes and microglia in amyotrophic lateral sclerosis and frontotemporal dementia. Front Cell Neurosci 9:414.

Rajendran L, Honsho M, Zahn TR, Keller P, Geiger KD, Verkade P, Simons K. 2006. Alzheimer's disease beta-amyloid peptides are released in association with exosomes. Proc Natl Acad Sci U S A 103(30):11172-7.

Ransohoff RM. 2016. A polarizing question: do M1 and M2 microglia exist? Nat Neurosci 19(8):987-91.

Ransohoff RM, Perry VH. 2009. Microglial physiology: unique stimuli, specialized responses. Annu Rev Immunol 27:119-45.

Raoul C, Estevez AG, Nishimune H, Cleveland DW, deLapeyriere O, Henderson CE, Haase G, Pettmann B. 2002. Motoneuron death triggered by a specific pathway downstream of Fas. potentiation by ALS-linked SOD1 mutations. Neuron 35(6):1067-83.

Raponi E, Agenes F, Delphin C, Assard N, Baudier J, Legraverend C, Deloulme JC. 2007. S100B expression defines a state in which GFAP-expressing cells lose their neural stem cell potential and acquire a more mature developmental stage. Glia 55(2):165-77.

Rawji KS, Mishra MK, Michaels NJ, Rivest S, Stys PK, Yong VW. 2016. Immunosenescence of microglia and macrophages: impact on the ageing central nervous system. Brain 139(Pt 3):653-61.

Raymond A, Ensslin MA, Shur BD. 2009. SED1/MFG-E8: a bi-motif protein that orchestrates diverse cellular interactions. J Cell Biochem 106(6):957-66.

Re DB, Le Verche V, Yu C, Amoroso MW, Politi KA, Phani S, Ikiz B, Hoffmann L, Koolen M, Nagata T and others. 2014. Necroptosis drives motor neuron death in models of both sporadic and familial ALS. Neuron 81(5):1001-8.

Reijn TS, Abdo WF, Schelhaas HJ, Verbeek MM. 2009. CSF neurofilament protein analysis in the differential diagnosis of ALS. J Neurol 256(4):615-9.

Reinhold AK, Rittner HL. 2017. Barrier function in the peripheral and central nervous system-a review. Pflugers Arch 469(1):123-134.

Ren L, Lubrich B, Biber K, Gebicke-Haerter PJ. 1999. Differential expression of inflammatory mediators in rat microglia cultured from different brain regions. Brain Res Mol Brain Res 65(2):198-205.

Renton AE, Chio A, Traynor BJ. 2014. State of play in amyotrophic lateral sclerosis genetics. Nat Neurosci 17(1):17-23.

Renton AE, Majounie E, Waite A, Simon-Sanchez J, Rollinson S, Gibbs JR, Schymick JC, Laaksovirta H, van Swieten JC, Myllykangas L and others. 2011. A hexanucleotide repeat expansion in C9ORF72 is the cause of chromosome 9p21-linked ALS-FTD. Neuron 72(2):257-68.

Ribeiro Xavier AL, Kress BT, Goldman SA, Lacerda de Menezes JR, Nedergaard M. 2015. A Distinct Population of Microglia Supports Adult Neurogenesis in the Subventricular Zone. J Neurosci 35(34):11848-61.

Rigato C, Buckinx R, Le-Corronc H, Rigo JM, Legendre P. 2011. Pattern of invasion of the embryonic mouse spinal cord by microglial cells at the time of the onset of functional neuronal networks. Glia 59(4):675-95.

Righi M, Mori L, De Libero G, Sironi M, Biondi A, Mantovani A, Donini SD, Ricciardi-Castagnoli P. 1989a. Monokine production by microglial cell clones. Eur J Immunol 19(8):1443-8.

Righi M, Pierani A, Boglia A, De Libero G, Mori L, Marini V, Ricciardi-Castagnoli P. 1989b. Generation of new oncogenic murine retroviruses by cotransfection of cloned AKR and MH2 proviruses. Oncogene 4(2):223-30.

Robberecht W, Philips T. 2013. The changing scene of amyotrophic lateral sclerosis. Nat Rev Neurosci 14(4):248-64.

Roberts K, Zeineddine R, Corcoran L, Li W, Campbell IL, Yerbury JJ. 2013. Extracellular aggregated Cu/Zn superoxide dismutase activates microglia to give a cytotoxic phenotype. Glia 61(3):409-19.

Rocha MC, Pousinha PA, Correia AM, Sebastiao AM, Ribeiro JA. 2013. Early changes of neuromuscular transmission in the SOD1(G93A) mice model of ALS start long before motor symptoms onset. PLoS One 8(9):e73846.

Roggenbuck J, Quick A, Kolb SJ. 2016. Genetic testing and genetic counseling for amyotrophic lateral sclerosis: an update for clinicians. Genet Med 19(3):267-274.

Rosen DR. 1993. Mutations in Cu/Zn superoxide dismutase gene are associated with familial amyotrophic lateral sclerosis. Nature 364(6435):362.

Roszer T. 2015. Understanding the Mysterious M2 Macrophage through Activation Markers and Effector Mechanisms. Mediators Inflamm 2015:816460.

Rothstein JD, Van Kammen M, Levey AI, Martin LJ, Kuncl RW. 1995. Selective loss of glial glutamate transporter GLT-1 in amyotrophic lateral sclerosis. Ann Neurol 38(1):73-84.

Rozas P, Bargsted L, Martinez F, Hetz C, Medinas DB. 2016. The ER proteostasis network in ALS: Determining the differential motoneuron vulnerability. Neurosci Lett 636:9-15.

Rufino-Ramos D, Albuquerque PR, Carmona V, Perfeito R, Nobre RJ, Pereira de Almeida L. 2017. Extracellular vesicles: Novel promising delivery systems for therapy of brain diseases. J Control Release 262:247-258.

Rupaimoole R, Slack FJ. 2017. MicroRNA therapeutics: towards a new era for the management of cancer and other diseases. Nat Rev Drug Discov 16(3):203-222.

Saba R, Gushue S, Huzarewich RL, Manguiat K, Medina S, Robertson C, Booth SA. 2012. MicroRNA 146a (miR-146a) is over-expressed during prion disease and modulates the innate immune response and the microglial activation state. PLoS One 7(2):e30832.

Saba R, Schratt GM. 2010. MicroRNAs in neuronal development, function and dysfunction. Brain Res 1338:3-13.

Saghazadeh A, Rezaei N. 2017. The role of timing in the treatment of spinal cord injury. Biomed Pharmacother 92:128-139.

Sanagi T, Yuasa S, Nakamura Y, Suzuki E, Aoki M, Warita H, Itoyama Y, Uchino S, Kohsaka S, Ohsawa K. 2010. Appearance of phagocytic microglia adjacent to motoneurons in spinal cord tissue from a presymptomatic transgenic rat model of amyotrophic lateral sclerosis. J Neurosci Res 88(12):2736-46.

Sanuki R, Onishi A, Koike C, Muramatsu R, Watanabe S, Muranishi Y, Irie S, Uneo S, Koyasu T, Matsui R and others. 2011. miR-124a is required for hippocampal axogenesis and retinal cone survival through Lhx2 suppression. Nat Neurosci 14(9):1125-34.

Sargsyan SA, Blackburn DJ, Barber SC, Grosskreutz J, De Vos KJ, Monk PN, Shaw PJ. 2011. A comparison of in vitro properties of resting SOD1 transgenic microglia reveals evidence of reduced neuroprotective function. BMC Neurosci 12:91.

Sarko DK, McKinney CE. 2017. Exosomes: Origins and Therapeutic Potential for Neurodegenerative Disease. Front Neurosci 11:82.

Sasaki S, Iwata M. 2007. Mitochondrial alterations in the spinal cord of patients with sporadic amyotrophic lateral sclerosis. J Neuropathol Exp Neurol 66(1):10-6.

Saura J. 2007. Microglial cells in astroglial cultures: a cautionary note. J Neuroinflammation 4:26.

Saura J, Tusell JM, Serratosa J. 2003. High-yield isolation of murine microglia by mild trypsinization. Glia 44(3):183-9.

Sbai O, Ferhat L, Bernard A, Gueye Y, Ould-Yahoui A, Thiolloy S, Charrat E, Charton G, Tremblay E, Risso JJ and others. 2008. Vesicular trafficking and secretion of matrix metalloproteinases-2, -9 and tissue inhibitor of metalloproteinases-1 in neuronal cells. Mol Cell Neurosci 39(4):549-68.

Schafer DP, Lehrman EK, Stevens B. 2013. The "quad-partite" synapse: microglia-synapse interactions in the developing and mature CNS. Glia 61(1):24-36.

Schampel A, Volovitch O, Koeniger T, Scholz CJ, Jorg S, Linker RA, Wischmeyer E, Wunsch M, Hell JW, Ergun S and others. 2017. Nimodipine fosters remyelination in a mouse model of multiple sclerosis and induces microglia-specific apoptosis. Proc Natl Acad Sci U S A 114(16):E3295-E3304.

Scheiblich H, Roloff F, Singh V, Stangel M, Stern M, Bicker G. 2014. Nitric oxide/cyclic GMP signaling regulates motility of a microglial cell line and primary microglia in vitro. Brain Res 1564:9-21.

Schiera G, Di Liegro CM, Di Liegro I. 2015. Extracellular Membrane Vesicles as Vehicles for Brain Cell-to-Cell Interactions in Physiological as well as Pathological Conditions. Biomed Res Int 2015:152926.

Schiffer D, Cordera S, Cavalla P, Migheli A. 1996. Reactive astrogliosis of the spinal cord in amyotrophic lateral sclerosis. J Neurol Sci 139 Suppl:27-33.

Schipke CG, Boucsein C, Ohlemeyer C, Kirchhoff F, Kettenmann H. 2002. Astrocyte Ca2+ waves trigger responses in microglial cells in brain slices. FASEB J 16(2):255-7.

Sen R, Smale ST. 2010. Selectivity of the NF-{kappa}B response. Cold Spring Harb Perspect Biol 2(4):a000257.

Shaw PJ, Ince PG, Falkous G, Mantle D. 1995. Oxidative damage to protein in sporadic motor neuron disease spinal cord. Ann Neurol 38(4):691-5.

Shechter R, Miller O, Yovel G, Rosenzweig N, London A, Ruckh J, Kim KW, Klein E, Kalchenko V, Bendel P and others. 2013. Recruitment of beneficial M2 macrophages to injured spinal cord is orchestrated by remote brain choroid plexus. Immunity 38(3):555-69.

Sheedy FJ, Palsson-McDermott E, Hennessy EJ, Martin C, O'Leary JJ, Ruan Q, Johnson DS, Chen Y, O'Neill LA. 2010. Negative regulation of TLR4 via targeting of the proinflammatory tumor suppressor PDCD4 by the microRNA miR-21. Nat Immunol 11(2):141-7.

Sheerin UM, Schneider SA, Carr L, Deuschl G, Hopfner F, Stamelou M, Wood NW, Bhatia KP. 2014. ALS2 mutations: juvenile amyotrophic lateral sclerosis and generalized dystonia. Neurology 82(12):1065-7.

Sheller S, Papaconstantinou J, Urrabaz-Garza R, Richardson L, Saade G, Salomon C, Menon R. 2016. Amnion-Epithelial-Cell-Derived Exosomes Demonstrate Physiologic State of Cell under Oxidative Stress. PLoS One 11(6):e0157614.

Shen M, Lu J, Dai W, Wang F, Xu L, Chen K, He L, Cheng P, Zhang Y, Wang C and others. 2013. Ethyl pyruvate ameliorates hepatic ischemia-reperfusion injury by inhibiting intrinsic pathway of apoptosis and autophagy. Mediators Inflamm 2013:461536.

Sheridan GK, Murphy KJ. 2013. Neuron-glia crosstalk in health and disease: fractalkine and CX3CR1 take centre stage. Open Biol 3(12):130181.

Shibata N, Hirano A, Hedley-Whyte ET, Dal Canto MC, Nagai R, Uchida K, Horiuchi S, Kawaguchi M, Yamamoto T, Kobayashi M. 2002. Selective formation of certain advanced glycation end products in spinal cord astrocytes of humans and mice with superoxide dismutase-1 mutation. Acta Neuropathol 104(2):171-8.

Shih RH, Wang CY, Yang CM. 2015. NF-kappaB Signaling Pathways in Neurological Inflammation: A Mini Review. Front Mol Neurosci 8:77.

Shimizu T, Smits R, Ikenaka K. 2016. Microglia-induced activation of non-canonical Wnt signaling aggravates neurodegeneration in demyelinating disorders. Mol Cell Biol.

Shinder GA, Lacourse MC, Minotti S, Durham HD. 2001. Mutant Cu/Zn-superoxide dismutase proteins have altered solubility and interact with heat shock/stress proteins in models of amyotrophic lateral sclerosis. J Biol Chem 276(16):12791-6.

Silva SL, Osorio C, Vaz AR, Barateiro A, Falcao AS, Silva RF, Brites D. 2011. Dynamics of neuron-glia interplay upon exposure to unconjugated bilirubin. J Neurochem 117(3):412-24.

Silva SL, Vaz AR, Barateiro A, Falcao AS, Fernandes A, Brito MA, Silva RF, Brites D. 2010. Features of bilirubin-induced reactive microglia: from phagocytosis to inflammation. Neurobiol Dis 40(3):663-75.

Silverman JM, Fernando SM, Grad LI, Hill AF, Turner BJ, Yerbury JJ, Cashman NR. 2016. Disease Mechanisms in ALS: Misfolded SOD1 Transferred Through Exosome-Dependent and Exosome-Independent Pathways. Cell Mol Neurobiol 36(3):377-81.

Simões AE, Pereira DM, Amaral JD, Nunes AF, Gomes SE, Rodrigues PM, Lo AC, D'Hooge R, Steer CJ, Thibodeau SN and others. 2013. Efficient recovery of proteins from multiple source samples after TRIzol((R)) or TRIzol((R))LS RNA extraction and long-term storage. BMC Genomics 14:181.

Singh VK, Kalsan M, Kumar N, Saini A, Chandra R. 2015. Induced pluripotent stem cells: applications in regenerative medicine, disease modeling, and drug discovery. Front Cell Dev Biol 3:2.

Sofroniew MV, Vinters HV. 2010. Astrocytes: biology and pathology. Acta Neuropathol 119(1):7-35.

Song GJ, Suk K. 2017. Pharmacological Modulation of Functional Phenotypes of Microglia in Neurodegenerative Diseases. Front Aging Neurosci 9:139.

Song L, Pei L, Yao S, Wu Y, Shang Y. 2017. NLRP3 Inflammasome in Neurological Diseases, from Functions to Therapies. Front Cell Neurosci 11:63.

Soon CP, Crouch PJ, Turner BJ, McLean CA, Laughton KM, Atkin JD, Masters CL, White AR, Li QX. 2010. Serum matrix metalloproteinase-9 activity is dysregulated with disease progression in the mutant SOD1 transgenic mice. Neuromuscul Disord 20(4):260-6.

Soria FN, Pampliega O, Bourdenx M, Meissner WG, Bezard E, Dehay B. 2017. Exosomes, an Unmasked Culprit in Neurodegenerative Diseases. Front Neurosci 11:26.

Soriano SG, Amaravadi LS, Wang YF, Zhou H, Yu GX, Tonra JR, Fairchild-Huntress V, Fang Q, Dunmore JH, Huszar D and others. 2002. Mice deficient in fractalkine are less susceptible to cerebral ischemia-reperfusion injury. J Neuroimmunol 125(1-2):59-65.

Sousa C, Biber K, Michelucci A. 2017. Cellular and Molecular Characterization of Microglia: A Unique Immune Cell Population. Front Immunol 8:198.

Spittau B, Rilka J, Steinfath E, Zoller T, Krieglstein K. 2014. TGFbeta1 increases microglia-mediated engulfment of apoptotic cells via upregulation of the milk fat globule-EGF factor 8. Glia 63(1):142-53.

Spreux-Varoquaux O, Bensimon G, Lacomblez L, Salachas F, Pradat PF, Le Forestier N, Marouan A, Dib M, Meininger V. 2002. Glutamate levels in cerebrospinal fluid in amyotrophic lateral sclerosis: a reappraisal using a new HPLC method with coulometric detection in a large cohort of patients. J Neurol Sci 193(2):73-8.

Sreedharan J, Blair IP, Tripathi VB, Hu X, Vance C, Rogelj B, Ackerley S, Durnall JC, Williams KL, Buratti E and others. 2008. TDP-43 mutations in familial and sporadic amyotrophic lateral sclerosis. Science 319(5870):1668-72.

Staniland AA, Clark AK, Wodarski R, Sasso O, Maione F, D'Acquisto F, Malcangio M. 2010. Reduced inflammatory and neuropathic pain and decreased spinal microglial response in fractalkine receptor (CX3CR1) knockout mice. J Neurochem 114(4):1143-57.

Stansley B, Post J, Hensley K. 2012. A comparative review of cell culture systems for the study of microglial biology in Alzheimer's disease. J Neuroinflammation 9:115.

Stefano L, Racchetti G, Bianco F, Passini N, Gupta RS, Panina Bordignon P, Meldolesi J. 2009. The surface-exposed chaperone, Hsp60, is an agonist of the microglial TREM2 receptor. J Neurochem 110(1):284-94.

Stranks AJ, Hansen AL, Panse I, Mortensen M, Ferguson DJ, Puleston DJ, Shenderov K, Watson AS, Veldhoen M, Phadwal K and others. 2015. Autophagy Controls Acquisition of Aging Features in Macrophages. J Innate Immun 7(4):375-91.

Streit WJ, Sammons NW, Kuhns AJ, Sparks DL. 2004. Dystrophic microglia in the aging human brain. Glia 45(2):208-12.

Streit WJ, Walter SA, Pennell NA. 1999. Reactive microgliosis. Prog Neurobiol 57(6):563-81.

Stutz A, Kolbe CC, Stahl R, Horvath GL, Franklin BS, van Ray O, Brinkschulte R, Geyer M, Meissner F, Latz E. 2017. NLRP3 inflammasome assembly is regulated by phosphorylation of the pyrin domain. J Exp Med 214(6):1725-1736.

Su P, Zhang J, Wang D, Zhao F, Cao Z, Aschner M, Luo W. 2016. The role of autophagy in modulation of neuroinflammation in microglia. Neuroscience 319:155-67.

Subramaniam SR, Federoff HJ. 2017. Targeting Microglial Activation States as a Therapeutic Avenue in Parkinson's Disease. Front Aging Neurosci 9:176.

Sumi N, Nishioku T, Takata F, Matsumoto J, Watanabe T, Shuto H, Yamauchi A, Dohgu S, Kataoka Y. 2009. Lipopolysaccharide-activated microglia induce dysfunction of the blood-brain barrier in rat microvascular endothelial cells co-cultured with microglia. Cell Mol Neurobiol 30(2):247-53.

Sun Y, Luo ZM, Guo XM, Su DF, Liu X. 2015. An updated role of microRNA-124 in central nervous system disorders: a review. Front Cell Neurosci 9:193.

Sunden-Cullberg J, Norrby-Teglund A, Rouhiainen A, Rauvala H, Herman G, Tracey KJ, Lee ML, Andersson J, Tokics L, Treutiger CJ. 2005. Persistent elevation of high mobility group box-1 protein (HMGB1) in patients with severe sepsis and septic shock. Crit Care Med 33(3):564-73.

Suzuki M, El-Hage N, Zou S, Hahn YK, Sorrell ME, Sturgill JL, Conrad DH, Knapp PE, Hauser KF. 2011. Fractalkine/CX3CL1 protects striatal neurons from synergistic morphine and HIV-1 Tat-induced dendritic losses and death. Mol Neurodegener 6:78.

Svahn AJ, Giacomotto J, Graeber MB, Rinkwitz S, Becker TS. 2016. miR-124 Contributes to the functional maturity of microglia. Dev Neurobiol 76(5):507-18.

Tafuri F, Ronchi D, Magri F, Comi GP, Corti S. 2015. SOD1 misplacing and mitochondrial dysfunction in amyotrophic lateral sclerosis pathogenesis. Front Cell Neurosci 9:336.

Taganov KD, Boldin MP, Chang KJ, Baltimore D. 2006. NF-kappaB-dependent induction of microRNA miR-146, an inhibitor targeted to signaling proteins of innate immune responses. Proc Natl Acad Sci U S A 103(33):12481-6.

Tahara K, Kim HD, Jin JJ, Maxwell JA, Li L, Fukuchi K. 2006. Role of toll-like receptor signalling in Abeta uptake and clearance. Brain 129(Pt 11):3006-19.

Takahashi K, Rochford CD, Neumann H. 2005. Clearance of apoptotic neurons without inflammation by microglial triggering receptor expressed on myeloid cells-2. J Exp Med 201(4):647-57.

Takahashi K, Tanabe K, Ohnuki M, Narita M, Ichisaka T, Tomoda K, Yamanaka S. 2007. Induction of pluripotent stem cells from adult human fibroblasts by defined factors. Cell 131(5):861-72.

Tambuyzer BR, Ponsaerts P, Nouwen EJ. 2009. Microglia: gatekeepers of central nervous system immunology. J Leukoc Biol 85(3):352-70.

Tang Y, Le W. 2016. Differential Roles of M1 and M2 Microglia in Neurodegenerative Diseases. Mol Neurobiol 53(2):1181-94.

Taraboletti G, D'Ascenzo S, Borsotti P, Giavazzi R, Pavan A, Dolo V. 2002. Shedding of the matrix metalloproteinases MMP-2, MMP-9, and MT1-MMP as membrane vesicle-associated components by endothelial cells. Am J Pathol 160(2):673-80.

Taylor JP, Brown RH, Jr., Cleveland DW. 2016. Decoding ALS: from genes to mechanism. Nature 539(7628):197-206.

Taylor RA, Chang CF, Goods BA, Hammond MD, Mac Grory B, Ai Y, Steinschneider AF, Renfroe SC, Askenase MH, McCullough LD and others. 2017. TGF-beta1 modulates microglial phenotype and promotes recovery after intracerebral hemorrhage. J Clin Invest 127(1):280-292.

Tefera TW, Wong Y, Barkl-Luke ME, Ngo ST, Thomas NK, McDonald TS, Borges K. 2016. Triheptanoin Protects Motor Neurons and Delays the Onset of Motor Symptoms in a Mouse Model of Amyotrophic Lateral Sclerosis. PLoS One 11(8):e0161816.

Thompson AG, Gray E, Heman-Ackah SM, Mager I, Talbot K, Andaloussi SE, Wood MJ, Turner MR. 2016. Extracellular vesicles in neurodegenerative disease - pathogenesis to biomarkers. Nat Rev Neurol 12(6):346-57.

Thomsen GM, Gowing G, Latter J, Chen M, Vit JP, Staggenborg K, Avalos P, Alkaslasi M, Ferraiuolo L, Likhite S and others. 2014a. Delayed disease onset and extended survival in the SOD1G93A rat model of amyotrophic lateral sclerosis after suppression of mutant SOD1 in the motor cortex. J Neurosci 34(47):15587-600.

Thomsen GM, Gowing G, Svendsen S, Svendsen CN. 2014b. The past, present and future of stem cell clinical trials for ALS. Exp Neurol 262 Pt B:127-37.

Tian B, Nowak DE, Brasier AR. 2005. A TNF-induced gene expression program under oscillatory NF-kappaB control. BMC Genomics 6:137.

Tiftikcioglu BI, Ilgezdi I, Zorlu Y, Sener U, Tokucoglu F. 2017. Long-term disability and progression in spinal onset multiple sclerosis. Acta Neurol Belg.

Tomankova T, Petrek M, Gallo J, Kriegova E. 2011. MicroRNAs: Emerging Regulators of Immune-Mediated Diseases. Scand J Immunol 75(2):129-41.

Tomlinson PR, Zheng Y, Fischer R, Heidasch R, Gardiner C, Evetts S, Hu M, Wade-Martins R, Turner MR, Morris J and others. 2015. Identification of distinct circulating exosomes in Parkinson's disease. Ann Clin Transl Neurol 2(4):353-61.

Torres-Platas SG, Comeau S, Rachalski A, Bo GD, Cruceanu C, Turecki G, Giros B, Mechawar N. 2014. Morphometric characterization of microglial phenotypes in human cerebral cortex. J Neuroinflammation 11:12.

Tremblay ME, Lowery RL, Majewska AK. 2010. Microglial interactions with synapses are modulated by visual experience. PLoS Biol 8(11):e1000527.

Trias E, Diaz-Amarilla P, Olivera-Bravo S, Isasi E, Drechsel DA, Lopez N, Bradford CS, Ireton KE, Beckman JS, Barbeito L. 2013. Phenotypic transition of microglia into astrocyte-like cells associated with disease onset in a model of inherited ALS. Front Cell Neurosci 7:274.

Tripathi P, Rodriguez-Muela N, Klim JR, de Boer AS, Agrawal S, Sandoe J, Lopes CS, Ogliari KS, Williams LA, Shear M and others. 2017. Reactive Astrocytes Promote ALS-like Degeneration and Intracellular Protein Aggregation in Human Motor Neurons by Disrupting Autophagy through TGF-beta1. Stem Cell Reports 9(2):667-680.

Tronel C, Largeau B, Santiago Ribeiro MJ, Guilloteau D, Dupont AC, Arlicot N. 2017. Molecular Targets for PET Imaging of Activated Microglia: The Current Situation and Future Expectations. Int J Mol Sci 18(4).

Tsuda M. 2016. Microglia in the spinal cord and neuropathic pain. J Diabetes Investig 7(1):17-26.

Tsuda M, Koga K, Chen T, Zhuo M. 2017. Neuronal and microglial mechanisms for neuropathic pain in the spinal dorsal horn and anterior cingulate cortex. J Neurochem 141(4):486-498.

Tsuda M, Shigemoto-Mogami Y, Koizumi S, Mizokoshi A, Kohsaka S, Salter MW, Inoue K. 2003. P2X4 receptors induced in spinal microglia gate tactile allodynia after nerve injury. Nature 424(6950):778-83.

Turner BJ, Talbot K. 2008. Transgenics, toxicity and therapeutics in rodent models of mutant SOD1-mediated familial ALS. Prog Neurobiol 85(1):94-134.

Turner M, Al-Chalabi A. 2002. Early symptom progression rate is related to ALS outcome: a prospective population-based study. Neurology 59(12):2012-3; author reply 2013.

Turner MR, Cagnin A, Turkheimer FE, Miller CC, Shaw CE, Brooks DJ, Leigh PN, Banati RB. 2004. Evidence of widespread cerebral microglial activation in amyotrophic lateral sclerosis: an [11C](R)-PK11195 positron emission tomography study. Neurobiol Dis 15(3):601-9.

Ueno M, Fujita Y, Tanaka T, Nakamura Y, Kikuta J, Ishii M, Yamashita T. 2013. Layer V cortical neurons require microglial support for survival during postnatal development. Nat Neurosci 16(5):543-51.

Urushitani M, Sik A, Sakurai T, Nukina N, Takahashi R, Julien JP. 2006. Chromogranin-mediated secretion of mutant superoxide dismutase proteins linked to amyotrophic lateral sclerosis. Nat Neurosci 9(1):108-18.

Valadi H, Ekstrom K, Bossios A, Sjostrand M, Lee JJ, Lotvall JO. 2007. Exosome-mediated transfer of mRNAs and microRNAs is a novel mechanism of genetic exchange between cells. Nat Cell Biol 9(6):654-9.

van Blitterswijk M, van Vught PW, van Es MA, Schelhaas HJ, van der Kooi AJ, de Visser M, Veldink JH, van den Berg LH. 2012. Novel optineurin mutations in sporadic amyotrophic lateral sclerosis patients. Neurobiol Aging 33(5):1016 e1-7.

Van Damme P, Robberecht W, Van Den Bosch L. 2017. Modelling amyotrophic lateral sclerosis: progress and possibilities. Dis Model Mech 10(5):537-549.

Van Den Bosch L. 2011. Genetic rodent models of amyotrophic lateral sclerosis. J Biomed Biotechnol 2011:348765.

van der Vos KE, Abels ER, Zhang X, Lai C, Carrizosa E, Oakley D, Prabhakar S, Mardini O, Crommentuijn MH, Skog J and others. 2016. Directly visualized glioblastoma-derived extracellular vesicles transfer RNA to microglia/macrophages in the brain. Neuro Oncol 18(1):58-69.

Vance C, Rogelj B, Hortobagyi T, De Vos KJ, Nishimura AL, Sreedharan J, Hu X, Smith B, Ruddy D, Wright P and others. 2009. Mutations in FUS, an RNA processing protein, cause familial amyotrophic lateral sclerosis type 6. Science 323(5918):1208-1211.

VanGuilder HD, Bixler GV, Brucklacher RM, Farley JA, Yan H, Warrington JP, Sonntag WE, Freeman WM. 2011. Concurrent hippocampal induction of MHC II pathway components and glial activation with advanced aging is not correlated with cognitive impairment. J Neuroinflammation 8:138.

Vargas MR, Johnson JA. 2010. Astrogliosis in amyotrophic lateral sclerosis: role and therapeutic potential of astrocytes. Neurotherapeutics 7(4):471-81.

Vaz AR, Cunha C, Gomes C, Schmucki N, Barbosa M, Brites D. 2015. Glycoursodeoxycholic acid reduces matrix metalloproteinase-9 and caspase-9 activation in a cellular model of superoxide dismutase-1 neurodegeneration. Mol Neurobiol 51(3):864-77.

Vaz AR, Gomes C, Cunha C, Brites D. 2016. Astrocytes in amyotrophic lateral sclerosis: harmful effects and strategies to afford neuroprotection. in New Development in Astrocytes Research. New York: NY: Nova Science Publishers.

Venegas C, Heneka MT. 2017. Danger-associated molecular patterns in Alzheimer's disease. J Leukoc Biol 101(1):87-98.

Verderio C, Matteoli M. 2001. ATP mediates calcium signaling between astrocytes and microglial cells: modulation by IFN-gamma. J Immunol 166(10):6383-91.

Veremeyko T, Siddiqui S, Sotnikov I, Yung A, Ponomarev ED. 2013. IL-4/IL-13-dependent and independent expression of miR-124 and its contribution to M2 phenotype of monocytic cells in normal conditions and during allergic inflammation. PLoS One 8(12):e81774.

Veyrat-Durebex C, Corcia P, Dangoumau A, Laumonnier F, Piver E, Gordon PH, Andres CR, Vourc'h P, Blasco H. 2014. Advances in cellular models to explore the pathophysiology of amyotrophic lateral sclerosis. Mol Neurobiol 49(2):966-83.

Vilhardt F. 2005. Microglia: phagocyte and glia cell. Int J Biochem Cell Biol 37(1):17-21.

Villadangos JA, Cardoso M, Steptoe RJ, van Berkel D, Pooley J, Carbone FR, Shortman K. 2001. MHC class II expression is regulated in dendritic cells independently of invariant chain degradation. Immunity 14(6):739-49.

Villarroya-Beltri C, Gutierrez-Vazquez C, Sanchez-Cabo F, Perez-Hernandez D, Vazquez J, Martin-Cofreces N, Martinez-Herrera DJ, Pascual-Montano A, Mittelbrunn M, Sanchez-Madrid F. 2013. Sumoylated hnRNPA2B1 controls the sorting of miRNAs into exosomes through binding to specific motifs. Nat Commun 4:2980.

Vincenti JE, Murphy L, Grabert K, McColl BW, Cancellotti E, Freeman TC, Manson JC. 2016. Defining the Microglia Response during the Time Course of Chronic Neurodegeneration. J Virol 90(6):3003-17.

Vinet J, Weering HR, Heinrich A, Kalin RE, Wegner A, Brouwer N, Heppner FL, Rooijen N, Boddeke HW, Biber K. 2012. Neuroprotective function for ramified microglia in hippocampal excitotoxicity. J Neuroinflammation 9:27.

Visvanathan J, Lee S, Lee B, Lee JW, Lee SK. 2007. The microRNA miR-124 antagonizes the anti-neural REST/SCP1 pathway during embryonic CNS development. Genes Dev 21(7):744-9.

Volonté C, Apolloni S, Parisi C. 2015. MicroRNAs: newcomers into the ALS picture. CNS Neurol Disord Drug Targets 14(2):194-207.

Vu LT, Bowser R. 2017. Fluid-Based Biomarkers for Amyotrophic Lateral Sclerosis. Neurotherapeutics 14(1):119-134.

Vucic S, Nicholson GA, Kiernan MC. 2008. Cortical hyperexcitability may precede the onset of familial amyotrophic lateral sclerosis. Brain 131(Pt 6):1540-50.

Vucic S, Rothstein JD, Kiernan MC. 2014. Advances in treating amyotrophic lateral sclerosis: insights from pathophysiological studies. Trends Neurosci 37(8):433-42.

Wake H, Moorhouse AJ, Jinno S, Kohsaka S, Nabekura J. 2009. Resting microglia directly monitor the functional state of synapses in vivo and determine the fate of ischemic terminals. J Neurosci 29(13):3974-80.

Walker DG, Lue LF. 2015. Immune phenotypes of microglia in human neurodegenerative disease: challenges to detecting microglial polarization in human brains. Alzheimers Res Ther 7(1):56.

Waller R, Goodall EF, Milo M, Cooper-Knock J, Da Costa M, Hobson E, Kazoka M, Wollff H, Heath PR, Shaw PJ and others. 2017. Serum miRNAs miR-206, 143-3p and 374b-5p as potential biomarkers for amyotrophic lateral sclerosis (ALS). Neurobiol Aging 55:123-131.

Walsh JG, Muruve DA, Power C. 2014. Inflammasomes in the CNS. Nat Rev Neurosci 15(2):84-97.

Walton NM, Sutter BM, Laywell ED, Levkoff LH, Kearns SM, Marshall GP, 2nd, Scheffler B, Steindler DA. 2006. Microglia instruct subventricular zone neurogenesis. Glia 54(8):815-25.

Wang K, Ye L, Lu H, Chen H, Zhang Y, Huang Y, Zheng JC. 2017a. TNF-alpha promotes extracellular vesicle release in mouse astrocytes through glutaminase. J Neuroinflammation 14(1):87.

Wang K, Zhang S, Weber J, Baxter D, Galas DJ. 2010. Export of microRNAs and microRNA-protective protein by mammalian cells. Nucleic Acids Res 38(20):7248-59.

Wang WY, Tan MS, Yu JT, Tan L. 2015a. Role of pro-inflammatory cytokines released from microglia in Alzheimer's disease. Ann Transl Med 3(10):136.

Wang Y, Balaji V, Kaniyappan S, Kruger L, Irsen S, Tepper K, Chandupatla R, Maetzler W, Schneider A, Mandelkow E and others. 2017b. The release and trans-synaptic transmission of Tau via exosomes. Mol Neurodegener 12(1):5.

Wang Y, Cella M, Mallinson K, Ulrich JD, Young KL, Robinette ML, Gilfillan S, Krishnan GM, Sudhakar S, Zinselmeyer BH and others. 2015b. TREM2 lipid sensing sustains the microglial response in an Alzheimer's disease model. Cell 160(6):1061-71.

Weekman EM, Sudduth TL, Abner EL, Popa GJ, Mendenhall MD, Brothers HM, Braun K, Greenstein A, Wilcock DM. 2014. Transition from an M1 to a mixed neuroinflammatory phenotype increases amyloid deposition in APP/PS1 transgenic mice. J Neuroinflammation 11:127.

Whyte CS, Bishop ET, Ruckerl D, Gaspar-Pereira S, Barker RN, Allen JE, Rees AJ, Wilson HM. 2011. Suppressor of cytokine signaling (SOCS)1 is a key determinant of differential macrophage activation and function. J Leukoc Biol 90(5):845-54.

Wilcock DM. 2012. A changing perspective on the role of neuroinflammation in Alzheimer's disease. Int J Alzheimers Dis 2012:495243.

Willekens SM, Van Weehaeghe D, Van Damme P, Van Laere K. 2016. Positron emission tomography in amyotrophic lateral sclerosis: Towards targeting of molecular pathological hallmarks. Eur J Nucl Med Mol Imaging 44(3):533-547.

Willemen HL, Huo XJ, Mao-Ying QL, Zijlstra J, Heijnen CJ, Kavelaars A. 2012. MicroRNA-124 as a novel treatment for persistent hyperalgesia. J Neuroinflammation 9:143.

Willingham SB, Allen IC, Bergstralh DT, Brickey WJ, Huang MT, Taxman DJ, Duncan JA, Ting JP. 2009. NLRP3 (NALP3, Cryopyrin) facilitates in vivo caspase-1 activation, necrosis, and HMGB1 release via inflammasome-dependent and -independent pathways. J Immunol 183(3):2008-15.

Wohleb ES. 2016. Neuron-Microglia Interactions in Mental Health Disorders: "For Better, and For Worse". Front Immunol 7:544.

Wolf SA, Boddeke HW, Kettenmann H. 2017. Microglia in Physiology and Disease. Annu Rev Physiol 79:619-643.

Wolf Y, Yona S, Kim KW, Jung S. 2013. Microglia, seen from the CX3CR1 angle. Front Cell Neurosci 7:26.

Wong WT. 2013. Microglial aging in the healthy CNS: phenotypes, drivers, and rejuvenation. Front Cell Neurosci 7:22.

Woodbury ME, Freilich RW, Cheng CJ, Asai H, Ikezu S, Boucher JD, Slack F, Ikezu T. 2015. miR-155 Is Essential for Inflammation-Induced Hippocampal Neurogenic Dysfunction. J Neurosci 35(26):9764-81.

Wu CH, Fallini C, Ticozzi N, Keagle PJ, Sapp PC, Piotrowska K, Lowe P, Koppers M, McKenna-Yasek D, Baron DM and others. 2012a. Mutations in the profilin 1 gene cause familial amyotrophic lateral sclerosis. Nature 488(7412):499-503.

Wu CX, Sun H, Liu Q, Guo H, Gong JP. 2012b. LPS induces HMGB1 relocation and release by activating the NF-kappaB-CBP signal transduction pathway in the murine macrophage-like cell line RAW264.7. J Surg Res 175(1):88-100.

Wu D, Cerutti C, Lopez-Ramirez MA, Pryce G, King-Robson J, Simpson JE, van der Pol SM, Hirst MC, de Vries HE, Sharrack B and others. 2015a. Brain endothelial miR-146a negatively modulates T-cell adhesion through repressing multiple targets to inhibit NF-kappaB activation. J Cereb Blood Flow Metab 35(3):412-23.

Wu DC, Re DB, Nagai M, Ischiropoulos H, Przedborski S. 2006. The inflammatory NADPH oxidase enzyme modulates motor neuron degeneration in amyotrophic lateral sclerosis mice. Proc Natl Acad Sci U S A 103(32):12132-7.

Wu J, Bie B, Yang H, Xu JJ, Brown DL, Naguib M. 2013. Suppression of central chemokine fractalkine receptor signaling alleviates amyloid-induced memory deficiency. Neurobiol Aging 34(12):2843-52.

Wu K, Zhu C, Yao Y, Wang X, Song J, Zhai J. 2016a. MicroRNA-155-enhanced autophagy in human gastric epithelial cell in response to Helicobacter pylori. Saudi J Gastroenterol 22(1):30-6.

Wu XQ, Dai Y, Yang Y, Huang C, Meng XM, Wu BM, Li J. 2016b. Emerging role of microRNAs in regulating macrophage activation and polarization in immune response and inflammation. Immunology 148(3):237-48.

Wu Y, Dissing-Olesen L, MacVicar BA, Stevens B. 2015b. Microglia: Dynamic Mediators of Synapse Development and Plasticity. Trends Immunol 36(10):605-13.

Wu Y, Singh S, Georgescu MM, Birge RB. 2005. A role for Mer tyrosine kinase in alphavbeta5 integrin-mediated phagocytosis of apoptotic cells. J Cell Sci 118(Pt 3):539-53.

Xiang W, Chao ZY, Feng DY. 2015. Role of Toll-like receptor/MYD88 signaling in neurodegenerative diseases. Rev Neurosci 26(4):407-14.

Xiao Q, Zhao W, Beers DR, Yen AA, Xie W, Henkel JS, Appel SH. 2007. Mutant SOD1(G93A) microglia are more neurotoxic relative to wild-type microglia. J Neurochem 102(6):2008-19.

Xiao T, Zhang W, Jiao B, Pan CZ, Liu X, Shen L. 2017. The role of exosomes in the pathogenesis of Alzheimer' disease. Transl Neurodegener 6:3.

Xu J, Dong H, Qian Q, Zhang X, Wang Y, Jin W, Qian Y. 2017. Astrocyte-derived CCL2 participates in surgery-induced cognitive dysfunction and neuroinflammation via evoking microglia activation. Behav Brain Res 332:145-153.

Xu Z, Ho S, Chang CC, Liu Z, Li M, Vasilescu ER, Clynes RA, Vlad G, Suciu-Foca N. 2014. ILT3.Fc inhibits the production of exosomes containing inflammatory microRNA in supernatants of alloactivated T cells. Hum Immunol 75(8):756-9.

Yamanaka K, Boillee S, Roberts EA, Garcia ML, McAlonis-Downes M, Mikse OR, Cleveland DW, Goldstein LS. 2008a. Mutant SOD1 in cell types other than motor neurons and oligodendrocytes accelerates onset of disease in ALS mice. Proc Natl Acad Sci U S A 105(21):7594-9.

Yamanaka K, Chun SJ, Boillee S, Fujimori-Tonou N, Yamashita H, Gutmann DH, Takahashi R, Misawa H, Cleveland DW. 2008b. Astrocytes as determinants of disease progression in inherited amyotrophic lateral sclerosis. Nat Neurosci 11(3):251-3.

Yamasaki R, Tanaka M, Fukunaga M, Tateishi T, Kikuchi H, Motomura K, Matsushita T, Ohyagi Y, Kira J. 2010. Restoration of microglial function by granulocyte-colony stimulating factor in ALS model mice. J Neuroimmunol 229(1-2):51-62.

Yang L, Blumbergs PC, Jones NR, Manavis J, Sarvestani GT, Ghabriel MN. 2004. Early expression and cellular localization of proinflammatory cytokines interleukin-1beta, interleukin-6, and tumor necrosis factor-alpha in human traumatic spinal cord injury. Spine (Phila Pa 1976) 29(9):966-71.

Yang WW, Sidman RL, Taksir TV, Treleaven CM, Fidler JA, Cheng SH, Dodge JC, Shihabuddin LS. 2010. Relationship between neuropathology and disease progression in the SOD1(G93A) ALS mouse. Exp Neurol 227(2):287-95.

Yao L, Kan EM, Lu J, Hao A, Dheen ST, Kaur C, Ling EA. 2013. Toll-like receptor 4 mediates microglial activation and production of inflammatory mediators in neonatal rat brain following hypoxia: role of TLR4 in hypoxic microglia. J Neuroinflammation 10:23.

Ye J, Jiang Z, Chen X, Liu M, Li J, Liu N. 2017. The role of autophagy in pro-inflammatory responses of microglia activation via mitochondrial reactive oxygen species in vitro. J Neurochem 142(2):215-230.

Yelamanchili SV, Lamberty BG, Rennard DA, Morsey BM, Hochfelder CG, Meays BM, Levy E, Fox HS. 2015. MiR-21 in Extracellular Vesicles Leads to Neurotoxicity via TLR7 Signaling in SIV Neurological Disease. PLoS Pathog 11(7):e1005032.

Yeo JG, Leong J, Arkachaisri T, Cai Y, Teo BH, Tan JH, Das L, Lu J. 2016. Proteolytic inactivation of nuclear alarmin high-mobility group box 1 by complement protease C1s during apoptosis. Cell Death Discov 2:16069.

Yeo YA, Martinez Gomez JM, Croxford JL, Gasser S, Ling EA, Schwarz H. 2012. CD137 ligand activated microglia induces oligodendrocyte apoptosis via reactive oxygen species. J Neuroinflammation 9:173.

Yiangou Y, Facer P, Durrenberger P, Chessell IP, Naylor A, Bountra C, Banati RR, Anand P. 2006. COX-2, CB2 and P2X7-immunoreactivities are increased in activated microglial

cells/macrophages of multiple sclerosis and amyotrophic lateral sclerosis spinal cord. BMC Neurol 6:12.

Yu A, Zhang T, Duan H, Pan Y, Zhang X, Yang G, Wang J, Deng Y, Yang Z. 2017. MiR-124 contributes to M2 polarization of microglia and confers brain inflammatory protection via the C/EBP-alpha pathway in intracerebral hemorrhage. Immunol Lett 182:1-11.

Yu HM, Zhao YM, Luo XG, Feng Y, Ren Y, Shang H, He ZY, Luo XM, Chen SD, Wang XY. 2012. Repeated lipopolysaccharide stimulation induces cellular senescence in BV2 cells. Neuroimmunomodulation 19(2):131-6.

Yu JY, Chung KH, Deo M, Thompson RC, Turner DL. 2008. MicroRNA miR-124 regulates neurite outgrowth during neuronal differentiation. Exp Cell Res 314(14):2618-33.

Yu M, Wang H, Ding A, Golenbock DT, Latz E, Czura CJ, Fenton MJ, Tracey KJ, Yang H. 2006. HMGB1 signals through toll-like receptor (TLR) 4 and TLR2. Shock 26(2):174-9.

Yuan J, Ge H, Liu W, Zhu H, Chen Y, Zhang X, Yang Y, Yin Y, Chen W, Wu W and others. 2017. M2 microglia promotes neurogenesis and oligodendrogenesis from neural stem/progenitor cells via the PPARgamma signaling pathway. Oncotarget 8(12):19855-19865.

Yuan K, Zhang X, Lv L, Zhang J, Liang W, Wang P. 2016. Fine-tuning the expression of microRNA-155 controls acetaminophen-induced liver inflammation. Int Immunopharmacol 40:339-346.

Yuyama K, Sun H, Mitsutake S, Igarashi Y. 2012. Sphingolipid-modulated exosome secretion promotes clearance of amyloid-beta by microglia. J Biol Chem 287(14):10977-89.

Zabel MK, Zhao L, Zhang Y, Gonzalez SR, Ma W, Wang X, Fariss RN, Wong WT. 2016. Microglial phagocytosis and activation underlying photoreceptor degeneration is regulated by CX3CL1-CX3CR1 signaling in a mouse model of retinitis pigmentosa. Glia 64(9):1479-91.

Zahednasab H, Balood M, Harirchian MH, Mesbah-Namin SA, Rahimian N, Siroos B. 2014. Increased autotaxin activity in multiple sclerosis. J Neuroimmunol 273(1-2):120-3.

Zhang F, Vadakkan KI, Kim SS, Wu LJ, Shang Y, Zhuo M. 2008. Selective activation of microglia in spinal cord but not higher cortical regions following nerve injury in adult mouse. Mol Pain 4:15.

Zhang G, He JL, Xie XY, Yu C. 2012a. LPS-induced iNOS expression in N9 microglial cells is suppressed by geniposide via ERK, p38 and nuclear factor-kappaB signaling pathways. Int J Mol Med 30(3):561-8.

Zhang L, Dong LY, Li YJ, Hong Z, Wei WS. 2012b. miR-21 represses FasL in microglia and protects against microglia-mediated neuronal cell death following hypoxia/ischemia. Glia 60(12):1888-95.

Zhang R, Gascon R, Miller RG, Gelinas DF, Mass J, Hadlock K, Jin X, Reis J, Narvaez A, McGrath MS. 2005. Evidence for systemic immune system alterations in sporadic amyotrophic lateral sclerosis (sALS). J Neuroimmunol 159(1-2):215-24.

Zhang W, Jiao B, Zhou M, Zhou T, Shen L. 2016. Modeling Alzheimer's Disease with Induced Pluripotent Stem Cells: Current Challenges and Future Concerns. Stem Cells Int 2016:7828049.

Zhang Y, Chen K, Sloan SA, Bennett ML, Scholze AR, O'Keeffe S, Phatnani HP, Guarnieri P, Caneda C, Ruderisch N and others. 2014. An RNA-sequencing transcriptome and splicing database of glia, neurons, and vascular cells of the cerebral cortex. J Neurosci 34(36):11929-47.

Zhang ZJ, Jiang BC, Gao YJ. 2017. Chemokines in neuron-glial cell interaction and pathogenesis of neuropathic pain. Cell Mol Life Sci 74(18):3275-3291.

Zhao S, Zhang L, Lian G, Wang X, Zhang H, Yao X, Yang J, Wu C. 2011. Sildenafil attenuates LPS-induced pro-inflammatory responses through down-regulation of intracellular ROS-related MAPK/NF-kappaB signaling pathways in N9 microglia. Int Immunopharmacol 11(4):468-74.

Zhao SC, Ma LS, Chu ZH, Xu H, Wu WQ, Liu F. 2017. Regulation of microglial activation in stroke. Acta Pharmacol Sin 38(4):445-458.

Zhao W, Beers DR, Appel SH. 2013. Immune-mediated mechanisms in the pathoprogression of amyotrophic lateral sclerosis. J Neuroimmune Pharmacol 8(4):888-99.

Zhao W, Beers DR, Bell S, Wang J, Wen S, Baloh RH, Appel SH. 2015. TDP-43 activates microglia through NF-kappaB and NLRP3 inflammasome. Exp Neurol 273:24-35.

Zhao W, Beers DR, Henkel JS, Zhang W, Urushitani M, Julien JP, Appel SH. 2010. Extracellular mutant SOD1 induces microglial-mediated motoneuron injury. Glia 58(2):231-43.

Zhong Z, Deane R, Ali Z, Parisi M, Shapovalov Y, O'Banion MK, Stojanovic K, Sagare A, Boillee S, Cleveland DW and others. 2008. ALS-causing SOD1 mutants generate vascular changes prior to motor neuron degeneration. Nat Neurosci 11(4):420-2.

Zhu H, Bhattacharyya B, Lin H, Gomez CM. 2013. Skeletal muscle calpain acts through nitric oxide and neural miRNAs to regulate acetylcholine release in motor nerve terminals. J Neurosci 33(17):7308-7324.

Zhu HT, Bian C, Yuan JC, Chu WH, Xiang X, Chen F, Wang CS, Feng H, Lin JK. 2014. Curcumin attenuates acute inflammatory injury by inhibiting the TLR4/MyD88/NF-kappaB signaling pathway in experimental traumatic brain injury. J Neuroinflammation 11:59.

Zhu Y, Hou H, Rezai-Zadeh K, Giunta B, Ruscin A, Gemma C, Jin J, Dragicevic N, Bradshaw P, Rasool S and others. 2011. CD45 deficiency drives amyloid-beta peptide oligomers and neuronal loss in Alzheimer's disease mice. J Neurosci 31(4):1355-65.

Zondler L, Feiler MS, Freischmidt A, Ruf WP, Ludolph AC, Danzer KM, Weishaupt JH. 2017. Impaired activation of ALS monocytes by exosomes. Immunol Cell Biol 95(2):207-214.

Zondler L, Muller K, Khalaji S, Bliederhauser C, Ruf WP, Grozdanov V, Thiemann M, Fundel-Clemes K, Freischmidt A, Holzmann K and others. 2016. Peripheral monocytes are functionally altered and invade the CNS in ALS patients. Acta Neuropathol 132(3):391-411.

Zou ZY, Cui LY, Sun Q, Li XG, Liu MS, Xu Y, Zhou Y, Yang XZ. 2012. De novo FUS gene mutations are associated with juvenile-onset sporadic amyotrophic lateral sclerosis in China. Neurobiol Aging 34(4):1312 e1-8.